UNIVERSITY OF SOUTHAMPTON

FACULTY OF MEDICINE, HEALTH AND LIFE SCIENCES

School of Biological Sciences

Autumnal senescence in a poplar plantation in response to elevated carbon dioxide, from cell to canopy

In one volume

by

Matthew James Tallis

March 2007.

UNIVERSITY OF SOUTHAMPTON

ABSTRACT

FACULTY OF MEDICINE, HEALTH AND LIFE SCIENCES
SCHOOL OF BIOLOGICAL SCIENCES

Doctor of Philosophy

AUTUMNAL SENESCENCE IN A POPLAR PLANTATION IN RESPONSE TO ELEVATED CARBON DIOXIDE, FROM CELL TO CANOPY

by Matthew James Tallis

Global data sets derived from remote sensing of terrestrial vegetation and phenological observations of bud set, leaf colour change and leaf drop have provided evidence for the recent extension of the growing season. Atmospheric carbon dioxide concentration has risen by ~ 39 % since pre-industrial times and is considered a strong driver for a mean global temperature rise. This increased temperature is generally thought to be the cause of the extension in the growing seasons. In this thesis the influence increased atmospheric carbon dioxide concentration may have on the autumnal phenology of a poplar plantation was examined.

Following up to six years growth in an atmosphere enriched with carbon dioxide (CO_2) using free air CO_2 enrichment technology, the autumnal phenology of two poplar genotypes was examined. Using remote sensing technology, at spatial and spectral resolutions varying from leaf level to airborne sensors, the changes in canopy spectral reflectance during senescence were monitored. These changes were associated with a delayed autumnal decline in canopy leaf area and leaf level chlorophyll concentration for the trees exposed to elevated CO_2. Associated with this was a decrease in both specific leaf area (leaf area per unit mass) and leaf nitrogen content (on a leaf mass basis). The extension of autumnal senescence in this plantation resulting from atmospheric CO_2 enrichment was estimated to contribute approximately 2 % to the annual gross primary production.

The change in gene expression associated with this delay was studied using microarray technology. Delayed senescence in elevated CO_2 was also evident at the level of gene expression, confirming the remotely-sensed observations. For the first time, an up-regulation of genes encoding enzymes within the pathways of phenylpropanoid metabolism were identified during autumnal senescence in elevated CO_2, inferring increased stress tolerance.

Table of contents

List of figures

Chapter 1

Chapter 2

Chapter 3

Chapter 4

Chapter 5

Figure number

List of tables

Chapter 1

Chapter 2

Chapter 3

Chapter 4

Chapter 5

Table number

Acknowledgements

I would like to thank my supervisors Gail Taylor and Franco Miglietta for help, support and guidance during this study. For help with obtaining leaf spectra in chapter two I wish to thank Dr. Jadunandan Dash (University of Southampton). I acknowledge his use of a number of spectra to calculate MTCI, and thank him for the opportunity to be involved in field scale validation of MTCI from the ENVISAT satellite, in collaboration with the European Space Agency. For the work in chapter two I would also like to thank Prof. Paul Curran (University of Bournemouth) Dr. Ann Rae (University of Southampton) and anonymous reviewers of New Phytologist for advice on data analysis, Dr. Matthew Terry for the loan of the light meter and Dave Baddams and Mick Cotton (all University of Southampton) for help in the green house.

I have been very fortunate to work in Italy in an international collaborative experiment and would like to thank all of my friends and colleagues past and present at the POP/EUROFACE consortium. In particular I would like to thank Dr. Carlo Calfapietra, Dr. Paolo De Angelis and Tullio Ora (University of Viterbo) for help and advice at the site.

Special mention must be made to those who helped me in the field especially Dr. Birgit Gielen and Christophe Stevnen (University of Antwerp) for the long hours during the autumn of 2004. I would also like to thank my supervisor Franco Miglietta for the loan of the GER 3700 and integrating sphere and advice with the set-up of the sphere and, along with Beniamino Gioli (IBMET-CNR Florence), for help with the airborne data collection and analysis. I would also like to thank Marion Liberloo (University of Antwerp) Dr. Marco Pecchiari (University of Udine) and Dr. Graham Clarkson (Vitacress salads) for assistance in the field in 2003. For advice on the statistical analysis for the field data I would like to thank Dr. C. Patrick Doncaster (University of Southampton), and for supplying the leaf nitrogen data I would like to thank Prof. Peter Freer-Smith (Forest Research).

All of my friends and colleagues in Gail's lab, past and present, must be thanked especially Dr. Nathaniel Street for help with microarray hybridisations, I would also like to thank Laura Graham, James Tucker and Rob Holmes here. I would further like to thank Dr. Nathaniel Street for advice on analysis of the microarray data in chapter five. For independent confirmation of the results from chapter five I thank Jing Zhang (University of

Southampton, visiting from the University of Peking) for providing me with data from the RT-qPCR she carried out. I also wish to thank Dr. Penny Tricker and Dr. Carol Wagstaff for reading this thesis and providing advice on editing.

Finally I must always thank my girlfriend Henrike for her love and support before and during this thesis, and for stopping me from working when appropriate, and my parents for there love and support.

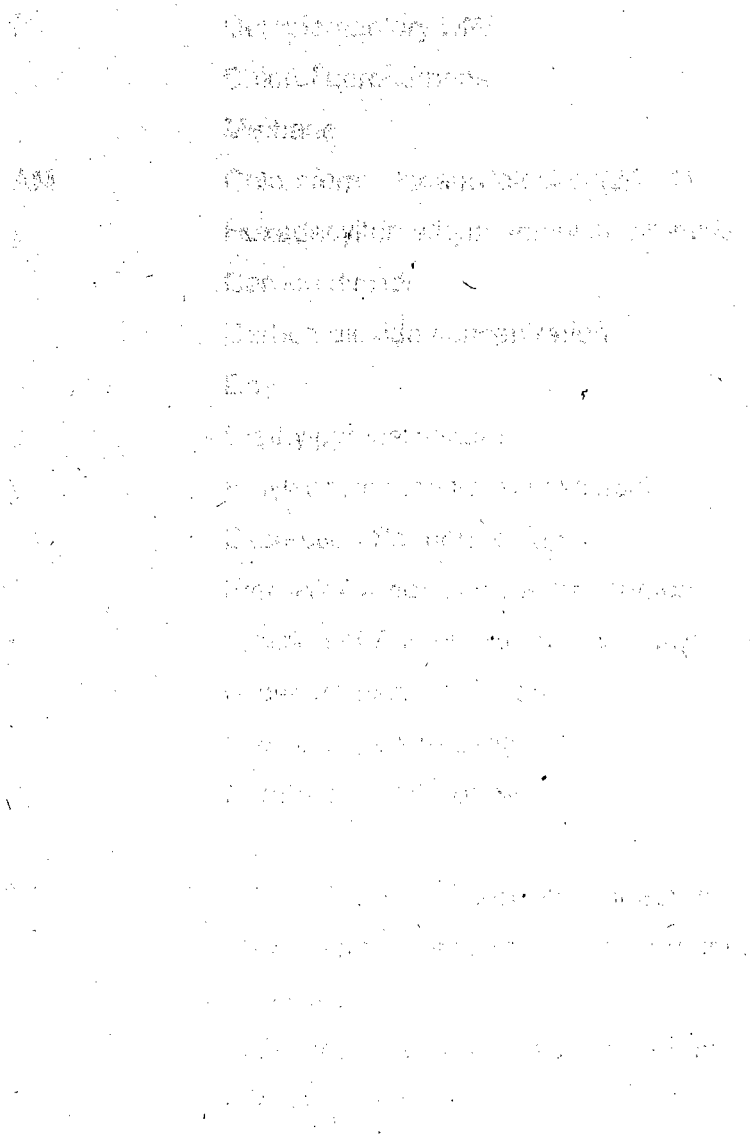

List of abbreviations and symbols

Abbreviation	*Definition*
APAR	Absorbed photosynthetically active radiation
A_{sat}	Light saturated photosynthesis
ANCOVA	Analysis of covariance
ANOVA	Analysis of variance
ATP	Adenosine triphosphate
C	Carbon
°C	Degrees Celsius
CCM	Chlorophyll Content Meter
cDNA	Complementary DNA
CFC	Chlorofluorocarbons
CH_4	Methane
CHISAM	Chloroform : Isoamylalcohol (24 : 1)
CTAB	Hexadecyltrimethylammonium bromide
CO_2	Carbon dioxide
$[CO_2]$	Carbon dioxide concentration
d	Day
DEPC	Diethylpyrocarbonate
EDTA	Ethylenediamine tetraacetic acid
EST	Expressed Sequence Tag
FACE	Free-Air Carbon Dioxide Enrichment
FPAR	Fraction of Photosynthetically Active Radiation
GPP	Gross Primary Production
GSL	Growing Season Length
Gt	Gigatonnes (10^9 tonnes)
Ha	Hectare
HEPES	4-(2-hydroxyethyl)-1-piperazineethanesulfonic acid
J_{max}	Maximum rate of electron transport contributing to RuBP regeneration
LAI	Leaf Area Index (m^2 foliage m^{-2} ground area)
LiCl	Lithium Chloride

Log_e	Natural Logarithm
Log_2	Log to the base two
LUE	Light Use Efficiency
mRNA	Messenger RNA
MNDVI	Modified Normalised Difference Vegetation Index
N	Nitrogen
NADPH	Reduced form of Nicotinamide Adenine Dinucleotide Phosphate
NDVI	Normalised Difference Vegetation Index
NPP	Net Primary Production
ODT	Oven Dried Tonne
OTC	Open Top Chamber
nm	Nanometre
% Nmass	Nitrogen content on a percentage mass basis
PCR	Polymerase Chain Reaction
Pg	Petagramme (10^{15} grams) or 10^9 tonnes or 1 Gt
3-PGA	3-phosphoglycerate
Pi	Inorganic Phosphate
PNUE	Photosynthetic Nitrogen Use Efficiency
ppm	Parts Per Million
PRI	Photochemical Reflectance Index
PSRI	Plant Senescence Reflectance Index
REDOX	Oxidation - Reduction reaction
REP	Red-Edge Position
RNA	Ribonucleic acid
ROS	Reactive Oxygen Species
rpm	Revolutions Per Minute
RT	Room Temperature
RT-qPCR	Reverse Transcriptase Quantitative PCR
Rubisco	Ribulose bisphosphate carboxylase / oxygenase
RuBP	Ribulose 1,5 bisphosphate
SE	Standard Error (of the mean)
SLA	Specific Leaf Area ($mm^2\ g^{-1}$)
SPAD	Soil Plant Analysis Development

SRC	Short Rotation Coppice
t	Tonne
$V_{c,max}$	Maximum velocity of carboxylation of Rubisco
WAI	Woody Area Index (m^2 timber m^{-2} ground area)
WUE	Water Use Efficiency

Chapter 1:

General introduction

1.1 Overview

This chapter presents a background to the capture of atmospheric carbon by forest trees. The transfer of carbon from the atmosphere to the terrestrial biosphere, through the process of photosynthesis, and the *in planta* cycling of that carbon in the form of carbohydrates, will be discussed. A particular emphasis will be placed upon how these processes are influenced by an increasing atmospheric carbon dioxide concentration [CO_2] and the consequences this could have on natural autumnal senescence.

This subject matter is important because the seasonal growth of Northern Hemisphere vegetation takes up atmospheric CO_2 and this sink for CO_2 has increased over recent decades. This enhanced sink may be explained by a greater magnitude of vegetation photosynthetic activity, resulting from increased surface temperatures and CO_2 fertilisation. However, this does not adequately explain the total increase in the sink for carbon and an increased duration of the growing seasons is a component of this response (Keeling *et al.*, 1996). The biomass accumulation of forest trees is important because, at the latest assessment, forests were considered to cover 30.3 % of total global land area and store approximately 283 Gt of carbon (FAO, 2006). An extended growing season has also been reported to increase carbon storage globally in the boreal zone of Northern latitude forests (Lucht *et al.*, 2002) and in the aspen boreal forests of North America (Chen *et al.*, 1999). Specifically, in terms of an extended autumnal period of between five to ten days in a deciduous forest in New England, gross production of that forest was increased by around 500 Kg C ha^{-1} in that year (Goulden *et al.*, 1996). At the global spatial scale Zhou *et al.*, (2001) identified an increase in the growing-season magnitude of NDVI (a surrogate for productivity) by around 20.9 %, 8.7 % and 12.4 % for spring, summer and autumn respectively across Eurasia, highlighting increased terrestrial productivity between the years 1981 – 1999. Climatic warming is generally considered a strong driver for an extension in the growing season; this is particularly true for earlier spring time events (Menzel 2000; Badeck *et al.*, 2004; Stöckli and Vidale 2004; Menzel *et al.*, 2006). However, the association of warming with autumnal phenological events is far weaker (Stöckli and Vidale 2004; Menzel *et al.* 2006).

Autumnal senescence is an active, genetically controlled process of plant development (Buchanan-Wollaston *et al.*, 2003) and for northern forest tree species the cue for this

process appears to be most strongly correlated with a shortening of the photoperiod (Richardson *et al.,* 2006), a feature evident for poplar species (Böhlenius *et al.,* 2006; Olsen *et al.*, 1997). Nevertheless, features other than day length influence progression of leaf senescence and the plant's leaf carbon to nitrogen balance is important (Wingler *et al.,* 2006). Therefore, to understand the influence increased atmospheric [CO_2] imparts on leaf senescence, we must also understand the processes during the growing season by which elevated CO_2 may influence the dynamic relationship of plant carbon to nitrogen balance.

Carbon dioxide enrichment of the atmosphere occurs with zero spatial limitation and has a multi-faceted role in influencing vegetation. This is the result of CO_2 impacting upon the site of global primary production; photosynthesis, as well as global temperature, both of which are intimately linked (Boisvenue and Running, 2006). This study takes into account the multiple biological scales over which vegetation responds to increasing atmospheric CO_2. This results from integrating knowledge of global remote sensing technology, leaf to canopy eco-physiology and spectral reflectance, with an understanding of changes in transcriptional response.

1.2 Atmospheric CO_2 Concentration, C_3 Photosynthesis and Global Warming

In 1772, Joseph Priestley observed that air contaminated by the burning of a candle could not support the life of a mouse; however addition of a sprig of mint to the same air enabled the mouse to survive (Priestley and Hey, 1772). This is explained by photosynthesis (*i*) through which approximately equal volumes of CO_2 and O_2 are exchanged by green plant material in the presence of light (Mc Donald, 2003).

$$\text{Carbon dioxide + water + sunlight} \longrightarrow \text{glucose + water + oxygen}$$

$$(6CO_2 + 12H_20 + \text{electromagnetic energy} \longrightarrow C_6H_{12}O_6 + 6H_20 + 6O_2) \qquad (i)$$

In the 1980s a mathematical model for C_3 photosynthesis was developed by Farquhar *et al.* (1980) and was based around the kinetic properties of the enzyme ribulose-1:5-bisphosphate carboxylase/oxygenase (Rubisco). Rubisco catalyses the binding of CO_2 with a 5 carbon (5C) compound, ribulose bisphosphate (RuBP) forming two 3C compounds (3-PGA). The enzyme Rubisco has a direct association with atmospheric CO_2 and the carboxylation of Rubisco is the only known reaction reported to respond directly to increasing atmospheric CO_2 (Long *et al.,* 2006). The model by Farquhar has proved a very robust predictor of C_3 photosynthesis for multiple species and conditions (Long *et al.*, 2004) and identifies three key processes which regulate the rate of photosynthesis. Two of these are associated with Rubisco; these are the maximum rate of CO_2 binding capacity (carboxylation capacity: $V_{c,max}$) of Rubisco and the regeneration of ribulose-1,5-bisphosphate (RuBP) the 5C substrate for Rubisco, which is limited by the rate of electron transport (J_{max}), determined by the *light reactions* of photosynthesis. A third process regulating the rate of C_3 photosynthesis is the rate of conversion of the C3 products from the Calvin cycle to sucrose and starch with the subsequent liberation of inorganic phosphate (Pi) for photophosphorylation (Farquhar *et al.*, 1980). As atmospheric carbon dioxide concentration [CO_2] increases it is predicted that the rate limiting step in photosynthesis will shift from $V_{c,max}$ which is not saturated at current [CO_2] (Drake *et al.*, 1997) towards processes involving regeneration of RuBP such as the light reactions (Sage, 1994), or the rate of export and subsequent metabolism of carbohydrate (Stitt, 1991).

Around 1860, John Tyndall identified the capacity of water vapour (H_2O) and CO_2 to absorb infrared radiation, and in 1896, Svante Arrhenius calculated that doubling the

concentration of atmospheric CO_2 would raise average global temperature by 5°C to 6°C (Mc Donald, 2003). This is not far from today's predictions; for example, of six alternative scenarios for climate change, scenario IS92a (one of the six, and considered 'business as usual') predicts a near doubling of atmospheric CO_2 concentration by 2100, to 700 ppm with an associated rise of 2.5 °C in global mean temperature (Houghton, 2004). It is also worth noting that global mean temperature rose by 0.6 °C during the twentieth century and that this rise was strongly associated with an increase in the radiative forcing of the atmosphere, a phenomenon termed global warming (Houghton 2004).

Global warming resulting from an increased radiative forcing of the atmosphere is the consequence of a process termed *The Greenhouse Effect*. The Greenhouse Effect can be considered the result of two distinct processes. One allows the existence of life, the *natural greenhouse effect*, predominantly the result of the radiative forcing of atmospheric H_2O increasing global temperature by 21 °C from an estimated - 6 °C for an atmosphere consisting of N_2 and O_2 only. The second is the *enhanced greenhouse effect* leading to what is commonly termed global warming. Global warming is generally assumed to be the consequence of the radiative forcing of the greenhouse gases CO_2, N_2O, CH_4, CFCs and tropospheric ozone. Houghton (2004) estimated CO_2 alone to provide 70 % of the increased radiative forcing to the atmosphere since a pre-industrial year of 1750. This is generally assumed to be the result of an approximate 35 % rise in atmospheric [CO_2] from near to 270 - 280 ppm prior to the industrial revolution (Prentice *et al.*, 2001; Francy *et al.*, 1999) to an average for 2004 of 377 ppm (Keeling and Whorf, 2004), and during 2005 the rate of annual increase also accelerated above that recorded since records began in March 1958 (Nösberger and Long, 2006). Direct sampling of atmospheric CO_2 began from a station on mount Mauna Loa, Hawaii, in 1958, by measuring the infrared radiation from a glowing coil of wire after a stream of sample air had passed over it (Keeling, 1998). Today atmospheric CO_2 concentration is measured by ten stations evenly distributed over both hemispheres from 82 °N to 90 °S which sample air at 30 minute intervals (Blasing and Jones, 2004), and in Feburary 2006 atmospheric [CO_2] peaked at 382 ppm (Nösberger and Long, 2006) a value possibly not seen for the last several million years (Pearson and Palmer 2000).

1.2.1 The terrestrial biomass carbon sink and atmospheric CO_2 concentration

An association between atmospheric [CO_2], global warming and forest growth has lead to activities such as afforestation and reforestation to be proposed under article 3.3 of the Kyoto Protocol as a potential mitigation strategy against global warming (UN, 1998; IPCC, 2001). The plants of the terrestrial biosphere are currently a store of approximately 500 x 10^{15} g carbon, or 500 PgC and the atmosphere, a slightly larger 730 PgC. At recent atmospheric CO_2 concentrations, 120 x 10^{15} g of carbon (120 PgC) are cycled each year between the terrestrial biosphere and the atmosphere (16 % of the atmospheric total), termed the gross primary production (GPP) (Prentice *et al.*, 2001; Scholes and Noble, 2001). Approximately half of this carbon is directly returned to the atmosphere through plant respiration, with the remaining carbon captured though the process of plant growth. This is termed the Net Primary Production (NPP) (Prentice *et al.*, 2001; Malhi 2002). Net primary production is the difference between gross photosynthesis and autotrophic respiration, and is a major determinant of the strength of the terrestrial carbon sink which may be considered to capture approximately 8 % of the atmospheric carbon pool (Malhi, 2002). The carbon taken up by NPP finally re-enters the carbon cycle through heterotrophic respiration which can occur via herbivory and plant decomposition or by the oxidation process of combustion. Some carbon is also transferred to relatively longer-term storage in soil pools (Malhi, 2002).

The ability of the terrestrial biosphere to capture atmospheric CO_2 in the presence of a changing climate may have implications on the magnitude of climate change and global biogeochemical cycling. For example, the European terrestrial biosphere currently acts as a net carbon sink of between 135 - 205 x 10^{12} g C y^{-1} which is estimated to account for 7 - 12 % of the 1995 anthropogenic carbon emissions of Europe (Janssens *et al.*, 2003). Between 1982-1990 land NPP was estimated as 56.4 x 10^{15} g C yr^{-1} for which forests contributed 33 % to the total global NPP and 62 % of the land NPP (Field *et al.*, 1998). Soils remain a major terrestrial store of carbon, approximately three times that of terrestrial vegetation (Malhi, 2002). However, over the short-term the largest influence on forest NPP and so the largest sink for CO_2 will be in the standing biomass of stems, branches and roots of trees (Geider *et al.*, 2001). This is supported by data from the POP/EUROFACE experiment, in which a short rotation coppice (SRC) plantation of poplar was exposed to growth in enriched atmospheric CO_2 (described in detail from page 11). At this site,

atmospheric CO_2 enrichment caused a stimulation of above ground biomass of 27 % after the first three year cycle, an increase of approximately 5 ODT $ha^{-1}yr^{-1}$ (Calfapietra *et al.*, 2003) and by 29 % after the second three year cycle with an increase of approximately 7 ODT ha^{-1} yr^{-1} (Liberloo *et al.*, 2006) averaged across genotypes. Whereas the percentage stimultion of below ground biomass was similar to above ground, the total increase in elevated CO_2 was estimated at 0.9 ODT $ha^{-1}yr^{-1}$ when avearged across genotypes (Liberloo *et al.*, 2006). Therefore, fast growing trees such as *Populus* may be a species to consider as a mitigation strategy against increasing atmospheric [CO_2] (Wittig *et al.*, 2005). Furthermore, as trees age the ratio of wood to leaf area increases, resulting in a decrease in NPP as the ratio of maintenance respiration to carbon capture increases (Geider *et al.*, 2001). As a result, cultural practices such as coppicing may help to stimulate the NPP per unit land area by maintaining a high leaf to wood area ratio.

In general, mathematical models of climatic change tend to agree that as CO_2 increases, an imbalance between terrestrial carbon uptake and respiration results, leading to increased NPP (also known as the *CO_2 fertilisation effect*); however the magnitude, duration and long term direction of this response is variable (Cao and Woodward, 1998; Cramer *et al.*, 2001). This is because models predict that, as atmospheric [CO_2] rises, photosynthesis saturates and soil respiration rates continue to rise with increasing temperature, and by 2050 the terrestrial biosphere becomes a source of CO_2 (Cox *et al.*, 2000; Knorr *et al.*, 2005). This leads to divergent estimates for the percentage of atmospheric CO_2 that could be captured by terrestrial biomass over this coming century. Estimates range from 5 % if photosynthesis saturates to 42 % if CO_2 fertilisation is maintained (Thompson *et al.*, 2004). Over recent years, it has become evident that carbon capture in the Northern Hemisphere is no longer increasing through the peak of the growing season. Increased summer temperatures and resultant forest drought stress have been provided as an explanation for this (Angert *et al.*, 2005; Bunn 2006) and forests are considered a source of carbon during these summer periods as they are also highly susceptible to fire (Angert *et al.*, 2005). This gives just one example of the complex variables which need consideration when estimating the future changes in atmosphere / biosphere carbon exchange.

1.3 Predicting future terrestrial biomass carbon capture

A classic study, combining both remote estimates of global photosynthetic activity and measurements of atmospheric [CO_2], identified a change in seasonal amplitude of the atmospheric CO_2 draw-down that was associated with increased seasonal photosynthetic activity of the Northern Hemisphere. The implication of this was an increase in the NPP of the Northern Hemisphere during the period of study (1981 and 1991) (Myneni *et al.*, 1997). Too increase the accuracy of predictions for future scenarios of climate change and to improve our understanding of the vegetation atmosphere feedbacks exposure of plants to increased atmospheric CO_2 concentration is carried out. To assess a global phenomenon, the scaling of the experimental approach becomes of paramount importance. In such a complex system, spatial scaling from molecular biology to global ecology, as well as a sufficient temporal scaling are generally required to interpret vegetation responses to carbon dioxide enrichment (Osmond *et al.*, 2004).

1.3.1 Experimental Design

Historically, small scale experiments were often employed to develop an understanding of plant physiological processes occurring in response to changing atmospheric chemistry. For example, senescence was presumed to be advanced due to an earlier shift in plant development in elevated CO_2 under laboratory conditions (Miller *et al.*, 1997); however such results can prove misleading if simply scaled up. Recent evidence from field scale experiments where whole vegetation canopies were exposed to elevated CO_2 through the process of free air carbon dioxide enrichment (FACE) identified a delay in senescence for *Populus tremuloides* (Karnosky *et al.*, 2003) and soybean (Dermody *et al.*, 2006). Körner *et al.* (2005) also identified increased leaf longevity for two (*Fagus sylvatica* and *Carpinus betulus*) of three mature dominant species growing in a Swiss deciduous forest exposed to 540 ppm [CO_2], with the third (*Quercus petracea*) showing decreased leaf longevity. Such results highlight the need for sufficient temporal and spatial scaling for a predictive understanding of future vegetation responses to climatic change. The issue of both spatial and temporal scale is also particularly relevant in accounting for future shifts in biodiversity which may result from climatic changes (Körner 2003).

A loss of photosynthetic potential is often a consequence of long-term growth in elevated CO_2 relative to ambient CO_2 (Curtis and Wang, 1998, Stitt and Krapp, 1999). However, this may not be a genuine response to elevated CO_2, but a feature of smaller scale studies using plants grown in pots which impose root restriction (Curtis and Wang, 1998; Sage 1994). Root restriction causes a change in plant source to sink balance, the balance between carbohydrate production and utilisation. Contrary to this proposed acclimation, the longest term data set of freely rooted field-grown plants (a perennial ryegrass, *Lolium perenne*) shows a sustained average increase in daily integrated C uptake of 36 % over 10 years of exposure to elevated CO_2 (Ainsworth *et al.*, 2003).

1.3.2 Free-Air Carbon dioxide Enrichment (FACE) Experimentation

Over recent years as technology has advanced for subjecting plants to future environments, in particular elevated CO_2, so too has the scale of experimental approaches. The use of Free-Air Carbon dioxide Enrichment technology (FACE) causes a reduction in experimental artefacts that have plagued growth chamber, glasshouse and open-top chamber (OTC) studies. Examples of these artefacts are changes in photon flux, the ratio of diffuse to total solar irradiance, temperature, humidity and wind stress, for example, OTCs are about 2 - 4 °C warmer than the ambient environment (Hendrey and Miglietta, 2006). Experimentally raising atmospheric CO_2 to 550 ppm (a common target value in FACE experiments, table 1.1) from today's ambient concentration of approximately 380 ppm is an increase of 46 % on todays and 96 % on a pre-industrial value. Some authors consider that CO_2 fertilisation of the biosphere may have already peaked following over two centuries of industrial releases of CO_2, and present FACE experiments are reporting responses that are sub-maximal (Körner 2003; Granados and Körner 2002) but relevant for estimating vegetation responses within this century.

The use of FACE technology provides CO_2 enrichment to a field-grown ecosystem of choice. Globally, there are 12 FACE experiments (Hendrey and Miglietta, 2006) and five of these are used for forest tree enrichment, see table 1.1. A system to expose a forest approximately 10 m tall, and containing an overstory of Loblolly pine, to an elevated [CO_2] was developed by Hendrey *et al.,* (1999). This system consists of a 30 m diameter experimental plots each containing 32 vertical pipes through which CO_2 enriched air is released at a pre-mixed desired target concentration using a high volume blower.

Table 1.1: Experimental descriptors of the five global forest FACE sites; adapted from Hendrey and Miglietta, (2006).

FACE site	Alternative name	Location	Target [CO_2] (ppm)	Dominant species	Reference / Web site
BangorFACE		Bangor, UK	580	*Alnus glutinosa* *Betula pendula* *Fagus sylvatica*	bangorface.org.uk
FACTS-I	DukeFACE	Orange County, NC, USA	Ambient +200	*Pinus taeda*	Hendrey *et al.*, 1999
FACTS-II	AspenFACE	Rhinelander, WI, USA	560	*Acer saccharum* March *Betula papyrifera* March *Populus tremulodies*	Karnosky *et al.*, 2003
ORNL FACE	Oak Ridge	Oak Ridge, TN, USA	565	*Liquidambar styracifluca*	Norby *et al.*, 2001
POPFACE EUROFACE	POP / EUROFACE	Viterbo, Italy	550	*Populus alba* *Populus x euramericana* *Populus nigra*	Miglietta *et al.*, 2001

The POP/EUROFACE facility designed by Miglietta *et al.* (2001) (figure 1.1) exposes three 22 m diameter experimental plots of short rotation coppice (SRC) poplar trees reaching a maximum of approximately 12 m in height (M. Liberloo pers. comm.) to elevated atmospheric CO_2. The overarching aims of this experiment are to determine the functional responses of a poplar, agro-forestry system, to actual and future atmospheric CO_2 concentrations, and to quantify carbon uptake, sequestration and loss in a future high CO_2 world. The benefit of this FACE system is that it requires no pre-mixing of CO_2 with air and no blowers for even distribution over the canopy. In this system pure CO_2 is released through holes of 0.3 mm diameter from octagonally arranged pipes enclosing the experimental area. The high velocity of CO_2 release through the small holes causes immediate mixing with ambient air allowing CO_2 enrichment at the desired target concentration of 550 ppm over the experimental plot. As well as reduced infra structure and cost, the absence of blowers in the Miglietta *et al.* system removes a possible confounding factor. Pinter *et al.* (2000) ascribed an observed advancement in senescence of wheat exposed to FACE to be more simply the result of blowers in the FACE facility increasing canopy temperature following night-time CO_2 enrichment. One major drawback of all FACE experiments to date is the consequence of a sudden abrupt change in the concentration of CO_2 exposure and not a gradual increase over time. A gradual increase in

CO_2 up to 550 ppm was shown to affect the mycorrhiza fungal community differently to the abrupt change in exposure typical of FACE experiments. The gradual increase treatment showed no significant changes with the ambient fungal community. In the abrupt change, common to FACE experimentation, a significant decline in mycorrhizal diversity was observed (Klironomos *et al.*, 2005).

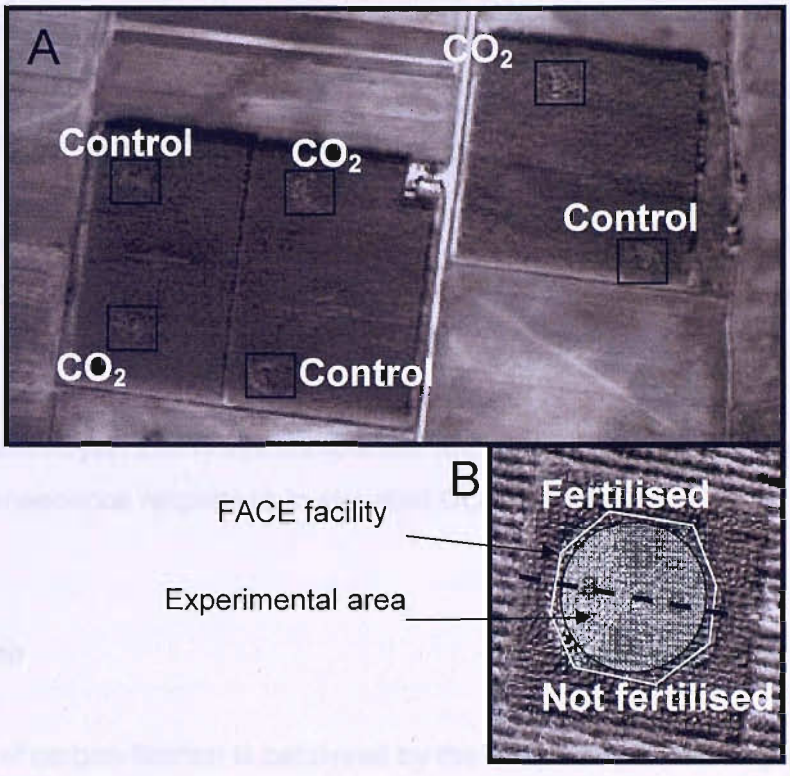

Figure 1.1: (A) The nine hectare POP/EUROFACE plantation. CO_2 represents to location of the FACE experimental plots and control the location of the control plots. (B), an example of one FACE experimental plot showing the location of the three *Populus* species, and the division into sub-plots of different soil nitrogen treatments. Species are labelled a, b and c for *P. alba*, *P. nigra* and *P. x euramericana* respectively. Image (A) was obtained from F. Miglietta and captured on 25.10.04 using a multispectral camera equipped with a single optic operated at three wide bandwidths centred on 550, 680 and 800 nm, mounted on a certified aircraft (Sky Arrow 650TCNS, Rome, Italy). This false colour image was captured using the red (680 nm) and NIR (800 nm) bandwidths and is displayed here in grey scale. Image (B) was taken from from www.unitus.it/euroface

1.4 Physiological responses to elevated atmospheric CO_2 influencing plant C:N balance.

Once the required experimental system has been achieved at the desired level of spatial and temporal scale, probing for vegetation responses to elevated atmospheric [CO_2] can begin. Again, as for experimental design, data acquisition can occur over multiple scales depending upon the nature of the hypothesis been tested. Some examples of scale from the same POP/EUROFACE experimental site are; documenting changes in gene expression (Taylor *et al.,* 2005), leaf level photosynthesis (Calfapietra *et al.,* 2005), leaf carbohydrate fluxes (Davey *et al.*, 2006), biomass production (Liberloo *et al.,* 2006), and modelling of total GPP (Wittig *et al.,* 2005). Plants only directly perceive a change in CO_2 through tissues exposed to the open air, such as guard cells and mesophyll cell walls and the carboxylation of Rubisco in C_3 plants (Long *et al.*, 2006). However gross changes in photosynthesis, respiration and stomatal conductance have all been reported to respond to increasing CO_2 concentration (Drake *et al.*, 1997). A discussion based upon how these three responses may influence autumnal senescence will follow. However, as whole plant nitrogen distribution controls the feedback regulation of photosynthesis via influencing sink activity (Paul and Foyer, 2001) this component will be discussed first as it may underpin many of the senescence responses in elevated CO_2 (Herrick and Thomas, 2003; Wingler *et al.*, 2004).

1.4.1 Rubisco

The initial site of carbon fixation is catalysed by the enzyme Rubisco. At present CO_2 concentrations, Rubisco is not saturated and the rate of carboxylation of Rubisco ($V_{c,max}$) may be considered a rate limiting factor for light saturated photosynthesis (Drake *et al.*, 1997). Rubisco can respond to increasing CO_2 by partitioning carbon flux through the major metabolic pathways of photosynthesis and photorespiration. Increasing [CO_2] increases carboxylation thereby competitively decreasing oxygenation and both these effects increase the rate of photosynthesis (Farquhar *et al.*, 1980). This is because competitive inhibition of carboxylation occurs by oxygenation of Rubisco and drives photorespiration which results in carbon loss and decreases the net efficiency of photosynthesis by between 20 - 40 % (Long *et al.,* 2004). This increase in carbon fixation by suppression of the photorespiratory pathway requires no additional light, water or nutrients, and therefore increases leaf efficiency in every respect (Drake *et al.*, 1997).

Dependent upon the plants internal and external environment, this extra carbon may be assimilated by the plant in the form of increased biomass and this is termed CO_2 fertilisation. However this is not always the case and the plant may acclimate to growth in elevated CO_2 via mechanisms which result in reduced photosynthetic carbon uptake (Curtis and Wang, 1998).

1.4.2 Acclimation of Rubisco to elevated CO_2

A generally consistent feature of acclimation to elevated CO_2 is reduced Rubisco content (Drake *et al.*, 1997, Moore *et al.*, 1999, Stitt, 1991). Long *et al.* (2004) calculated a highly significant reduction in Rubisco content (19 %) with, importantly, a significant increase in light-saturated photosynthesis (A_{sat}) of C_3 plants (34 %). In C_3 plants as much as 75 % of cellular nitrogen (N) is present in the chloroplasts of mesophyll cells with Rubisco representing a major fraction of this leaf N (Hörtensteiner and Feller, 2002). Leaf nitrogen is consistently reduced in elevated CO_2 (Craine and Reich, 2001, Makino and Mae, 1999, Stitt and Krapp, 1999) and rice plants that were grown in elevated CO_2 reallocated N away from leaves to leaf sheaths and roots (Makino *et al.*, 2000). This indicates a possible whole plant regulation of photosynthesis in respect of N allocation that can lead to an increase in N use efficiency (NUE) of plants growing in elevated CO_2 (Stitt and Krapp, 1999). It has also been suggested, that when N is not a limiting resource, a greater photosynthetic rate will be sustained in elevated CO_2 when compared with that in ambient CO_2 (Sage, 1994; Stitt and Krapp, 1999).

1.4.3 Implications from the acclimation responses of Rubisco

The close correlation between carbon and nitrogen signalling in respect of Rubisco content was seen by growing tobacco in elevated CO_2 with N fertilisation. Although the carbohydrate content of leaves increased, there was little loss of Rubisco and no photosynthetic down regulation (Geiger *et al.*, 1999). These observations contradict studies which implicate a build up of soluble sugars in leaves as a cause of Rubisco down regulation and subsequent reduction in photosynthesis (Cheng *et al.*, 1998). It appears that carbohydrate accumulation may, but not always, lead to down regulation of Rubisco. Paul and Foyer (2001) discuss the whole plant C:N balance in response to the whole plant source-sink relationship as applying the principal control over photosynthesis. So it

appears that leaf nitrogen is redistributed in an attempt to optimise the plant C:N balance, and the maintenance of this balance appears implicit in the ability of plants to continually capture carbon in a CO_2-enriched atmosphere. Therefore, when N is limiting, forest carbon capture will become limited (Oren *et al.,* 2001) in an attempt to maintain plant C:N balance.

1.4.4 The whole plant influence on photosynthesis

A description of how the initial site of CO_2 capture (Rubisco) can influence plant response to elevated CO_2 has previously been outlined, and this response appears dependent upon whole plant C:N status. Terashima *et al.* (2005) explain that a mature leaf senses its photosynthetic status by monitoring its sugar concentration. When demand for photosynthate is large, the sugar concentration of this leaf is low, due to vigorous translocation of photosynthate to sink organs (such as expanding leaves, roots and timber), and a high photosynthetic potential exists. Whereas, when demand for photosynthate is low, leaf sugar concentration will rise, and a reduced photosynthetic potential results from a process termed sugar repression of photosynthesis (Koch, 1996). In the review by Koch (1996) the notion of feast and famine responses was put forward. Essentially low sugar status (famine) enhances photosynthesis, reserve mobilisation and export, whereas sugar abundance (feast) promotes growth and carbohydrate storage and down regulates photosynthesis (Koch, 1996).

A leaf can be both a source and sink for photosynthate, depending upon leaf developmental stage. Leaf sugar-associated down regulation of leaf photosynthetic rates, and Rubisco content, was not observed until leaves were more than 60 % expanded (Moore *et al.,* 1999). In Terashima *et al.* (2005) the authors also discuss their unpublished data, which shows that, while leaves are actively expanding, sugar repression of photosynthetic activity does not occur. It could be concluded that expanding leaves, which are sinks for photoassimilate, respond differently in elevated CO_2 than expanded leaves which are generally sources for photoassimilate. This may be exemplified in the biomass response of *Populus deltoides* to growth in elevated CO_2. In a short term experiment carried out in greenhouses on one year old *P. deltoides* saplings, the ratio of expanding to expanded leaves controlled the growth response to elevated CO_2 (Wait *et al.,* 1999). Furthermore, after three years of FACE exposure to elevated CO_2 *P. x euramericana* leaves continued to expand for longer than in ambient CO_2 (Taylor *et al.*, 2003), and also

exhibited increased photosynthetic assimilation (Bernacchi *et al.*, 2003) and above ground biomass (Calfapietra *et al.*, 2003).

Manipulation of plant growth habit has provided good evidence for the influence of sink strength on carbon capture. In determinate plants, the main axis terminates in a floral bud, for example maize and wheat, and in indeterminate plants, e.g. poplar and soybean, buds form in an axillary position. This results in determinate plants having a genetically limited capacity to add new sinks for photosynthate and this determinism is absent in indeterminate plants (Long *et al.*, 2004). Using a single gene mutation, Ainsworth *et al.* (2004) developed a determinate form of soybean from an indeterminate parental genetic source. Both forms showed similar photosynthetic rates in ambient CO_2 conditions but, in elevated CO_2, the determinant form exhibited a large decrease in $V_{c,max}$ while the wild type did not. This highlights evidence that the ability of the plant to utilise increased carbohydrate by the addition of more sinks drives the photosynthetic response and thus the carbon capture ability of the plant in elevated CO_2. This supports the evidence of root restriction in earlier experiments being proposed as a mechanism for the observed down regulation of photosynthesis in elevated CO_2. Therefore, crucial to our understanding of photosynthetic acclimation in elevated CO_2 is an understanding of the leaf photosynthetic processes in relation to whole plant carbohydrate production and utilisation status. By exposing leaflets of soybean plants to a different [CO_2] than the rest of the plant, Sims *et al.* (1998) concluded that whole plant requirement for photosynthate (sink strength) could influence leaf physiology independently of individual leaf carbohydrate status, and that feedback inhibition of photosynthesis is primarily a function of the whole plant environment and is independent of the local CO_2 environment (Sims *et al.*, 1998).

The utilisation of triose phosphates (3C compounds) in end product synthesis (of sucrose, starch and amino acids) is determined by sink requirements and also determines the rate at which inorganic phosphate (Pi) is recycled back to the chloroplast to drive photosynthesis (Paul and Foyer 2001) (see figure 1.2). Shading experiments in Pi-deficient plants (artificially increasing sink demand relative to source supply) can off-set this limitation (Pieters *et al.*, 2001) and so negate photosynthetic down-regulation. One mechanism that may by-pass Pi limitation of photosynthesis is that of starch synthesis. Reduced *Pi* in the chloroplast increases the glycerate-3-phosphate to Pi ratio and so activates ADP-glucose pyrophosphorylase (AGPase), a key enzyme involved in starch

synthesis. This results in increased leaf starch accumulation (Nielsen *et al.,* 1998) and retention of Pi in the chloroplast. By comparing transgenic *Solanum tuberosum* L. (potato) plants that were unable to accumulate leaf starch due to leaf mesophyll-specific antisense expression of *AGPB* a subunit of AGPase, with the wild type. Ludewig *et al.* (1998) concluded that accumulation of starch is not responsible for photosynthetic down regulation and was not accompanied by reduced Rubisco activity. In many species leaf starch may act as a transient sink (Heineke *et al.,* 1999; Paul and Foyer, 2001) reducing end product limitation feedback imposed by poor sink strength. Following three to four years FACE exposure to elevated CO_2 a significant increase in mature leaf starch was evident for both *P. x euramericana* and *P. nigra* trees at the POP/EUROFACE site. This has been proposed as a mechanism by which sugar repression of photosynthesis was avoided and an increased photosynthetic rate attained (Davey *et al.,* 2006).

1.5 Sensing of leaf source:sink status

Carbohydrates such as sucrose or the storage form starch are the end products of photosynthesis. Beginning with the process of glycolysis in the cytosol, these compounds are ultimately oxidised during respiratory metabolism, providing free-energy and ATP for plant maintenance and growth, (Lawlor, 2001). To enter glycolysis sucrose is initially hydrolysed by the family of enzymes known as plant invertases (ß-fructofuranosidase) resulting in the irreversible conversion of sucrose into fructose and glucose (Roitsch and Gonzalez, 2004). An initial step in the process of glycolysis occurs through the reversible phosphorylation of glucose to glucose 6-phosphate (G6P) catalysed by the enzyme hexokinase. Further to entering glycolysis, phosphorylated glucose can also be utilised in the resynthesis of sucrose in a process known as sucrose cycling (figure 1.2). Any relative limitation in leaf sucrose export and utilisation may stimulate this process of sucrose cycling within mesophyll cells of mature leaves initiating a futile cycle of glucose phosphorylation through hexokinase (Moore *et al.,* 1999). The primary carbohydrate signal regulating photosynthesis would be generated by a glucose flux through hexokinase as a result of futile sucrose cycling resulting in photosynthetic down regulation (Moore *et al.,* 1999). In other words, low sucrose export which is considered the consequence of limited sink metabolism, will result in an increase in the futile cycling of sucrose via G6P, which feeds back to regulate photosynthesis by a hexokinase derived signal (figure 1.2). This mechanism has been proposed to regulate the plant source sink balance in elevated CO_2

(Moore *et al.,* 1999) and is strictly dependent upon the developmental stage of the leaf. Actively expanding sink leaves do not respond to sugar repression of photosynthesis (Terashima *et al.,* 2005).

Recent work with *Arabidopsis* has identified signals important in the response of stomata to [CO_2], by which developing leaves respond to the CO_2 environment of mature leaves, independent to the CO_2 environment of the developing leaf (Lake *et al.*, 2001). A systemic CO_2 signal between the source and sink leaves has been proposed by which sink leaves respond to the CO_2 environment of source leaves, and for stomatal development a gene responsible for this signal has been identified (Gray *et al.*, 2000). There is also evidence to suggest that sink leaf carbohydrate status mirrors that of the source leaf so linking photosynthetic response in elevated CO_2 with sink leaf development (Coupe *et al.*, 2006).

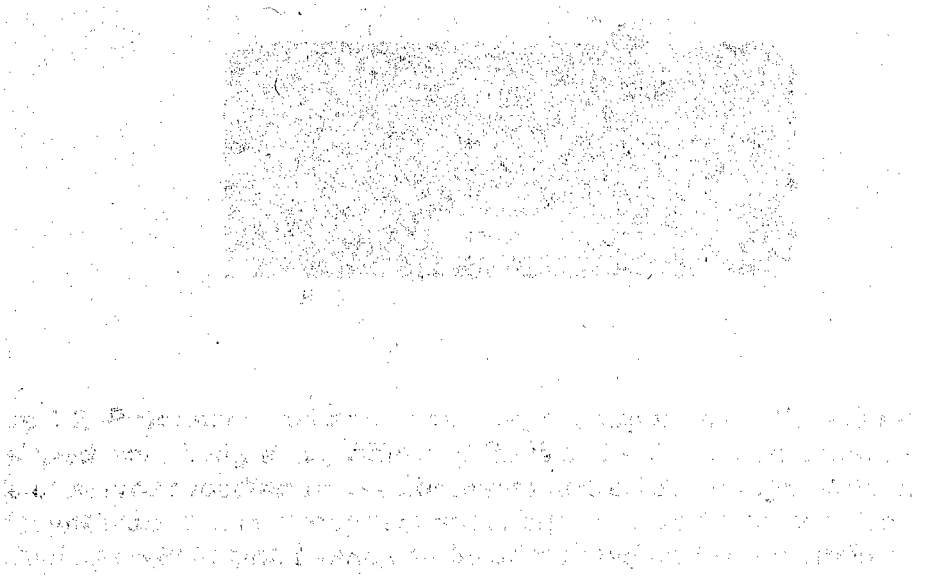

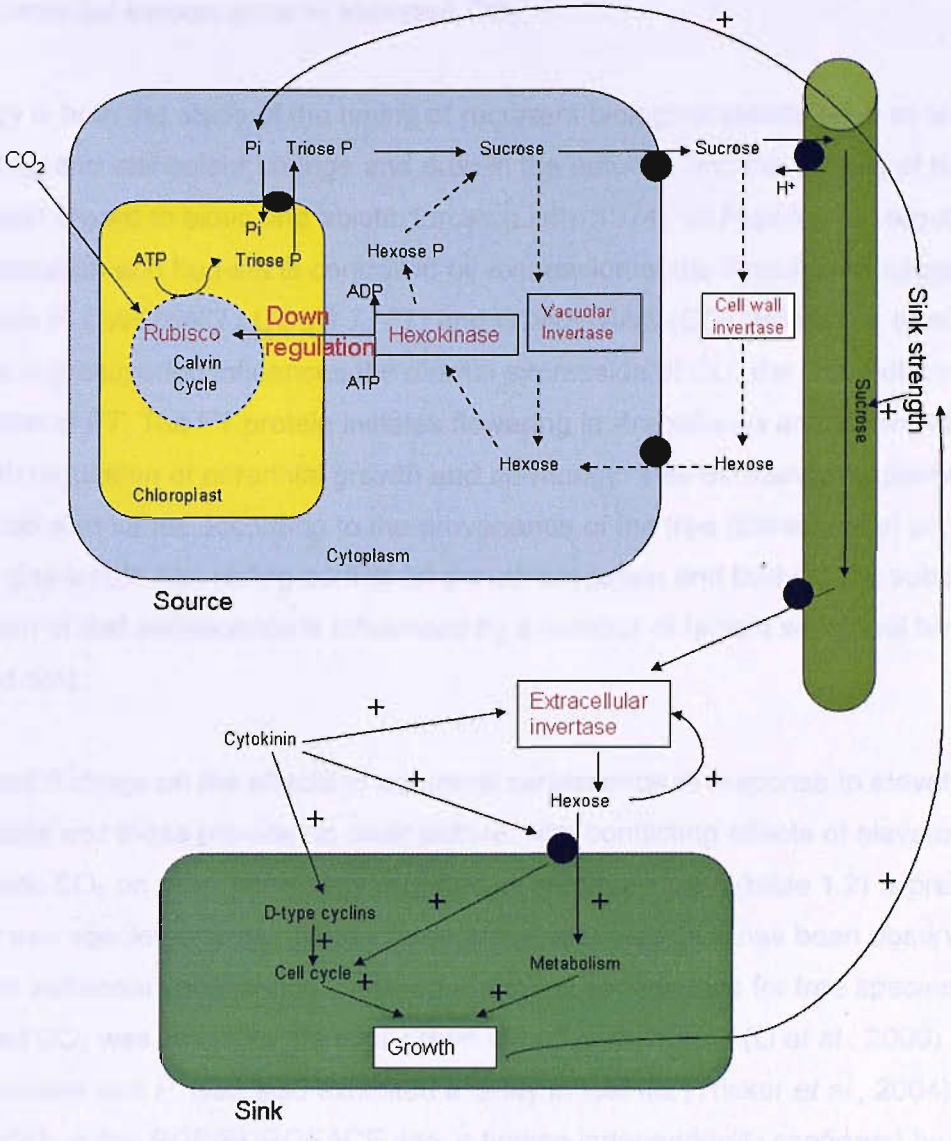

Figure 1.2: Proposed mechanism connecting sugar flux with sink metabolism, *developed from Long et al., 2004 and Roitsch 1999. Dashed arrows represent a futile cycle of sucrose leading to hexokinase-mediated down regulation of photosynthesis if sink strength is not adequate. Solid arrows represent a process by which growth in sink tissue can be stimulated and so maintain sink strength*

1.6 Autumnal senescence in elevated CO_2

Phenology is both the study of the timing of recurrent biological events such as leafing out in the spring and leaf colour change and drop in the autumn, and the causes of these timings, with regard to biotic and abiotic forces (Lieth, 1974). In *Populus* the regulation of growth cessation and bud-set is controlled by expression of the *Populus* orthologs of *Arabidopsis FLOWERING LOCUS T* (*FT*) and *CONSTANS* (*CO*) (Böhlenius *et al.*, 2006). A change in photoperiod influences the diurnal expression of *CO*, the CO protein induces transcription of *FT*. The FT protein initiates flowering in *Arabidopsis* and is involved in the day-length regulation of perennial growth and dormancy. This dormancy response to photoperiod also varies according to the provenance of the tree (Böhlenius *et al.*, 2006). Although day-length has strong control on growth cessation and bud-set the subsequent progression of leaf senescence is influenced by a number of factors which will be discussed next.

Only limited findings on the effects of autumnal senescence in response to elevated CO_2 are available and these provide no clear picture, with conflicting effects of elevated atmospheric CO_2 on plant phenology reported. A summary table (table 1.2) is presented for forest tree species displaying the influence that elevated CO_2 has been observed to have upon autumnal senescence. Delayed autumnal senescence for tree species growing in elevated CO_2 was found for the ever-green *Quercus myrtiifolia* (Li *et al.*, 2000). *Populus* x *euramericana* and *P. alba* also exhibited a delay in leaf fall (Tricker *et al.*, 2004) in elevated CO_2 at the POP/EUROFACE site, a finding independently confirmed by Cotrufo *et al.* (2005) who reported an earlier fall of leaves from ambient CO_2 grown trees. However, no significant effect was apparent on the timing of bud-set in these species (Calfapietra *et al.*, 2003). An increased carbon gain capacity in *Q. rubra* shade leaves was also found during a simulated autumn in elevated CO_2 (Cavender-Bares *et al.*, 2000). In elevated CO_2 advanced senescence was documented for *Pinus sylvestris* (Jach and Ceulemans, 1999) and *Populus trichocarpa* (Sigurdsson, 2001) but this advancement was reduced for *P. trichocarpa* upon application of nitrogen fertiliser (Sigurdsson, 2001).

Table 1.2: The influence of elevated atmospheric [CO_2] on the progression of autumnal senescence for a number of forest tree species.

Species	CO_2 exposure system	Influence of CO_2 on senescence	Reference
L. tulipifera	OTC no irrigation	No effect	Gunderson *et al.*, 1993
P. sylvestris	OTC (forest soil)	Advanced	Jach and Ceulemans, 1999
Q. alba	OTC no irrigation	No effect	Gunderson *et al.*, 1993
Q. myrtiifolia	OTC (forest soil)	Delayed	Li *et al.*, 2000
P. trichocarpa	Whole tree chambers	Advanced	Sigurdsson, 2001
Q. rubra	Glasshouse: Sun leaves Glasshouse: Shade leaves	Advanced Delayed	Cavender-Bares *et al.*, 2000 Cavender-Bares *et al.*, 2000
L. styraciflua	FACE	No effect	Herrick and Thomas, 2003
P. alba, *P. x euramericana*	FACE	Delayed	Tricker *et al.*, 2004
P. tremulodies	FACE	Delayed	Karnosky *et al.*, 2003
P. triocarpa X P. deltoides	OTC	Delayed	Rae *et al.*, 2006
Fagus and Carpinus *Quercus*	WebFACE WebFACe	Delayed Advanced	Körner *et al.*, 2005 Körner *et al.*, 2005

No effect of elevated CO_2 was apparent on *Liquidambar styraciflua* leaf fall, although late season photosynthesis was stimulated in both sun and shade leaves in this indeterminate tree (Herrick and Thomas, 2003). Conflicting results also occur for non-tree species including the determinate species barley (*Hordeum vulgare* L. cv. Alexis) (Fangmeier *et al.,* 2000) and potato (*Solanum tuberosum* L.) which has characteristically very large sink organs, (Miglietta *et al.,* 1998), and showed advanced senescence in elevated CO_2 while C_3 grasses exhibited delayed senescence (Craine and Reich, 2001) as did indeterminate soybean (Miglietta *et al.,* 1993; Dermody *et al.,* 2006). An example of the variability of this senescence response can be seen for *Liquidambar styraciflua* (sweetgum) which shows both no change (Herrick and Thomas, 2003) or advanced senescence (Norby *et al* 2003) in elevated CO_2 at two FACE sites in the USA. In a mixed mature deciduous forest in Switzerland, four years of exposure to elevated CO_2 increased leaf duration of two dominant species (*Fagus sylvatica* and *Carpinus betulus*) by five to six days while the third dominant species (*Quercus petraea*) leaf duration was reduced by five days (Körner *et al.,* 2005).

1.6.1 Leaf economic traits

Generally in elevated CO_2, light-saturated photosynthesis (A_{sat}) is increased and leaf nitrogen is decreased (Long *et al.,* 2004) resulting in increased photosynthetic nitrogen use efficiency (PNUE). This is a well-documented adaptation (Drake *et al.,* 1997; Stitt and Krapp, 1999), which, at the whole stand level, was weakly associated with increased longevity (Reich *et al.,* 1992). Reduced leaf nitrogen on a leaf mass basis is also associated with increased leaf longevity (Reich *et al.,* 1992, 1997), as is reduced specific leaf area ($mm^2\ g^{-1}$) (Reich *et al.,* 1997), which is also often a consequence of growth in elevated CO_2 (Norby *et al.,* 1999). These features, reduced SLA, decreased leaf N on a mass basis and increased leaf longevity, have all been associated with *Populus* exposed to elevated CO_2 for three years using FACE technology (Tricker *et al.,* 2004). To this end the question posed by Hikosaka (2005) "why are there no species that have both high productivity (photosynthetic capacity or high biomass production per unit N in the plant body) and long persistence (leaf life span or mean residence time of nitrogen)" may in some way begin to be answered by elevated CO_2 studies. The reasoning behind the question of Hikosaka (2005) is that the fraction of N partitioned to cell walls resulting in decreasing SLA is at the expense of N allocation to photosynthetic components, so the correlation between decreased SLA and longevity occurs at the expense of photosynthetic capacity. It appears in elevated CO_2 that a leaf with decreased SLA and so increased "toughness" (Hikosaka, 2005) and associated increased longevity (Reich *et al.,* 1997) exists with increased photosynthetic capacity (Long *et al.,* 2004). This could be due to a reduced requirement for nitrogen investment in Rubisco (Makino *et al.,* 2000; Drake *et al.,* 1997). Nitrogen is therefore available to be partitioned to the cell walls with the associated decreased SLA and increased leaf persistence, with no loss in photosynthetic capacity.

Generally the C:N ratio of leaves is increased in elevated CO_2. This is the result of an average increase in soluble sugars and insoluble starch by 20 % and 80 % respectively (Long *et al.,* 2004) and the redistribution of N away from Rubisco to sink organs (Makino *et al.,* 2000). Herrick and Thomas (2003) hypothesize that, for species which show an increased net photosynthesis in elevated CO_2, the increased C:N ratio of such leaves will result in delayed autumnal senescence. In other words in the absence of photosynthetic down-regulation a later season positive leaf carbon balalnce will result in delayed senescence. Whereas, Sigurdsson (2001), suggests that, if N is limiting, an increased C:N

disparity in elevated CO_2 will result in the earlier onset of senescence as a mechanism to balance the C:N disparity through leaf loss and N remobilisation. Therefore, if N is limiting, an increased C:N ratio in leaves growing in elevated CO_2 will result in a homeostatic adjustment through earlier senescence, so reducing the source to sink ratio and thereby remobilising N to re-address the leaf / plant C:N balance. For the ever-green *Q. myrtifolia* Li *et al.* (2000) suggest that a lower leaf N in elevated CO_2 results in less demand for N from older leaves to satisfy the growth of new leaves.

1.6.2 Source / sink balance and carbohydrate flux

The association of sugar flux, hexokinase and senescence was demonstrated when genetically transformed *Arabidopsis* plants over- and under-expressing hexokinase were grown on 3 % glucose and exhibited accelerated and delayed senescence phenotypes respectively (Xiao *et al.,* 2000). Tomato plants also showed accelerated senescence when overexpressing *Arabidopsis* hexokinase-1 (Dai *et al.,* 1999), whereas an *Arabidopsis* mutant lacking hexokinase-1 exhibited delayed senescence (Moore *et al.,* 2003). Wingler *et al.* (2004) documented that *Arabidopsis* plants grown on 2 % glucose and 30 mM N agar exhibited delayed senescence, and for those grown on 2 % glucose with a reduced nutrient (4.7 mM N) agar, senescence was advanced. It was concluded that increased sugar accumulation in the leaves of nitrogen-deficient *Arabidopsis* could be due to decreased sugar utilisation for the synthesis of N demanding amino acids and proteins. This increased ratio of carbohydrate production to carbohydrate utilisation (an increased source to sink ratio) is thought to promote senescence (Pourtau *et al.,* 2004). With sufficient N an increased glucose supply delayed senescence, suggesting that, if balanced by sink activity, an increase at the source can result in delayed senescence.

A consistent feature of growth in elevated CO_2 in FACE experiments is an increase in fine root growth and turnover (Lukac *et al.,* 2003; Norby, 2004). Further to this being a sink for photoassimilate this may be a further adaptation to growth in elevated CO_2 that delays senescence through the increased delivery of cytokinin to leaves (Yong *et al.,* 2000). Maintenance of sink strength has further been implied in the regulation of senescence through the use of shading experiments. When whole plants were shaded (artificially increasing sink:source ratio) senescence was delayed, however, shading of individual leaves or leaf parts advanced their senescence (Weaver and Amasino, 2001).

1.6.3 Reactive oxygen species (ROS).

Reactive oxygen species (ROS) cause cellular damage and death by oxidising proteins, unsaturated fatty acids and DNA. They are involved in leaf senescence (Navabpour *et al.,* 2003), and many other processes such as the hyper-sensitive response and are also cellular signalling molecules. Chloroplasts are considered the site of much ROS generation, the result of the redox reactions in photosynthesis (Lawlor, 2001). In simple terms photosynthesis is the conversion of energy, from a discrete portion of electromagnetic radiation, referred to as the photosynthetically active radiation (PAR electromagnetic radiation existing between 400 and 700 nm), to chemical energy for plant metabolism (Lawlor, 2001). Chlorophylls the initial site of photon energy capture are composed of a hydrophilic porphyrin head of five rings, at the centre of which is a magnesium atom; a long hydrophobic tail anchors the molecule to the hydrophobic portion of a chlorophyll binding protein and to the thylokoid membrane (Mc Donald, 2003). One photon of PAR excites one electron within one chlorophyll molecule to a higher unstable energy state, to re-gain stability this energy has to be lost (Taiz and Zeiger, 2002). In terms of carbon capture this energy is lost in *photochemistry*; it is transferred to the chemical reactions of photosynthesis. When the irradiance environment or leaf physiology are such that more energy is input than is used in photochemistry, this energy can be re-emitted as a photon of light in a process termed *fluorescence* (Horton *et al.,* 1994). A further form of energy dissipation by *non-photochemical quenching* is also carried out by another class of pigments, the carotenoids of the xanthophyll cycle. Under excess light, violaxanthin is rapidly converted to zeaxanthin via antheraxanthin (DemmigAdams and Adams, 1996), the increased number of conjugated C-C bonds in zeaxanthin allows this pigment to accept electrons from excited chlorophyll and dissipate this energy harmlessly as heat. These forms of energy dissipation are required to limit the potentially damaging effect irradiance can have on photosystems through photoinhibition (Long *et al.,* 1994).

Few plants have CO_2 fixation rates high enough to use all of the energy (in the form of excited electrons) in photochemistry (Long *et al.*, 1994). Therefore, alternative electron acceptors other than CO_2 are required and these acceptors can include molecular oxygen. Molecular oxygen as an alternative electron acceptor results in the production of (ROS), such as extremely reactive superoxide radicals and singlet oxygen, and leads to photoinhibition and oxidative stress (Zimmerman and Zentgraf, 2005). In elevated CO_2 with sufficient N an increased potential for photochemistry over that of non-photochemical

energy dissipation was observed for the grass *Dactylis glomerata.* This was explained as the result of an increased requirement for electrons in photochemistry relative to other electron sinks (Hymus *et al.,* 2001). This process may influence senescence by reducing the potential for ROS production, the opposite was observed in elevated CO_2 when N was limiting and photoinhibition was increased (Hymus *et al.,* 2001). *Arabidopsis* mutants *ore1*, *ore3* and *ore9* which exhibit a delay in senescence were also identified as having a greater tolerance to oxidative stress and a close correlation between oxidative stress tolerance and leaf longevity was concluded (Woo *et al.,* 2004). Lifelong exposure of *Quercus pubescens* and *Q. ilex* to elevated CO_2 resulted in a reduction in superoxide dismutase (SOD), an enzyme involved in the removal of ROS. As no reduction in chlorophyll or foliar proteins also occurred, the reduced levels of SOD were concluded as being the result of a decreased intrinsic oxidative stress in elevated CO_2 because of an enhanced assimilation and decreased photorespiration (Schwanz and Polle, 1998). Furthermore, light use efficiency (LUE) calculated as the ratio of above ground biomass per unit of absorbed photosynthetically active radiation (PAR), was increased by between 14 - 28 % across all three poplar species growing in elevated CO_2, at the POP/EUROFACE site (Liberloo *et al.,* 2006). This implied a reduction in photoinhibition as more energy was partitioned to photochemistry. From a synthesis of the four established forest face sites (table 1.1, not including BangorFACE), a universal increase in NPP particularly at lower LAI values was attributed to increased light use efficiency (Norby *et al.,* 2005).

1.6.4 Photorespiration

The contribution that photorespiration may make towards the progression of leaf senescence is complicated to interpret. This is because photorespiration is reported to increase the production of ROS (Zimmerman and Zentgraf, 2005) which may be considered a process to increase the potential for leaf senescence. On the other hand, photorespiration may serve as a mechanism to dissipate excess ATP and NADPH produced when circumstances are such that carbon fixation is not a sufficient sink for these products of the light reactions, thus preventing damage to the photosynthetic apparatus (Taiz and Zieger, 2002). Nevertheless, an increased glycine / serine ratio in pre-senescent *Arabidopsis* leaves was identified as the best metabolite marker for senescence and this high gly/ ser ratio is commonly the result of increased photorespiration (Diaz *et al.,* 2005). The increase in Rubisco carboxylation ($V_{c,max}$) and competitive inhibition of

oxygenation that results in elevated CO_2 reduces photorespiration (Drake et al 1997); this process may affect senescence by influencing ROS production. The converse of this was observed in soybean where experimentally decreasing the CO_2:O_2 ratio resulted in rapid senescence and this was ascribed to increased photorespiration (Widholm and Ogren, 1969).

1.6.5 Stomatal conductance

Reduced stomatal conductance is frequently observed in elevated CO_2 and is considered to persist in the long-term (Bettarini *et al.*, 1998; Tricker *et al.,* 2005). As a result of increased carboxylation efficiency, this effect does not generally result in a decreased A_{sat} (Long *et al.,* 2004) but does increase water use efficiency (WUE) (Tricker *et al.,* 2005). This increased WUE may reduce plant stress, particularly during periods of water deficiency, as implied from observing differing species responses of mature trees following natural drought in the UK (Beerling *et al.,* 1996). Decreased drought stress could influence the timing of autumnal senescence particularly when increased ROS production, associated with drought stress, is considered (Street *et al.,* 2006). The reduced transpiration, per unit leaf area, associated with reduced stomatal conductance may also indirectly result in enhanced canopy temperature as the partitioning of absorbed solar radiation between sensible heat (the heat that is transported from the canopy to the surroundings via conduction, convection or radiation) and evapotranspiration is altered (Sellers, *et al.,* 1996). This temperature response to elevated CO_2 is clearly seen at SoyFACE where a significant increase in temperature by approximately 1 °C was observed in the FACE plots (Long *et al.,* 2006a) and where a delayed senescence was also apparent (Dermody *et al.,* 2006). Reduced stomatal conductance may therefore influence senescence by ameliorating drought stress and changing canopy temperature.

1.7 Identification of genetic responses for tree growth and senescence in elevated CO_2.

As one of a few primary substrates for plant survival, it is not surprising to find that historical changes in atmospheric CO_2 have been a driving force behind plant evolution. Angiosperms first appeared around 140 million years ago during dynamic changes in atmospheric composition and global temperature; within 10 -30 million years of their initial appearance angiosperms dominated the species composition of many flora world wide (Field and Arens, 2005). The initial radiation of angiosperms into pre-existing plant

communities, of which conifers were the dominant gymnosperm, occurred during a transition from icehouse to greenhouse conditions resulting from an abrupt increase in atmospheric CO_2 (Jahren *et al.*, 2000). During the maximal glaciation of the late Pleistocene (18 000 - 20 000 years ago) atmospheric [CO_2] ranged between 180 - 200 ppm (Petit *et al.,* 1999) and most plant species today can be considered to have existed during this time (Ward and Kelly, 2004). Therefore, on this geological time scale, all currently represented species may be presumed to possess the genetic capacity or phenotypic plasticity to respond to changes in atmospheric [CO_2] (Ward and Kelly, 2004). Genetic studies using plants exposed to elevated CO_2 may therefore begin to provide insight into possible pathways and resulting genotypes that favour this environment (Rae *et al.,* 2006; Ward and Kelly, 2004).

Charles Darwin's theory of evolution via natural selection implies a conservation of favourable developmental and metabolic pathways and so the genes encoding these pathways may exist within wide taxonomic groups. This allows for the selection of a number of specifically targeted species (model species) to represent wide taxonomic groups. For example, *Arabidopsis thaliana* (thale cress) was the first plant species selected as a model used to represent plant biology (The *Arabidopsis* Genome Initiative, 2000). However, *Arabidopsis* may not represent tree species, which differ fundamentally in a number of ways such as, a long juvenile stage, long lifespan, dormancy, seasonal senescence and wood production. Poplar is now recognised as a model tree species (Taylor *et al.,* 2002), and the recent sequencing of the poplar genome has shown the value of this, with 5248 of a predicted 45, 555 protein-coding loci in poplar exhibiting no homology/orthology in *Arabidopsis* (approximately 12 % of all predicted genes) (Tuskan *et al.,* 2006).

The recent use of microarray technology can be used to identify changes in gene expression that occur in response to an environmental change. Therefore the genes responsive to this change, and resulting pathways associated with metabolic/ phenotypic changes may be inferred. For example, responses to elevated CO_2 (Taylor *et al.,* 2005), drought (Street *et al.,* 2006), both elevated ozone and elevated CO_2 (Gupta *et al.,* 2005), and natural autumnal senescence (Andersson *et al.,* 2004) have all been studied in *Populus* using microarray technology. The details of microarray technology will be covered in Chapter five of this thesis. Transcript profiling through the use of microarray technology,

offers an unprecedented opportunity for insight into processes such as leaf senescence for which genetic control may be pleiotropic or highly redundant and for which understanding is limited (Andersson *et al.*, 2004 Bhalerao *et al.*, 2003 Buchanan-Wollaston 2003; 2005, Pourtau *et al.*, 2006). However, it is important to keep in mind that typically less than 50 % of protein abundance can be explained by change in mRNA (Feder and Walser, 2005). As Feder and Walser (2005) state "the flip of a coin is more likely to give a prediction of proteome changes to stress than is mRNA abundance". An example of this can be seen in photosynthetic acclimation to elevated CO_2 as a decreased Rubisco protein level does not always correlate with transcript abundance (Moore *et al.*, 1999). To gain an integrated functional understanding of how elevated CO_2 confers the phenotype of interest requires integrating knowledge of the transcriptome, proteome and metabolome (Feder and Walser, 2005), (figure 1.3).

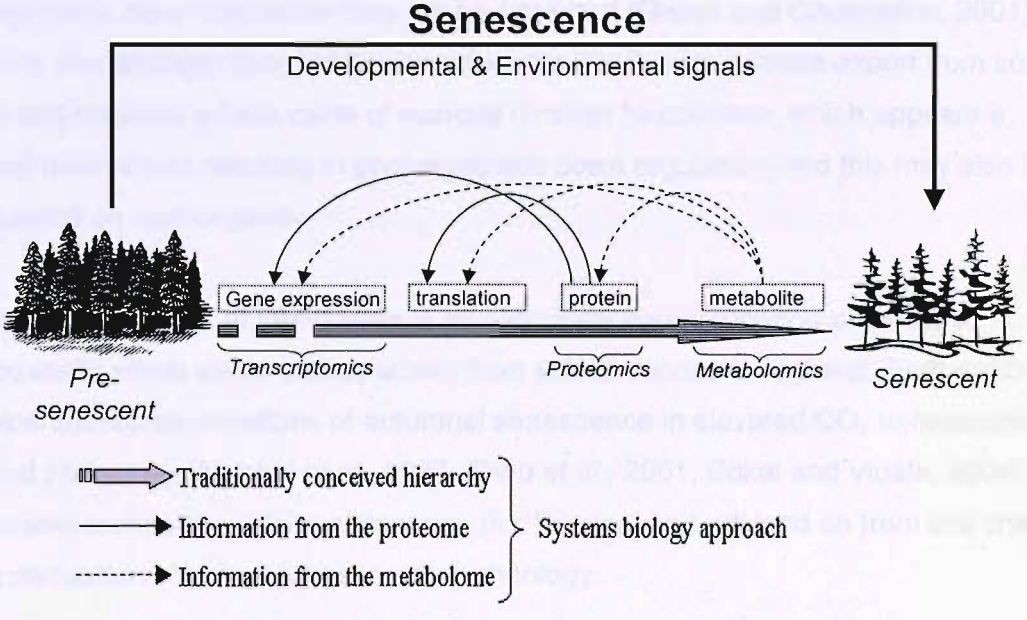

Figure 1.3: Representation of the systems biology approach, identifying processes involved in conferring a phenotypic response. Figure based on an image from Goodacre (2004).

Presently nothing is published concerning transcriptional responses to senescence in elevated CO_2 and, in the absence of any robust targeted hypothesis a microarray approach may be a good starting point. However, this will only be beneficial to our understanding of canopy senescence in elevated CO_2 if the experimental system is ecologically relevant, the gross canopy changes during senescence are well documented and the sampling strategy is representative.

1.8 Summary

Clearly plant growth in elevated CO_2 is influenced by a complex interaction of environmental variables. The use of differing experimental methodologies, such as, irrigation, fertilisation and CO_2 enrichment technology may also confound conclusions relating to the CO_2 response. Plant carbohydrate concentration clearly influences photosynthetic potential and is influenced by atmospheric CO_2. The complex interaction between growth habit and resource availability influences the photosynthetic response to increased atmospheric CO_2, which may be predominantly expressed through a carbohydrate derived signal. These signals are generally considered to be transduced from a carbohydrate flux through hexokinase, as opposed to steady-state levels. Through the complex interaction of sugars with metabolic processes, in those species showing both physiological and morphological plasticity and indeterminate growth habit such as poplar, photosynthetic down regulation may not be expected (Gielen and Ceulemans, 2001). Sufficient sink strength may provide an adequate conduit for sucrose export from source leaves and so avoid a futile cycle of sucrose through hexokinase, which appears a principal mechanism resulting in photosynthetic down regulation, and this may also impart an influence on leaf longevity.

Autumnal senescence of forest trees is an extremely heterogeneous process, a heterogeneity which exists across scales from leaf to canopy to regional. Furthermore, to link experimental observations of autumnal senescence in elevated CO_2 to measurements of global phenology (Myneni *et al.,* 1997; Zhou *et al.,* 2001; Sökal and Vidale, 2004) a comparable technology will be necessary. For this reason I will lead on from this chapter with a discussion about remote sensing technology.

1.9 Reflectance based estimates of vegetation characteristics

The technology behind reflectance based remote sensing of vegetation allows for spatial sampling over multiple scales from the leaf to the canopy and up to global monitoring. For example, in the case of satellite-based sensors, the Medium Resolution Imaging Spectrometer (MERIS) sensor onboard the ENVISAT satellite will provide global coverage at a spatial resolution of 300 m every three days. The discrete band-widths of spectra taken by this sensor can accurately represent chlorophyll content, in the form of the MERIS Terrestrial Chlorophyll Index (MTCI) (Dash and Curran, 2004). The Advanced Very High Resolution Radiometer (AVHRR) on board the NOAA satellite samples spectra which are related to LAI, the fraction of absorbed PAR (FPAR) and chlorophyll content. This is commonly used to estimate global phenology, via calculations of Normalised Difference Vegetation Index (NDVI) (Zhou et al., 2001) (see page34). However, NDVI has proved less sensitive to estimate the high chlorophyll content commonly found in forests and MTCI was considered superior (Dash and Curran, 2004). In this section of Chapter one a short review of the non-destructive sampling of vegetation characteristics, by remote sensing, will be presented. This review will first consider the biophysical processes leading to vegetation-specific reflectance spectra and then follow with a discussion identifying what knowledge can be gained from such spectra. It will become apparent that leaf chlorophyll content and green leaf area index are readily identifiable using reflectance spectroscopy. With chlorophyll content influencing canopy spectral reflectance and being a marker for senescence (Buchanan-Wollaston, *et al.,* 2003), reflectance spectroscopy is a technique used to monitor senescence and growing season duration from the leaf (Merzlyak *et al.,* 1999) to the global (Zhou *et al.,* 2001) scale.

1.9.1 A very brief introduction to electromagnetic radiation

In the 1600s Sir Isaac Newton demonstrated that white light is composed of a spectrum of visible colours, and proposed that light was made up of tiny particles (corpuscles). Following this discovery the nature of electromagnetic radiation has been debated between a particle theory and a wave theory. Generally electromagnetic radiation is considered to show dual properties of both waves and particles, and in this model a wave consists of discrete units called photons (McDonald, 2003). The energy present in a photon (the quanta) is equal to a constant (*h*) (Plank`s constant 6.62x 10^{-34} J s) x the

frequency of the wave. As the frequency of a wave is equal to another constant (*c*) (the speed of light) divided by the wavelength, then, in simple terms the energy present in a photon can be considered inversely proportional to the wavelength (McDonald, 2003).

1.9.2 Photosynthesis and electromagnetic radiation

The energy present in PAR (also know as visible light) ranges from 290 kJ mol^{-1} - 184 kJ mol^{-1}, (mean for violet 400-425 nm to mean for red 640-700 nm, respectively) (McDonald, 2003). Irradiance of longer wavelengths than the visible, the near infrared irradiance (NIR) (> 740 nm), has less energy (85 kJ mol^{-1}) and this energy is insufficient to be involved in the REDOX reactions of photosynthesis (McDonald, 2003). The energy in NIR has the detrimental influence of imparting a large heat load on the leaf and so is scattered and strongly reflected by the spongy mesophyll cells of a healthy leaf (Jenssens, 2000) (figure 1.4). This gives rise to the characteristic "red-edge" associated with reflectance spectra of green vegetation (Penuelas and Filella, 1998) (figure 1.5). Reflectance around this red edge feature has been used to characterise gross photosynthetic trends and identified a general increased photosynthetic activity for large portions of the Northern Hemisphere between 1982 - 1999 (Slayback *et al.,* 2003).

Approximately 90 % of the intercepted incident radiation in the PAR region is absorbed by plant pigments, the remainder is either reflected or transmitted through the leaf (Jones, 1993) (figure 1.5). Numerous pigments with overlapping absorption spectra are responsible for absorption in the PAR region with the greatest portion being absorbed by chlorophylls a and b and the carotenoids (Blackburn, 1998). Chlorophyll a absorbs maximally at wavelengths centred on 430 and 660 nm and chlorophyll b peaks at 450 and 650 nm (Jensen, 2000). The former absorption band of both chlorophylls is in the blue region of the spectrum with the latter in the red.

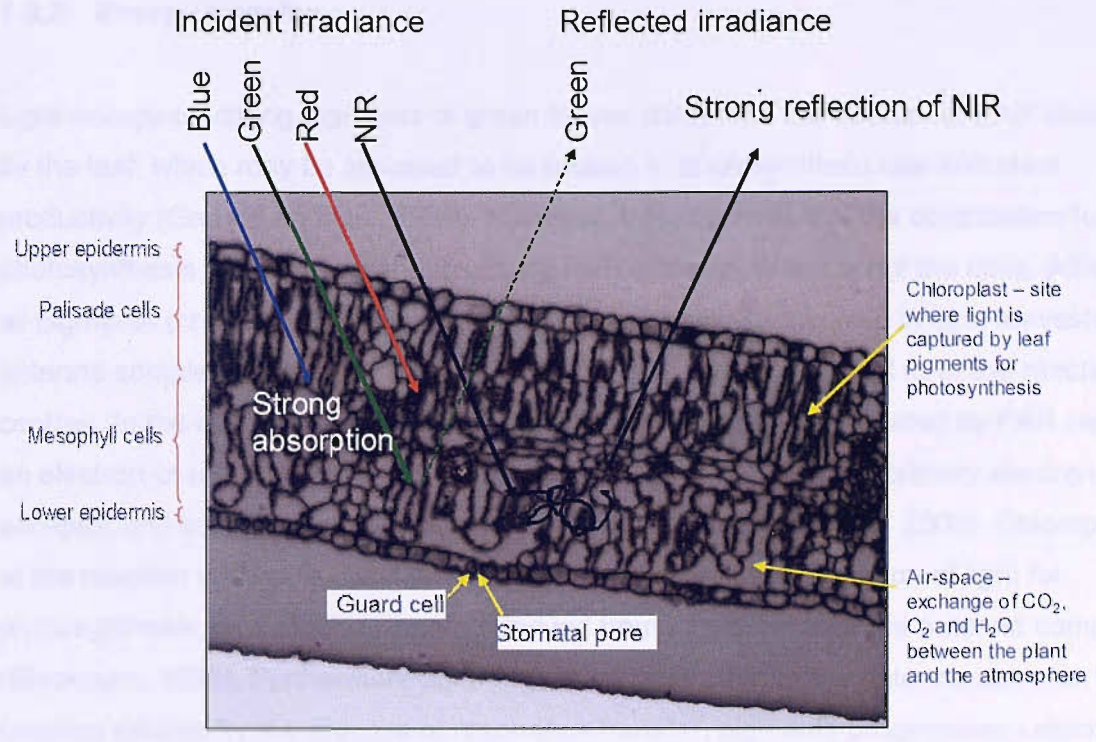

Figure 1.4: A cross section of a P. deltoides leaf showing cellular and organelle interactions with electromagnetic radiation in the visible and near infrared (NIR) portion of the spectrum.

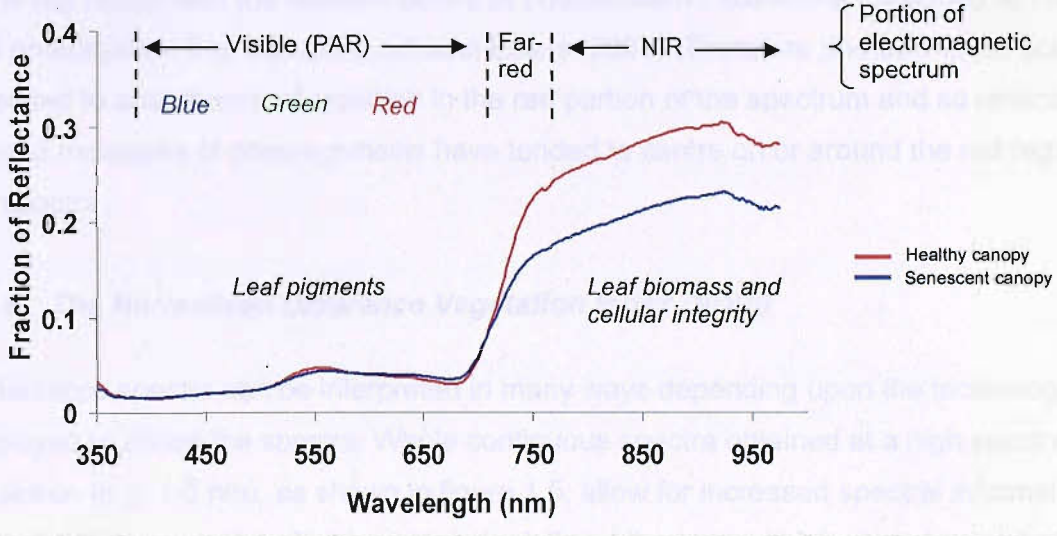

Figure 1.5: An example of the reflectance spectra obtained above the canopy of *P. x euramericana* at EUROFACE 2004, using a GER 3700 with a 23 ° field of view fibre optic. The spectra of both a healthy and more senescent canopy are shown and so are the dominant canopy components that influence the reflectance spectra.

1.9.3 Energy transfer

Light energy-capturing pigments of green leaves determine the amount of PAR absorbed by the leaf, which may be assumed to be related to photosynthetic rate and plant productivity (Gamon and Qiu, 1999). However, this assumes that the contribution to photosynthesis of each pigment absorbing PAR is equal, which is not the case. Although all pigments (chlorophylls and carotenoids) form a complex involved in light harvesting (the antenna complex), it is a specific pair of chlorophyll a molecules that form the reaction centres. In the reaction centres, the excitation energy (initially generated by PAR raising an electron of a pigment to a higher energy level) is donated to the primary electron acceptor and the light reactions of photosynthesis begin (McDonald, 2003). Chlorophyll a at the reaction centres is considered the limiting factor in the utilisation of light for photosynthesis, as it receives energy derived from all pigments of the antenna complex (Blackburn, 1998). Furthermore as energy is transferred from the antenna complex to the reaction centres by the process of resonance transfer, pigments progressively absorb at a longer wavelength and therefore lower energy. This has the outcome of decreasing the probability of reverse energy transfer away from the reaction centres as an energy input would be required (Taiz and Zeiger, 2002). As such, the reaction centres maximally absorb in the red region with the reaction centre of photosystem I absorbing maximally at 700 nm and photosystem II at 680 nm (Lack and Evans, 2001). Therefore photosynthetic potential is related to absorbance of radiation in the red portion of the spectrum and so reflectance-derived measures of photosynthesis have tended to centre on or around the red region of the spectra.

1.9.4 The Normalised Difference Vegetation Index (NDVI)

Reflectance spectra can be interpreted in many ways depending upon the technology employed to obtain the spectra. Whole continuous spectra obtained at a high spectral resolution (e.g. 1-3 nm), as shown in figure 1.5, allow for increased spectral information normally at the expense of high spatial resolution. However, at high spatial resolution, global level satellite-based radiometers sample discrete wide wave bands (Plummer *et al.*, 1995), from which vegetation indices of spectral reflectance are often calculated. In general most spectral measures of vegetation pigmentation are based around the sharp

transition between reflectance of red and near infrared radiation (Penuelas and Filella, 1998).

The amount of absorbed PAR (APAR) has been related to net primary production (NPP) via a light use efficiency (LUE) conversion factor (ε), a coefficient defining the carbon fixed per unit radiation intercepted for unstressed vegetation (Monteith, 1977). However LUE is regulated by temperature, water, [CO_2], nutrient availability, growth stage and pathogens creating large variations in (ε) and thus complicating estimates of NPP (Dawson *et al.,* 2003). Nevertheless indices calculated from remote measurements of reflectance, such as the normalised difference vegetation index (NDVI), provide a global method to estimate NPP when factors such as water availability and temperature are taken into account (Field *et al.* 1998).

The simple ratio (SR) (*ii*) described as the first true vegetation index (Jensens, 2000) gives a ratio of the NIR : red reflectance. From the leaf properties discussed above it can be seen that abundant green tissue has a low red and high near IR reflectance so a high value of SR.

(*ii*) $SR = \frac{R_{NIR}}{R_{Red}}$ (*iii*) $NDVI = \frac{R_{NIR} - R_{Red}}{R_{NIR} + R_{Red}}$

Where R_{NIR} and R_{Red} are reflectances in NIR and red wavelengths respectively.

The Normalised Difference Vegetation Index (NDVI) (*iii*) is a means of calculating the contrast between the red and near IR reflection of solar radiation, which is characteristic of vegetation and has superseded the SR. Such data have been strongly correlated with the fraction of PAR (FPAR) intercepted by canopies (Myneni *et al.,* 1997).

1.10 General summary

At multiple scales, from leaf to canopy to global, the interaction between vegetation and electromagnetic radiation is measurable using optical sensors. This interaction is dominated by leaf structure and pigments. Autumnal senescence in deciduous trees is characterised by changes in the colouration of leaves which reflects chlorophyll loss, a process monitored globally using remote sensing technology, providing evidence for extended growing seasons (Zhou *et al.,* 2001). Applied at variable spatial and temporal scales, this technology has the potential to measure the highly heterogeneous process of senescence. This heterogeneity must be correctly represented in measurements if the process of senescence is to be accurately measured. It is therefore considered that remote sensing technology could provide a complement to the techniques employed in measuring the influence elevated atmospheric CO_2 has on autumnal senescence.

1.11 Aims and objectives

The objectives of this thesis are to monitor the progression of autumnal senescence in a short rotation poplar plantation exposed to elevated atmospheric CO_2. Earlier work attempting to quantify the influence elevated atmospheric CO_2 has on forest tree autumnal senescence has generally been carried out the individual leaf level. At this level measurements of chlorophyll content and gas exchange were generally used to estimate changes in whole canopy senescence. Autumnal senescence is associated with a high degree of within canopy variability for leaf chlorophyll content and leaf gas exchange. Therefore the principal objective of this thesis is to obtain data across the multiple scales from the whole canopy, to the individual leaf to cellular gene expression.

The aims are therefore:

- To identify a suitable approach to monitor autumnal senescence at the whole canopy scale. Therefore identifying, at the whole canopy scale, the influence that an elevated atmospheric [CO_2] has on autumnal senescence.
- To calibrate these canopy scale measurements of autumnal senescence with changes occurring at the individual leaf scale. Therefore identifying individual leaves that best represent the changes of the whole canopy, and further identifying leaf level processes that may contribute to the canopy scale findings.
- To carry out a microarray analysis of the indivdual leaves. Therefore identifying changes in gene expression occurring during autumnal senescence. In particular attempt to identify genes that appear responsive to an elevated atmospheric [CO_2] that could contribute to the findings at larger experimental scales.

Chapter 2:

Non-destructive estimates of *Populus* leaf pigment content and the influence of leaf contact irradiance

2.1 Overview

In this chapter non-destructive estimates of leaf pigment content will be determined using spectral reflectance. As declining leaf chlorophyll content is considered a symptom of leaf senescence (Buchanan-Wollaston *et al.,* 2003) then an accurate estimate of leaf chlorophyll content will be informative in understanding the progression of autumnal senescence. A non-destructive estimate of leaf carotenoid content will also be determined because of the photoprotective role these pigments provide, particularly so as chlorophyll levels decline during autumnal senescence (Merzlyak *et al.,* 1999).

Reflectance-based estimates of leaf pigment content can only provide relative values that may be influenced by inter-species leaf properties and environmental variables. Therefore it is important to calibrate these estimates with chemically-extracted leaf pigments from the species in question, obtaining a calibrated non-destructive estimate of leaf pigment content. A calibration equation can then be obtained from the regression between the non-destructive estimates and quantified extracted leaf pigment. In this chapter chemically-extracted leaf chlorophyll and total carotenoid content will be correlated with spectral reflectance indices. Chlorophyll content data obtained using commercially available leaf chlorophyll content meters are reported to be influenced by the leaf irradiance environment (Hoel and Solhaug, 1998). The influence of leaf-contact irradiance upon spectral indices will also be explored, and any possible error in calibration will be discussed.

2.2 Introduction

Chloroplasts are the sites where light capture by pigments, predominantly chlorophyll, drives carbon assimilation (Lawlor, 2001). The amount of chlorophyll in a leaf can give indirect information on leaf nutrient status (Gitelson *et al.,* 2003), stress physiology (Carter and Knapp, 2001) and the progression of autumnal senescence (Buchanan-Wollaston *et al.,* 2003; Keskitalo *et al.,* 2005). Therefore, accurate quantification of chlorophyll content can be used to produce an indicator of vegetation condition, yield potential and phenology.

When plants are exposed to higher levels of irradiance than those required by photosynthesis, chloroplasts may be damaged in a process termed photoinhibition (Long *et al.,* 1994). To overcome this damage plants have evolved several protective mechanisms such as energy dissipation through pigments of the xanthophyll cycle (Demmig-Adams and Adams, 1996) and chlorophyll fluorescence (Horton *et al.,* 1994). The level of irradiance incident on a leaf surface can also influence the amount and distribution of chloroplasts within that leaf (Wada *et al.,* 2003). This is considered a further protective mechanism, which involves the relocation of chloroplasts from the periclinal upper cell surface to the anticlinal cell walls, so reducing the area available for light capture (Kasahara *et al.,* 2002). These photorelocations are present among a wide range of taxa including algae, mosses and vascular plants (Haupt and Scheuerlein, 1990). *Arabidopsis* mutants defective in the gene for phototropin2 (*phot2-1*, a blue-light receptor), exhibited no chloroplast avoidance response. The transmittance of white-light through leaves of these mutant plants did not change with increasing light intensity. However, in the wild-type plants as light intensity increased the amount transmitted through the leaf also increased in response to chloroplast avoidance. The maximum chloroplast avoidance response occured in *Arabidopsis* at 500 μmol m^{-2} s^{-1} of white light and is a response considered important for plant survival (Kasahara *et al.,* 2002). This process is also apparent in natural field conditions in which chloroplasts were reported to be in motion most of the time during daylight hours (Williams *et al.,* 2003). This photorelocation process explains the under-estimation of chlorophyll content at high levels of irradiance using a hand-held chlorophyll content meter (Soil Plant Analysis Development, SPAD). Hoel and Solhaug (1998) reported an 8 - 15 % decline in SPAD values under high irradiance relative to low.

Plant growth environment and species differences are well documented to influence leaf spectral properties (Billings and Morris, 1951; Knapp and Carter, 1998); however, short term changes to irradiance have not been addressed. In this chapter it is hypothesised that when leaves are exposed to increasing low levels of irradiance (approximately 0 - 20 µmol s^{-1} m^{-2} up to 300 µmol s^{-1} m^{-2}) short term physiological mechanisms such as chloroplast avoidance may influence spectral properties in the red region.

Although, irradiance levels for remote sensing measurements, under natural light conditions, range between 1500 - 2000 µmol m^{-2} s^{-1}. The levels used in the research presented here ranged between 0 µmol m^{-2} s^{-1} and 300 µmol m^{-2} s^{-1}. These levels were chosen because this was; (1) within the maximum range predicted for chloroplast avoidance, (2) not associated with a temperature change between low and medium irradiance although an increase of 1 °C was noted for high irradiance environment (3) unlikely to affect the chlorophyll content (the co-variate) a pre-requisite for analysis of covariance (ANCOVA) (Underwood, 1997), and (4) this range in irradiance was similar to that used when identifying the influence of irradiance on SPAD estimates (5 - 250 µmol m^{-2} s^{-1}, Hoel and Solhaugh, 1998). These four features allow the testing of the hypothesis that short term physiological responses to irradiance may influence spectral estimates of leaf chlorophyll content.

Importantly, a comparison between reflectance-based spectral indices and identification of those indices showing the strongest correlation with leaf chlorophyll content will be carried out. As will the identification of a reflectance estimate of total leaf carotenoid content.

2.3 Materials and methods

2.3.1 Leaf material

Recently planted cuttings of poplar (*P. deltoides*) were grown in individual pots in a greenhouse (maximum temperature 20°C, minimum temperature 12°C and day light duration 16 hours) to a size for which no shading of the lower canopy was evident (approx 50 - 70 cm). A visibly wide range of leaf greenness existed between plants and those representing this range were selected. Eleven trees across this range were subjected to three levels of irradiance treatment each for two hours: 300 µmol m^2 s^{-1} of PAR referred to as high irradiance, 150 µmol s^{-1} m^{-2} referred to as medium irradiance and 0-20 µmol s^{-1} m^{-2} referred to as low irradiance. The irradiance treatment was given by manipulating canopy position under the growth lamps present in the greenhouse (400 W Son-T bulbs, OSRAM, Germany) and PPFD was measured using a PAR light meter (LI-250, *LI-COR*, Inc., Nebraska, USA). Following each irradiance treatment, one leaf from each of the eleven poplar trees was selected and three 22 mm diameter leaf discs were removed per leaf. As leaf maturity may influence spectral properties due to mesophyll differentiation, leaves from between the sixth and eighth node down the stem from the first fully unfurled leaf near the apical bud were selected and these leaves were considered to have a fully differentiated mesophyll (Rodriguez-Acosta pers. comm.2005). Leaves within this age range were randomly selected for each irradiance treatment. A total of 33 discs from each irradiance treatment were examined; both spectral reflectance and chlorophyll content meters were used to estimate the chlorophyll content of the disc, and the chlorophyll of the disc was then chemically extracted and quantified spectrophotometrically.

2.3.2 Hand-held chlorophyll content meters

After each irradiance treatment, three leaves per tree were selected and chlorophyll content estimated using two hand-held chlorophyll content meters. One measurement per leaf was taken with the Chlorophyll Content Meter 200 (CCM-200, Opti-Sciences, MA. USA). A further chlorophyll estimate was taken using the SPAD-502 (Minolta Camera Co., Osaka, Japan) however, due to the smaller sampling area of the SPAD-502 10 replicate measures were taken and the mean calculated to represent the area measured by the CCM-200.

The CCM-200 has a 0.71 cm^2 sampling area and estimates chlorophyll content by measuring the absorbance of red (centred on 660 nm) and NIR (centred on 940 nm) light. The SPAD-502 is essentially the same but the sampling area is 0.06 cm^2 and the measure of red absorbance is centred on 650 nm (Richardson *et al.,* 2002). Immediately following each leaf measurement with the CCM-200 and SPAD-502, the portion of leaf containing the area measured was removed and spectral reflectance of the disc was measured using the GER 1500. Each disc was visually homogeneous for green colouration within disc, but between leaves a large heterogeneity of greenness was observed. Finally the leaf disc was placed in 1 ml of DMF (N, N-dimethylformamide; analytical grade; Fisher Scientific) to allow a spectrophotometric estimate of extracted chlorophyll content.

2.3.3 Spectral measurements

Spectral reflectance was measured using a GER-1500 field spectrometer; this sensor acquires data over 350 nm – 1050 nm with a sampling bandwidth of 1.5 nm and a resolution of 3 nm (GER, Buffalo, NY, USA. Mod. 1500). The GER 1500 was used with a 4° field-of-view (FOV) lens and each leaf disc was placed directly below this lens on a platform covered with a black cloth used to minimise background reflectance. The focal length was calculated such that the instantaneous field-of-view (IFOV) of the sensor lay well within the perimeter of the disc and three technical replicate spectral reflectance measurements were taken per disc. An artificial light source, a 1 kW video lamp, was used as the source of illumination for all spectral measurements and it was placed at a zenith angle of 10°. All spectral reflectance measurements were acquired under this same background irradiance within approximately one minute after leaf removal from the treatment irradiance. The radiance of each disc recorded by the GER-1500 was converted to absolute reflectance. This was done by taking the ratio of the target (leaf) with the reference spectral data obtained by measuring radiance from a pure white reflectance panel, for which reflectance is > 99 % between 400 -1500 nm (Spectrolon., Labsphere). A correction was then applied using a calibration specific to that reference-panel (Maclellan *et al.*, 2006); this correction was carried out by Dr. J. Dash (Dept. Geography, University of Southampton).

For each disc, five indices (*ii* - *vi*) reported to represent leaf chlorophyll content were correlated with extracted leaf chlorophyll content and two indices (*vii-viii*) documented to represent leaf carotenoid content were correlated with extracted leaf carotenoid content.

1. The Simple Ratio (SR) (Jensens 2000)

$$SR = \frac{R_{800}}{R_{680}} \quad (ii)$$

Where R_{800} and R_{680} are reflectances in NIR and red wavelengths respectively.

2. Normalised Difference Vegetation Index ($NDVI_{680}$) (Sims and Gammon, 2002)

$$NDVI = \frac{R_{800} - R_{680}}{R_{800} + R_{R680}} \quad (iii)$$

Where R_{800} and R_{680} are reflectances in NIR and red wavelengths respectively.

3. A chlorophyll specific Normalised Difference Vegetation Index the modified NDVI (MNDVI) (Gitelson and Merzlayk, 1994)

$$\text{Modified NDVI (MNDVI)} = \frac{R_{750} - R_{705}}{R_{750} + R_{705}} \quad (iv)$$

Where R_{750} and R_{705} are reflectances in NIR and red wavelengths respectively.

4. Red edge position (REP) estimated using the maximum of the first derivative of the reflectance spectra (D_λ), and then identified as the wavelength (between 680 - 740 nm) at which the maximum derivative value exists (Dawson and Curran, 1998).

$$D_{\lambda(i)} = \frac{R_{\lambda(i)} - R_{\lambda(i-1)}}{\Delta\lambda} \quad (v)$$

Where, $R_{\lambda(i)}$ and $R_{\lambda(i-1)}$ are reflectances at wavelength i, and i-1, respectively.

5. Red edge position (REP) estimated using the first derivative reflectance spectra smoothed to 3 nm and then identified as the wavelength (between 680 - 740 nm) at which the maximum value of this smoothed data exists (*vi*)

6. The Photochemical reflectance index (PRI) (Gamon *et al.*, 1997).

$$\text{PRI} = \frac{R_{531} - R_{570}}{R_{531} + R_{570}} \qquad (vii)$$

where R_{531} is reflectance at a wavelength sensitive to changes in the xanthophyll epoxidation state (ie changes between violaxanthin and zeaxanthin) and R_{570} is reference reflectance of a wavelength unaffected by xanthophyll activity. By measuring changes in xanthophyll activity the PRI has been described as a reflectance assessment of light use efficiency (LUE) (Gamon *et al.,* 1997). As well as estimating LUE, the PRI has also been reported to effectively predict chlorophyll to carotenoid ratio (Guo and Trotter, 2004).

7. The Plant senescence reflectance index (PSRI) , an index designed to specifically measure leaf carotenoid to chlorophyll ratio, (Merzlyak *et al.,* 1999)

$$\text{PSRI} = \frac{R_{678} - R_{500}}{R_{750}} \qquad (viii)$$

where R_{678} is reflectance in a wavelength sensitive to chlorophyll absorbance, R_{500} is reflectance in a wavelength sensitive to carotenoid absorbance and R_{750} is considered outside pigment influence and so used for normalizing, as for the MNDVI.

8. Based on the logical assumption that reflection of PAR is dominated by combined absorption of chlorophylls *a*, *b* and total carotenoids, a further carotenoid reflectance index (*ix*) was developed using two functions: the total reflectance of PAR and the reflectance index exhibiting the strongest correlation with leaf chlorophyll content. Total reflectance of PAR can be considered as inversely proportional to total PAR-absorbing pigment content, and this value divided by chlorophyll content should therefore respond inversely with total leaf carotenoid content. Based upon these assumptions the most effective carotenoid content index for poplar was calculated as:

$$\text{Carotenoid Index} = \frac{R_{500-680}}{MNDVI} \qquad (ix)$$

where $R_{500-680}$ is the sum of the reflectance between 500 nm and 680 nm and MNDVI is the modified normalized difference vegetation index (*iv*)

2.3.4 *Analysis of the spectrum (400 - 800 nm)*

To visually identify any spectral features relating to irradiance treatment that may be obscured or lost when spectra are condensed to a usable informative index, spectra were grouped as high or low with respect to chlorophyll content. High chlorophyll content were identified as leaves containing greater than 500 mg m^{-2} chlorophyll for which high and medium irradiance n = 11 and low irradiance n =6. Low chlorophyll content leaves were those containing between 10 - 50 mg m^{-2} chlorophyll for which high and medium irradiance n = 11 and for low n = 8

2.3.5 *Estimating chemically-extractable leaf chlorophyll content*

Immediately following the spectral measurement, discs were placed in 1 ml of DMF (N, N-dimethylformamide; analytical grade; Fisher Scientific). DMF is a superior solvent to others, such as acetone, for the purposes of chlorophyll extraction, as it overcomes problems such as incomplete extraction and variable evaporation during processes such as maceration, centrifugation, filtration and spectrophotometric analysis (Wellburn, 1994). Direct leaf immersion in DMF resulted in equally efficient chlorophyll extraction as pre-grinding the leaf and then immersing (Moran and Porath, 1980). Therefore, leaf discs were left immersed in DMF and kept at 4 °C in the dark for at least 48 hrs for the extraction of leaf pigments. Each sample was diluted 1:12 with DMF to fall within the sensitive linear range of the spectrophotometer. Diluted sample (1 ml) was placed in a quartz cuvette of 10 mm path length and 1 ml of DMF was placed in an identical cuvette as a blank. The mean of the three technical replicate dilutions for each biological sample was used to represent the pigment content within that sample. Chlorophyll and carotenoid content was determined by measuring absorbance at 664, 647 and 480 nm using a spectrophotometer (U-2000 Hitachi) and calculated using the specific extinction coefficients described in Wellburn (1994) for a spectrophotometer of 1 - 4 nm resolution range.

Chlorophyll *a* (Chl *a*) $= 11.65*A_{664}-2.69*A_{647}$ (*x*)

Chlorophyll *b* (Chl *b*) $= 20.81*A_{647} - 4.53*A_{664}$ (*xi*)

Total carotenoids (car) $= \frac{1000A_{480} - 0.89(\text{Chl a}) - 52.02(\text{Chl b})}{245}$ (*xii*)

With a known sample area (380 mm^2) chlorophyll content was expressed as mg m^{-2}.

2.3.6 Data analysis

Linear regression was used to identify the goodness of fit for the correlation between extracted leaf chlorophyll content (the independent *X* axis variable) and each different non-destructive estimate of chlorophyll content (the dependent or response *Y* axis variable). This same approach was also used to identify spectral estimates of leaf carotenoid content. Linear regression was applied across all irradiance treatments, then to each irradiance treatment independently, in order to identify any influence irradiance may have upon the strength of the correlation between remotely sensed index and chlorophyll content. Two outliers were removed, the result of atypical spectral data, within the medium irradiance treatment (n = 31). To fit the curvilinear response of SR and NDVI to the linear model used, a transformation was carried out by taking the $\log_e$ of the chlorophyll content. In the case of the carotenoid index a Log_e transformation of both axes was required. An analysis of covariance (ANCOVA) was used to quantify the relationship between non-destructive measurement and the effect of irradiance, on the correlation with chlorophyll content. Non-destructive measurements were the response variable, irradiance treatments the effect and chlorophyll content the covariate. The *P* value obtained from the *F* test for the effect of irradiance would identify the significance of any change in intercept of the regression between remotely sensed measurement and chlorophyll content, for a change in irradiance. Importantly in this analysis any significant change in the gradient of this correlation, with a change in irradiance, would be identified by the *P* value of the F test for the interaction between irradiance and chlorophyll content. Such a significant interaction would indicate that any influence irradiance level may have upon remotely sensed measurement is dependent upon the chlorophyll content.

In an applied context the predictive equations for chlorophyll content from these non-destructive measurements were calculated. The predictive equations were calculated using the grouping method of Wald (Curran and Hay, 1986), in which a regression line was fitted mid way between the regression of *Y* on *X* and the regression of *X* on *Y* in the form $X = \beta Y + \alpha$. The example data set in Curran and Hay (1986) was used to ensure correct calculation. The two remotely sensed indices exhibiting either the strongest or weakest linear correlation with chlorophyll content were presented displaying the grouping method of Wald in comparison with the regression of *Y* on *X* and *X* on *Y*. ANCOVA and linear regression were carried out in Minitab 14.0, (Minitab Inc., Philadelphia) and the grouping

method of Wald calculated using excel (Microsoft Office Excel ver. 11; 1985-2003 Microsoft Corporation)

2.4 Results

2.4.1 Visual inspection of whole spectra between 400 - 800 nm

Condensing spectra at 1 nm resolution down to specific indices that use only small bands of these continuous spectra has two outcomes. On the positive side the complex nature of whole spectra is simply condensed to one usable calibrated value of chlorophyll content. However, on the negative side, much information may be excluded or overlooked. Spectra were grouped per irradiance treatment across a similar chlorophyll content range to highlight spectral features that may be related with irradiance. Reflectance spectra for poplar with a chlorophyll content range of 500- 650 mg m^{-2} and corresponding to low (n = 6), medium (n = 11) and high (n = 10) levels of irradiance are presented in figure 2.1 A low chlorophyll content group (10 - 50 mg m^{-2}) corresponding to low (n = 8), medium (n = 9) and high (n = 11) levels of irradiance was also examined and is also presented in figure 2.1. A clear increase in reflectance is evident for leaves of the high chlorophyll content group exposed to high irradiance when compared with the medium and low irradiance treatments.

2.4.2 Non-destructive estimates of leaf chlorophyll content

The chlorophyll content estimated by the two hand-held chlorophyll content meters showed a linear response with increasing chlorophyll content, across all three irradiance treatments. These results are presented in figure 2.2. The pre-transformed curvilinear responses of SR and NDVI and the linear response of all other indices (MNDVI and REP estimates) with chlorophyll content are also given in figure 2.2.

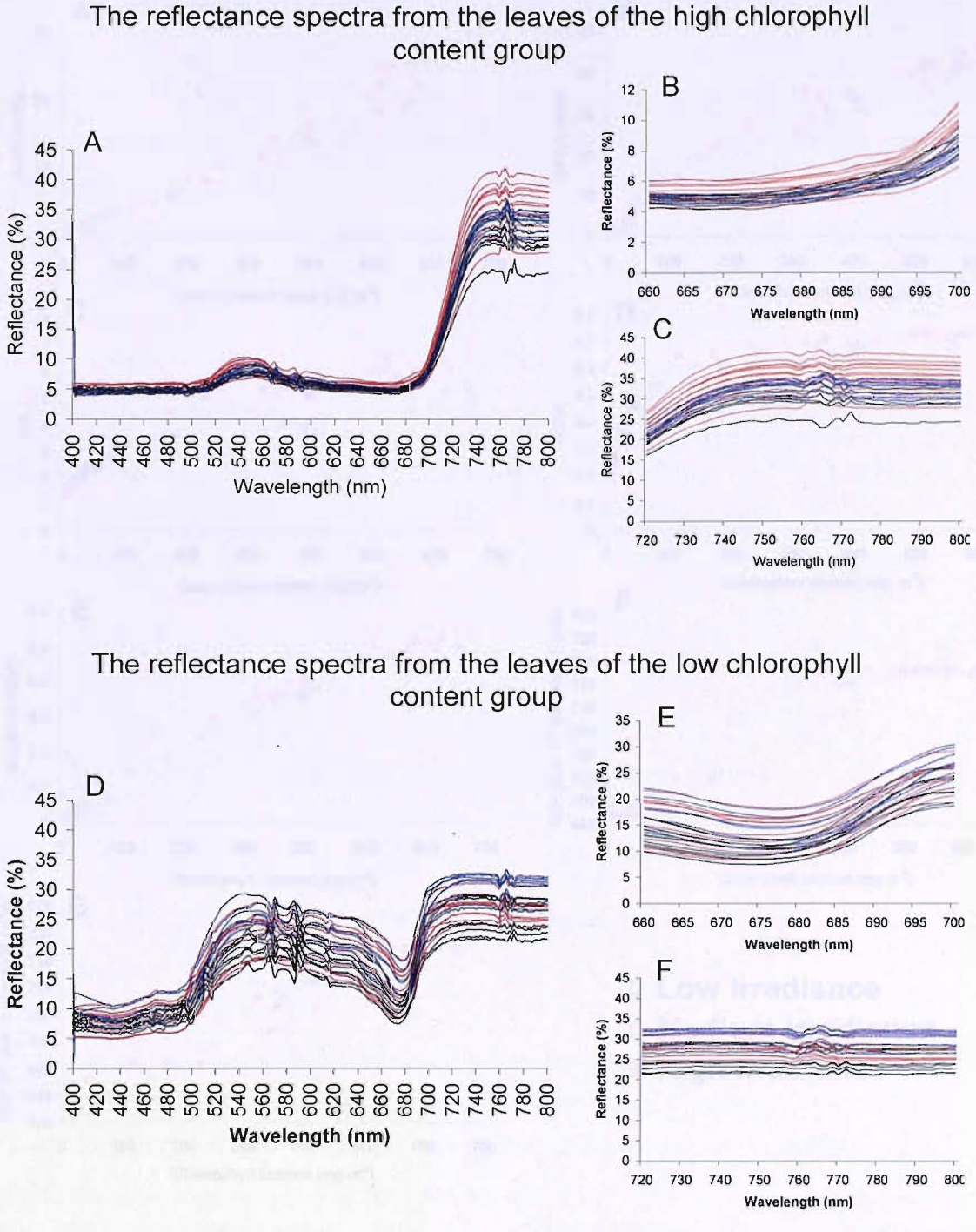

Figure 2.1: The reflectance spectra for the high chlorophyll content leaves (> 500 mg m^{-2}) between 400 to 800 nm (A), and for the separate bands in the red (680 - 700 nm) (B), and red edge to NIR (720 - 800 nm) (C). The reflectance spectra for the low (10 - 50 mg m^{-2}) chlorophyll content leaves between 400 to 800 nm (D), and for the separate bands in the red (680 - 700 nm) (E), and red edge to NIR (720 - 800 nm) (F). The reflectance spectra obtained under the high (——), medium (——) and low (——) irradiance treatments are shown.

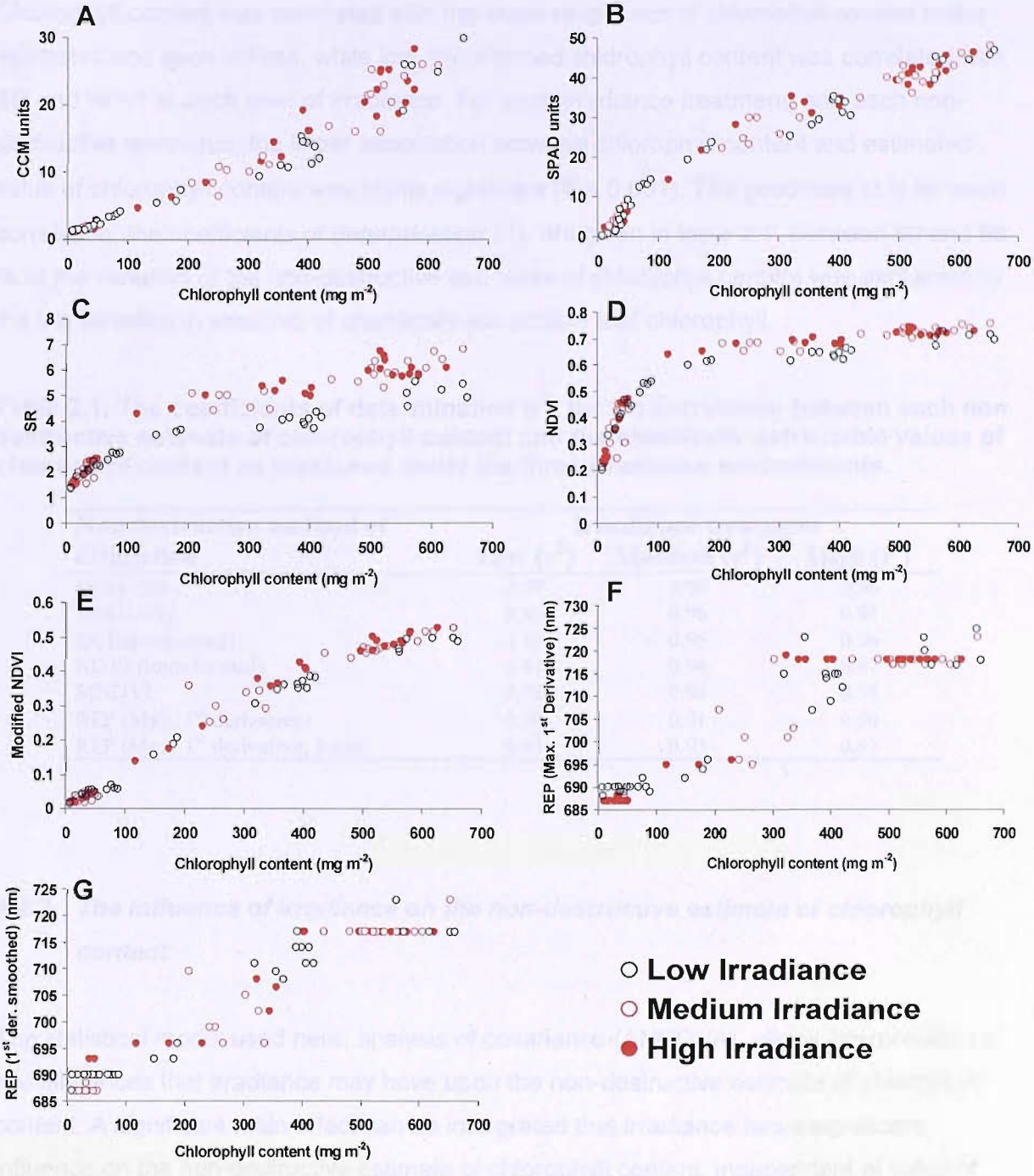

Figure 2.2: The relationships between chemically-extractable leaf chlorophyll content and (A) CCM value, (B) SPAD value, (C) SR, (D) NDVI, (E) modified NDVI, (F) REP estimated using the maximum of first derivative, (G) REP estimated using the maximum of first derivative and smoothed to 3 nm at the three levels of irradiance.

Chlorophyll content was correlated with the linear responses of chlorophyll content meter estimates and each indices, while $\log_e$ transformed chlorophyll content was correlated with SR and NDVI at each level of irradiance. For each irradiance treatment, and each non-destructive technique, the linear association between chlorophyll content and estimated value of chlorophyll content was highly significant ($P \leq 0.001$). The goodness of fit for each correlation, the *coefficients of determination* (r^2), are given in table 2.1. Between 90 and 98 % of the variation of the non-destructive estimates of chlorophyll content was explained by the the variation in amounts of chemically-extractable leaf chlorophyll.

Table 2.1: The coefficients of determination (r^2) for the correlation between each non destructive estimate of chlorophyll content and the chemically-extractable values of chlorophyll content as measured under the three irradiance environments.

Non destructive method of estimation	Irradiance treatment		
	Low (r^2)	Medium (r^2)	High (r^2)
CCM-200	0.93	0.95	0.96
SPAD-502	0.95	0.96	0.96
SR (transformed)	0.92	0.95	0.96
NDVI (transformed)	0.97	0.94	0.97
MNDVI	0.98	0.96	0.98
REP (Max. 1st derivative)	0.90	0.91	0.90
REP (Max. 1st derivative, 3 nm)	0.93	0.93	0.93

2.4.3 The influence of irradiance on the non-destructive estimate of chlorophyll content

The statistical model used here, analysis of covariance (ANCOVA), allows interpretation of two influences that irradiance may have upon the non-destructive estimate of chlorophyll content. A significant main effect can be interpreted that irradiance has a significant influence on the non-destructive estimate of chlorophyll content, independent of value of chemically-extractable leaf chlorophyll. A significant interaction between irradiance and chemically-extractable leaf chlorophyll content identifies that the effect irradiance has on the non-destructive estimate is influenced by the value of chemically-extractable leaf chlorophyll. The results of the ANCOVA are given in table 2.2.

Table 2.2: The *P* value of the ANCOVA between irradiance treatment and non-destructive estimate of leaf chlorophyll content. Those estimates considered significantly ($P \leq 0.05$) influenced by irradiance are highlighted in bold.

Non destructive estimate of chlorophyll content	ANCOVA (p value)	
	Main effect	Interaction
CCM-200	$F_{2,93} = 0.18, P = 0.832$	$F_{2,93} = 0.16, P = 0.849$
SPAD-502	$F_{2,93} = 0.58, P = 0.560$	$F_{2,93} = 0.81, P = 0.450$
SR (transformed)	$F_{2,91} = 8.88, \mathbf{P \leq 0.001}$	$F_{2,91} = 14.4, \mathbf{P \leq 0.001}$
NDVI (transformed)	$F_{2,91} = 3.05, \mathbf{P = 0.052}$	$F_{2,91} = 4.73, \mathbf{P = 0.011}$
Modified NDVI	$F_{2,91} = 0.25, P = 0.781$	$F_{2,91} = 2.32, P = 0.104$
REP (Max. 1st derivative)	$F_{2,91} = 0.45, P = 0.638$	$F_{2,91} = 0.30, P = 0.744$
REP (Max. 1st derivative, 3 nm)	$F_{2,91} = 1.01, P = 0.368$	$F_{2,91} = 0.24, P = 0.787$

The error associated with switching axis to gain an estimate of chemically-extractable leaf chlorophyll content from a non-destructive value was small. This was observed using the non-destructive estimates with both the lowest ($r^2 = 0.90$, REP estimated as the maximum of the 1st derivative) and the highest ($r^2 = 0.98$, modified NDVI) coefficient of determination for chemically-extractable leaf chlorophyll estimated under low irradiance. For these two indices the results from the linear regression of *Y* on *X* were compared with those for the incorrect predictive regression of *X* on *Y* and that calculated using the grouping method of Wald (see figure 2.3). The plots obtained for the predictive equations, calculated by the grouping method of Wald, for each non-destructive estimate of leaf chlorophyll content and obtained under each irradiance treatment are given in figure 2.4. Both the fitted equations for the regression of Y on X and the predictive equations calculated using the grouping method of Wald are reported in table 2.3. There was a general tendency for the predictive (calibration) equation calculated using the grouping method of Wald to result in a lower estimate of leaf chlorophyll content under high irradiance than when the same approach was calibrated under low irradiance.

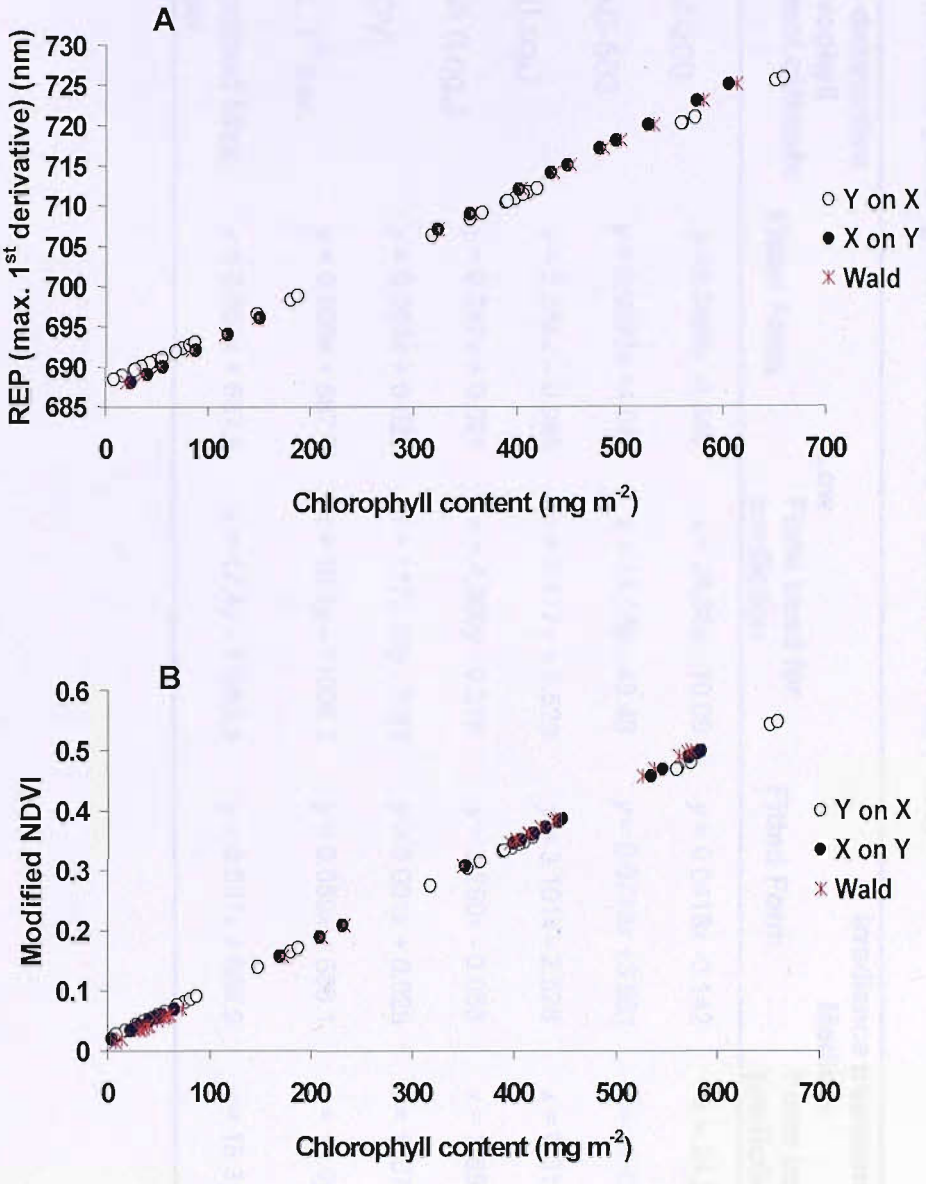

Figure 2.3: The linear regression of *X* on *Y*, *Y* on *X* and that calculated using the grouping method of Wald for (A) chemically-extractable leaf chlorophyll content and REP estimated as the maximum of the 1st derivative and (B) chemically-extractable leaf chlorophyll content and the modified NDVI.

Table 2.3: The linear calibration equations used to convert index to chlorophyll content value for each indices under each level of irradiance, calculated using the Wald grouping method discussed in Curran and Hay (1986)

Non-destructive chlorophyll content estimate	Irradiance treatment					
	Low		Medium		High	
	Fitted Form	Form used for prediction	Fitted Form	Form used for prediction	Fitted Form	Form used for prediction
CCM-200	y =0.0409x -0.348	x = 26.85y - 10.09	y = 0.0418x -0.142	x = 24.33y - 5.70	y =0.0419x + 0.185	x = 23.73y + 0.769
SPAD-502	y = 0.0693x +4.043	x = 14.05y - 49.49	y = 0.0713x +3.551	x = 14.127y - 51.51	y = 0.0741x +2.627	x = 13.95y - 44.68
SR (Log_e)	y = 2.036x – 0.985	x = 0.477y + 0.529	y = 3.101x - 2.528	x = 0.319y + 0.825	y = 2.815x - 1.77	x = 0.349y + 0.653
NDVI (Log_e)	y = 0.247x + 0.021	x = 4.300y - 0.216	y = 0.290x - 0.058	x = 3.652y + 0.083	y = 0.285x + 0.043	x = 3.863y - 0.012
MNDVI	y = 0.001x + 0.020	x = 1172.29y - 9.52	y = 0.001x + 0.028	x = 1207.2y - 36.53	y = 0.001x + 0.020	x = 1128.4y - 20.66
Max. 1^{st} der.	y = 0.058x + 687.7	x = 16.1y - 11005.2	y = 0.059x + 686.1	x = 16.9y - 11554.7	y = 0.06x + 686.84	x = 15.9y - 10913.3
Smoothed Max. 1^{st} der.	y = 0.055x + 687.9	x = 17.4y - 11953.5	y = 0.057x + 685.9	x = 18.3y - 12537.8	y = 0.056x + 687.0	x = 17.0y - 11685.5

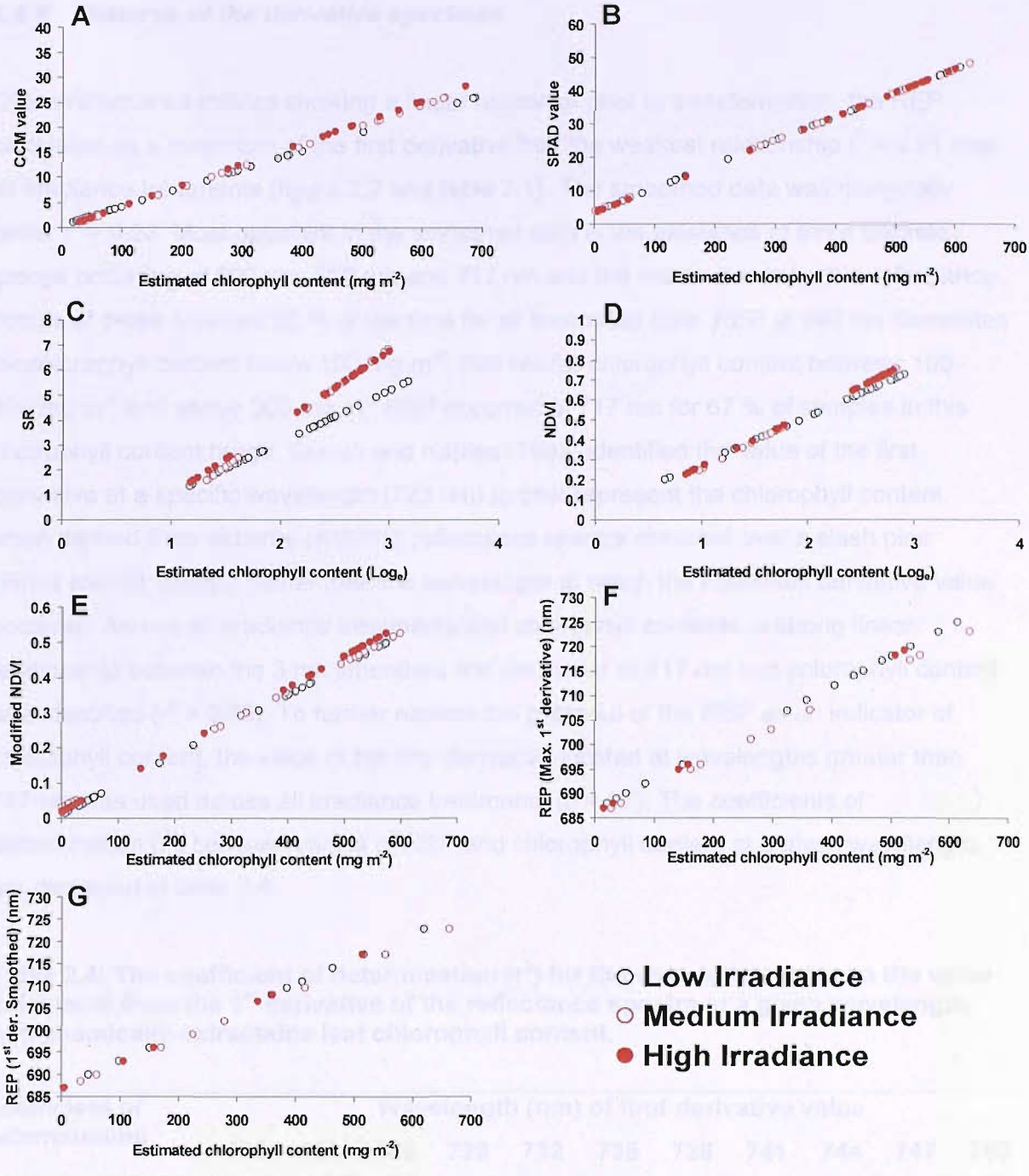

Figure 2.4: The calibration plots calculated using the grouping method of Wald to convert non-destructive estimate of chlorophyll content to a calibrated value using (A) CCM value, (B) SPAD value, (C) SR, (D) NDVI, (E) modified NDVI, (F) REP estimated using the maximum of first derivative, (G) REP estimated using the maximum of first derivative and smoothed to 3 nm at the three levels of irradiance.

2.4.4 Features of the derivative spectrum

Of the reflectance indices showing a linear response prior to transformation, the REP calculated as a maximum of the first derivative had the weakest relationship $r^2 = 0.91$ over all irradiance treatments (figure 2.2 and table 2.1). The smoothed data was marginally better $r^2 = 0.93$. Most apparent in the smoothed data is the existence of three discrete groups occurring at 690 nm, 696 nm and 717 nm and the maximum derivative reflectance occurs at these 3 values 52 % of the time for all smoothed data. REP at 690 nm dominates for chlorophyll content below 100 mg m^{-2}, 696 nm for chlorophyll content between 100 - 300 mg m^{-2} and above 300 mg m^{-2} REP occurred at 717 nm for 67 % of samples in this chlorophyll content range. Curran and Kupiec (1995) identified the value of the first derivative at a specific wavelength (723 nm) to best represent the chlorophyll content, when derived from airborne (AVIRIS) reflectance spectra obtained over a slash pine (*Pinus elliottii*) canopy, rather than the wavelength at which the maximum derivative value occurred. Across all irradiance treatments and chlorophyll contents, a strong linear relationship between the 3 nm smoothed first derivative at 717 nm and chlorophyll content was identified ($r^2 = 0.89$). To further explore the potential of the REP as an indicator of chlorophyll content, the value of the first derivative located at wavelengths greater than 717 nm was used across all irradiance treatments ($n = 97$). The coefficients of determination (r^2) between values of REP and chlorophyll content at a given wavelength are displayed in table 2.4.

Table 2.4: The coefficient of determination (r^2) for the correlation between the value calculated from the 1st derivative of the reflectance spectra at a given wavelength, and chemically-extractable leaf chlorophyll content.

Coefficient of determination	Wavelength (nm) of first derivative value										
	720	723	726	729	732	735	738	741	744	747	750
r^2	0.93	0.95	0.95	0.96	0.94	0.93	0.92	0.92	0.83	0.58	0.24

The derivative spectra for each irradiance treatment can be seen in figure 2.5. At 1 nm resolution and existing across all values of chlorophyll content for the medium and high irradiance treatments a depression centred on 722 nm can be seen. Smoothing the data to 3 nm removes this feature which is also absent at the 1 nm resolution for the low irradiance treated leaves.

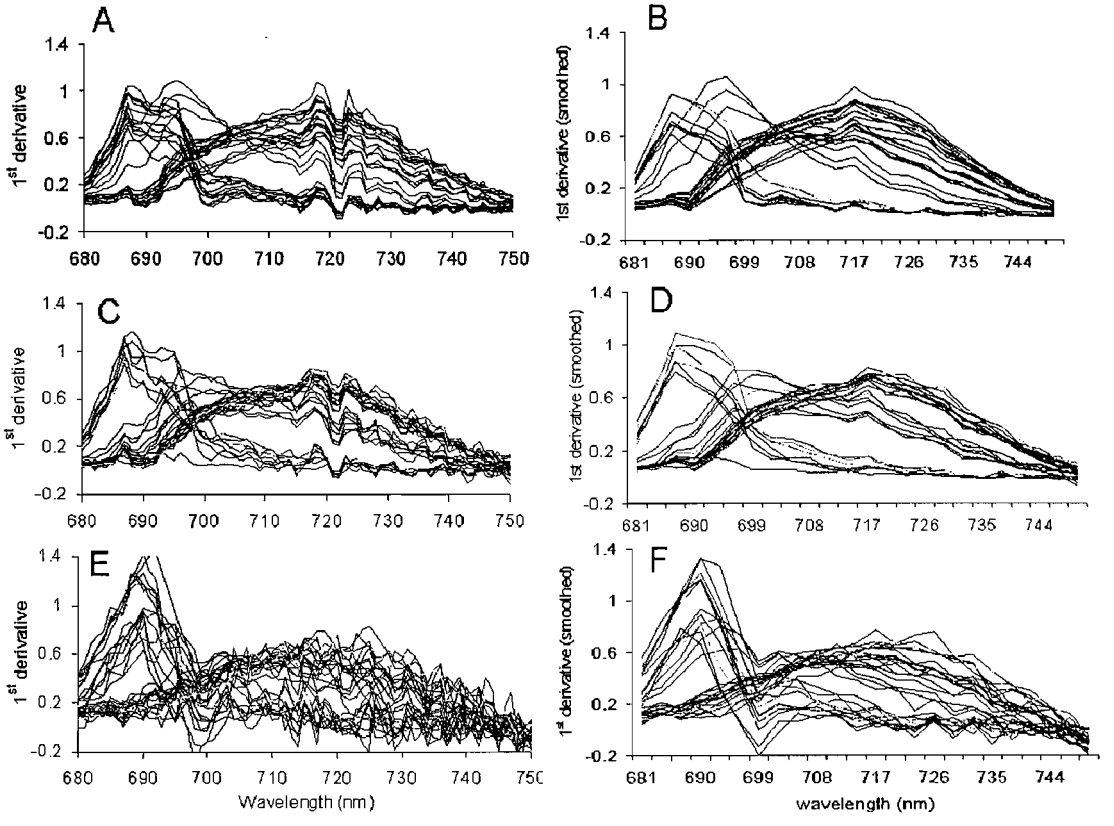

Figure 2.5: The 1st derivative spectra between 680 to 750 nm at 1 nm resolution for (A) high, (C) medium, and (E) low irradiance respectively. The 1st derivative spectra obtained from reflectance smoothed to 3 nm are shown in (B), (D) and (F) for high, medium and low irradiance treatments respectively.

2.4.5 Leaf carotenoid content

Across the wide range in chlorophyll content (100 - 660 mg m^{-2}) carotenoid to chlorophyll ratio remained generally constant. For leaves with chlorophyll content below 50 mg m^{-2} the carotenoid to chlorophyll ratio increased exponentially (Figure 2.6). The Plant Senescing Reflectance Index (PSRI) (Merzlyak *et al.,* 1999) is reported to be sensitive to changes in the carotenoid to chlorophyll ratio for leaves having below 100 mg m^{-2} chlorophyll. Additionally the Plant Reflectance Index (PRI) is reported to predict carotenoid to chlorophyll ratio across a wide variety of species (Guo and Trotter, 2004). Below 100 mg m^{-2} chlorophyll, the PSRI was a weak predictor of leaf carotenoid to chlorophyll ratio (r^2 = 0.49), this improved for leaves having below 50 mg m^{-2} chlorophyll (r^2 = 0.68). Whereas the PRI was not a predictor of leaf carotenoid to chlorophyll ratio, r^2 = 0.008 and 0.036 for below 100 mg m^{-2} of leaf chlorophyll and below 50 mg m^{-2} of leaf chlorophyll respectively.

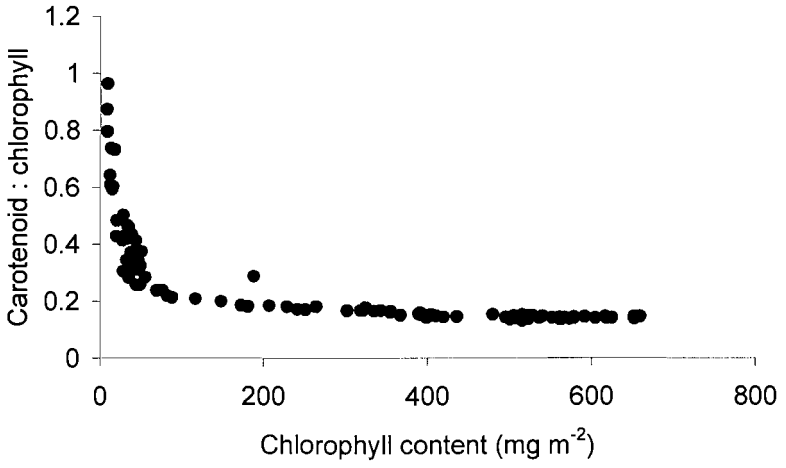

Figure 2.6: The change in leaf carotenoid : chlorophyll ratio between leaves of different chlorophyll content (*n* = 99).

Using the 97 samples for which MNDVI exhibited a strong linear correlation with leaf chlorophyll content, the carotenoid index (*xi*) showed a curvilinear response with total leaf carotenoid content which ranged between 6.7 mg m^{-2} and 95.8 mg m^{-2} (figure 2.7). Log_e transformation of the carotenoid index removed this curvilinear response and resulted in the Log_e carotenoid index exhibiting a very strong negative correlation (r^2 = 0.97) with Log_e extracted carotenoid content as shown in figure 2.8. It is worth remembering that increased reflectance in the visible portion of the spectrum will be negatively associated with pigment content and so any index related with this feature will have a negative association with pigment content.

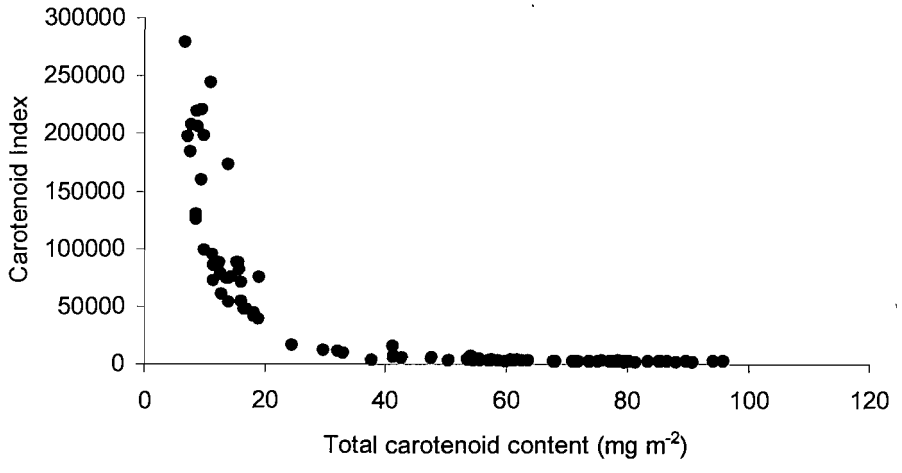

Figure 2.7: The relationship between chemically-extractable leaf carotenoid content and the non-destructive estimate of leaf carotenoid content (the carotenoid index) (*n* = 97).

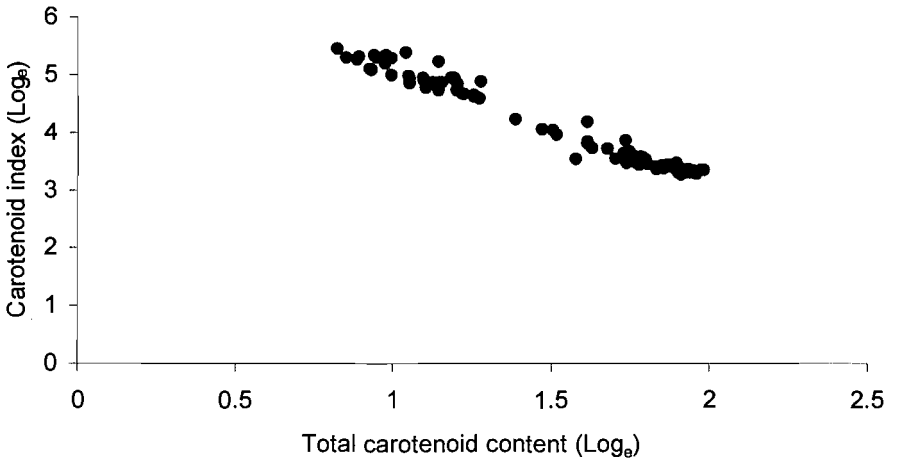

Figure 2.8: The linear relationship between Log$_e$ chemically-extractable leaf carotenoid content and the non-destructive estimate of leaf carotenoid content calculated as the Log$_e$ of the carotenoid index (n = 97, r^2 = 0.97).

2.5 Discussion

In this chapter spectral reflectance estimates of leaf pigment content were carried out after the leaves had been exposed to increasingly low levels of irradiance. Spectral indices of chlorophyll content were calculated and the relationship with leaf chlorophyll content analysed and compared with that of standard hand-held chlorophyll content meters.

2.5.1 Non-destructive estimates of leaf chlorophyll content

Irrespective of irradiance treatment, and also with combining data across all irradiance treatments such that n = 97 for reflectance-based values and n = 99 for the hand-held instruments, non-destructive estimates of leaf chlorophyll content were generally very good. The coefficients of determination ranged from an r^2 value of 0.90 for REP estimated as the maximum of the first derivative to 0.98 for the MNDVI (table 2.1). This indicated that a ratio-based estimate between the red and NIR is superior to a derivative based estimate of REP so long as the bands used for the ratio-based estimate are very close to the red edge limit for chlorophyll absorption. The curvilinear response of both SR and NDVI (figure 2.2) is generally considered the result of low levels of chlorophyll saturating absorption at wavelengths in the middle of the red band (680 nm). This feature is improved by using absorbance towards the edge of the chlorophyll-absorbing red band (705 nm) (Gamon and Surfus, 1999; Gitelson and Merzlyak, 1994), results consistent with data reported here.

The CCM-200 and the SPAD-502 both exhibited very strong coefficients of determination for total leaf chlorophyll content (r^2 = 0.95 and r^2 = 0.96, n=99, respectively) (table 2.1). The CCM exhibits a linear response across the wide dynamic range of chlorophyll content (8 - 660 mg m^{-2} chlorophyll) although scatter around the best fit line increases with increasing chlorophyll content. The SPAD-502 exhibits less scatter than the CCM-200 at high chlorophyll content, but a slight curvilinear response dominated by a steeper gradient below 100 mg m^{-2} can be seen indicating a slight tendency towards saturation at chlorophyll content values greater than 100 mg m^{-2} (figure 2.2). Both instruments measure absorbance of red light (centred on 650 nm and 660nm for SPAD-502 and CCM-200 respectively) and both obtain a reference in the NIR centred on 940 nm (Richardson *et al.*, 2002). The small difference between the SPAD-502 and the CCM-200 estimates of leaf chlorophyll content may be explained by two features. Feature one is that the two

instruments measure transmitted red irradiance centred on a different red wavelength. Feature two could be the sampling strategy. The mean of 10 techincal replicate measurements of the leaf were obtained by the SPAD-502 that represented each biological replicate. Whereas no technical replicates were taken for the CCM-200. This increased replication is a more representative strategy as indicated by the increased coefficient of determination for the SPAD-502, when compared with the CCM-200. Irrespective of the difference between CCM-200 and SPAD-502, an explanation should be sought as to why these approaches are less prone to saturation than NDVI. NDVI uses reflectance in the centre of the red band (680 nm); this is closer to the red edge absorption maxima than both the CCM-200 and SPAD-502 (660 and 650 nm respectively) and should therefore be less prone to saturation. One reason could be that chlorophyll content measured by the CCM-200 and SPAD-502 is estimated from transmitted irradiance compared with NDVI which is calculated from reflected irradiance.

The red edge position calculated using the first derivative of the leaf reflectance spectra between 660 - 750 nm, and reported as the wavelength at which the maximum derivative value occurs, was a good estimator of chlorophyll content (r^2 = 0.91) but the poorest of all those examined (table 2.1). It was improved by smoothing the data (r^2 = 0.93), although the greatest improvement was made through estimating chlorophyll content as a function of the value of the first derivative at a given wavelength at the edge of the maximum chlorophyll absorbance as reported by Curran and Kupiec (1995). For the leaves tested here, the derivative reflectance at 729 nm provided the best derivative estimate of leaf chlorophyll content explaining 96 % of the variation (table 2.4). This could result for two reasons, (1) this long wavelength is at the edge of the chlorophyll absorbance range and therefore avoids saturation and (2) other influences upon the derivative reflectance such as chlorophyll fluorescence are reported at shorter wavelengths such as 688, 697 and 710 nm (Zarco-Tejada *et al.,* 2003). Data reported here show that 52 % of the values for the maximum of the first derivative spectra occur at three specific wavelengths, 690, 696 and 717 nm (figure 2.5). These positions are similar to those reported to respond to steady-state chlorophyll fluorescence (Zarco-Tejada *et al.,* 2003) and may explain the poorer performance of this index as a direct estimator of chlorophyll content. Such a process may also explain the trough at 722 nm in the 1 nm resolution derivative spectra (figure 2.5). This trough resulted from a subtle increase in reflectance between 716 and 718 nm and existed across the total chlorophyll content range and was generally absent in the spectra

for low irradiance. Although reported here as a poorer and more complicated estimate of leaf chlorophyll content, the maximum of the derivative spectra results from changes within the red edge position and not simply from ratios obtained using data from either side of the red edge position such as the NDVI. The derivative spectra is therefore less influenced by interfering background absorption (Dawson and Curran, 1998) indicating the increased value of this approach when background features may have a large influence upon the reflectance spectra, as may be encountered when obtaining field-based spectra of senescing tree canopies.

2.5.2 Non-destructive estimates of leaf carotenoid content

The two spectral approaches reported to estimate both leaf carotenoid content and leaf chlorophyll:carotenoid ratio, the PRI (Guo and Trotter, 2004) and the PRSI (Mezlyak *et al.*, 1999) were both poor estimators of these components in poplar leaves. However, the carotenoid index reported here was an excellent predictor of leaf carotenoid content. Due to the nature of the calculation, the units for this index are large and wide ranging, ranging from 1820 to 279036 for a leaf carotenoid content range of 6.7 mg m^{-2} to 81.3 mg m^{-2} respectively. This results in the *Y* axis changing by a factor of 153 across this range in chlorophyll content (figure 2.7). The saturation of this index by a leaf carotenoid content of above 20 mg m^{-2} may be a genuine feature of this index or a response to this vast change in units. Whatever the reason for this curvilinear response, it was overcome by Log_e transformation of both axes resulting in a spectral estimate explaining 97 % of the change in leaf carotenoid content (figure 2.8). The form of this index takes into account all reflectance across 500 -680 nm (a large component of the PAR) and it is logical to assume that this approach may also estimate leaf chlorophyll:carotenoid ratio. The correlation between log_e transformed carotenoid index on the untransformed ratio of chlorophyll:carotenoid content, again displayed a strong significant negative association (r^2 =0.92; $P \leq 0.001$).

2.5.3 Observing the whole spectrum between 400 - 800 nm

Within the high chlorophyll content group, and with an increase in irradiance, an increase in leaf reflectance between 400 nm to 800 nm of the electromagnetic spectrum was observed. No consistent features between irradiance and spectral reflectance were

observed for the low chlorophyll content group (figure 2.1). This increase in reflectance was considered to be the result of a short-term (two hour) adaptive response of the leaf to irradiance, because all leaf spectra were rapidly obtained under the same incident irradiance. In the red region of the spectrum reflectance is dominated by absorption of photosynthetic pigments contained in the chloroplast. In the NIR region of the spectrum reflectance at 800 nm has been reported to be most correlated with mesophyll cell surface:airspace volume, per unit leaf area, for 48 species of angiosperm and is generally considered a measure of leaf cellular integrity (Slaton *et al.,* 2001). Under the highest irradiance treatment, this increase in reflectance resulted in a change in the value of chlorophyll content predicted by a number of standard remotely-sensed measurements. If obtained under medium to high irradiance, remote measurement would predict lower chlorophyll content than when measured under low irradiance. For most indices this under-estimation with high irradiance was seen to increase with increasing chlorophyll content, a feature that was significant for both SR and NDVI (figure 2.4 and table 2.2).

2.5.4 The influence of irradiance on reflectance indices

Under this changing irradiance (from 0 - 300 μmol s^{-1} m^{-2}), both stomatal aperture size and conductance are reported to increase linearly, with stomatal conductance generally becoming saturated between 400 -1000 μmol s^{-1} m^{-2} (Willmer and Fricker, 1996). It is therefore further hypothesized that short-term changes in stomatal response to changing irradiance may affect NIR reflectance. For example, the refractive index between leaf airspaces and hydrated mesophyll cells influences NIR reflectance (Woolley, 1971) and leaf turgor and mesophyll to airspace volume both of which are documented to influence NIR reflectance (Slaton *et al.,* 2001). In response to this hypothesis, and data reported here, stomatal conductance was measured on these trees although at a later date (approximately three months after spectral analysis). The same trees were taken representing the high chlorophyll content group and one tree was subjected to high irradiance (700 μmol s^{-1} m^{-2}) or or low (20 μmol s^{-1} m^{-2}). Stomatal conductance was measured with a portable steady-state porometer Li-1600 (*LI-COR* inc. Lincoln, Nebraska, USA) on each of leaves five, six and seven and ten replicate measurements were taken per leaf. For all leaves stomatal conductance was greater under the high irradiance treatment (data are presented in appendix B). Alternatively a temperature increase with increasing irradiance may be responsible for this, although this factor was not apparent

from measurements taken during the initial experimental set-up. Under high irradiance, and for the high chlorophyll content group, a uniform increase in visible leaf reflectance was apparent and this was absent in the low chlorophyll content group (figure 2.1). This could be the result of chloroplast avoidance as a mechanism to reduce photoinhibition, as reported by Hoel and Solhaug (1998) when estimating chlorophyll content using a SPAD-502 . However, of all the techniques used in this study, the SPAD-502 appeared to be the least influenced by the irradiance environment. The indices for which a significant interaction between irradiance level and chlorophyll content occurred (SR and NDVI) were further examined using the predictive forms of the regression between remotely-sensed index and chlorophyll content. These indices were used to predict the maximum value of chlorophyll extracted from the low irradiance treatment (660 mg m^{-2} = 2.8 log). When the SR value of 4.75 was input in to the low irradiance calibration equation, a log_e chlorophyll content of 2.8 was predicted, as expected. However, when this same SR value was input into the high irradiance calibration, a log_e chlorophyll content of 2.3 was predicted, an underestimation of 20 %. Using this same approach an underestimation of 5 % was also calculated for the NDVI.

2.5.5 Summary

In summary indices calculated from remotely-sensed reflectance provide an excellent means to estimate leaf chlorophyll content; for simplicity and predictability MNDVI may be considered the best of these indices. The calculation of an estimate of both total leaf carotenoid content and leaf chlorophyll:carotenoid content may increase the potential application of this technology to monitor the progression of autumnal senescence in poplar. The use of calibrated remote estimates to derive a quantitative value of chlorophyll content should be used with caution particularly in the field as external factors such as changing irradiance can lead to a change in index value irrespective of changing chlorophyll content.

Chapter 3:

Canopy senescence in elevated carbon dioxide

3.1 Overview

The consequences of long-term growth in elevated atmospheric CO_2 on canopy senescence, for a fast growing poplar coppice plantation, will be explored in this chapter. The influence that enrichment of atmospheric CO_2 may have on leaf level processes during senescence is of fundamental importance in order to understand the mechanisms involved. Nevertheless, the heterogeneity of internal and external leaf environments that results in a typical canopy or plantation stand creates a large variability of responses at the leaf level, especially when factors such as PNUE, LUE, SLA, carbohydrate content and irradiance environment are all documented to influence senescence (Hikosaka *et al.,* 2005; Wingler *et al.,* 2006). Therefore, only if any consistent autumnal response can be integrated across the whole canopy or stand level may it then be considered to influence the carbon balance, as documented by Goulden *et al.,* (1996). In this chapter, and for the first time to my knowledge, the change in GPP that results from the influence elevated atmospheric CO_2 has on canopy senescence will be estimated.

3.2 Introduction

Leaf senescence is considered the genetically controlled final stage of leaf development and during senescence a general decline in leaf protein and RNA levels parallels a loss in photosynthetic activity (Buchanan-Wollaston *et al.,* 2003). Phenological events such as budding, leafing or flowering of plants in the spring or leaf colour change and fall in the autumn have received much attention as they may be a sensitive and easily observable indicator of changes in the biosphere (Menzel and Fabian, 1999). An analysis of over 1700 species showed that climate change is already affecting living systems with significant shifts in plant phenology (Parmesan and Yohe, 2003). These shifts in phenology include a well-documented extension of the growing season (Menzel and Fabian, 1999; Menzel *et al.,* 2006; Myneni *et al.,* 1997; Zhou *et al.,* 2001) which has been ascribed to global warming and considered a fingerprint for global change (Penuelas and Filella, 2001; Root *et al.,* 2003). Across Europe, a 6 day earlier leaf unfolding and delay of 4.8 days in leaf autumn colouring between 1959 and 1993 was identified (Menzel and Fabian, 1999). Remotely sensed values of Normalised Difference Vegetation Index (NDVI) which is now widely used as an index of green vegetation amount (Peñuelas and Filella 1998; Dawson *et al.,* 2003) give large scale supporting evidence for this. Between 1981 and 1991 NDVI data taken from orbiting satellites show a spring advance of 8 days and a 4-day delay in autumn senescence across Europe (Myneni *et al.,* 1997). An 18-day extension of the growing season in Eurasia between 1982 to 1999 and 12 day extension in North America has also been identified through a more recent analysis of NDVI data (Zhou *et al.,* 2001).

These changes in phenology have been attributed to warmer temperatures causing longer growing seasons (Menzel *et al.,* 2006; Menzel and Fabian, 1999; Peñuelas, and Filella, 2001; Root *et al.,* 2003; Zhou *et al.,* 2001), but others have cautioned of a weaker relationship between temperature and the timing of autumnal events when compared with that of spring events (Menzel *et al.,* 2006; Stöckli, and Vidale, 2004). In the most comprehensive meta-analysis to date, consisting of 125, 000 observations from 21 European countries, taken between 1971 and 2000 and using 542 plant species, Menzel *et al.* (2006) reported the correlation between an advanced spring phenophase and warming patterns of 19 European countries to be strong and significant ($r = -0.69$, $P < 0.001$). However the association between warming and the autumnal phenophase was described by Menzel *et al.* (2006) as 'vague'. The correlation between leaf color change

and drop and the temperature trends for 14 European countries was weak and non-significant (r = 0.003, *P* =0.99). Moreover of the leaf coloring events only 52 % were delayed and only 15 % of these were significant. This contrasts sharply with that of spring events which showed 78 % were earlier and that 31 % of these were significant.. Field data validation from phenological modelling of a Northern forest indicates accumulated chilling degree days to account for less in the autumnal decline of a forest canopy than accumulated heating degree days accounts for leafing out of a spring canopy,(Richardson *et al.,* 2006). Across Europe, during the last 30 years, autumnal senescence has been delayed by between 1.3 - 1.8 days decade^{-1} (Menzel *et al.,* 2006 and Menzel and Fabian, 1999, respectively). With atmospheric [CO_2] documented to influence autumnal phenology, it is hypothesized that elevated CO_2 would delay autumnal senescence in highly productive, indeterminate, non-sink limited poplar trees.

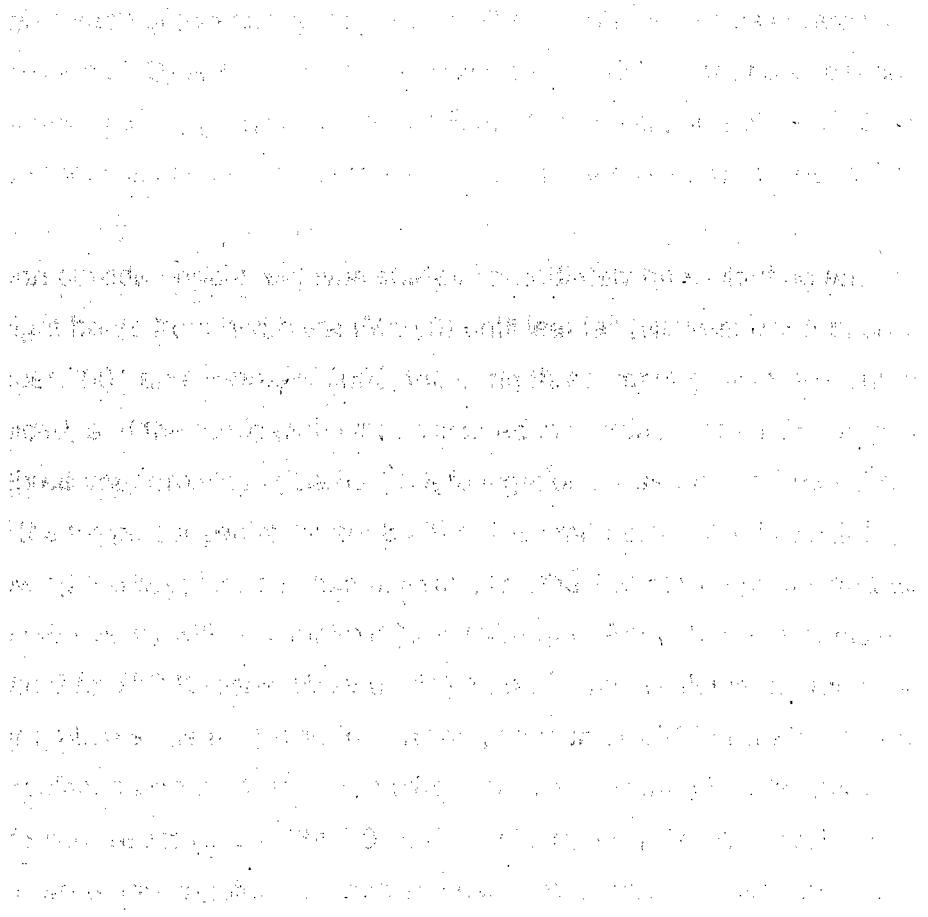

3.3 Materials and Methods

3.3.1 Plant material and experimental set up

The 9 hectare POP/EUROFACE experimental plantation (http://www.unitus.it/euroface/) is located in central Italy (Tuscania; 42°22`-N, 11°48`-E, alt 150m) and is dominated by a typically Mediterranean climate. It is situated on former agricultural fields, which up until 50 years ago were covered by woody vegetation (Scarascia-Mugnozza *et al.,* 2005). The site was planted during the spring of 1999 and consists of a plantation of *Populus* x *euramericana* Dode (Guiner) (*P. deltoides* Bart. ex Marsh. x *P. nigra* L., genotype I-214) at a density of 5000 trees ha^{-1}, planted at 2 m x 1 m spacing. Within the plantation six experimental plots of 314 m^2 were planted with each of *P. alba* L. (genotype 2AS11), *P. nigra* L. (genotype Jean Pourtet) and *P.* x *euramericana* (genotype I-214), at a spacing of 1m x 1m (10^4 trees ha^{-1}). The experimental plots were divided into three equal segments each planted with one clone, and further sub-divided in half using a physical barrier penetrating to 1 metre depth in the soil, such that each species was represented by 58 plants in each of two sub-plots per plot. Three plots served as controls receiving atmospheric CO_2 and three plots received CO_2 enrichment at a target concentration of 550 µmol mol^{-1} via octagonal-shaped FACE rings. A description of the FACE facility design and performance is given by (Miglietta *et al.,* 2001), and is summarised in Chapter 1.

Carbon dioxide enrichment was started immediately after planting and maintained during day light hours from bud burst (March) until leaf fall (November) of each year. Between October 2001 and February 2002, following three years growth, the entire plantation was coppiced, and the fumigation was continued in March 2002 for the re-growth. During the first three year growing cycle the CO_2 fumigation measured at 1 min intervals was within 20 % of the target concentration for 80 % of the time as detailed in Tricker *et al,* (2004). Following the coppice, one half of each plot (the sub-plot) representing all the clones was provided weekly with a combined NPK (Nitrogen, Phosphorus, Potassium) fertiliser (a ratio of 20:6:6 for N:P:K respectively at 212 kg ha^{-1} + micro-elements) for 16 weeks through the drip irrigation system. During the growing season of 2003 and 2004 this combined fertiliser was replaced with an ammonium nitrate nutrient treatment for twenty weeks (2003) and twenty two weeks (2004) (34:0:0, N:P:K, 290 kg ha^{-1}). Throughout the entire experiment all plants were drip irrigated at a rate estimated to match transpiration (approximately six to

ten mm per day). Characterisation of the canopy and climatic variables following planting up to the commencement of this study are provided in Tricker *et al.* (2005).

The study described here was carried out during the end of the 2003 and 2004 growing seasons following 5 and 6 years exposure to free air carbon dioxide enrichment. In 2003 the mean [CO_2] within the FACE plots was 535.9 ± 20.4 ppm and within 20 % of the target concentration of 550 ppm for 72.2 % of the time and this reduced to 70 % for 2004. Climatic variables were different for each year and in 2003 senescence data were collected between the 24th September and the 9th November during which time the mean minimum daily temperature was 11.2 °C (range 18.0 °C to 3.7 °C, lowest value on 26th October) and mean maximum daily temperature was 22.0 °C (range 32.0 °C to 11.3 °C, lowest value on 07th November). Mean photosynthetically active radiation (PAR) was 3419.4 MJ m^{-2} d^{-1} (range 6262.0 MJ m^{-2} d^{-1} to 468.8 MJ m^{-2} d^{-1} lowest value on 7th November). In 2004 measurements were made between 14th September and 4th November during which time mean minimum daily temperature was 14.4 °C (range 19.0 °C to 8.8 °C, lowest value on 29th September) and mean daily maximum temperature was 25.9 °C (range 31.9 °C to 19.9 °C, lowest value on 27th October). Mean photosynthetically active radiation (PAR) was 2477.5 MJ m^{-2} d^{-1} (range 4168.6 MJ m^{-2} d^{-1} to 1094.1 MJ m^{-2} d^{-1} lowest value on 29th October). In general 2003 was characterised by a very hot dry summer, reported in the literature as the 2003 European heat wave (Ciais *et al.*, 2005) whereas 2004 was characterised by an unseasonable warm extended autumnal senescence period. *Populus* x *euramericana* Dode (Guinier), a genotype of Italian origin and exhibiting very strong apical control, and *Populus. nigra* L., a genotype of French origin exhibiting less but still good apical control, were the species selected for study. The third species *Populus alba* L. was not selected, the highly different reflective properties between the adaxial and abaxial leaf surfaces as well as leaf hairs were considered confounding factors to reflectance spectroscopy as reported by Levizou *et al.*,(2005).

3.3.2 *Characterisation of canopy senescence*

3.3.2.1 Leaf Area Index

Canopy leaf area index (LAI m^2 of leaves / m^2 of ground) was estimated using the LAI-2000 Plant canopy analyser (Li-cor, Inc., Nebraska, USA) with a 90° view lens cap in 2003

and a 45° view lens cap in 2004 allowing for an increase in canopy height. The LAI-2000 associated optical sensor (LAI -2050) consists of a near hemi-spherical (148°) view which is projected on to five detectors arranged in concentric rings. Each concentric ring measures the transmittance of irradiance of < 490 nm through the canopy (any radiation above 490 nm is filtered out). The rings are centred on at 7 °, 23 °, 38 °, 53 °, and 68 ° from nadir with each subtending between 11 ° to 13 ° from this centre. Detector 1 centred on (7 °) measures transmittance from approximately straight overhead and detector 5 centred on (68 °) measures transmittance from approximately 22 ° above the horizon.

For an accurate assessment of LAI, the LAI-2000 has four assumptions in the following order of importance, which must be satisfied:

A. The foliage is considered black: Little radiation is assumed to be reflected or transmitted through the canopy. The optical filter ensures this, as little radiation below 490 nm is reflected or transmitted by foliage. However, unless measured under diffuse irradiance, sun flecks may penetrate the canopy resulting in an underestimation of LAI.

B. The foliage is randomly distributed around the plant: *P. x euramericana* with very good apical control appeared to satisfy this assumption but *P. nigra* with less apical control, and therefore bushier, appeared to exhibit small amounts foliage clumping evident from hemispherical photography (Calfapietra, pers. comm.).

C. The foliage elements are small: Individual leaves should be small compared to the area of view of each ring. The dense planting resulted in few leaves existing within the lower canopy during the period of measurement.

D. The foliage is azimuthally randomly arranged: the foliage exists in all compass directions for each plant. A closed, uniformly planted canopy of even height within species appeared to satisfy this assumption.

One value of leaf area index is then calculated by measuring the diffuse radiation above the canopy and then of *n* number of points below the canopy. The non-intercepted radiation is measured to estimate gaps in the canopy. The probability of a beam of radiation being intercepted whist passing through the canopy is proportional to the path

length, foliage density and foliage orientation. The automated calculation of LAI is then derived from the probability of seeing the sky whilst looking up through the canopy (*LI-COR*, 1990).

Measurements were taken with the LAI-2000 at sunrise and sunset, so avoiding any direct light penetration of the canopy and during uniform sky conditions. Following a reference value which was obtained in open skies clear of the canopy, 14 below canopy measurements as described in Gielen *et al.* (2001) were taken and this was replicated four times per sub-plot for each of the six experimental plots, at each time of measurement. As optical values of LAI theoretically include stems and branches, following total leaf drop an estimate of wood area index, WAI (m^2 of woody tissue / m^2 of ground) (Liberloo *et al.*, 2005), was conducted in the same way except that the function A/B = 1 was set to allow for no foliage (*LI-COR*, 1990). Little above ground woody tissue growth late in senescence after bud set was assumed, so LAI was re-estimated by subtracting the WAI from the LAI for the final two estimates of LAI in both years. In 2003 only *P. x euramericana* canopy LAI was measured whereas in 2004 both *P. x euramericana* and *P. nigra* were measured.

3.3.2.2. Ground-based canopy reflectance

Ground- based canopy reflectance was measured for *P. x euramericana* and *P. nigra* with a field portable spectroradiometer (GER 3700) (GER, Buffalo, NY, USA. Mod. 3700). The GER 3700 measures across the spectral range of between 350 nm to 2500 nm. The spectral resolution was 3.0 nm between 350 nm to 1050 nm with a sampling bandwidth of 1.5 nm, and only data collected between 350 nm to 1050 nm were used for further analysis. In this way the spectra sampled by the GER 3700 may be considered to be acquired at the same spectral resolution as the raw data for the GER 1500 used in chapter two.

Spectral measurements were taken between the hours of 10.30 and 15.00 (2003) when solar zenith angle was calculated to be less than 60° (as calculated using http://solardat.uoregon.edu/cgi-bin/SolarPositionCalculator.cgi), and 11.00 - 14.00 (2004), as recommended by NERC EPFS (Fogwell, 2006). All measurements were taken under uniform clear sky conditions at approximately 1m above the canopy, except for *P. nigra* (26.10.04) which was carried out under uniform hazy cloud. This was done using a fibre

optic with a view angle of 23° that was directed away from any FACE infrastructure at 45° from nadir directly into the canopy, therefore maximising canopy view. A reference reading was taken before every measurement using a white reference panel (Spectralon, Labsphere, North Sutton, NH, USA) to account for changing incident irradiation. All treatments were measured during this time period on a single day to reduce any day of year influence and diurnal effects were minimised by confining the timing of measurements as close to solar noon as was logistically possible. Canopy reflectance was calculated as the ratio between the measurements taken above the canopy (target) and those of the white panel (reference) for each measurement. Within sub-plot replicate measurements (four in 2003, and six in 2004) were taken to account for azimuth variation, with respect to confounding factors such as FACE infrastructure and different species. In 2004 canopy reflectance of *P. x euramericana* was taken on 1st and 23rd October and *P. nigra* on 2nd and 26th October, whereas in 2003 both species were measured on the 15th October.

Two pigment-specific reflectance indices (as detailed in Chapter 2) were calculated from these data, these were;

1. A chlorophyll specific NDVI; the Modified NDVI (MNDVI) (*vi*) (Gamon and Surfus, 1999, Gitelson and Merzlyak, 1994).

2. The value of the first derivative spectrum (*vii*) at 729 nm,
A further NDVI was also calculated using the narrow bandwidth at the centre of the wider bandwidths generally used for large spatial NDVI assessments and global phenological monitoring (NDVI) (*v*).

3.3.2.3 Airborne spectral reflectance

Airborne measurements were made using a multispectral camera equipped with a single optic (Duncan Tech, USA Mod. MS4100) operated at three wide bandwidths centred on 550, 680 and 800 nm. The camera (field of view of 60°) was mounted on a certified aircraft (Sky Arrow 650TCNS, Rome, Italy) flying at 200 m (2003) and both 200m and 1000m (2004) above the experimental area. Measurements were taken during cloud free periods around solar noon on 1st November 2003, 31st July 2004 and 25th October 2004,

Normalized Difference Vegetation Index (NDVI) was calculated from these airborne measurements as $(R_{NIR} - R_{Red}) / (R_{NIR} + R_{Red})$.

3.3.3 *Estimating gross primary production (GPP)*

To estimate the GPP resulting from a CO_2-induced shift in autumnal phenology of *P. x euramericana*; nitrogen treatments were pooled. Taking at least three estimates of the LAI measured from bud set and throughout senescence, a regression equation was calculated for this linear decline between LAI (Y axis) and time (X axis). When extrapolating forward in time using this regression, for each species under each CO_2 treatment, the divergence in number of days for a 50 % decline in canopy LAI was calculated inorder to estimate the number of days senescence was delayed under elevated CO_2. Data were extracted from Wittig *et al.* (2005). The mean monthly GPP (g C m^{-2} d^{-1}) of *P. x euramericana* exposed to elevated CO_2 at the POP/EUROFACE site and estimated in 2001 when a closed canopy existed were taken. The relationship between day of year (X axis) and GPP (Y axis) was explained by a cubic function in the form $y = 2E^{-06}x^3 - 0.0021x^2 + 0.542x - 27.289$ (r^2 = 0.98). The mean number of days shift in the autumnal phenophase (10 day advanced in control conditions) of *P. x euramericana* calculated in this study was applied to the model. Assuming that any phenological shifts resulting from elevated CO_2 would be accounted for in this relationship, the GPP resulting from an elevated CO_2 stimulated shift in the autumnal phenophase was crudely estimated as the difference between the areas under the two curves.

3.3.4 *Experimental design*

Six plots were identified within the nine hectare site and adjacent plots were spatially separated by approximately 100 m (Scarascia-Mugnozza *et al.*, 2005). The surrounding landscape was considered undulating but the gradient between plots was only 1 - 6 % (Hoosebeek *et al.*, 2004). An initial soil survey based on C and N contents between selected plots revealed one plot (plot 5, a FACE plot) to be underrepresented by both C and N content when compared with the other plots (Hoosebeek *et al.*, 2004). Nevertheless three blocks were identified, each block represented by two plots, one of which received ambient CO_2 conditions and the other elevated CO_2, see Plate 3.1. Conditions within blocks were considered homogeneous for environmental variables and the statistical

model was based on a randomised complete block design with a block as a random untested factor (Tricker *et al.,* 2004). One assumption implicit for this type of statistical analysis is that a block is homogenous for environmental variables, and that blocks are placed to represent the spatial variability of the site (Sokal and Rolf, 1998). This assumption may have been satisfied during the first coppice rotation from 1999 - 2001, however during the second rotation (2002 - 2004) during which time data for this thesis were collected this assumption appeared violated (Tricker *et al.,* 2005). This may be seen in the false colour image of Plate 3.1, where a large heterogeneity between the plots of block three is clearly visible. If the originally planned statistical model were still used, such heterogeneity could now result in both type I (false positive) and type II (false negative) errors in interpreting significance of results. The influence of these types of error may be exemplified when the LAI data reported in this chapter are compared with those of Liberloo *et al.* (2005). Although increased replication of measurement was employed here, the general methodology was identical to that of Liberloo *et al.,* (2005), and not surprisingly so were the actual measured LAI values. The difference results in the statistical interpretation; Liberloo *et al.,* (2005) assume blocks to be homogeneous and therefore do not include a random block factor in the statistical model, resulting in a highly statistically significant stimulation of LAI in elevated CO_2 during most times of measurement. The significance of this stimulation may be genuine, however, in this chapter, the observed and measured block heterogeneity was considered and random block was included as a factor in the statistical model. Responses initially considered as significant using the old model are no longer significant but a significant block x treatment interaction was observed. Testing the variance associated with the blocks in the statistical analysis means that the response to CO_2 enrichment is measured against the background environmental variables, and in this case the likelihood of committing a type I error is reduced. However, this approach may increase the likelihood of introducing a type II error. A type II error may result here because the significant block x CO_2 interaction (the result of site heterogeneity) masks a genuine significant effect of the treatment. Where appropriate, the likelihood of committing a type II error was also reduced by using the data analysis employed in this chapter. This was achieved through the principle that autumnal senescence is uni-directional over time and measurement of senescence progression was expressed as a percentage change over time, respective to each sub-plot, using equation (*xiii*)

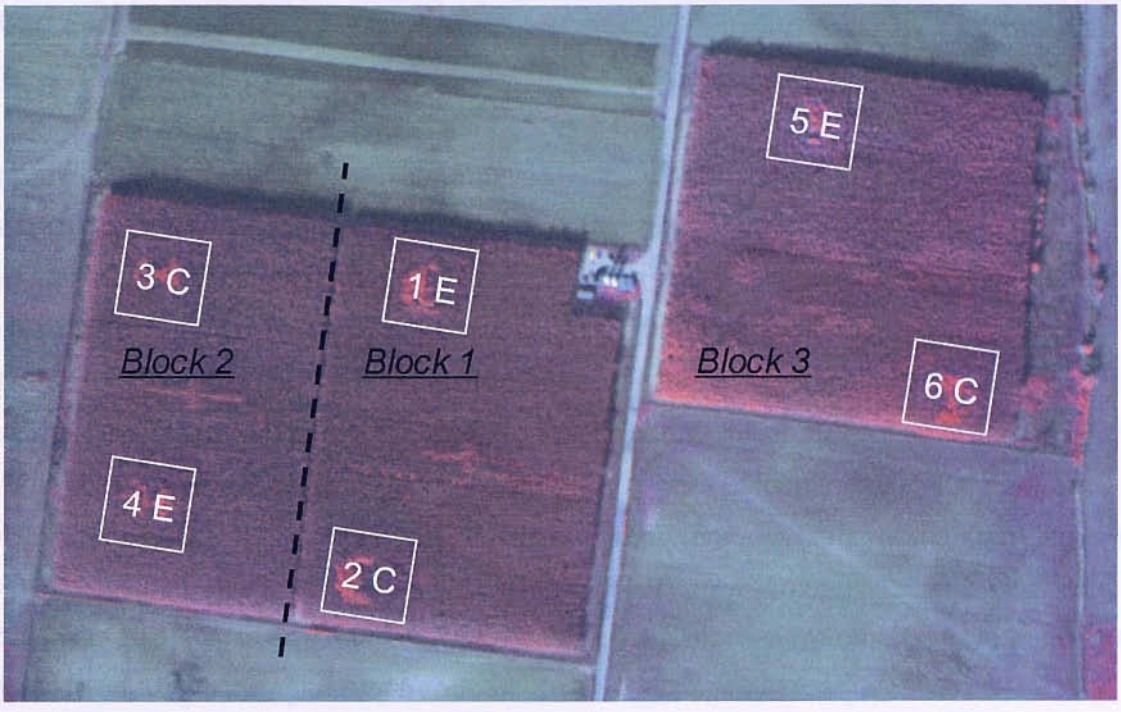

Plate 3.1: Aerial view of the EUROFACE site obtained on 25.10.04 using a multispectral camera (Duncan Tech, USA Mod. MS4100). This image was captured using optics centered on red (680 nm) and NIR (800 nm) bandwidths and an increased intensity of red colour corresponds to an increased greenness of the canopy. The white boxes indicate the location of the experimental plots, which are numbered 1 to 6 according to the POP/EUROFACE terminology. Plots labelled E corresponds to the FACE experimental plots and those labelled C are the control plots. The blocking arrangement of the whole nine hectare site is given. Block three is located on a separate field and (— -) indicates the boundary of blocks one and two. The within block variation in canopy greenness can be seen in block three indicated by a non-uniform intensity of red colouration across this block. The summed area of both fields is nine hectares and as a guide to scale the distance between adjacent experimental plots is at least 100 m (Scarascia-Mugnozza *et al.* 2005).

$$\left(\frac{Plot\ mean_{end\ October} - Plot\ mean_{start\ October}}{Plot\ mean_{start\ October}} \right) \times 100 \qquad (xiii)$$

This allowed the change in each sub-plot to be expressed relative to the initial value, now normalised to zero, so further reducing the contribution of any background variability and reducing the likelihood of committing both type I and type II errors.

3.3.5 Statistical analysis.

To test the hypothesis that elevated atmospheric CO_2 influences the progression of autumnal senescence, the most informative results were considered to be those measuring the percentage response over time due to the reduced likelihood of confounding environmental variability. Although, replicate measures of canopy reflectance and LAI were taken, measuring the same exact replicate area within each sub-plot between time periods was not possible due to light breezes and positional influences; therefore, the mean sub-plot value was the independent unit of replication. This resulted in zero error degrees of freedom if a four-way ANOVA were calculated to include species, nitrogen fertilisation, CO_2 exposure and random block. The previous randomised complete block design was analysed using a three-way ANOVA between species, nitrogen fertilisation and CO_2 exposure and all interactions with block were omitted from the model. This allowed 14 error degrees of freedom.

3.3.5.1 *Error degrees of freedom and the statistical model*

At the POP/EUROFACE site nitrogen fertilisation had no influence on growth, LAI and biomass production (Liberloo *et al.,* 2006), and this was considered the result of the earlier agricultural land-use history creating a high background concentration of nutrients (Hoosbeck *et al.,* 2004; Liberloo *et al.,* 2006). The absence of any substantial N decline in the soil between 1998 and 2004 indicates that mineralization was high and ambient soil N was sufficient to sustain growth (Liberloo *et al.,* 2006). Furthermore, no effect of N fertilisation was reported on photosynthetic parameters (Calfapietra *et al.,* 2005; Tricker *et al.,* 2005) or water use efficiency (Tricker *et al.,* 2005). However, Calfapietra *et al,* (2005) identified an increase in leaf N per unit leaf mass (N_{mass}) in response to fertilisation, and this variable is considered an important trait in determining leaf longevity (Reich *et al.,* 1997, 1999). As both species are reported to respond to elevated CO_2 by exhibiting a similar % increases in biomass (Gielen *et al.,* 2003; Liberloo *et al.,* 2006), resulting in increased NPP (Gielen *et al.,* 2005) they are therefore not considered to be sink limited. For reasons discussed in chapter one it was a reasonable assumption that both species would respond similarly in elevated CO_2 during autumnal senescence. Indeed, a study of leaf retention confirmed that it was increased in both species (although only marginally for *P. nigra* (Tricker *et al.,* 2004)) and this was re-inforced by leaf litter fall data (Cotrufo *et al.,*

2005). Therefore, and in line with the original hypothesis, species was not tested in the percentage change response. This allowed 12 error degrees of freedom with which to examine the effects of CO_2, fertilisation and all interactions with block (the statistical model is given in table 3.1). The assumption that species may respond similarly appeared valid because residuals were normally and not binomially distributed. This approach allowed statistical interpretation of the influence of both elevated CO_2 and nitrogen fertilisation on autumnal senescence, while taking into account heterogeneous background environmental variables, at the expense of a statistical interpretation of the species responses, although this may still be visually inspected.

Table 3.1: The statistical model used to examine the influence of both elevated atmospheric CO_2 and nitrogen fertilisation upon autumnal senescence

Response	=	N	+	CO_2	+	Block	+	N*CO_2	+	N*Block	+	CO_2*Block	+	N*CO_2*Block	+	ε
df	=	1	+	1	+	2	+	1	+	2	+	2	+	2	+	12

The statistical model was based on the split-plot design of Tricker *et al.* (2005) which was used to overcome the heterogeneity at this site. The split-plot design had two levels of CO_2 (ambient and elevated) in separate plots within each of the three random blocks (plate 3.1), and two nitrogen fertilisation levels (N) (fertilised and not fertilised) in separate subplots within each plot of each block (see chapter one figure 1.1). As plot was the independent unit of replication $n = 3$ per treatment. All data were analysed using a general linear model analysis of variance (ANOVA) in Minitab 14.0, (Minitab Inc., Philadelphia) with the model (*xiv*):

$$\text{Response} = \text{Block}' \mid CO_2 \mid \text{N} \qquad (xiv)$$

This split-plot design meant that the effect of [CO_2] was tested against error MS[Block'*CO_2] with two error degrees of freedom. This results in the effect of [CO_2] being sought from average within-block differences and therefore it is not obscured by the natural heterogeneity between blocks (C. P. Doncaster, pers. comm.). This conservative analysis is limited by only having two denominator degrees of freedom; the power was increased by *post-hoc* pooling (Doncaster and Davey, 2006). Post-hoc pooling was planned for CO_2 effects where the error term of Block' x CO_2 yielded $P \geq 0.25$ against the

error MS (Underwood 1997). In these cases MS for CO_2 was then tested against the combined SS for ([CO_2*block $_{(2\ d.f.)}$] + [error $_{(12\ d.f.)}$]) with the resulting 1 / 14 degrees of freedom, so the pool MS can now be calculated as pool SS / 14. The F value for the response to CO_2 can now be calculated as CO_2 MS / pool MS with the numerator and denominator degrees of freedom being 1 and 14 respectively. N and N*CO_2 were both tested against a pooled error MS of [Block'*N + Block'*CO_2*N] with 4 error degrees of freedom. Again, if the pooled error MS of [Block'*N + Block'*CO_2*N] yielded $P \geq 0.25$ against the error MS, then both N and CO_2*N were tested by post hoc pooling against an error MS of [Block'*N + Block'*CO_2*N+ total error of sp'(N*CO_2*block')] (Tricker *et al.*, 2005; Doncaster and Davey, 2006). In the case of the percentage change data this gave 16 error degrees of freedom.

In the AspenFACE experiment a similar approach to the statistical analysis was adopted. For example, the CO_2 FACE rings and control plots at this site contain genotype combinations in experimentally fixed orders and can therefore be considered a sub-plot factor within the main treatment plot. The authors state that the block by treatment interaction should be tested in order to determine the appropriate error model structure (Dickson *et al.*, 2000). The Duke FACE experiment has also experienced the development of site heterogeneity over time, such that the pairing of FACE and control plots due to similarities at the onset of experimentation no longer appears valid. This was overcome in the statistical analysis by incorporating pre-experimentation plots characteristics as a covariate in the ANOVA (Schlesinger *et al.*, 2006). However, this approach may neglect any progressive influence of treatment upon these plot characteristics. For example, an increase in new soil carbon was observed in the elevated CO_2 plots at EUROFACE (Gielen *et al.*, 2005).

This split plot design can be considered conservative because although it may increase the likelihood of a type II error it substantially reduces the chance of the more dangerous false positive (Type I) error (Dytham 1999). This is because any statistical significance of treatment is now determined over that of natural background variation, whereas, when block remained untested it could not be determined if block heterogeneity drove the response and lead to type I error.

All percentage change values were negative; for the data to satisfy the assumptions of ANOVA they were made positive by first squaring and then taking the square root. These positive values were first divided by 100 so that all values lay between 0 and 1 and an arcsine transformation was performed. This transformation was carried out in Microsoft Office Excel. Given the limited statistical power of the small number of plots (n = 3) data were considered marginally significant for $P \leq 0.10$ (Ellsworth *et al.*, 2004) and significant for $P \leq 0.05$.

3.3.5.2 *Statistical analysis at each time point*

Within sub-plot replication allowed error degrees of freedom when the statistical model described above was used at each time point for each species. The mean value of the sub-plot canopy reflectance, which was used for the % change calculations, consisted of six replicate measurements of canopy reflectance in 2004 and four in 2003. Therefore, at each time point this replication within sub-plot allowed 60 and 36 error degrees of freedom respectively. The four replicate measures of LAI for each sub-plot allowed 36 error degrees of freedom. Because of this within sub-plot measurement replication all interactions with block could be tested against the error variation of Replicate' (Block'* CO_2*N). As pixel resolution from the aircraft data was such that number of pixels per sub-plot were greater than number of trees; pixels could not be independent measurements. Therefore during each independent time of flight mean NDVI per sub-plot was the true replicate value.

3.4 Results

3.4.1 Leaf area index

Autumnal decline of end season LAI for *P. x euramericana* was delayed in elevated CO_2 causing a stimulation in LAI of 30 - 35 % and 20 - 25 % at the end of five and six years growth when expressed relative to the ambient CO_2. A similar trend after six years of growth in elevated CO_2 resulted in late season LAI being stimulated by 10 % for *P. nigra*. The late season whole canopy decline in LAI is given in figure 3.2. This rate of change in canopy LAI is expressed as a percentage change in canopy LAI for each treatment relative to the canopy LAI measured at the end of August. In 2004 the rate of change in canopy LAI is calculated with respect to the value of LAI obtained on the 31st August (Julian Day 244) for both *P. x euramericana*, and *P. nigra*. In 2003 the rate of change in canopy LAI is calculated with respect to the value of LAI obtained on the 23rd August (Julian Day 236) for *P. x euramericana* only. For both species and both years the total decline of canopy LAI was reduced in elevated CO_2 at the last time of measurement. In all cases this appeared the result of a reduced rate of leaf loss in the elevated CO_2 exposed canopies, although some variation to this rate of decline was evident (see figure 3.2). The leaf only retention (estimated by LAI-WAI) was stimulated by between 20 - 80 % and 15 - 40 % following 5 and 6 years' growth of *P. x euramericana* in elevated CO_2 and between 5 - 20 % for *Populus nigra* (figure 3.3). This end season stimulation of leaf retention was significant in elevated CO_2 for the last time point in 2004 (01 - 03.11.04) ($F_{1,2}$ = 14.09, P = 0.06 when sought from within block differences prior to *post hoc* pooling; and $F_{1,14}$ = 12.36, P = 0.003, from post hoc pooling), but fertilisation had very little influence on this response, figure 3.3. In 2003, for *P. x euramericana* only, CO_2 stimulated end season leaf retention by between 25 - 100 % (mid October - early November respectively, see figure 3.3), but this stimulation was not significant. Site heterogeneity may account for this, however, as with no error degrees of freedom (only one species examined in that year) the CO_2 effect was tested against block'*CO_2 with only two degrees of freedom.

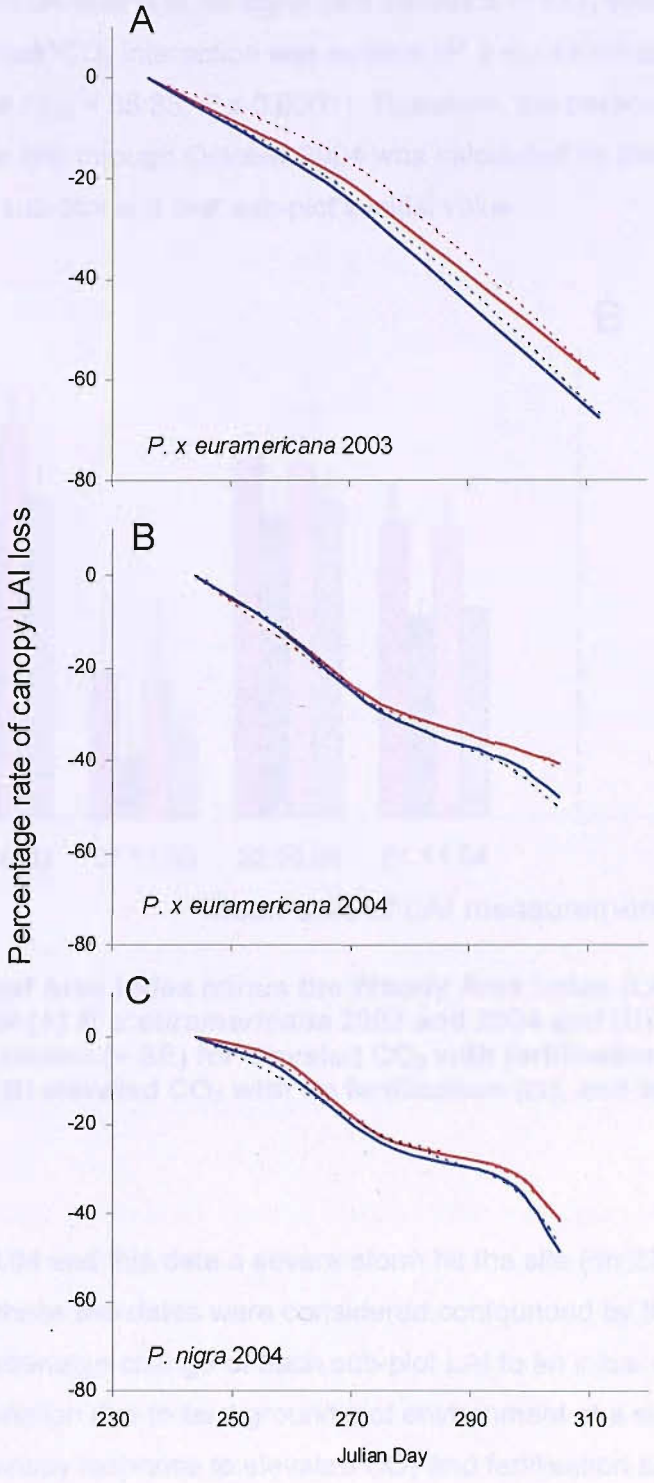

Figure 3.2: The percentage rate of decline in canopy LAI for canopies exposed to either elevated CO_2 with fertilisation (——), elevated CO_2 with no fertilisation (- - - -), ambient CO_2 with fertilisation (——) and ambient CO_2 with no fertilisation (- - - -). Figures (A) and (B) are for *P. x euramericana* in 2003 and 2004 respectively, and (C) is for *P. nigra* in 2004.

On mean date 01.10.04 their was no significant influence of CO_2 treatment on LAI, but a highly significant block*CO_2 interaction was evident (*P. x euramericana* $F_{2,36} = 51.8$, $P \leq 0.0001$ and *P. nigra* $F_{2,36} = 55.33$, $P \leq 0.0001$). Therefore, the decline in canopy leaf area index from this time and through October 2004 was calculated by the percentage reduction respective of each sub-plot and that sub-plot's initial value.

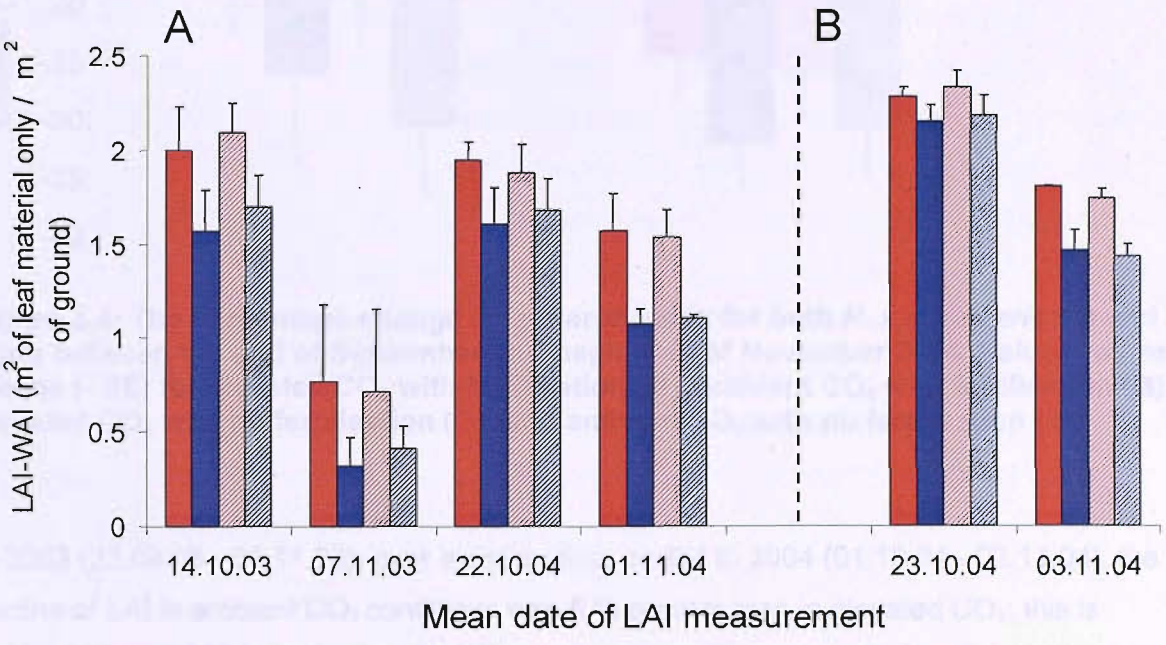

Figure 3.3: The Leaf Area Index minus the Woody Area Index (LAI - WAI) for the final two time points for (A) *P. x euramericana* 2003 and 2004 and (B) *P. nigra* 2004 only. Values represent means (+ SE) for elevated CO_2 with fertilisation (■), ambient CO_2 with fertilisation (■) elevated CO_2 with no fertilisation (▨), and ambient CO_2 with no fertilisation (▨).

Between the 14.09.04 and this date a severe storm hit the site (on 27.09.04), therefore changes between these two dates were considered confounded by the storm. By normalising the percentage change of each sub-plot LAI to an initial value of zero, any within treatment variation due to background plot environment at a single time point is reduced and the canopy response to elevated CO_2 and fertilisation across this autumn time period can be identified. The percentage change in canopy LAI throughout October 2004 was significantly reduced by elevated CO_2 ($F_{1,2} = 9.95$, $P = 0.088$ when sought from within block differences; $F_{1,14} = 5.93$, $P = 0.029$ from *post hoc* pooling), and fertilisation had little influence on this (figure 3.4).

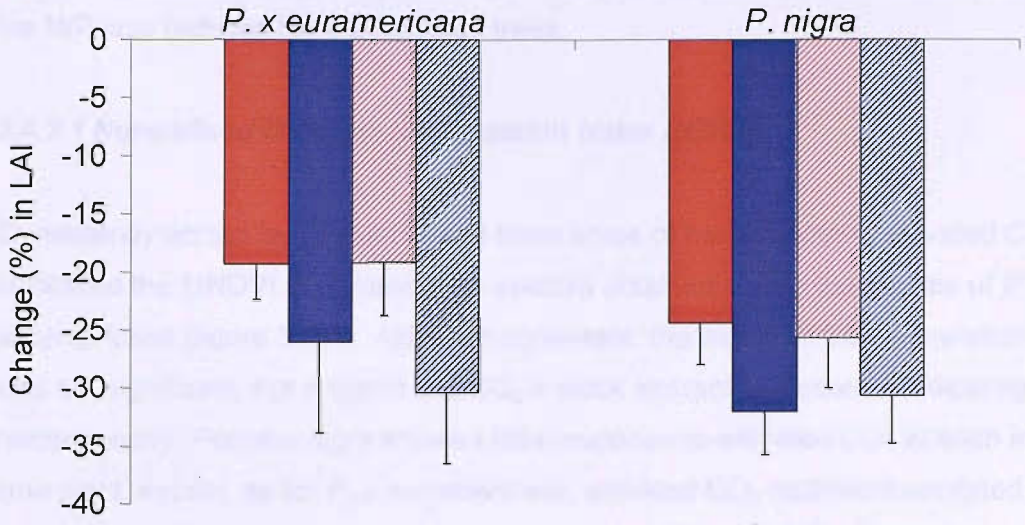

Figure 3.4: The percentage change in leaf area index for both *P. x euramericana* and *P. nigra* between the end of September and beginning of November 2004. Values represent means (- SE) for elevated CO_2 with fertilisation (■), ambient CO_2 with fertilisation (■) elevated CO_2 with no fertilisation (▨), and ambient CO_2 with no fertilisation (▨).

In 2003 (22.09.03 - 07.11.03), over a similar time period to 2004 (01.10.04 - 03.11.04), the decline of LAI in ambient CO_2 conditions was 6 % greater then in elevated CO_2; this is comparable to 2004 (see figure 3.4). However, this reduction was not significant but a highly significant block*CO_2 interaction was evident ($F_{2,2} = 677.44$, $P \leq 0.001$).

3.4.2 Canopy level spectral reflectance

Prior to interpreting the reflectance spectra derived from the canopy in the form of a vegetation index, a visual inspection of the mean canopy spectra (figure 3.5) can also be informative. In the two bands that are most informative about vegetation condition, the red and the NIR, an interesting species response to elevated CO_2 and autumnal senescence becomes apparent. For *P. x euramericana* (figure 3.5, A) increased reflectance in the NIR is evident in elevated CO_2 indicating increased leaf mass and/ or cellular integrity. For *P. nigra* (figure 3.5, C and D) the canopy in elevated CO_2 is characterised by decreased reflectance in the red band indicating increased chlorophyll content (Peñuelas and Filella 1998). Contrary to the spectra from *P. x euramericana* canopy, a decreased reflectance in

the NIR is evident for the CO_2 exposed P. nigra canopies. For both species reflectance in the NIR was reduced for the fertilised trees.

3.4.2.1 Normalised Difference Vegetation Index (NDVI).

Consistently across two autumns and three times of measurement, elevated CO_2 increased the MNDVI calculated from spectra obtained above the canopy of *P. x euramericana* (figure 3.6 A). Although consistent, the elevated CO_2 stimulation in MNDVI was not significant, but a significant CO_2 x block interaction occurred indicating large site heterogeneity. *Populus nigra* showed little response to elevated CO_2 at each individual time point, except, as for *P. x euramericana*, elevated CO_2 treatment exhibited the largest value of MNDVI at the latest time of measurement (figure 3.6 B). A significant CO_2 x block interaction was again apparent (table 3.2). Fertilisation had no significant effect on LAI during senescence, and little influence throughout the growing season (Liberloo *et al.*, 2006). However, at an individual time point of measurement in 2004, fertilisation was seen to significantly reduce MNDVI for *P. x euramericana* (23.10.04) and *P. nigra* (02.10.04) (figure 3.6 and table.3.2).

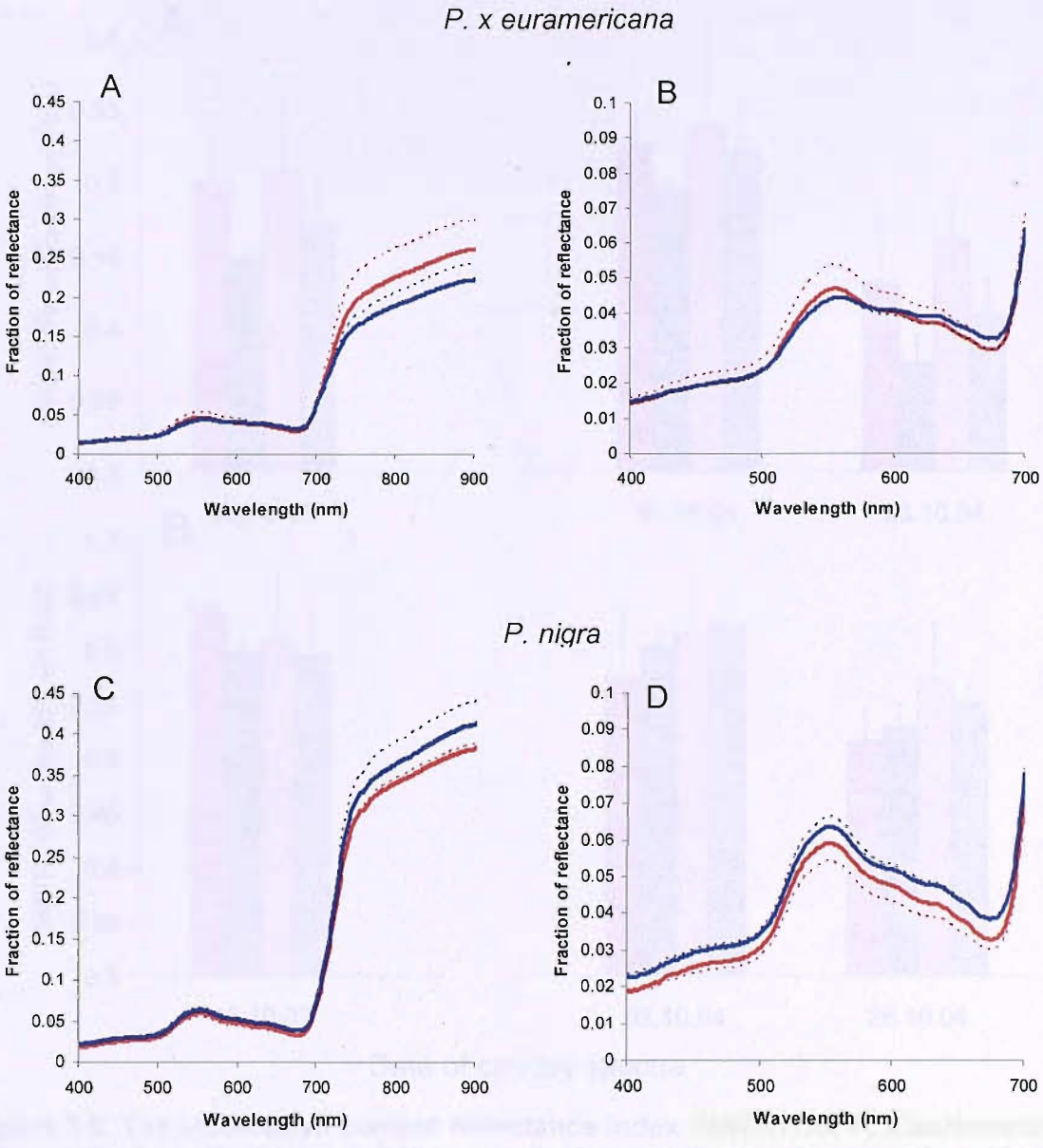

Figure 3.5: The fraction of reflectance between 400 and 900 nm obtained over the canopy of *P. x euramericana* (23.10.04) (A), and the spectral reflectance of just the visible portion (400 -700 nm) over the same canopy (B). The fraction of reflectance between 400 and 900 nm obtained over the canopy of *P. nigra* (26.10.04) (C) and the spectral reflectance of just the visible portion (400 -700 nm) over the same canopy (D). Reflectance spectra are for elevated CO_2 with fertilisation (——), elevated CO_2 with no fertilisation (- - -), ambient CO_2 with fertilisation (—) and ambient CO_2 with no fertilisation (- - -).

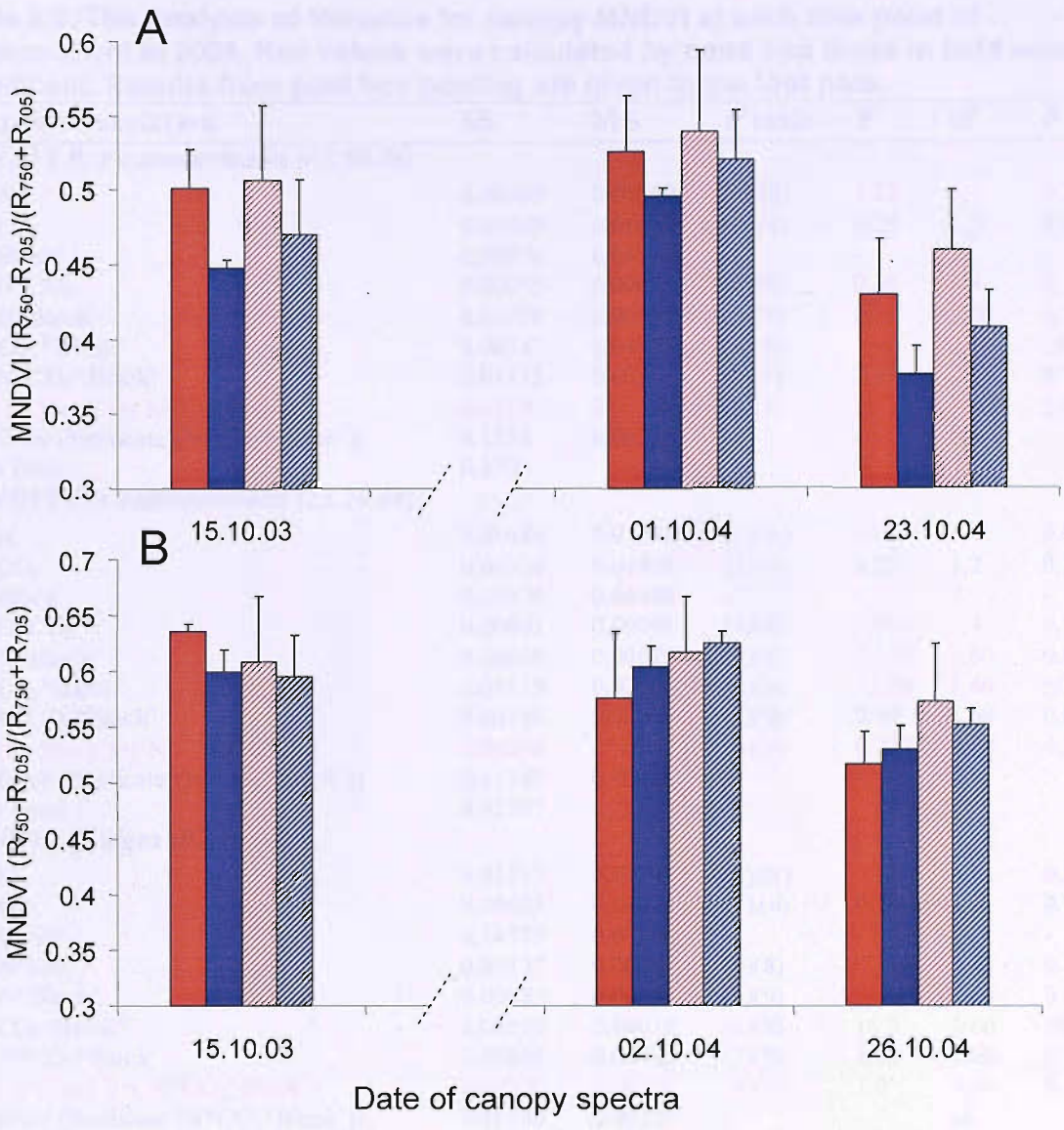

Figure 3.6: The chlorophyll content reflectance index (MNDVI) for *P. x euramericana* (A), and *P. nigra* (B) obtained at three single time points over two autumn periods. *X* axis crosses *Y* at 0.3, and values represent means (+ SE) for elevated CO_2 with fertilisation (■), ambient CO_2 with fertilisation (■) elevated CO_2 with no fertilisation (▨), and ambient CO_2 with no fertilisation (▨).

Table 3.2: The Analysis of Variance for canopy MNDVI at each time point of measurement in 2004. Red values were calculated by hand and those in bold were significant. Results from post hoc pooling are given in the foot note.

Source of variation	SS	MS	*F* ratio	*F*	df	*P*
MNDVI P. x euramericana (01.10.04)						
(1) N	0.00669	0.00669	(1)/(8)	1.22	1,4	0.30
(2) CO_2	0.01069	0.01069	(2),(6)	0.25	1,2	0.67
(3) Block'	0.09076	0.04538	-	-	2	-
(4) N*CO_2	0.00055	0.00055	(4)(8)	0.10	1,4	0.76
(5) N*Block'	0.01078	0.00539	(5)(9)	2.10	2,60	0.13
(6) CO_2*Block'	0.08547	0.04273	(6)(9)	16.7	2,60	**≤0.001**
(7) N*CO_2*Block'	0.01112	0.00556	(7)(9)	2.17	2,60	0.12
(8) (N*Block')+(N*CO_2*Block')	0.0219	0.00546	(8)(9)	2.13	4,60	**0.09**
(9) Error (Replicate'(N*CO_2*Block'))	0.1536	0.00256	-	-	60	-
(10) Total	0.370				71	
MNDVI P. x euramericana (23.10.04)						
(1) N	0.01684	0.01684	(1)/(8)	32.7	1,4	**0.005**[a]
(2) CO_2	0.04956	0.04956	(2),(6)	0.25	1,2	0.3
(3) Block'	0.08976	0.04488	-	-	2	-
(4) N*CO_2	0.00001	0.00001	(4)(8)	0.004	1,4	0.9[b]
(5) N*Block'	0.00058	0.00029	(5)(9)	0.156	2,60	0.86
(6) CO_2*Block'	0.05119	0.02560	(6)(9)	13.76	2,60	**≤0.001**
(7) N*CO_2*Block'	0.00149	0.00074	(7)(9)	0.40	2,60	0.67
(8) (N*Block')+(N*CO_2*Block')	0.00206	0.00052	(8)(9)	0.277	4,60	0.89
(9) Error (Replicate'(N*CO_2*Block'))	0.11165	0.00186	-	-	60	
(10) Total	0.32107				71	
MNDVI P. nigra (02.10.04)						
(1) N	0.01717	0.01717	(1)/(8)	72.3	1,4	**0.001**[c]
(2) CO_2	0.00625	0.00625	(2),(6)	0.16	1,2	0.73
(3) Block'	0.14779	0.07300	-	-	2	-
(4) N*CO_2	0.00177	0.00177	(4)(8)	0.75	1,4	0.44[d]
(5) N*Block'	0.00083	0.00041	(5)(9)	0.17	2,60	0.84
(6) CO_2*Block'	0.08020	0.04010	(6)(9)	16.9	2,60	**≤0.001**
(7) N*CO_2*Block'	0.00868	0.00433	(7)(9)	1.83	2,60	0.17
(8) (N*Block')+(N*CO_2*Block')	0.00950	0.00207	(8)(9)	1.0	4,60	0.41
(9) Error (Replicate'(N*CO_2*Block'))	0.14190	0.00237	-	-	60	
(10) Total	0.40450				71	
MNDVI P. nigra (26.10.04)						
(1) N	0.02737	0.02737	(1)/(8)	2.58	1,4	0.18
(2) CO_2	0.00029	0.00029	(2),(6)	0.02	1,2	0.89
(3) Block'	0.08259	0.04129	-	-	2	-
(4) N*CO_2	0.00540	0.00540	(4)(8)	0.5	1,4	0.52
(5) N*Block'	0.03831	0.01915	(5)(9)	8.15	2,60	**≤0.001**
(6) CO_2*Block'	0.02582	0.01291	(6)(9)	5.49	2,60	**0.006**
(7) N*CO_2*Block'	0.00411	0.00205	(7)(9)	0.87	2,60	0.42
(8) (N*Block')+(N*CO_2*Block')	0.04242	0.01060	(8)(9)	4.5	4,60	**0.003**
(9) Error (Replicate'(N*CO_2*Block'))	0.14104	0.00235	-	-	60	
(10) Total	0.32492				71	

[a]N pooled $F_{1,64} = 9.48$, $P =$ **0.003**
[b]N*CO_2 pooled $F_{1,64} = \leq 0.01$, $P = 0.94$
[c]N pooled $F_{1,64} = 7.26$, $P =$ **0.009**
[d]N*CO_2 pooled $F_{1,64} = 0.75$, $P = 0.39$

As for canopy LAI, the percentage change in canopy MNDVI through October 2004 was calculated in an attempt to reduce the contribution of both type I and type II errors. The percentage change in canopy MNDVI throughout October 2004 was significantly reduced by elevated CO_2 ($F_{1,2}$ = 252.17, P = 0.010 when sought from within block differences prior to *post hoc* pooling; and $F_{1,14}$ = 4.56, P = 0.05 from *post hoc* pooling). When MNDVI was measured as a percentage change, fertilisation was no longer significant; however, for *P. x euramericana* fertilisation appeared to increase the decline in MNDVI, whereas, for *P. nigra* in the elevated CO_2 treatment, fertilisation reduced this decline (figure.3.7) and in ambient CO_2 fertilisation appeared to have no influence.

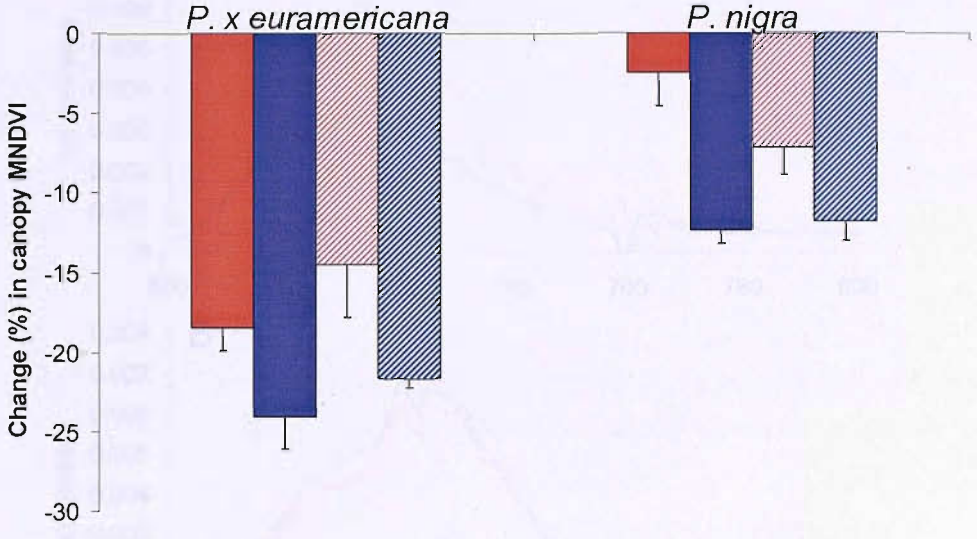

Figure 3.7: The percentage change in canopy MNDVI through October 2004. Values represent means (n=3) (- SE) for elevated CO_2 with fertilisation (■), ambient CO_2 with fertilisation (■), elevated CO_2 with no fertilisation (▨) and ambient CO_2 with no fertilisation (▨).

The classical vegetation index NDVI employed in global phenological research followed the same pattern of decline as MNDVI, however the percentage change over this time period was smaller, ranging from -6 % to -13 % for *P. x euramericana* and -1.8 % to -6 % for *P. nigra.* As for MNDVI the percentage change of NDVI was also significantly reduced by elevated CO_2 ($F_{1,2}$ = 15.68, P = 0.058 when sought from within block differences and $F_{1,14}$ = 6.08, P = 0.03 from *post hoc* pooling). Although not significant the influence of fertilisation was comparable to the influence on MNDVI (data not shown).

3.4.2.2 The first derivative spectra

The first derivative spectrum was calculated to identify features within the red edge that may be absent from both the reflectance spectra and reflectance indices (Zarco-Tejada *et al.*, 2003; Smith *et al.*, 2004). The first derivatives of the reflectance spectra reported in figure 3.5 are presented in figure 3.8.

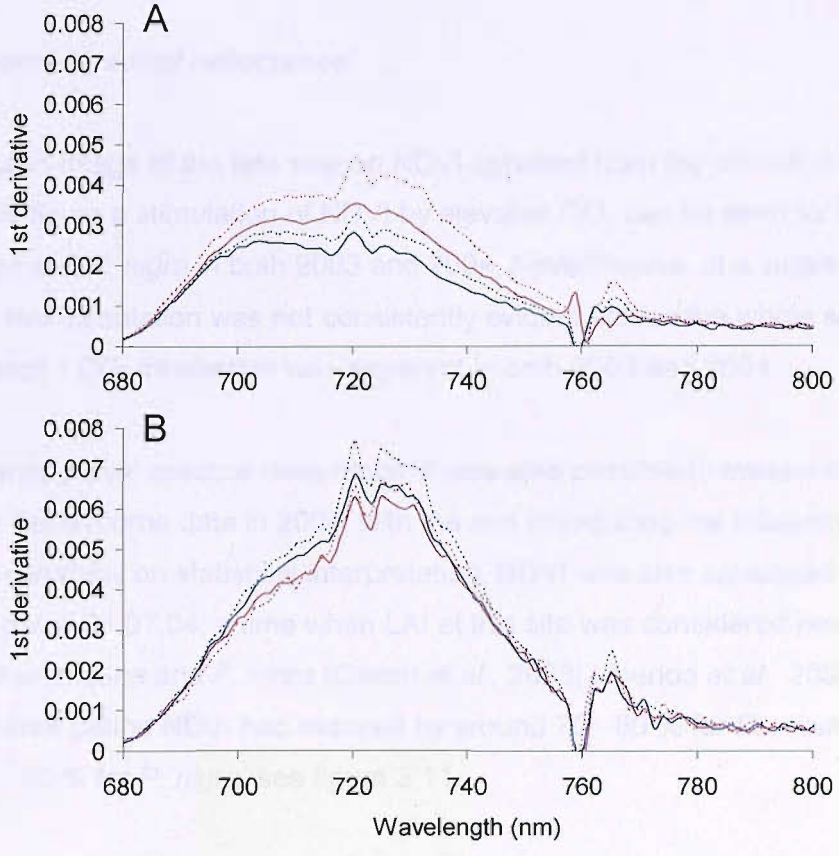

Figure 3.8: The first derivative spectra between 680 and 800 nm of the reflectance spectra obtained above the canopies of (A) *P. x euramericana* and (B) *P. nigra* on 23.10.04 and 26.10.04 respectively. Derivative spectra are for elevated CO_2 with fertilisation (—), elevated CO_2 with no fertilisation (- -), ambient CO_2 with fertilisation (—) and ambient CO_2 with no fertilisation (- -).

At this late time point in senescence it can be clearly seen that the wavelength at which the maximum value of the derivative spectrum occurs is always at the same position (720 nm) irrespective of species or treatment. Therefore, the blue shift of the peak of the derivative spectrum associated with stress is absent here and will not be informative as to

the progression of senescence. However, features within the derivative spectra may contribute information related to canopy stress (Smith *et al.,* 2004; Zarco-Tejada *et al.,* 2003). Using the technique employed by Curran and Kupiec (1995) and data from chapter two of this thesis, the value of the derivative spectra at 729 nm was identified to best represent chlorophyll content of poplar. In response to this, the percentage change in the derivative spectra at 729 nm was calculated during October 2004. Although this change was reduced in elevated CO_2 for *P. x euramericana*, no difference between treatments was seen for *P. nigra* and treatment effect was not significant (data not shown).

3.4.3 Airborne spectral reflectance

A false coloured image of the late season NDVI obtained from the aircraft is given in figure 3.9. From this figure a stimulation of NDVI by elevated CO_2 can be seen for both *P. x euramericana* and *P. nigra* in both 2003 and 2004. Nevertheless, at a single time point in senescence this stimulation was not consistently evident across the whole site and a significant block * CO_2 interaction was apparent in both 2003 and 2004.

As for the canopy level spectral reflectance, it was also possible to measure the change over time for the airborne data in 2004, with the aim of reducing the influence of background variability on statistical interpretation. NDVI was also calculated from an earlier flight dated 31.07.04, a time when LAI at this site was considered near maximal for both *P. x euramericana* and *P. nigra* (Gielen *et al.,* 2003; Liberloo *et al.,* 2005). Over this three month time period NDVI had reduced by around 70 - 80 % for *P. x euramericana* and between 40 - 50 % for *P. nigra*, see figure 3.11.

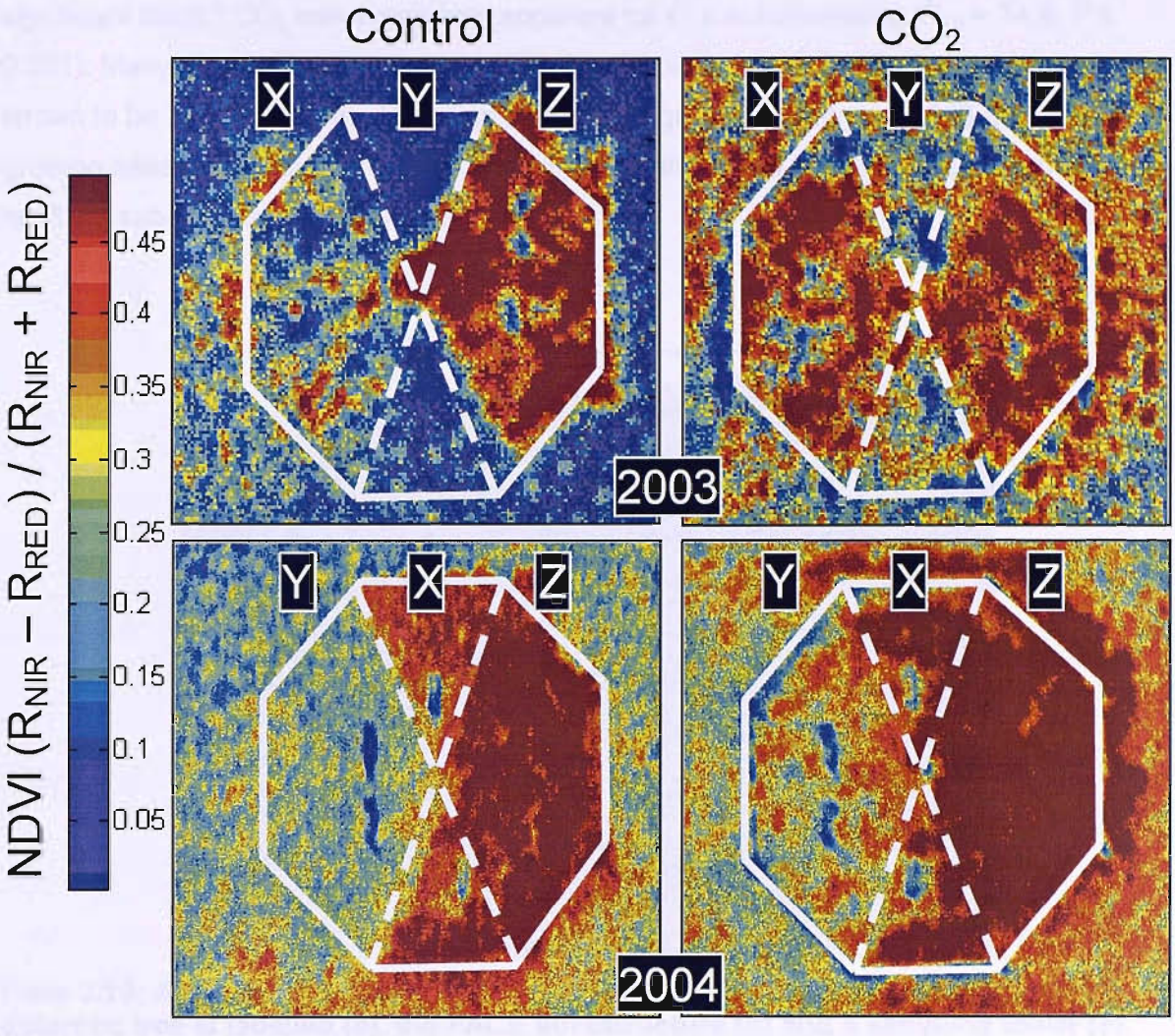

Figure 3.9: The NDVI (R_{NIR} - R_{red}) /(R_{NIR} + R_{red}) measured using a wide bandwidth multispectral camera from a Sky Arrow aircraft on 1st November 2003 and 25th October 2004. NDVI is represented for *P. nigra* (x) and *P.x euramericana* (y) in both years and treatments, also shown is NDVI of *P. alba* (z).

Using the statistical model previously described for the percentage change data, and following arcsine transformation, the residuals were not normally distributed and a binomial distribution was apparent. This binominal distribution was the result of segregation between individual species responses; a response not apparent for the smaller temporal and spatial resolution of other measurements. In this case, each species was tested independently in the statistical model and nitrogen excluded, so allowing 6 error degrees of freedom and the arcsine transformed data were now normally distributed. At this larger spatial and increased temporal resolution, when compared with canopy level reflectance, treatment did not significantly influence the decline in NDVI for *P. nigra*. However, a highly

significant block'* CO_2 interaction was apparent for *P. x euramericana* ($F_{2,6}$ = 74.8, P ≤ 0.001). Many trees within the elevated CO_2 plot of block 3 (plot 5; see figure 3.1) were known to be highly chlorotic a process that has progressed during the 2003 and 2004 growing seasons. Plate 3.10 shows an example of individual chlorotic trees taken from a fertilised sub-plot located within plot 5.

Plate 3.10: A fertilised sub-plot within the FACE plot number 5. An individual chlorotic tree is labelled (*a*), the FACE infrastructure (*b*) and a sampling tower (*c*).

As it was not possible to avoid these diseased trees from the aircraft images (as it was for ground level data) subsequent analysis of the aircraft NDVI data was carried out with the removal of block 3. This resulted in reducing the site heterogeneity, and removing the significance of the block*CO_2 interaction ($F_{1,4}$ = 0.02, P = 0.890). At this lower replication (n = 2) elevated CO_2 significantly reduced the decline in airborne NDVI for *P. x euramericana* ($F_{1,1}$ = 1501.36, P = 0.016) (figure3.11).

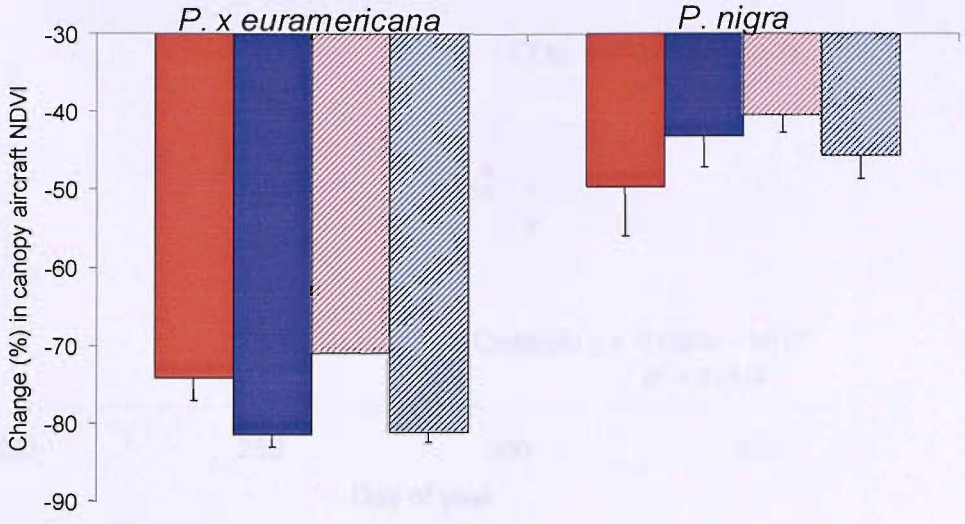

Figure 3.11: The percentage change in canopy NDVI (R_{NIR} - R_{red}) / (R_{NIR} + R_{red}) calculated from the airborne spectral reflectance obtained on 31st July 2004 and 25th October 2004. *X* axis crosses *Y* at -30 %, and values represent means (*n* = 2) (- SE) for elevated CO_2 with fertilisation (■), ambient CO_2 with fertilisation (■), elevated CO_2 with no fertilisation (▨) and ambient CO_2 with no fertilisation (▨).

3.4.4 Estimating GPP

The linear regression between LAI and day of year was calculated using the final three (*P.* x *euramericana* 2003 and *P. nigra* 2004) or four (*P. x euramericana* 2004) time points of LAI measurements obtained at and after bud set. This regression equation was used to estimate the number of days difference between CO_2 treatments for a decline of 50 % in LAI. The regression for *P. x euramericana* LAI taken in 2004 is given in figure 3.12 as an example of this process. Elevated CO_2 treatment resulted in a 5 and 15 day delay in a 50 % reduction of canopy LAI for *P. x euramericana* in years 2003 and 2004 respectively, while in 2004 a 12 day delay was calculated for *P. nigra*.

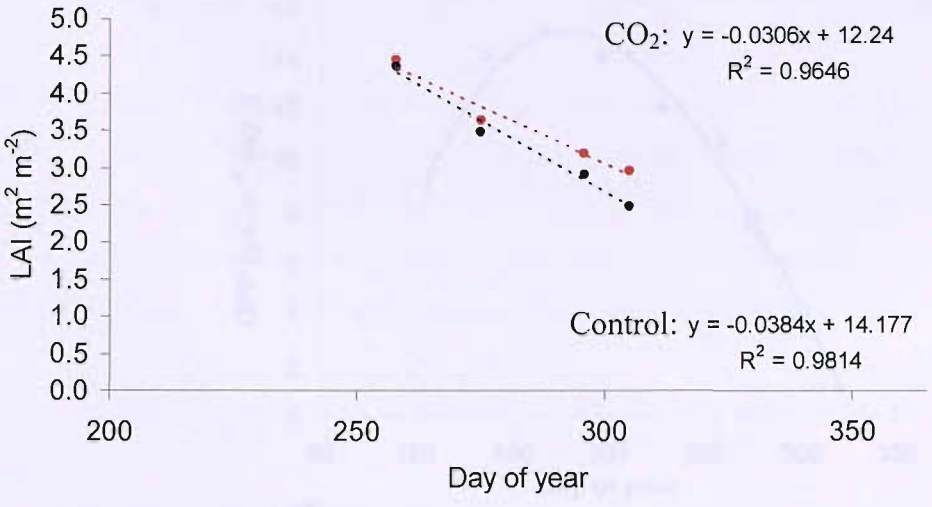

Figure 3.12: The linear regression between LAI and day of year for *P. x euramericana* during the end of the 2004 growing season. The linear best fit line for LAI values taken in elevated CO_2 is represented by (- -) and for LAI values taken in ambient CO2 by (- -). The coefficient of determination (r^2) and regression equations are reported for both treatments.

Over six years of exposure to elevated CO_2 and two years of data, a mean delay in senescence for *P. x euramericana* was estimated to be 10 days. The start of this 10 day delay can be approximated from the divergence in decline of LAI, which in 2004 was day 275 (as seen in figure 3.2). When this 10 day delay initiated on day 275 was modelled using the data from Wittig *et al.* (2005), a 2 % increase in GPP could be predicted. These modelled data are presented in figure 3.13.

A

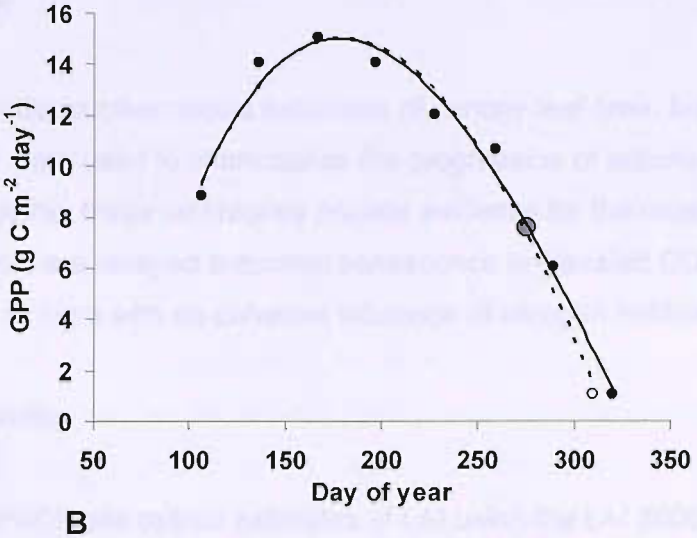

B

Consequence of 10 days delayed senescence
0. 55 t C ha^{-1} (2.04 % increased GPP)
2. 02 t CO_2 equivalents ha^{-1} (GPP)
1. 21 t CO_2 equivalents ha^{-1} (NPP)

Figure 3.13: (A) The GPP for a *P. x euramericana* canopy growing under 550 ppm [CO_2] from the data of Wittig *et al* (2005) (—). The effects of altering the rate of decline in LAI and consequently senescence are shown. The decline in LAI reported here diverged at day 275 (●), and in ambient CO_2 (- - -) senescence was considered advanced by 10 days when compared with senescence in elevated CO_2. (B): Also reported is the influence of this delay calculated as the % difference under each curve, assuming NPP is 60 % of GPP as reported for this site in Wittig *et al* (2005).

3.5 Discussion

In this chapter non-destructive optical estimates of canopy leaf area, leaf retention and chlorophyll content were used to characterise the progression of autumnal senescence in elevated CO_2. Together these techniques provide evidence for the most important findings of this chapter, which is a delayed autumnal senescence in elevated CO_2 for both *P. x euramericana* and *P. nigra* with no coherent influence of nitrogen fertilisation.

3.5.1 Leaf area index

At the POP/EUROFACE site optical estimates of LAI using the LAI 2000 have shown to be a reliable estimator of LAI when compared to that determined allometrically (Liberloo *et al.*, 2004). The end season stimulation in optical values of LAI was not confounded by aboveground woody biomass. This is because upon subtraction of this factor the stimulation in LAI was still apparent and significant. During the first three years of growth independent confirmation of this is provided by Cotrufo *et al.* (2005) theses authors identified an earlier autumnal leaf fall for the control canopy relative to the elevated CO_2 exposed canopy. The number of day's difference for a 50 % decline in LAI relative to the bud-set value of LAI was taken as an estimate of the time difference for the progression of senescence in either elevated or ambient CO_2. This difference was estimated to be either 5 days in 2003 or 15 days in 2004 for *P. x euramericana* and 12 days in 2004 for *P. nigra.*

3.5.2 Canopy level Vegetation Indices

For both species the canopy reflectance indices of MNDVI and NDVI showed a similar response to elevated CO_2 during the autumn with the change in both indices being significantly reduced. This elevated CO_2-stimulated reduction was more evident for the MNDVI which is considered more sensitive, than the NDVI, to a wide range of chlorophyll content (Gamon and Surfus, 1999). The NDVI is considered to be more of an integrated measure of green biomass that is saturated by low chlorophyll content (Sims and Gamon, 2002). At each time of measurement the influence of elevated CO_2 on MNDVI was not apparent for *P. nigra*, whereas for the earlier senescing species *P. x euramericana* MNDVI was stimulated by elevated CO_2 at each time of measurement for both years. This stimulation was not significant but there was a significant interaction of block with CO_2

treatment at every time of measurement for both species. Fertilisation significantly reduced the MNDVI at the end of October for *P. x euramericana* whereas the same effect of fertilisation was observed at the beginning of October for *P. nigra*. This may account for the apparent species-specific influence fertilisation has on the percentage change of MNDVI. In elevated CO_2, fertilisation appears to stimulate senescence for *P. x euramericana* and delay it for *P. nigra* relative to the unfertilised CO_2 treatments.

To determine the influence of elevated CO_2 on autumnal senescence it appears justified to account for site heterogeneity by expressing the percentage change of each replicate plot. The unidirectional progression of autumnal senescence overtime allows for this process, and the absence of block interactions with treatments validates this process.

3.5.2.1 The derivative spectra

The derivative spectra exhibit multiple peaks with a maximum peak at 720 nm for all treatments and species. However, these derivative spectra differ in the values of the first derivative at a given wavelength, and therefore the gradient of the maximum inflection point within the red edge and not the REP appears influenced by treatment. The multiple peaks display a pattern remarkably similar to that observed by Smith *et al.* (2004) over an experimental grass land. Stress induced by root anoxia of this grass resulted in a reduction in the peak at around 725 nm and a relative increase in the broad shoulder at 702 nm. This "double peak" shift was also documented by Zarco-Tejada *et al.* (2003) when a canopy of *Acer* was exposed to heat and humidity stress, and correlated strongly with steady-state fluorescence. The authors concluded that the change in the double peak was the result of a stress induced decline in natural steady-state fluorescence and a shift towards increased plant heat production to dissipate excess energy. The first derivative spectra for *P. x euramericana* would indicate that the ambient CO_2 and fertilised treatment is the most stressed, elevated CO_2 the least and both elevated CO_2 with fertilisation, and ambient CO_2 in-between (figure 3.8), which is precisely the order of decline in MNDVI (figure 3.7).

3.5.3 *Whole site NDVI*

The broadband NDVI taken from airborne images (figure 3.9) was obtained over a far greater spatial range that the canopy level measurements. Furthermore, when measured from nadir, spectra will be mostly influenced by top canopy leaves and the contribution from mid canopy leaf density will be lost and the soil background increased. The canopy level spectral assessment taken at 45° from nadir will sample reflected light from shade leaves and so integrate a greater portion of the canopy than that obtained by the aircraft. At this spatial range site heterogeneity was very apparent and was the only significant feature. The inclusion of diseased trees (figure 3.10) will also contribute to this heterogeneity, nevertheless when such features were taken into account and considering the temporal range from peak growing season to late senescence, a significant reduction in the senescence induced decline of NDVI was evident for *P. x euramericana*.

3.5.4 *Estimating GPP*

By using a combination of both photosynthetic and phenological data form a mature Oak forest in the U.K., Morecroft *et al.* (2003) suggest that climatic conditions during the autumnal period, such as lower irradiance, have the result that changes in the timing of autumnal phenology have a smaller impact on forest carbon balance than changes in spring time phenology. However, for a short rotation coppice poplar and using $^{14}CO_2$, Nelson and Isebrands (1983) identified that late season leaf retention exhibited photosynthetic rates high enough to contribute important quantities of photosynthate for radial stem growth, root growth and reserve storage in the stems and roots, and so could be considered to influence NPP. Both *P. nigra* and *P. x euramericana* showed a significant increase in standing root biomass in elevated CO_2, with substantial peaks observed in November (Lukac *et al.,* 2003). The significant delay in autumnal decline of LAI documented here may offer an explanation for the end season increased root biomass of these species, which was more evident when growing in elevated CO_2.

Extended functionality of the canopy will be important for any autumnal increase in GPP in elevated CO_2 relative to ambient. Although functionality was not directly measured in this chapter, both the percentage change in canopy level MNDVI and NDVI were significantly reduced by elevated CO_2. The question therefore arises "is the relatively delayed decline

in canopy chlorophyll content in elevated CO_2 simply the result of a greater number of leaves with the same individual chlorophyll content as the leaves in ambient CO_2 or is it the result of individual leaves having relatively more chlorophyll content in elevated CO_2?" Although the LAI data reported here indicate greater leaf retention in elevated CO_2 the answer to this question will be further explored in chapter four. The answer is important in determining the influence elevated CO_2 has on the progression of senescence, but does not necessarily affect the autumnal GPP, because with respect to species specific and environmental variables, gross canopy chlorophyll content will influence GPP irrespective of how it is maintained. During the first three years of growth, elevated CO_2 significantly increased the cumulative GPP (g C m^{-2}) of *P. nigra* and *P. x euramericana* by 17 and 25 % respectively (Wittig *et al.,* 2005). Taking the daily integrated GPP obtained from a closed canopy (year 2001) from Wittig *et al.* (2005), a delay in senescence of 10 days for *P. x euramericana* under such conditions would contribute approximately 2 % to the season GPP. Support for this may come from the canopy MNDVI measurements and also a significant stimulation of both $V_{c,max}$ and J_{max} for *P. nigra*, measured on 6th November 2004 (*P. x euramericana* was not measured) (Taylor *et al.,* 2007 *in submission*). Light saturated photosynthesis was also measured for *P. x euramericana* (between 01.09.03 and 03.09.03) when all buds were visibly closed and a stimulation in elevated CO_2 was evident (Tricker *et al.,* 2005)

3.5.5 Summary

In summary, this chapter identifies a delay of autumnal senescence for two *Populus* species growing in elevated atmospheric CO_2. This delay was consistent over two years but stronger evidence is provided by the repeated sampling in 2004 providing a mechanism to identify the CO_2 effect against a high degree of background environmental heterogeneity. In this chapter an attempt to understand the significance of this delay on GPP was undertaken and this provided evidence of an estimated 2 % increase in GPP. However, on a cautionary note, over multiple seasons a functionally extended canopy later in the autumn may not always have a positive impact upon gross season GPP. In the AspenFACE experiment a delayed bud-set and leaf fall was observed for *P. tremuloides* exposed to elevated CO_2 (Karnosky *et al.,* 2003). This resulted in dormant season die back of the terminal buds and branches that were exposed to frost prior to senescence and adequate frost hardening (Isebrands *et al.,* 2001). This dieback was most apparent for

aspen clone 271 (Isebrands *et al.,* 2001), which is also the clone observed to exhibit the greatest response to an elevated CO_2 delay in senescence (Karnosky pers. comm.). Furthermore, on a global scale, an extended growing season, although providing an increased sink for atmospheric CO_2 (Keeling *et al.,* 1996) may actually have a detrimental effect in mitigating global warming due to decreasing surface albedo (Betts, 2000).

Chapter 4:

Canopy senescence assessed at the leaf level

4.1 Overview

Non-destructive estimates of vegetation features such as chlorophyll content and LAI are very valuable in senescence research. This is because such estimates give values that are integrated over whole heterogeneous canopies, as documented in chapter three. However, equally valuable in understanding the influence that elevated CO_2 has on senescence is destructive sampling at the leaf level. This allows quantitative data to support or contradict the non-destructive estimates of canopy senescence and therefore develop our understanding of this process. In this chapter both SLA and leaf nitrogen as a percentage of leaf dry mass (N_{mass}) will be measured, as will leaf chlorophyll content. As SLA and N_{mass} are negatively associated with leaf longevity (Reich *et al.,* 1997; 1999), the influence elevated CO_2 has on these variables during the end of the season can be explored through destructive sampling. Furthermore, direct chemical extraction of leaf chlorophyll content provides a quantitative measure of senescence progression in elevated CO_2. As canopy spectral properties are the sum of multiple leaves and background variables it is important to understand the spectral properties of individual leaves in the absence of background variables, to determine the influence such leaves have on the integrated canopy spectra. In this chapter spectral reflectance and transmittance will also be determined for senescent leaves from the POP/EUROFACE site.

4.2 Introduction

Leaf senescence occurs throughout the growing season in an attempt to optimise the canopy nitrogen profile in relation to canopy irradiance profile, and so maximise photosynthetic nitrogen use efficiency (PNUE). This process is termed leaf turnover rate, in which leaves with a decreased PNUE (shaded or old leaves) senesce to allow N to be recycled to younger upper canopy sun leaves, so optimising canopy PNUE (Hikosaka, 2005). Old leaves are also considered an alternative N source for sink metabolism when N uptake from roots does not meet the demand from sinks. Leaf turnover rate is therefore a consequence of environmental factors such as shading and N availability (Hikosaka 2005), but also a consequence of genetically determined developmental aging (Buchanan-Wollaston *et al.,* 2003). At the end of the growing season, as environmental variables decrease photosynthetic potential, leaf senescence results in an attempt to conserve and re-cycle nutrients such as N and P for the next growing season. This form of senescence also results in the seasonal dormancy of deciduous trees as a mechanism to survive detrimental environmental variables via a temporary cessation of bud growth (Taiz and Zeiger, 2002) and this process can be termed autumnal senescence as opposed to leaf turnover rate. Leaf life span in relation to leaf N is confusing, because on one hand physiological experimentation identifies N deficiency as accelerating senescence (Wingler *et al.,* 2004); whereas large scale ecological observations indicate that leaf N_{mass} declines with increasing leaf longevity (Reich *et al.,* 1997). Using canopy models Hikosaka (2003) neatly solves this discrepancy and identifies one complexity in experimentation with senescence, namely temporal resolution. By with-holding N to a plant and so reducing N uptake rate, leaf longevity rapidly decreases and senescence is advanced. However, over time (approx 200 days), leaf longevity increases to a greater amount at this lower N uptake rate, than was previously identified at the higher N up-take rate. Hikosaka (2003) explains this to result from an initial decline in canopy LAI upon N depletion (increased leaf senescence) to a new steady-state level of a lower LAI with increased leaf longevity. Moreover, a positive relationship between leaf N_{mass} and SLA is apparent and a decline in both is associated with increasing leaf longevity (Reich *et al.,* 1997; 1999, Wright *et al.,* 2004). Although decreased SLA is strongly associated with decreased N_{mass}, it is also associated with increased leaf N_{area}. N content per unit leaf mass is reduced but per unit leaf area N content is increased (Hikosaka *et al.* 2005). Therefore factors that determine SLA and leaf C:N balance appear to influence leaf longevity. Whether SLA is determined

by increased leaf mass per unit leaf thickness or simply thicker leaves may also be important, as internal leaf CO_2 diffusion will be affected and may influence photosynthetic rate.

Under controlled conditions reflectance spectroscopy can yield more information about individual leaves than is possible at the whole canopy level. This becomes possible through the measurement of radiation that is both reflected from and transmitted through the leaf. Most visible radiation is absorbed by leaf pigments and so little is reflected or transmitted (Jackson 1986). Of the radiation that is absorbed some may be rapidly released as fluorescence, so contributing to that reflected, or more slowly as long wave thermal emission (Gammon and Qiu, 1999). A large portion of the NIR is diffused and scattered by the mesophyll cells. Here multiple reflections and refractions at the interface between hydrated mesophyll cells and airspaces scatter NIR upwards out of the leaf, designated reflected NIR the remainder is scattered downwards and designated transmitted NIR, very little if any is absorbed (Jackson 1986). Therefore changes in the absorption of radiation by leaves during senescence can be examined across the visible and into the NIR using the assumption that radiation in this range is either reflected, transmitted or absorbed (Jackson, 1986; Merzlyak *et al.,* 2004). As the thermal radiation exists at wavelengths longer than those measured in this chapter (3000 - 20, 000 nm) it is not considered to influence the spectra between 400 - 1100 nm. Nevertheless this thermal radiation would be a very important factor to take into account for future work on elevated CO_2 and senescence inorder to identify the influence of stomatal conductance and leaf temperature.

4.3 Materials and methods

4.3.1 Leaf selection

Ten trees were selected for each of *P.* x *euramericana* and *P. nigra* in each sub-plot of the experimental plots at the POP/EUROFACE site (see chapter three) on 24th September 2003. At this time the *P. x euramericana* buds had set and no new leaf production was evident in *P. nigra*. The stem, above the tenth leaf down, counted from the first leaf not associated with the apical bud, was labelled as a reference. The next leaf proximal to the apical bud from this reference was considered leaf nine, then leaf eight etc. Main stems and co-dominant lateral branches were selected such that the labelled leaf ten was a uniform height (approx 0.3 m) from the canopy top across all treatments and not shaded by the canopy. In 2004 twenty stems were selected on the 14th September and labelled in accordance with the system used in 2003. In 2003 all leaf level analyses were carried out on leaf nine selected from only two of the three blocks; block three was omitted for logistical reasons. In 2004 leaves nine to eleven were selected, at each time of harvest the same leaf number was selected across all treatments and all three blocks were used.

4.3.2 Sampling for leaf spectral measurements

Harvesting for leaf spectral measurements was only carried out during 2004. A minimum of six leaves from each sub-plot were sampled at each harvest and there was a minimum time of 30 minutes between sampling and the end of spectral measurements. Samplings took place on 19.09.04, 3.10.04, 18-19.10.04 and 1.11.04 for *P. x euramericana* and 20.09.04, 4.10.04, 21.10.04, and 30-31.10.04 for *P. nigra*. When sampling took place over two days this was to increase replication so that $n = 9$ per sub-plot on these days. In a pilot experiment, the potential of the 30 minute time delay between harvesting and completion of the spectral measurements was carried out. This was done in order to identify any possible influence on the leaf spectra of the length of time after harvest. A time course of spectral reflectance and transmittance was carried out on one single randomly selected green *P. x euramericana* leaf. Six measurements of both transmittance and reflectance were obtained 20 minutes after harvest. Ten minutes also elapsed between the first and last of the six measurements. In response to results from this time course, the petioles of

all leaves subsequently sampled for the spectral analysis were immediately re-cut under water and remained under water until all spectral measurements were obtained. As autumnal senescence is a unidirectional process over time the whole site was aimed to be sampled within one day to avoid an additional day of year influence at each time of sampling. As a result of this, and to reduce any diurnal factors confounding the spectral measurements, three replicate leaves were sampled from each sub-plot once in the time period between 07.30 and 12.00 and again between 12.30 and 18.00, on each single day.

4.3.3 Leaf level spectral assessment

Irradiance transmitted and reflected from individual leaves was measured using a GER 3700 spectroradiometer (GER, Buffalo, NY, USA. Mod. 3700). The spectroradiometer was attached to an integrating sphere (Macam Livingston Scotland UK) via a light proof seal. This was achieved using a one meter fibre optic with a 23° field of view. This integrating sphere contains three entrance ports and a movable light source attached to a fourth entrance port with a slide operated opening between light source and sphere. At all times irradiance from within the sphere was sampled via the fibre optic cable attached to the sphere via a port positioned at 90° to the light source and all other ports remained closed (see plate 4.1, A). The irradiance transmitted or reflected from a leaf was measured relative to that which originated from the light source which was maintained at six volts, and provided approximately 100 µmol m^{-2} s^{-1} of PAR.

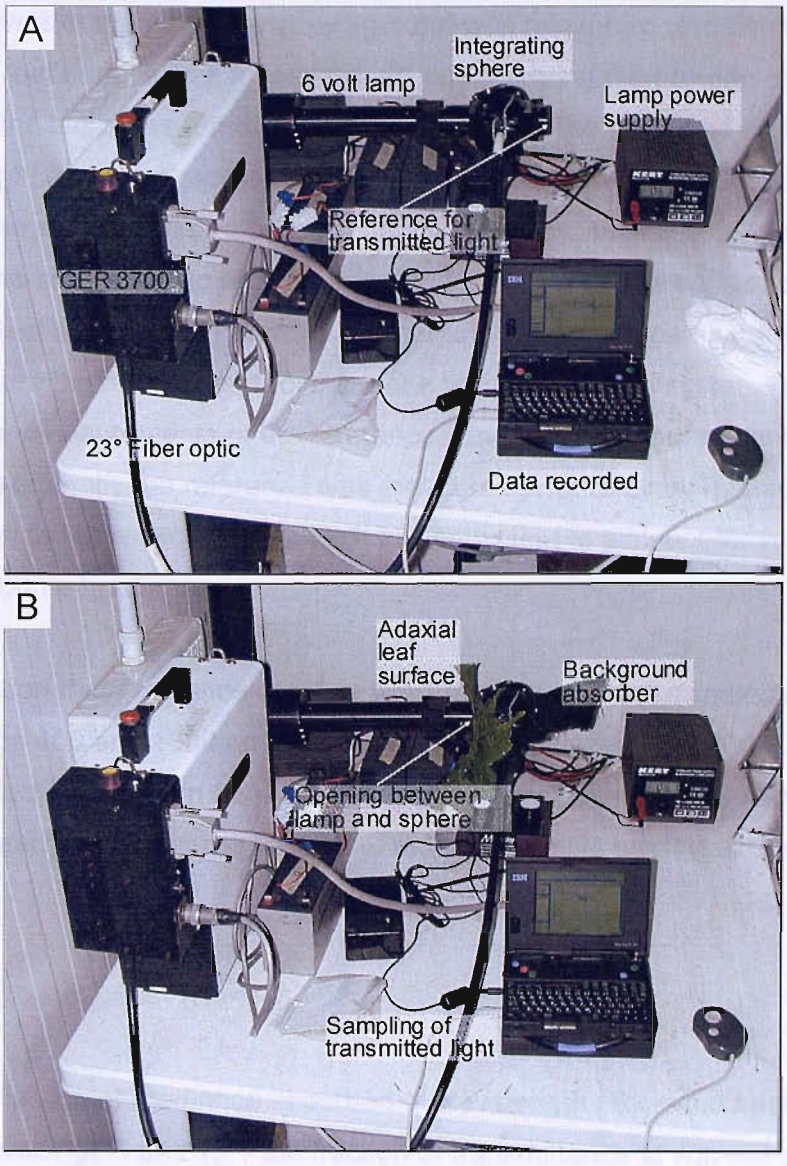

Plate 4.1: The equipment set up for measuring reflected and transmitted irradiance from *Populus* leaves at EUROFACE site during the autumn of 2004. The closed system used to measure the reference radiance prior to measuring leaf transmitted irradiance (A), and for measuring leaf transmitted irradiance (B) are shown.

Irradiance transmitted through the leaf was measured using the set up shown in plate 4.1 (A) and (B). Plate 4.1 (A) shows how the light source (labelled 6 volt lamp) was initially sampled from within the sphere after contact with the inner white coating of the closed port parallel to the light source (labelled reference for transmitted light). As shown in plate 4.1 (B) this reference port was then removed and the opening blocked with a black fabric absorber (≈ 100 % absorption) and a leaf was placed between the light source and the integrating sphere via the slide operated opening (approx. 10 mm diameter) with the adaxial leaf surface facing the light source. In this way only light that was transmitted

through the leaf was sampled and any background was minimised. Irradiance reflected from the adaxial leaf surface was measured without changing the position of the fibre optic. However, the lamp was removed and re-attached to the port used as the reference for transmitted light and the absorbent black material was then placed over the original lamp position. The sampling fibre optic was now situated between the light source and the slide opening. The slide opening allowed a leaf to be placed on the surface of the sphere with the adaxial leaf surface facing inward or alternatively a white card was placed in this position to measure the reference irradiance. The variability of this system was first tested by taking multiple measurements of the references used for both leaf transmittance and reflectance. Subsequently the reference was measured prior to every measurement of irradiance transmitted or reflectance by each individual leaf to account for very small changes in the source irradiance.

With the assumption that irradiance is either absorbed, transmitted or reflected by the leaf between the range 400 and 1000 nm (Jackson, 1986; Merzlyak *et al.,* 2004), the absorbed light was calculated as shown in (*xv*). Further to observing these gross spectral changes through time for each treatment the fraction of reflectance data was taken and the MNDVI (*vi*) calculated.

$$A_{(i)} = 1 - (R_{(i)}+T_{(i)}) \qquad (xv)$$

where $A_{(i)}$ = the fraction of irradiance absorbed at wavelength *i* $R_{(i)}$ = the fraction of reflectance at wavelength *i* and $T_{(i)}$ = the fraction of transmittance at wavelength *i*.

4.3.4 Chlorophyll analysis

In 2003 three leaves were selected in each sub-plot of two blocks (block 1 and 2) on 26th September and again on 16th October except on this latter date for *P. x euramericana* only one labelled leaf existed in the fertilised sub-plot of control plot number three. Almost immediately a disc of known area was taken from the middle of the basal intervienal area of each leaf and placed in 1 ml N,N-dimethylformamide (DMF; analytical grade; Fisher Scientific) and stored at 4 °C in the dark. Following a 1:4 dilution of samples with DMF, total chlorophyll was determined by measuring absorbance at 647 and 664 nm using a spectrophotometer (U-2000 Hitachi) and calculated using the extinction coefficients in

Wellburn (1994). With a known sample size chlorophyll content was then expressed as mg m^{-2}. In 2004 on 21st September (both species) and again on 18th October (*P. x euramericana*) and 2nd November (*P. nigra*) whole leaves from each sub-plot were sampled and flash frozen in liquid nitrogen (N_2) and stored at -80 °C. At a later date, four whole leaves from each sub-plot (three for *P. x euramericana* on 21st September from the ambient nitrogen sub-plot of plot 5) were taken from -80 °C storage and homogenised in liquid N_2 using a pestle and mortar. A 1.5 ml eppendorf tube containing 1 ml of DMF was taken and zeroed on a mass balance, a consistent volume of homogenised leaf material was added and the mass retaken in order to calculate the mass of sample contained in the DMF. This approached was carried as it allowed the same leaves used for chlorophyll extraction to also be used for RNA extraction. Samples were left in DMF for 48 hours at 4 °C in the dark and total chlorophyll along with total carotenoids were quantified on a leaf mass basis using the extinction coefficients of Wellburn (1994) after measuring absorbance at 480, 647 and 664 nm. Three technical replicate dilutions (1:4) were carried out on each biological replicate, the mean of which was the sample mean. A two way ANOVA was carried out at each time point, for each species, to identify if the mass of sample taken was biased for CO_2 or N treatments. No significant effect was seen at any time and therefore the change in mass of each sample (mean = 0.07 mg ± 0.02 standard deviations) was not considered to influence the interpretation of treatment effects on chlorophyll content. Moreover, linear regression was also carried out between mass of sample (*X* axis) and chlorophyll content expressed on a leaf mass basis (*Y* axis) (n = 191). Although a negative association was identified this was very weak (r^2 = 0.14).

4.3.5 Specific leaf area

Specific leaf area SLA ($mm^2 g^{-1}$ dry weight) was calculated from the leaves sampled for chlorophyll content determination in 2003. Immediately following harvest, leaf area was traced around on a labelled paper bag in which the leaf was then stored. Leaves were oven dried at 80 °C for at least 72 hours and leaf dry weight obtained. Leaf area was obtained from the traced image using Metamorph (Metamorph version 5, Universal Image Corporation, Philadelphia, USA) and the area of the disc removed for chlorophyll quantification was deducted. In 2004 leaves used for spectral reflectance measurements were also retained for SLA calculation. Six leaves per sub-plot for each of *P. x euramericana* (19.09.04) and *P. nigra* (20.09.04) and between six to nine leaves per sub-

plot for *P. x euramericana* (18-19.10.04) and six leaves for *P. nigra* (21.10.04) were used. SLA was calculated as described for 2003 except that no leaf disc was removed and leaf area was measured using ImageJ (ImageJ ver. 1.24o. National Institutes of health. http://rsb.info.nih.gov/ij/). The absence of a leaf trace on the bags of *P. nigra* samples from the ambient nitrogen sub-plot of plot 3 collected in the morning sampling period of the 21.10.04 excluded these from the analysis as SLA could not be calculated. In 2004 the leaves sampled for SLA were originally used for the spectral assessment therefore they were discretely sampled in the morning and afternoon periods. This sampling process also allowed the testing of a time of day influence on SLA.

4.3.6 Percentage Leaf N_{mass}

Three replicate oven dried leaves used for determination of SLA from each sub-plot harvested in the morning sampling period were analysed for leaf nitrogen content by François Bochereau of Forest Research (Forest Research, Alice Holt Lodge, Farnham, Surrey GU10 4LH). Leaves were ground to a fine powder, subjected to a sulphuric acid digest and then measured using continuous flow analysis (System 4, ChemLab, Great Dunmow, U.K. and Series 2000, Burkard Scientific, Uxbridge, U.K implemented by MB Scientific Services Ltd., Longstanton, U.K.).

4.3.7 Statistical analysis

The experimental design and statistical model are described in detail in chapter three and unless otherwise stated data were normally distributed, displayed homogeneity of variance and plot was considered the unit of replication. Table 4.1 gives the detail of the F ratios and calculations for the F test employed in this experimental design for the leaf chlorophyll concentration data of 2004.

As in chapter three, all data reporting the percentage change of the response variable was arcsine transformed and tested irrespective of species in the model (table 3.1) so allowing 12 error degrees of freedom. The existence of both positive and negative values in the data reporting the percentage change in chemically-extracted leaf carotenoid content would create error if all values were made positive for arcsine transformation. Therefore, and for carotenoid content only, the untransformed percentage change data were

analysed in the ANOVA. This was deemed suitable considering the residuals exhibited a normal distribution and homogeneity of variance. At individual time points, within sub-plot replication of sampling allowed error variation of Replicate'(Block'*CO_2*N), and therefore sufficient error degrees of freedom so that all interactions with block could be studied. Consequently statistical interpretation of each species response at each time point could be examined. The changes in leaf spectra respective of treatment were observed over the time period between 19.09.04 to 01.11.04 for *P. x euramericana* and 20.09.04 to 31.10.04 for *P. nigra*. In response to these observations the percentage change in mean absorbance between 700 and 710 nm (the red edge of chlorophyll absorbance) and 800 to 810 nm (in the NIR) was calculated. Following arcsine normalisation the treatment response was analysed using the split-plot design described in chapter three.

4.4 Results

4.4.1 Leaf spectral properties - pilot test.

Both the white reflective reference surfaces, from which the fraction of transmitted or reflected irradiance was calculated, were analysed across the range 400 - 1000 nm. Stability of irradiance between 400 nm to approximately 850 nm was a requirement for further spectral analysis of leaf properties. Figure 4.2 A and B show the stability of the reference irradiance when the integrating sphere is set up for measuring irradiance which is either (A) transmitted or (B) reflected from a leaf. A low intensity of irradiance in the blue portion of the spectrum was indentified. This low intensity was considered to contribute to the noise in the blue portion when the percentage of leaf reflectance and transmittance was calculated. Less visible and more NIR was transmitted through the leaf than reflected by the leaf (figure 4.2, C and D respectively). Irradiance that is transmitted through the leaf generally forms a plateau in the NIR (igure 4.2, C), whereas that measured from the reference surface declines in this range (figure 4.2, A). Therefore, when the fraction of transmitted irradiance is calculated, an artificial increase in the NIR becomes apparent (figure 4.2, E). This was considered an artefact of the experimental set up because the white reflective surface of the reference port for transmitted irradiance appeared to absorb a portion of NIR irradiance (figure 4.2, A). Irradiance reflected from the leaf adaxial surface also formed a plateau in the NIR (figure 4.2, D) as did that from the reference (figure 4.2, B). Therefore no instrumental artefact was considered to influence the fraction of reflected light (figure 4.2, F).

A general decline in the transmitted NIR irradiance was noted between sampling at time one and time six between which a time lag of ten minutes occurred (figure 4.2, C and E). This decline was absent for the reflected irradiance (figure 4.2, D and F). Transmitted irradiance has passed through the leaf and was influenced by more leaf structural components than reflected irradiance. Such structural influences on transmittance can be channelling of light by palisade cells, scattering of light by spongy mesophyll cells and internal reflectance of light by the abaxial epidermis (Vogelmann, 1993). It was considered that leaf water loss may influence cellular turgor and so NIR transmittance, via a change in the refractive index between hydrated spongy mesophyll cells and airspaces (Jackson, 1986). In response to this, all further leaves for spectral analysis were harvested and

petioles immediately re-cut under water to avoid desiccation. No decline in the percentage of transmitted NIR was then evidient for up to two hours after harvest.

4.4.2 Spectral properties of experimental leaves

Figure 4.3, A, B and C show the fraction of reflectance, transmittance and the calculated fraction of absorbance for leaves of *P. x euramericana* harvested on 1st November 2004 and figure 4.4, A, B and C show the fraction of reflectance, transmittance and the calculated fraction of absorbance for leaves of *P. nigra* harvested between 30th and 31st of October 2004. For both species and across all treatments the mean maximum fraction of absorbed visible light was 0.87 (87 %) with the mean wavelength for maximal absorbance occurring at 676 nm and 673 nm for *P. x euramericana* and *P. nigra* respectively. The increase in transmitted irradiance at wavelengths greater than 750 nm was considered not to be a genuine biological feature and the result of the reference port. As this same reference was used for all measurements of transmittance, this apparent feature was consistent throughout (figure 4.2, A for example), thus allowing relative comparisons of transmittance over time and between treatments. For both species a general decreased transmittance of NIR irradiance in the ambient CO_2 fertilised sub-plot was apparent (figure 4.3, B for *P. x euramericana*, figure 4.4, B for *P. nigra*), moreover, decreased NIR reflectance in this treatment was also apparent for *P. x euramericana* (figure 4.3, A). This resulted in an increased absorbance of NIR irradiance for this treatment for both species.

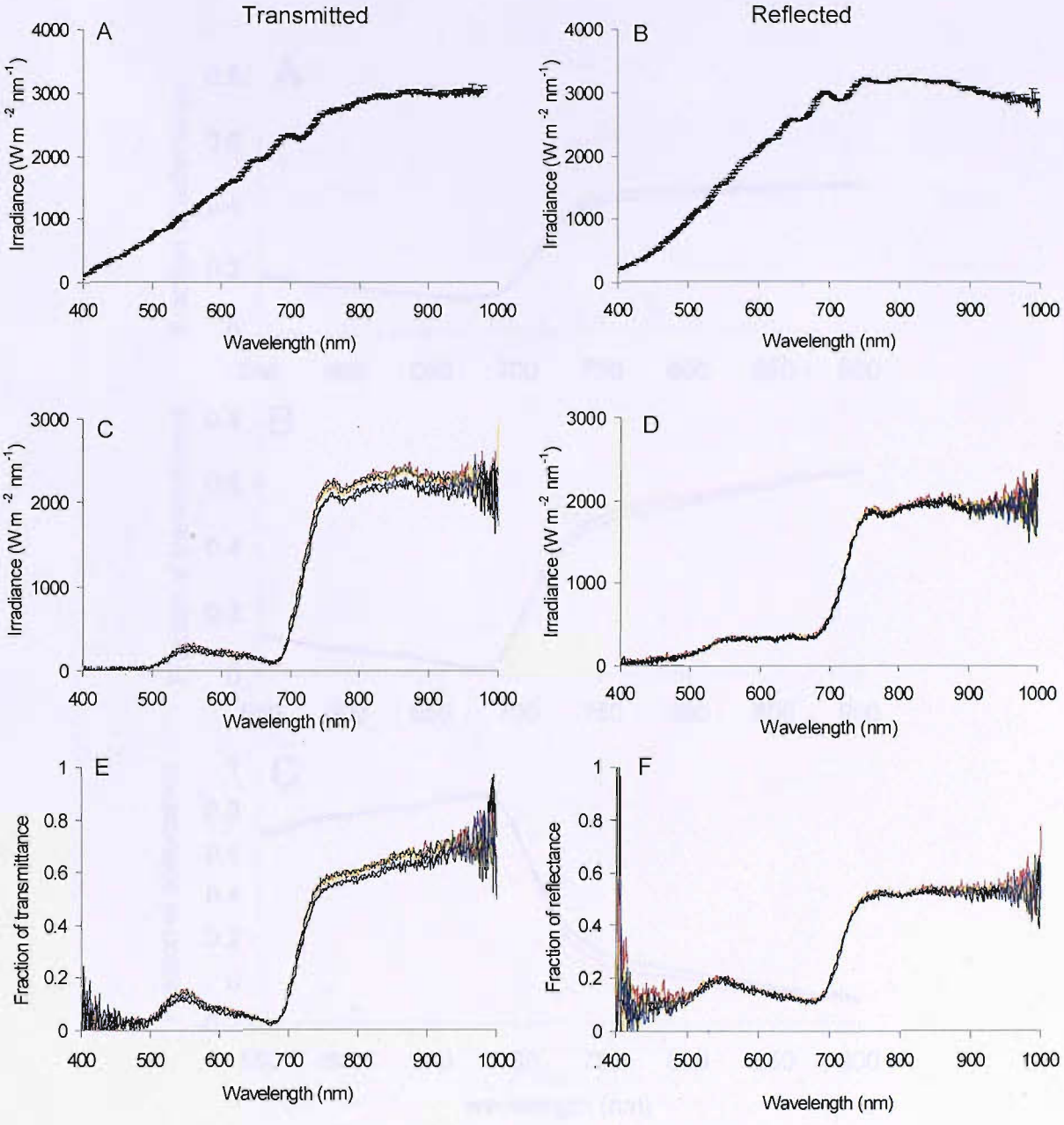

Figure 4.2: Testing the approach to measure leaf reflectance and transmittance between 400 to 1000 nm. Displayed are the mean (*n* = 6) (+ SE) for the reference irradiance from the reference port of the integrating sphere used to assess leaf transmittance (A) and reflectance (B) between 400 to 1000 nm. The irradiance transmitted (C) or reflected (D) from a *P. x euramericana* leaf and the respective fraction of transmittance (E) and reflectance (F) from that same leaf are given. The leaf spectral properties were measured at time 1 (—) (20 minutes after harvest) through to time six (—) (30 minutes after harvest). The intermediated time 2 (—) time 3 (—), time 4 (—) and time 5 (—) are also shown.

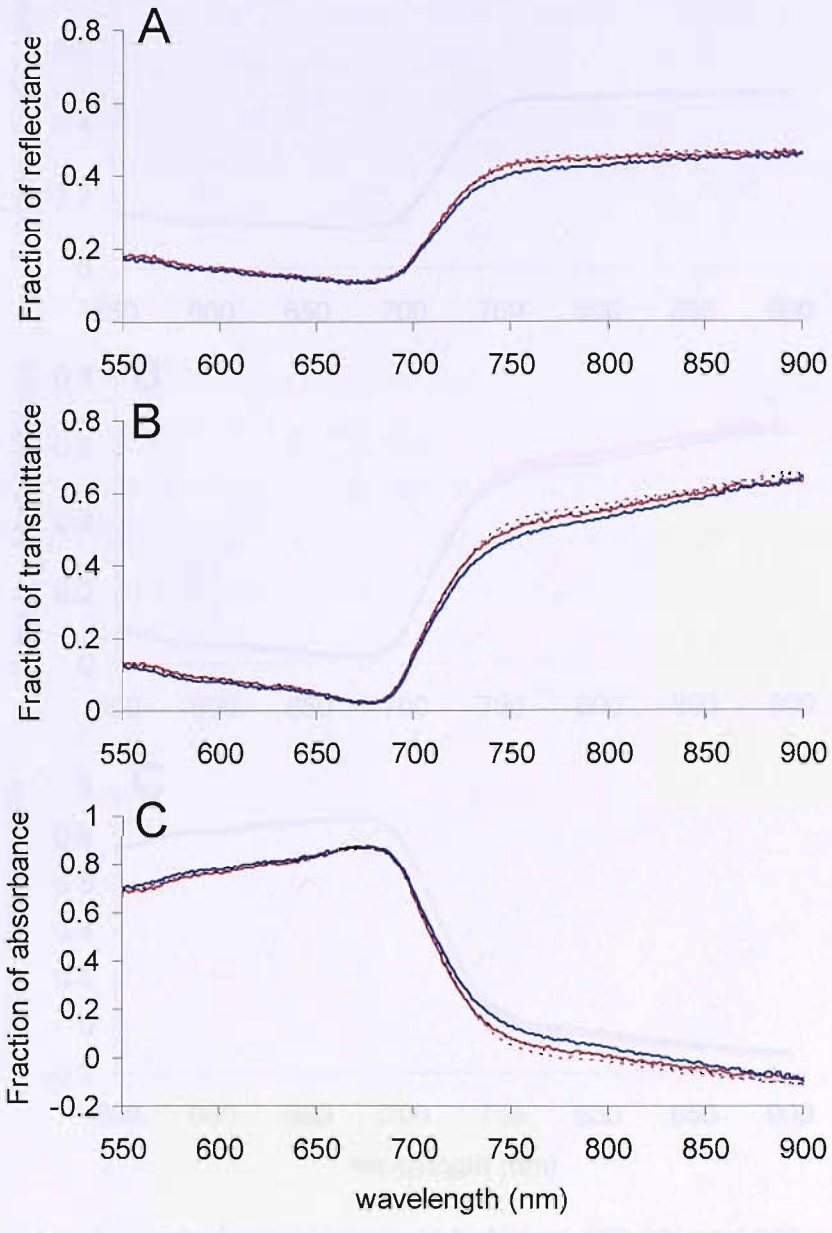

Figure 4.3: Leaf level spectral measurements between 550 nm and 900 nm obtained on 01.11.04 for *P. x euramericana*. The mean fraction of reflectance, transmittance and absorbance is shown for A, B and C respectively. Spectra are for elevated CO_2 with fertilisation (——), ambient CO_2 with fertilisation (——), elevated CO_2 with no fertilisation (- - - -), and ambient CO_2 with no fertilisation (- - - -).

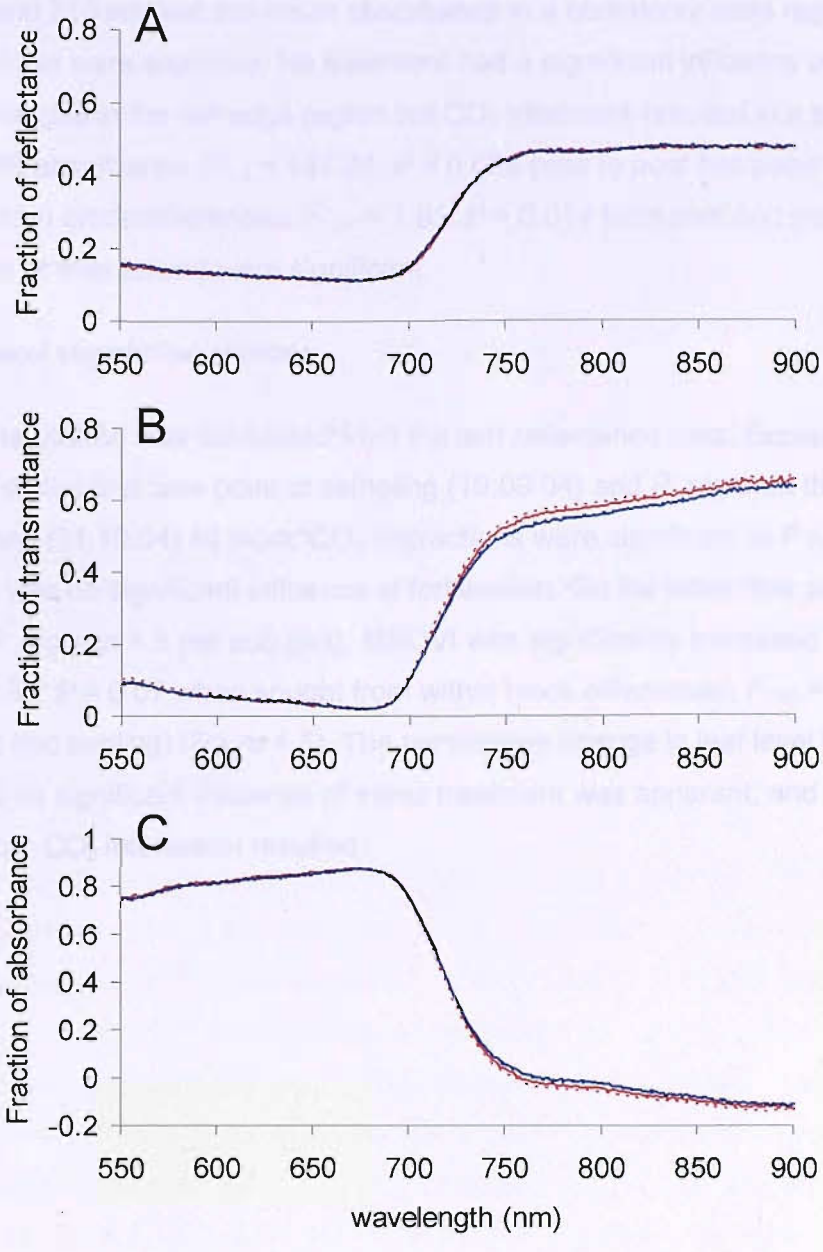

Figure 4.4: Leaf level spectral measurements between 550 nm and 900 nm obtained between 30 and 31.10.04 for *P. nigra*. The mean fraction of reflectance, transmittance and absorbance is shown for A, B and C respectively. Spectra are for elevated CO_2 with fertilisation (——), ambient CO_2 with fertilisation (——), elevated CO_2 with no fertilisation (- - - -), and ambient CO_2 with no fertilisation (- - - -).

Leaf level spectral properties were analysed during the course of autumnal senescence and a percentage change of spectral characteristics was calculated. To assess these changes, the mean absorbance at the red edge of the chlorophyll absorbance feature

between 700 and 710 nm and the mean absorbance in a commonly used region of the NIR 800 to 810 nm were analysed. No treatment had a significant influence over absorbance changes in the red edge region but CO_2 treatment resulted in a significant reduction in NIR absorbance ($F_{1,2}$ = 187.94, P = 0.005 prior to *post hoc* pooling when sought from within block differences; $F_{1,14}$ = 7.95, P = 0.014 from *post hoc* pooling). No other treatment or interactions were significant.

4.4.2.1 Leaf-level vegetation indices

During 2004 the MNDVI was calculated from the leaf reflectance data. Except for *P. x euramericana* on the first time point of sampling (19.09.04) and *P. nigra* on the last time point of sampling (31.10.04) all block*CO_2 interactions were significant at P ≤ 0.07 and at all times there was no significant influence of fertilisation. On the latter time point of sampling for *P. nigra* (n = 9 per sub-plot), MNDVI was significantly increased by elevated CO_2 ($F_{1,2}$ = 12.30, P = 0.07 when sought from within block differences; $F_{1,98}$ = 4.65, P = 0.03 from *post hoc* pooling) (figure 4.5). The percentage change in leaf level MNDVI was calculated and no significant influence of either treatment was apparent, and also no significant block* CO_2 interaction resulted.

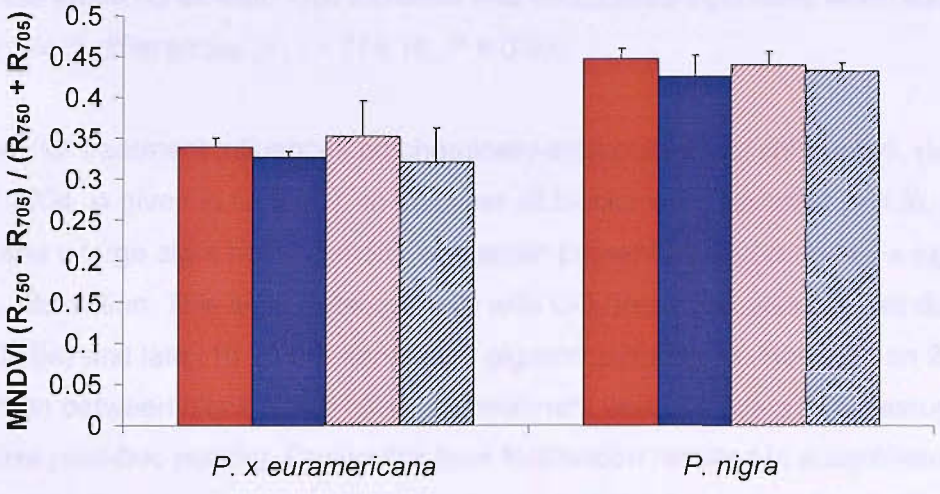

Figure 4.5: Mean leaf Modified NDVI for both *P. x euramericana* (01.11.04) and *P. nigra* (31.10.04). Values represent means of plots (*n* = 2) (+ SE) for elevated CO_2 with fertilisation (■), ambient CO_2 with fertilisation (■), elevated CO_2 with no fertilisation (▨) and ambient CO_2 with no fertilisation (▨).

4.4.3 Leaf pigment content

In 2003 (figure 4.6) chemically-extractable leaf chlorophyll was expressed on a leaf area basis. This is because only the area of leaf material was known for the pigment extraction. During this year only blocks one and two were sampled (*n* = 2). Late into the senescent period of 2003 (on 16.10.03), for both species, there were no significant effects of either CO_2 or fertiliser treatments on the amount of chemically-extractable leaf cholorphyll. However, during this time, a large site heterogeneity was present as evidenced by a significant interaction between block and CO_2 treatment ($F_{1,14}$ = 4.52, P = 0.05, for *P. x euramericana*; $F_{1,15}$ = 7.52, P = 0. 02, for *P. nigra*). This significant site heterogeneity was also evident for *P. nigra* during the earlier measurements (26.09.03), as evidenced by a significant interaction between block and CO_2 treatment ($F_{1,16}$ = 5.14, P = 0.04). At this same earlier time point (26.09.03) the site heterogeneity was considered small enough (the P value for block * CO_2 interaction was $P > 0.25$) to allow for post-hoc pooling. Again elevated CO_2 treatment had no significant influence on the amount of chemically-extractable leaf chlorophyll when the variance of the whole site was taken into account ($F_{1,17}$ = 0.97, P = 0.34 from post hoc pooling). However elevated CO_2 caused an increase of between 2 and 6 % in chemically-extractable chlorophyll content of *P. x euramericana*

leaves on the 26.09.03 as well. This increase was considered significant when sought only from within block differences ($F_{1,1}$ = 774.16, P = 0.02).

The ANOVA for treatment influences on chemically-extractable leaf chlorophyll, during the autumn of 2004, is given in table 4.1. In this year all blocks were sampled (n = 3). For *P. x euramericana* a large sight heterogeneity was again present as evidenced by a significant block*CO_2 interaction. This sight heterogeneity with CO_2 treatment was present during the early (21.09.04) and late (18.10.04) senescent pigment extractions. However on 21.09.04 the interaction between block and fertilisation treatment was considered low enough (P < 0.25) to allow *post-hoc* pooling. During this time fertilisation resulted in a significantly reduced chemically-extractable leaf chlorophyll (P = 0.078) when within block differences were calculated. However when the whole site variance was taken into account through *post-hoc* pooling the effect of fertilisation on chemically-extractable leaf chlorophyll was no longer considered to be significant (see table 4.1 and figure 4.7 A). For *P. nigra* no treatment effects on the amount of chemically-extractable leaf chlorophyll were considered to be significant (see figure 4.7, B; table 4.1).

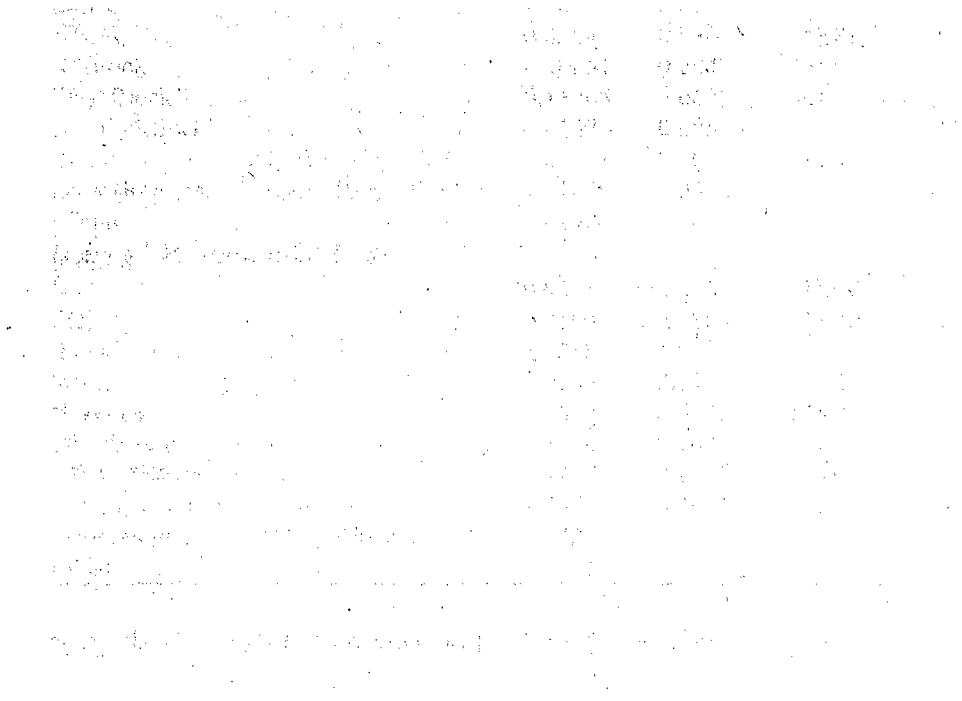

Table 4.1: The Analysis of Variance for leaf chlorophyll concentration (mg g^{-1}) at each time point of measurement in 2004. Red values were calculated by hand and those in bold were significant. Results from post hoc pooling are given in the foot note

Source of variation	SS	MS	*F* ratio	*F*	df	*P*
[chl] mg g^{-1} P. x euramericana (21.09.04)						
(1) N	0.01379	0.01379	(1)/(8)	0.113	1,4	0.754[a]
(2) CO_2	0.11771	0.11771	(2),(6)	0.36	1,2	0.611
(3) Block'	3.18477	1.64110	-	-	2	
(4) N*CO_2	0.08678	0.08678	(4)(8)	0.81	1,4	0.419[b]
(5) N*Block'	0.05002	0.02501	(5)(9)	0.27	2,35	0.765
(6) CO_2*Block'	0.97369	0.48685	(6)(9)	5.27	2,35	**0.01**
(7) N*CO_2*Block'	0.43718	0.43718	(7)(9)	2.37	2,35	0.109
(8) (N*Block')+(N*CO_2*Block')	0.4872	0.1218	(8)(9)	1.32	4,35	0.282
(9) Error (Replicate'(N*CO_2*Block'))	3.23141	0.09233	-	-	35	-
(10) Total	8.09535				46	
[chl] mg g^{-1} P. x euramericana (18.10.04)						
(1) N	0.07003	0.07003	(1)/(8)	5.54	1,4	**0.078**[c]
(2) CO_2	0.21955	0.21955	(2),(6)	1.11	1,2	0.403
(3) Block'	1.67476	0.83738	-	-	2	
(4) N*CO_2	0.04703	0.04703	(4)(8)	3.72	1,4	0.126[d]
(5) N*Block'	0.02552	0.01276	(5)(9)	0.20	2,36	0.820
(6) CO_2*Block'	0.39687	0.19843	(6)(9)	3.17	2,36	**0.054**
(7) N*CO_2*Block'	0.02507	0.01254	(7)(9)	0.20	2,36	0.820
(8) (N*Block')+(N*CO_2*Block')	0.05059	0.01265	(8)(9)	0.20	4,36	0.937
(9) Error (Replicate'(N*CO_2*Block'))	2.25622	0.06267	-	-	36	-
(10) Total	4.71505				47	
[chl] mg g^{-1} P. nigra (21.09.04)						
(1) N	0.11828	0.11828	(1)/(8)	1.12	1,4	0.350
(2) CO_2	0.12007	0.12007	(2),(6)	1.79	1,2	0.313[e]
(3) Block'	1.34743	0.67371	-	-	2	
(4) N*CO_2	0.03043	0.03043	(4)(8)	0.29	1,4	0.619
(5) N*Block'	0.40861	0.20430	(5)(9)	4.21	2,36	**0.023**
(6) CO_2*Block'	0.13405	0.06703	(6)(9)	1.38	2,36	0.265
(7) N*CO_2*Block'	0.01320	0.00660	(7)(9)	0.14	2,36	0.873
(8) (N*Block')+(N*CO_2*Block')	0.42181	0.10545	(8)(9)	2.17	4,36	**0.092**
(9) Error (Replicate'(N*CO_2*Block'))	1.74698	0.04853	-	-	36	-
(10) Total	3.91904				47	
[chl] mg g^{-1} P. nigra (02.11.04)						
(1) N	0.0358	0.0358	(1)/(8)	0.09	1,4	0.779
(2) CO_2	0.2869	0.2869	(2),(6)	1.77	1,2	0.315[f]
(3) Block'	3.8288	1.9144	-	-	2	
(4) N*CO_2	0.0764	0.0764	(4)(8)	0.21	1,4	0.671
(5) N*Block'	1.0696	0.5348	(5)(9)	2.43	2,36	0.102
(6) CO_2*Block'	0.3250	0.1625	(6)(9)	0.74	2,36	0.484
(7) N*CO_2*Block'	0.3957	0.1979	(7)(9)	0.90	2,36	0.416
(8) (N*Block')+(N*CO_2*Block')	1.4653	0.3663	(8)(9)	1.66	4,36	**0.181**
(9) Error (Replicate'(N*CO_2*Block'))	7.9229	0.2201	-	-	36	-
(10) Total	13.941				47	

([a-f] are applicable for post hoc pooling, all are not significant at P < 0.1)

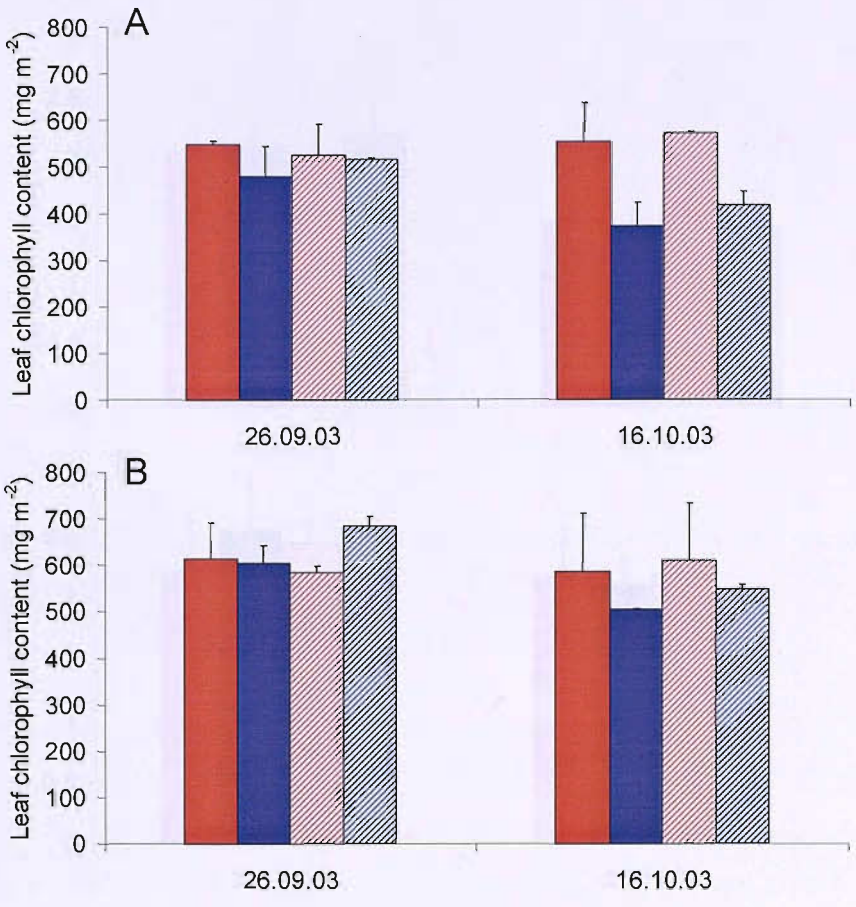

Figure 4.6: Mean extracted leaf chlorophyll content for *P. x euramericana* (A) and *P. nigra* (B) for leaves harvested in 2003. Values represent means of plots (*n* = 2) (+ SE) for elevated CO_2 with fertilisation (■), ambient CO_2 with fertilisation (■), elevated CO_2 with no fertilisation (▨) and ambient CO_2 with no fertilisation (▨).

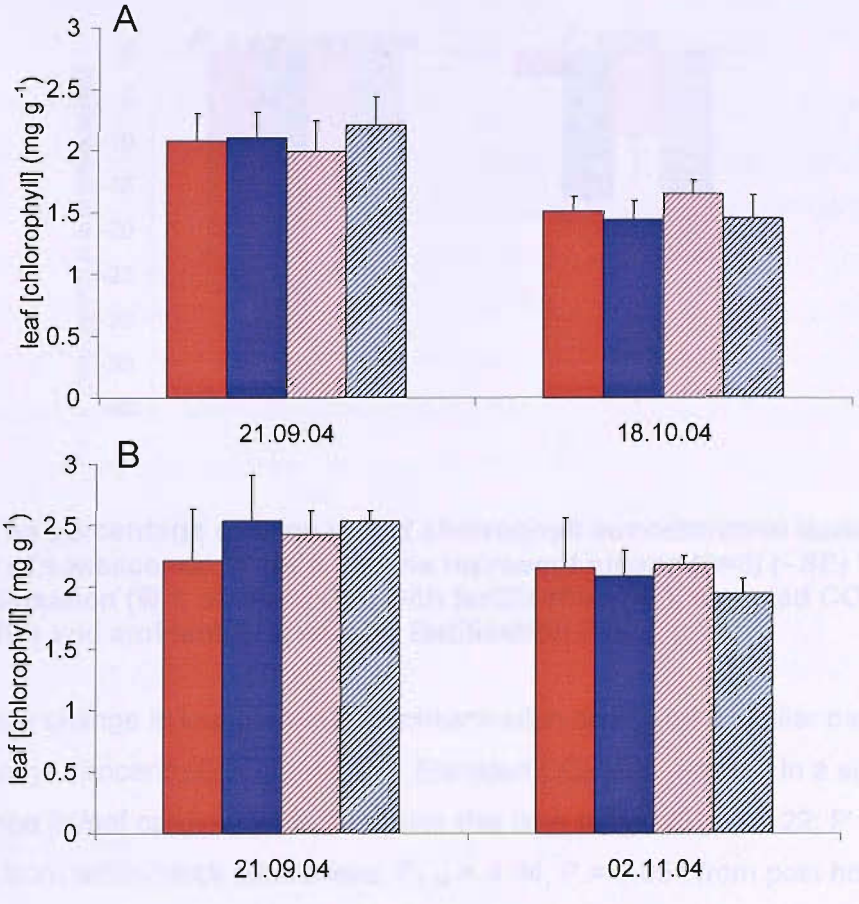

Figure 4.7: Mean extracted leaf chlorophyll concentration for *P. x euramericana* (A) and *P. nigra* (B) for leaves harvested in 2004. Values represent means of plots (*n* = 3) (+ SE) for elevated CO_2 with fertilisation (■), ambient CO_2 with fertilisation (■), elevated CO_2 with no fertilisation (▨) and ambient CO_2 with no fertilisation (▨).

To address the issue of site heterogeneity as evident from the significant block interactions, leaf chlorophyll concentration was expressed as a percentage change (figure 4.8). During the progression of autumnal senescence in 2004, elevated CO_2 significantly reduced the autumnal decline in leaf chlorophyll concentration ($F_{1,2}$ = 24.91, P = 0.038 when sought from within block differences, and $F_{1,14}$ = 8.32, P = 0.01 from *post hoc* pooling). No significant effects were evident for the percentage change in leaf chlorophyll content during 2003 (when only two blocks were sampled) and the block* CO_2 interaction was such that post hoc pooling was not permissible ($F_{1,8}$ = 2.58, P = 0.15).

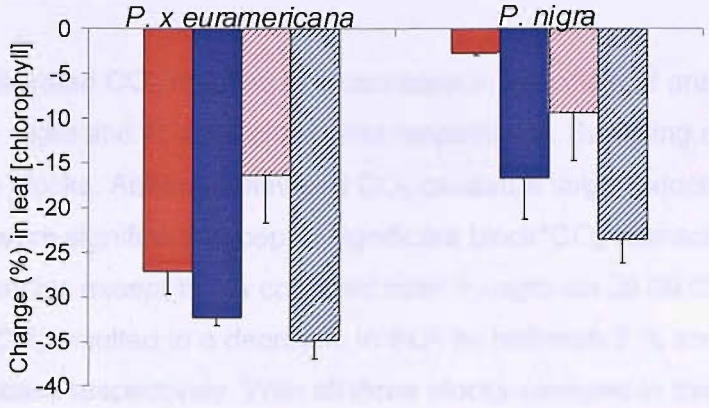

Figure 4.8: The percentage change in leaf chlorophyll concentration during the progression of senescence in 2004. Values represent means (n=3) (- SE) for elevated CO_2 with fertilisation (■), ambient CO_2 with fertilisation (■), elevated CO_2 with no fertilisation (▨) and ambient CO_2 with no fertilisation (▨).

The percentage change in leaf carotenoid concentration displayed a similar pattern to that of leaf chlorophyll concentration (figure 4.9). Elevated CO_2 also resulted in a significantly reduced change in leaf carotenoid content over this time period ($F_{1,2}$ = 9.22; P = 0.094 when sought from within block differences, $F_{1,14}$ = 4.44; P = 0.054 from post hoc pooling). No interactions with block were significant and neither was the influence of fertilisation.

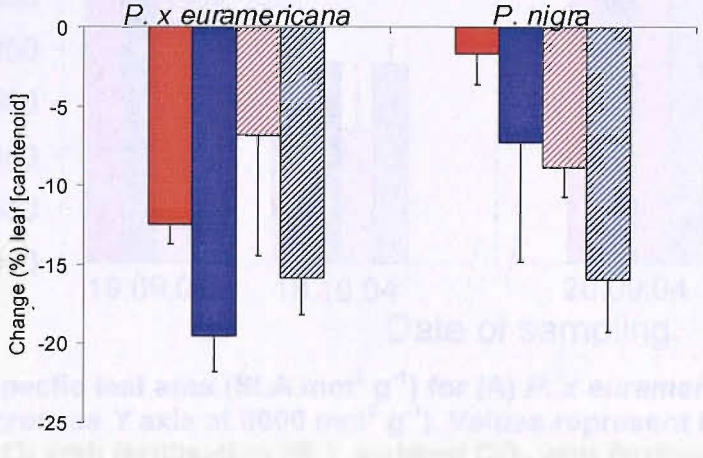

Figure 4.9: The percentage change in leaf carotenoid concentration during the progression of senescence in 2004. Values represent means (n=3) (- SE) for elevated CO_2 with fertilisation (■), ambient CO_2 with fertilisation (■), elevated CO_2 with no fertilisation (▨) and ambient CO_2 with no fertilisation (▨).

4.4.4 *Specific leaf area*

In October 2003 elevated CO_2 resulted in a decrease in specific leaf area by between 15 % and 18 % for *P. nigra* and *P. x euramericana* respectively. Sampling during this year was from only two blocks. Although elevated CO_2 caused a large reduction in SLA no treatment effects were significant except a significant block*CO_2 interaction was evident at $P \leq 0.03$ for all samples except those collected from *P. nigra* on 26.09.03. In late October of 2004 elevated CO_2 resulted in a decrease in SLA by between 5 % and 6 % for *P. nigra* and *P. x euramericana* respectively. With all three blocks sampled in this year the block*CO_2 interaction was highly significant at all times ($P \leq 0.04$). Except for fertilisation causing a significant increase in the SLA of *P. nigra* on the 20.09.04 ($F_{1,4} = 7.9$; $P = 0.048$ when tested from within block differences) no other treatments had a significant effect on SLA (see figure 4.10). Also evident for both species in figure 4.10 is a general decline in SLA as senescence progresses, a feature which was also evident from the SLA data collected in 2003.

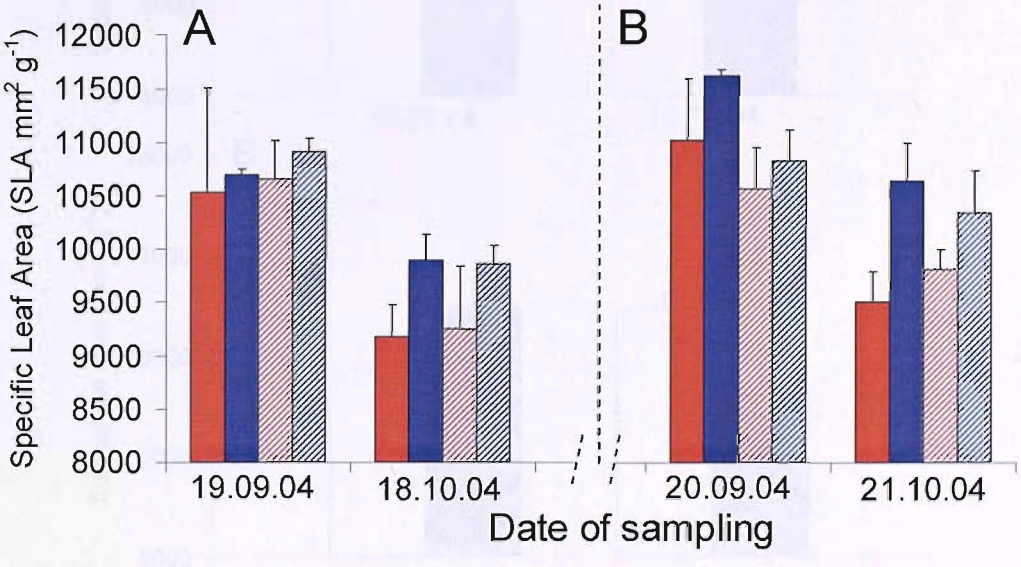

Figure 4.10: Specfic leaf area (SLA $mm^2\ g^{-1}$) for (A) *P. x euramericana* and (B) *P. nigra* (*X* axis crosses *Y* axis at 8000 $mm^2\ g^{-1}$). Values represent means (n = 3) (+ SE) for elevated CO_2 with fertilisation (■), ambient CO_2 with fertilisation (■), elevated CO_2 with no fertilisation (▨) and ambient CO_2 with no fertilisation (▨).

In 2004 it was possible to assess the diurnal influence on SLA for each sampling time point (figure 4.11). A one-way ANOVA was carried out to determine the influence of either am or pm leaf sampling time upon SLA. The mean SLA for each sub-plot was calculated and this was the unit of replication, such that n = 12 per species and time period, except for *P. nigra* when n = 11 due to the absence of the ambient nitrogen sub-plot, am time period leaf area traces of plot 3. At both times and for both species SLA was reduced in the afternoon when compared with the morning. This reduction was significant for *P. nigra* ($F_{1,22}$ = 9.56; P = 0.005, and $F_{1,21}$ = 5.32; P = 0.031 for 20.09.04 and 21.10.04 sampling time points respectively).

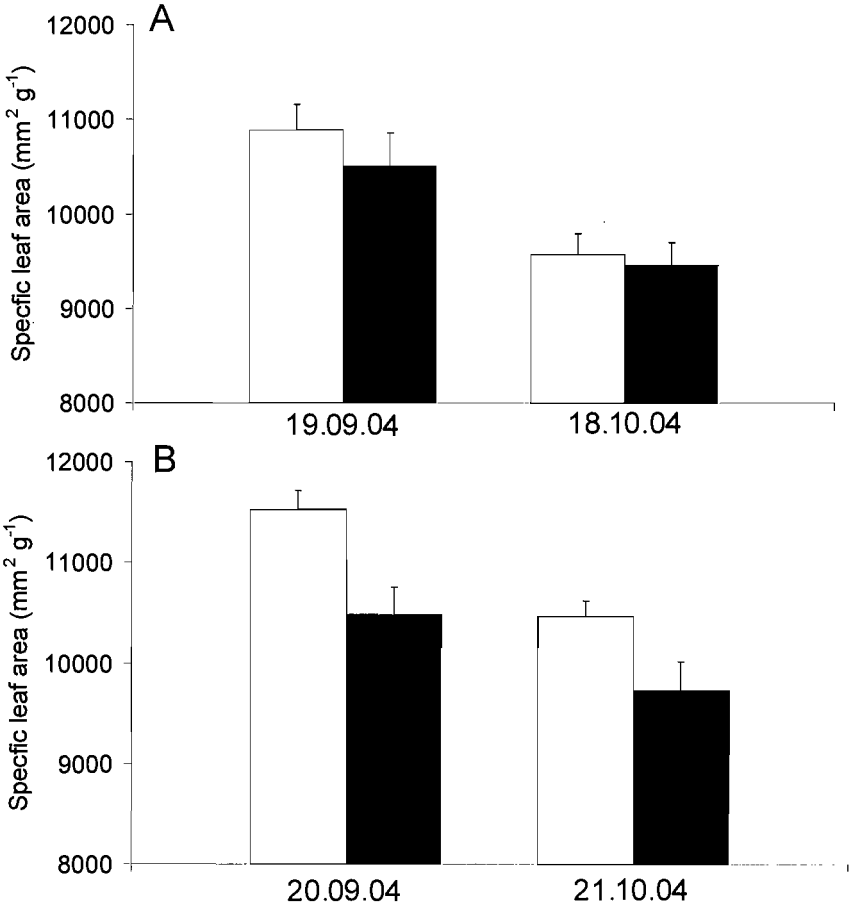

Figure 4.11: The influence of either morning (□) or afternoon (■) sampling time periods on specific leaf area (SLA) for (A) *P. x euramericana* and (B) *P. nigra* (*X* axis crosses *Y* axis at 8000 mm^2 g^{-1}). Values are means (n = 12, except *P. nigra* 21.10.04 when n = 11) (+ SE).

4.4.5 *Leaf Nitrogen (% N_{mass})*

During the last time point of sampling, leaf nitrogen was between approximately 2.3 and 2.5 % of leaf dry mass for *P. x euramericana* (18.10.04), and between approximately 2.6 and 2.9 % for *P. nigra* (21.10.04), figure 4.12. At this time point of sampling, and for *P. x euramericana* only, elevated CO_2 resulted in a significantly reduced leaf N_{mass} ($P = 0.018$), as shown in the footnote of table 4.2. Table 4.2 gives the results of the ANOVA for each time point of leaf N_{mass} measurements. The percentage decline in leaf N_{mass} was also calculated between the two time points of measurement. This ranged from between an 18 - 23 % decline for *P. x euramericana* and a 5 - 12 % decline for *P. nigra*, and no treatment effects or interactions with block were significant for the decline in leaf N_{mass}.

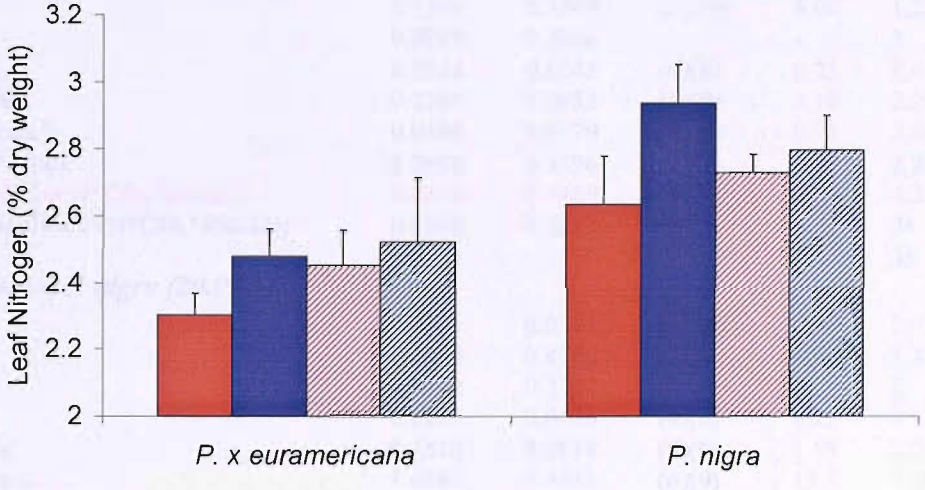

Figure 4.12: Leaf Nitrogen content (N_{mass}) as a percentage of leaf dry weight for both *P. x euramericana* and *P. nigra* (*X* axis crosses *Y* axis at 2 %). Values represent means ($n = 3$) (+ SE) for elevated CO_2 with fertilisation (■), ambient CO_2 with fertilisation (■), elevated CO_2 with no fertilisation (▨) and ambient CO_2 with no fertilisation (▨).

Table 4.2: The Analysis of Variance for leaf N_{mass} (% dry mass) at each time point of measurement in 2004. Red values were calculated by hand and those in bold were significant. Results from post hoc pooling are given in the foot note

Source of variation	SS	MS	*F* ratio	*F*	df	*P*
N (%dry mass) P. x euramericana (19.09.04)						
(1) N	0.0084	0.0084	(1)/(8)	0.19	1,4	0.685
(2) CO_2	0.0240	0.0240	(2),(6)	0.95	1,2	0.433[a]
(3) Block'	0.8869	0.4434	-	-	2	-
(4) N*CO_2	0.0506	0.0506	(4)(8)	1.15	1,4	0.344
(5) N*Block'	0.1545	0.0773	(5)(9)	2.59	2,24	**0.096**
(6) CO_2*Block'	0.0506	0.0253	(6)(9)	0.85	2,24	0.444
(7) N*CO_2*Block'	0.0216	0.0108	(7)(9)	0.36	2,24	0.699
(8) (N*Block')+(N*CO_2*Block')	0.1762	0.0440	(8)(9)	1.48	4,24	0.239
(9) Error (Replicate'(N*CO_2*Block'))	0.7150	0.0298	-	-	24	-
(10) Total	1.9117				35	
N (%dry mass) P. x euramericana (18.10.04)						
(1) N	0.0803	0.0803	(1)/(8)	0.74	1,4	0.438
(2) CO_2	0.1369	0.1369	(2),(6)	8.06	1,2	0.105[b]
(3) Block'	0.5799	0.2900	-	-	2	-
(4) N*CO_2	0.0245	0.0245	(4)(8)	0.23	1,4	0.657
(5) N*Block'	0.1366	0.0683	(5)(9)	3.15	2,24	**0.061**
(6) CO_2*Block'	0.0340	0.0170	(6)(9)	0.78	2,24	0.470
(7) N*CO_2*Block'	0.2992	0.1496	(7)(9)	6.89	2,24	**0.004**
(8) (N*Block')+(N*CO_2*Block')	0.4358	0.1089	(8)(9)	5.02	4,24	**0.004**
(9) Error (Replicate'(N*CO_2*Block'))	0.5208	0.0217	-	-	24	-
(10) Total	1.8121				35	
N (%dry mass)P. nigra (20.09.04)						
(1) N	0.0261	0.0261	(1)/(8)	0.52	1,4	0.512[c]
(2) CO_2	0.4160	0.4160	(2),(6)	0.76	1,2	0.474
(3) Block'	0.7402	0.3701	-	-	2	-
(4) N*CO_2	0.0125	0.0125	(4)(8)	0.25	1,4	0.643[d]
(5) N*Block'	0.1310	0.0655	(5)(9)	1.59	2,24	0.243
(6) CO_2*Block'	1.0882	0.5441	(6)(9)	13.2	2,24	**≤ 0.001**
(7) N*CO_2*Block'	0.0684	0.0342	(7)(9)	0.83	2,24	0.447
(8) (N*Block')+(N*CO_2*Block')	0.1994	0.0499	(8)(9)	1.21	4,24	0.332
(9) Error (Replicate'(N*CO_2*Block'))	0.9867	0.0411	-	-	24	-
(10) Total	3.469				35	
N (%dry mass) P. nigra (21.10.04)						
(1) N	0.0042	0.0042	(1)/(8)	0.05	1,4	0.842
(2) CO_2	0.3080	0.3080	(2),(6)	1.29	1,2	0.375
(3) Block'	0.0038	0.0019	-	-	2	-
(4) N*CO_2	0.1260	0.1260	(4)(8)	1.36	1,4	0.309
(5) N*Block'	0.0755	0.0377	(5)(9)	0.71	2,24	0.502
(6) CO_2*Block'	0.4793	0.2396	(6)(9)	4.52	2,24	**0.022**
(7) N*CO_2*Block'	0.2954	0.1477	(7)(9)	2.79	2,24	0.082
(8) (N*Block')+(N*CO_2*Block')	0.3709	0.0927	(8)(9)	1.75	4,24	0.172
(9) Error (Replicate'(N*CO_2*Block'))	1.2713	0.0530	-	-	24	-
(10) Total	2.5636				35	

([a-d] are applicable for post hoc pooling, only CO_2[b] is significant $F_{1,26} = 6.42$, $P = 0.018$).

4.5 Discussion

There are several important findings from this chapter but the most important could be considered the confirmation of the conclusions from chapter three through quantifying chemically-extracted leaf chlorophyll content. A further unexpected finding was the diurnal influence on SLA which indicates this factor should always be considered whenever sampling for SLA in the field.

4.5.1 SLA and leaf N_{mass}

In this chapter the leaf traits SLA and N_{mass} were measured during senescence for both *P. x euramericana* and *P. nigra* following up to six years growth in elevated CO_2. For both species SLA declined by approximately 10 % as senescence progressed from late September to late October (figure 4.10), and in elevated relative to ambient CO_2 SLA was between 8 to 18 % less depending on year and species. This reduction in SLA, between elevated and ambient CO_2 is within the range reported for both species measured during the growing season of the first three years of growth (Tricker *et al.*, 2004). During September of 2004 fertilisation significantly increased the SLA of *P. nigra* (figure 4.10). In 2003 the same significant effect of fertilisation was identified for *P. x euramericana* (Calfapietra *et al.*, 2005) and the authors attributed this to a fertilisation-induced stimulation of leaf area. An analysis of global data covering 2548 species indicated that a decreased SLA is associated with increased leaf longevity (Wright *et al.*, 2004). Moreover, leaf N_{mass} was positively correlated with SLA (Reich *et al.*, 1999) and therefore a decrease in SLA and related increase in leaf longevity is associated with a decrease in leaf N_{mass} (Reich *et al.*, 1999; Wright *et al.*, 2004). The association between SLA and N_{mass} is supported by data presented here. Leaf N_{mass} was reduced in both species exposed to elevated CO_2, and more so in the fertilised trees (18.10.04). In a meta analysis of results from FACE experimentation SLA and N_{mass} were both reduced in elevated CO_2 by approximately 10 % each (Long *et al.*, 2004), but canopy longevity was not measured. To my knowledge the association between these three factors has not been drawn for forest trees except that Tricker *et al.* (2004) and Rae *et al.* (2006) documented both increased leaf longevity and decreased SLA in *Populus* when exposed to elevated CO_2. In C_3 grasses Craine and Reich (2001) reported a significantly increased longevity in elevated CO_2 with an associated decrease in leaf N_{mass}, but elevated CO_2 had no effect on SLA. The authors

concluded that the longevity response to CO_2 was more associated with changes in N cycling and leaf N, than with increases in photosynthesis.

4.5.2 Leaf pigment changes

The environmental variation across the whole site had the most significant influence on the amount of chemically-extractable leaf pigments obtained after exposure to each experimental treatment. Attempts to normalise the influence of environmental variation on the statistical analysis were successful. Using this normalised data and over the time period anaysed in 2004 the autumnal change in chemically-extractable leaf chlorophyll was significantly reduced by the elevated CO_2 treatment. With changes in leaf chlorophyll considered the first visible indication of senescence (Buchanan-Wollaston *et al.*, 2003) this reduced change implies a delay in autumnal senescence in elevated CO_2. To answer the question posed in chapter 3, increased autumnal canopy chlorophyll content (as measured remotely) appears to be the result of both a reduction in the decline of LAI and a reduction in the decline of individual leaf chlorophyll concentration. Fertilisation had no significant influence on this response, but it is notable that, in elevated CO_2, fertilisation increased the decline in chlorophyll concentration during the autumn for *P. x euramericana* whereas the opposite was observed for *P. nigra* (figure 4.8). This same trend in response to autumnal senescence progression was also evident at the canopy level when MNDVI was calculated. The amount of chemically-extractable leaf chlorophyll measured in 2003 (figure 4.6) showed the same trend as for 2004 and was significantly increased in late September in elevated CO_2 for *P. x euramericana*. However, the low replication in this year (n = 2) resulted in a large standard error which was the result of significant block interactions with treatments. Furthermore, with leaves in elevated CO_2 exhibiting more mass per unit area (decreased SLA) the measurement of chemically-extractable leaf chlorophyll in 2004 (based on leaf mass) was considered a more suitable approach to monitor senescence between elevated and ambient CO_2. This is because these estimates will be less influenced by SLA than estimating chemically-extractable leaf chlorophyll on a leaf area basis as was carried out in 2003. The decline in chemically-extractable leaf carotenoid content was also significantly reduced in elevated CO_2 for both species (figure 4.9). Leaf pigments extracted from a portion of individally homogenised upper canopy leaves support the non-destructive findings of chapter 3. The chemical confirmation of the large spatial non-destructive analysis of chapter 3 indicates that senescence is delayed in elevated

CO_2 for these two species. Furthermore this also shows the potential for scaling up information collected at the leaf level to the canopy level.

4.5.3 Leaf spectral analysis

The changes in MNDVI were calculated at the leaf level and the influence of treatments was not as apparent as for extracted leaf chlorophyll. At all times block interactions with treatments were significant, except for *P. nigra* late in the season (31.10.04) when the block interaction with CO_2 was not significant and a marginally significant increase in leaf level MNDVI in elevated CO_2 was evident. Over time, the trend in percentage change in MNDVI was similar to that reported for chlorophyll concentration and canopy MNDVI for *P. x euramericana* although differences between treatments were less and not significant. Little change was evident for *P. nigra*. The small sample area measured (approximately 0.78 cm^2) per leaf may account for the lack of statistical support for the whole canopy measurements. Furthermore, the existence of leaf pathogens such as rust may influence surface reflectance properties although during the first three years of growth no significant difference was documented for rust attacks between treatments (Scarascia-Mugnozza *et al.*, 2006). There is also evidence that CO_2 may influence leaf surface reflectance irrespective of chlorophyll content, possibly through changing surface wax properties (Thomas, 2005). In elevated CO_2 an increase in surface wax amount was documented for *P. tremuloides* (Karnosky *et al.*, 2003). Unfortunately leaf surface waxes were not quantified in this research, but the changes in extracted leaf pigment content provide strong support for the conclusions from canopy remote sensing irrespective of any effects of leaf wax.

Observing a portion of both the visible and NIR spectra (550 - 900 nm) can provide information about leaf changes during senescence. Over this portion of the spectrum the largest observed difference was an increase in NIR absorbance as senescence progressed. This increase in NIR absorbance was significantly reduced in elevated CO_2. The increased NIR absorbance in ambient CO_2 was estimated from both a decrease in reflectance and transmittance of NIR from leaves of *P. x euramericana*, whereas for leaves of *P. nigra* only a decreased transmittance of NIR was evident in the ambient CO_2-grown leaves (figure 4.3 and 4.4 respectively). The reflectance and transmittance of NIR within the band measured here is increased by leaf thickness (Knapp and Carter, 1998) and also

hydration of mesophyll cell walls relative to the airscapes (Jackson, 1986). The amount of NIR reflectance was best predicted by a combination of the ratio of mesophyll cell surface area exposed to airspaces per unit leaf area; the presence of a cuticle thicker than 1 μm; and bicolouration. The correlation between all these three variables and NIR reflectance was strong (r^2 = 0.93) for 48 species examined by Slaton *et al.* (2001). For *P. x euramericana* during the second year's growth in elevated CO_2 a significant increase in both spongy mesophyll and palisade cell area as well as a small non-significant increase in leaf thickness has been documented (Taylor *et al.*, 2003). If still present after six years exposure, this may account for the features observed here. For irradiance between 770 and 800 nm, Woolley (1971) identified a direct increase in absorbance upon leaf drying, browning, and injury. Therefore the reduction in stomatal conductance and increased water use efficiency documented for *P. x euramericana* exposed to elevated CO_2 at this site (Tricker *et al.*, 2005) may also contribute to the observed decrease in NIR absorbance in elevated CO_2, through the associated increases in cellular hydration.

4.5.4 Diurnal changes in SLA

The diurnal influence on SLA may provide an explanation as to how decreased SLA increases leaf longevity. SLA decreased for both species as senescence progressed (figure 4.11) and this decrease was more apparent in the afternoon, a diurnal effect which was significant for *P. nigra*. Following exposure to 1200 ppm CO_2 *P. deltoides* leaves became depleted in glucose at 16.00 hours and this was considered to be the result of a shift in metabolism towards increasing starch synthesis (Walter *et al.*, 2005). An increased level of leaf starch has also been reported to contribute to a decreased SLA in elevated CO_2 (Pritchard *et al.*, 1999) and in elevated CO_2 prior to coppice increased leaf starch was evident in leaves of both *P. x euramericana* and *P. nigra*. In 2003, after coppice, only *P. x euramericana* was examined and the same trend was apparent (Davey *et al.*, 2006). Using *Arabidopsis* mutants with defects in starch metabolism Gibon *et al.* (2004) identified starch production as important for plant maintenance during the latter part of the night when day length was short, as is typical for the autumnal period.

4.5.5 Summary

In summary, the delay in autumnal senescence documentated in chapter 3 can also be identified at the individual leaf level. This gives strong support for this delay and also suggests that data collected at the leaf level can be scaled up to explain the findings at the whole canopy level. Elevated CO_2 reduced the autumnal decline in chemically-extractable leaf pigment content. The influence of fertilisation is again difficult to interpret. The first summary point could be that fertilisation has no effect because it has no influence on the leaf % N_{mass}. Alternatively as data is consistent at both the canopy and leaf level it can be considered that fertilisation has no effect at this site on senescence in ambient CO_2, but in elevated CO_2 fertilisation has a divergent effect on senescence progression depending on species (although no CO_2 * N interactions were significant). Moreover, the previous agricultural land use history of this site may confound direct interpretation of fertilisation effects for extrapolation outside of this plantation.

Chapter 5:

Changes in gene expression during autumnal senescence in elevated carbon dioxide

5.1 Overview

Both canopy level non-destructive approaches and leaf level destructive approaches have identified a delay in the natural autumnal senescence of two poplar genotypes growing in elevated atmospheric CO_2. The same trend from both approaches has identified the leaf level sampling strategy in chapter four as adequate to represent the different senescence response observed at the canopy level.

In this chapter an attempt to identify cellular processes occurring during autumnal senescence, which may provide a clue as to the mechanisms that are responsible for the delayed senescence, will be carried out. In the absence of any substantiated hypothesis targeted to specific mechanisms, microarray technology will be used to identify target genes expressed during senescence in elevated CO_2. An overview of the molecular biology and biochemistry relating to microarray technology will be given and the advantages and disadvantages of this approach will also be discussed.

5.2 Introduction

It is now generally accepted that leaf senescence is the final stage of leaf development and is genetically controlled to maximise nutrient mobilisation and recycling (Buchanan-Wollaston *et al.,* 2003; Quirino *et al.,* 2000). Unlike animals, plants are sessile organisms (depending on temporal and spatial scale, i.e. within one generation and at the whole plant scale), and one response to an unfavourable environment is to remove those parts of the plant that are not essential (Buchanan-Wollaston, 1997). With this in mind it may not be surprising to find that a wide breadth of environmental stresses, defence responses and age-dependent triggers for senescence result in a highly conserved sequence of cellular events irrespective of the trigger (Lim *et al.,* 2003; Quirino *et al.,* 2000). This sequence of cellular degradation begins with the chloroplast and massive N remobilisation, with the mitochondria and nucleus remaining intact until very late stages of senescence (Lim *et al.,* 2003). The mitochondria and nucleus are required because senescence is energetically demanding (mitochondria) and genetically coordinated (nucleus) but nuclear degradation is also an important source of re-mobilised phosphorous (Dangl *et al.*, 2000).

As exemplified from studies of autumnal senescence in *Populus tremula* (aspen) senescence is associated with a massive decline in leaf RNA abundance (Bhalerao *et al.,* 2003) which parallels the decline in leaf chlorophyll concentration, and the efficiency of photosynthesis (Keskitalo *et al.,* 2005). Nevertheless, the inhibition of senescence through the application of inhibitors of RNA and protein synthesis, as well as anoxia and respiratory inhibition, identifies senescence as an active process requiring gene expression (Noodén 1988). The synthesis of RNA during senescence results in senescence-associated genes (*SAG*s), a term not favoured by Buchanan-Wollaston (2003) who considered senescence-enhanced genes (*SEN* genes) a more accurate term. This may be to indicate that many (amount unknown) *SAG*s are expressed during normal growth, with their expression enhanced during senescence. In addition to those *SEN* genes, *SAG12*, a cysteine protease is considered unique to senescence and a marker for natural autumnal developmental senescence (Weaver *et al.,* 1998).

Numerous studies, mostly involving Arabidopsis, have attempted to identify SEN genes and the differential expression of SEN genes in response to different triggers of senescence and these are discussed in the following reviews: Buchanan-Wollaston,

(2003); Quirino *et al.,* (2000); Yoshida, (2003); Lim *et al.,* (2003) and Wingler *et al.,* (2006). In summary many SEN genes are involved and cross talk exists between stress responses, hormonal regulation of aging, sugar signalling and the light environment, and very much is still unknown. For example, in just one study which involved sequencing cDNA clones from senescing *Arabidopsis* leaves, 70 new SEN genes were identified (Gepstein *et al.,* 2003). The four most abundant genes found in senescing Aspen leaves were also among the most abundant in senescing Arabidopsis. These were genes encoding metallothionein, early-light -inducible-proteins (ELIP), proteases and components of the ubiquitin degradation pathway (Gepstein *et al.,* 2003). The most dominant senescence-associated proteases are cysteine proteases, which are vacuole localized enzymes, and this is highly consistent between *Arabidopsis* and *Populus* (Gepstein *et al.,* 2003). So during early senescence while the vacuole is intact a role for reactive oxygen species (ROS) has been proposed in the early degradation of the stroma enzyme Rubisco (Buchanan-Wollaston *et al.,* 2003), and so a ROS-associated decline in membrane integrity may be an early senescence symptom (McKersie *et al.,* 1988). This process was also suggested as a mechanism for the initial degradation of chloroplast proteins in aspen leaves (Andersson *et al.,* 2004), although the authors caution that unknown chloroplast proteases may be involved. Early stage senescence is a reversible process and it is proposed that only when stroma and thylakoid components come into contact with vacuole and extraplastidial enzymes, a process requiring membrane rupture, does senescence become irreversible (Hörtensteiner and Feller, 2002). The metabolically-active nature of senescence means that it is an oxidative process and therefore generates ROS (Dangl *et al.,* 2000). Although evident in early phase senescence, excess ROS during this phase would initiate terminal senescence and be catastrophic to the orderly process and efficient nutrient remobilisation (Gepstein *et al.,* 2003). As senescence is a plastic response which can adapt to environmental conditions to optimise plant C:N status and nutrient remobilisation (Wingler *et al.,* 2006), it seems a reasonable assumption that this plasticity will exist during early stages of senescence, which appears dominated by a balance between ROS and ROS-scavenging mechanisms (Dangl *et al.,* 2000). In a similar vein Keskitalo *et al.* (2005) ask the question "is there a point of no return in autumnal senescence of aspen leaves". To give a temporal aspect to the process of senescence, and in answer to this question, the authors propose that reversibility of senescence is only possible during phase 1, up until 11th September in this experiment, with leaf abscission occurring approximately 1 month later. It is also imperative to remember that the single

most important contributory factor to the timing of senescence in *Populus* is the change in photoperiod (Böhlenius *et al.,* 2006; Keskitalo *et al.,* 2005). This indicates the complexity that exists between the signals and the progression of senescence when attempting to delineate the mechanisms that contribute to delayed autumnal senescence as a result of elevated CO_2.

To date, two studies have attempted to disentangle the complexity of senescence at the level of gene expression in forest trees, and both of these studies were carried out on one aspen (*P. tremula*) tree in northern Sweden (Bhalerao *et al.,* 2003; Andersson *et al.,* 2004). Bhalerao *et al.,* (2003) identified 35 genes that were unique to the autumn aspen leaf cDNA library, when compared with a cDNA library produced from a young but fully expanded aspen leaf and these were designated as *Paul* (*Populus autumn leaves*) 1-35. Andersson *et al.,* (2004) analyzed changes in gene expression during the progression of autumnal senescence relative to the gene expression of a common reference pool collected from leaves of 20 trees on 4th September, and differential gene expression was assessed using microarray technology. Over 3000 genes were significantly expressed over the time course of senescence with many of the *Paul* genes among those most highly expressed. Among the 200 most highly expressed transcripts were many representing genes of unknown function.

In this chapter and for the first time, the gene expression in the leaves of freely growing poplar trees exposed to elevated CO_2 following six years of growth will be explored during natural autumnal senescence. The differential gene expression between elevated CO_2 and ambient CO_2 growing trees will be investigated using microarray technology.

5.2.1 Microarray technology

The abundance of specific sequences of mRNA in a reference material and therefore the expression of the associated gene can be assessed through the exacting and mutual selectivity of complementary base pairing, an exploitable process considered to provide the core to the revolution in molecular biology (Southern *et al.,* 1999). Microarray technology is based on the complementary base pairing of strands of nucleic acids and can be considered a high through-put variant of the Northern blot. In Northern blot hybridisation RNA from the experimental sample is separated by denaturing agarose gel

electrophoresis and these separated products are immobilised on to a nitrocellulose membrane. A radioactive single-stranded nucleotide sequence specific to the gene of interest (the probe) is then "blotted" onto the nitrocellulose membrane and incubated. The existence of radioactivity on the blot can lead to the conclusion that the gene of interest is present in the experimental sample (Watson *et al.,* 1992). cDNA Microarray technology can be considered the reverse of this blotting process with many thousands of probes used at once, a diagram of the process of cDNA microarray hybridisation is give in figure 5.1.

cDNA microarrays are produced by robotically spotting multiple probes representing specific genes or ESTs (expressed sequence tags, discussed next) of interest, at a very high density on a suitable matrix which is often glass based. For example, the density of the poplar microarray produced by the Platform for Integrated Clone Management (PICME) is up to 26,000 probes in an area of a typical microscope slide (www.picme.at). The "target" is a labelled representation of cellular mRNA pools (Duggan *et al.,* 1999). Typically RNA is extracted from material under control and treatment conditions, in the case of this chapter this may be leaves from either ambient CO_2-(control) or elevated CO_2-(treatment) grown trees. The mRNA is selected from the total RNA pool by using an oligo-dT primer to select for the poly (A) tail unique to mRNA and this is subsequently reverse transcribed to cDNA. The cDNA representation from each pool is labelled with a fluorescent fluorophore-dUTP conjugate which emits specific wavelengths upon excitation with a laser. Most commonly used are Cy3-dUTP which emits at 568 nm (therefore appearing green, G) and is used to label control cDNA and Cy5-dUTP which emits at 667 nm (therefore appearing red, R) and is used to label treated cDNA. Following hydridisation between spotted probes and labelled targets the slide is exposed to a laser and the ratio of the fluorescence between the two dyes corresponds to the abundance of each probe relative to the control and treated samples. It is important to outline terminology at this stage. An EST spotted cDNA microarray hybridisation experiment informs upon the relative abundance of an EST sequence in a treated sample. The general terminology is to refer to the gene encoding the mRNA of the respective EST to be either up- or down-regulated by the treatment with respect to the relative abundance of the labelled target in the treated sample. However it is important to note that no knowledge of changes in gene regulation is directly measured, a change in regulation is assumed from relative measures

of mRNA abundance, therefore when discussing the RG ratios and the activity of the corresponding gene the terms up- or down-expressed will be used.

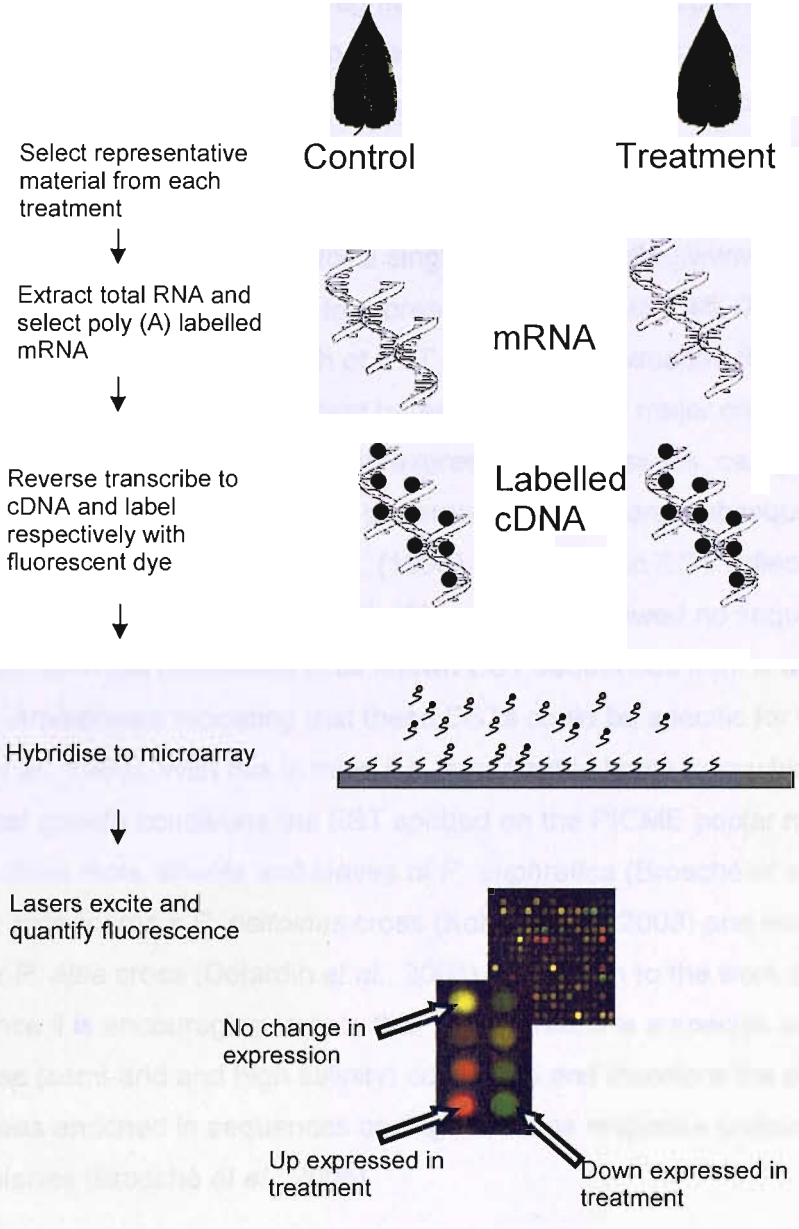

Figure 5.1: A schematic representation of the analysis of gene transcription using cDNA microarry technology. Leaf images were obtained from N.R. Street (University of Southampton) and nucleic acids adapted from an image by Darryl Leia of the National Human-Genome Research Institute and obtained via www.googleimages.co.uk

5.2.2 Expressed Sequence Tags (ESTs)

In order to sequence the human genome a technique termed EST (expressed sequence tag) sequencing was identified. In view of gene discovery, this technique was considered superior (in terms of time and cost) to that of whole genomic DNA sequencing (Adams *et al.,* 1991). ESTs are sequenced fragments of cDNA, as the cDNA is reverse transcribed from mRNA then ESTs represent partial sequences of genes from total DNA, a vast amount of which consists of non-coding sequences. In 1993 a data base was set up as a repository for all the EST sequence information and currently contains sequence information of 369, 237 *Populus* ESTs with 89, 943 *Populus* trichocarpa ESTs representing the most numerous for a single genotype (http://www.ncbi.nlm.nih.gov; as of 22.09.06). These are now known to represent approximately 45, 000 genes (Tuskan *et al.,* 2006). When exploiting this wealth of EST sequence information through the use of microarray technology, it is important to remember that a major criticism of this approach is the difficultly in obtaining every mRNA expressed in all tissues, cell types and developmental stages from which to generate the cDNA and subsequent ESTs (Adams *et al.,* 1991). For example, Sterky *et al.,* (1998) generated an EST collection from wood-forming tissue of *Populus*. Up to 12 % of these ESTs showed no sequence similarity to any sequence in the databases of all known EST sequences from a wide array of species including *Arabidopsis* indicating that these ESTs could be specific for wood formation (Sterky *et al.,* 1998). With this in mind it is important to know from which sources and under what growth conditions the EST spotted on the PICME poplar microarray originate. They are from roots, shoots and leaves of *P. euphratica* (Brosché *et al.*, 2005), root tissue from a *P. trichocarpa* x *P. deltoides* cross (Kohler *et al.*, 2003) and wood tissue from a *P. tremula* x *P. alba* cross (Déjardin *et al.*, 2004). In relation to the work documented here on senescence it is encouraging to note that *P. euphratica* is a species adapted to growth in high stress (semi-arid and high salinity) conditions and therefore the cDNA library from this species was enriched in sequences coding for stress response proteins such as metallothiones (Brosché *et al.,* 2005).

The assignment of biological function to raw sequence information is termed annotation. Annotation can result from comparing the sequence similarity (homology) with sequences from other organisms using sequence alignment algorithms, such as BLAST (Basic Local Alignment Search Tool). For example, BLAST can be applied to a cross species

nucleotide comparison for the existence of the queried gene or with amino acid sequences to identify the most likely gene product. Therefore, depending upon the species, the number of ESTs, the sequence analysis of the EST, and functional analysis of the gene corresponding to the EST, a cDNA microarray experiment may be considered a bit like finding a needle in a haystack when you only have anecdotal evidence as to what a needle is. Nevertheless at the limits of this current and rapidly expanding technology microarrays have provided substantial insight into genes involved in senescence. For example in one study 800 genes showing a reproducible increase in transcription during *Arabidopsis* leaf senescence were identified (Buchanan-Wollaston *et al.,* 2005). Furthermore, Buchanan-Wollaston *et al.* (2005) showed transcriptional evidence for a similarity in common processes during senescence, whereas, differences were also shown and attributed to different stress pathways induced to extend the viability of senescing cells. For example, genes related to flavonoid synthesis showed increased expression in developmental senescence only, and were absent in dark-induced senescence (Buchanan-Wollaston *et al.,* 2005).

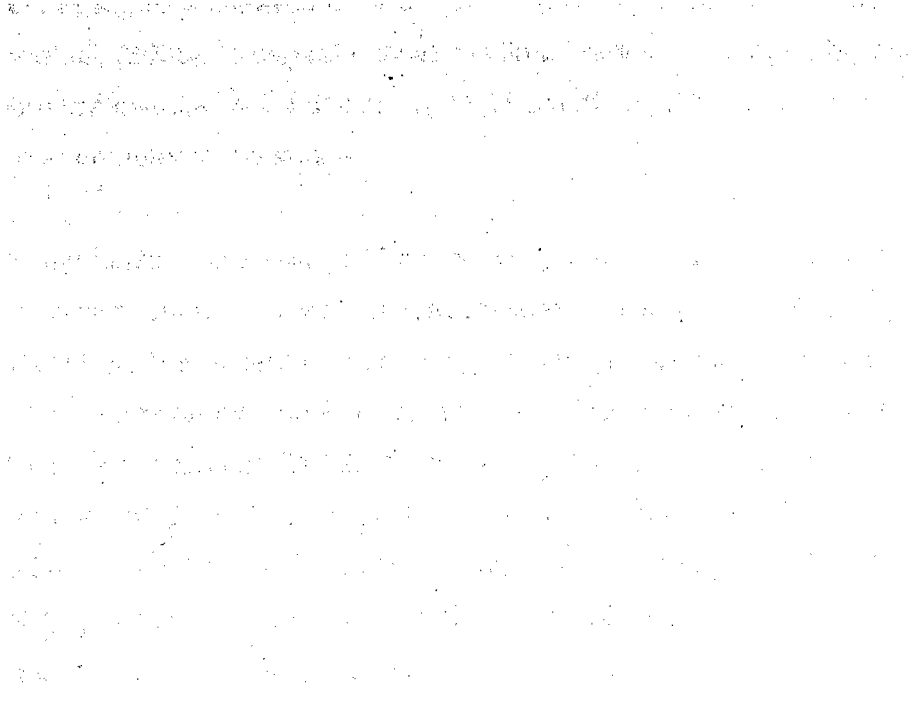

5.3 Materials and Methods

5.3.1 Leaf sampling

Trees growing in the experimental plots of the POP/EUROFACE site (chapter three) were selected and leaves were removed with scissors at the leaf base so that the petiole remained attached to the stem. Immediately following removal the leaf was sealed in a pre-prepared labelled foil packet and within ten seconds of removal was placed in liquid N_2. All samples were then stored at - 80 °C except during transportation from Italy to the UK, when leaves were stored on dry ice (CO_2) at approximately - 60 to - 70 °C.

Pre-senescent leaf material was sampled prior to the labelling of trees for following the course of senescence (as described in chapter four). These leaves were sampled with respect to leaf number one which was considered the first fully unfurled leaf that was approximately 30 mm in length. Leaf nine was the ninth leaf down the stem from reference leaf one. This sampled leaf nine was considered mature as leaf area was maximal and expansion had finished (Taylor *et al.*, 2003). Four replicate leaves were sampled from each sub-plot as described above, for *P. x euramericana* (31.08.04) and *P. nigra* (01.09.04). Due to the length of time (approx 3 hrs) to sample each species, and the potential for confounding factors of environmental and diurnal influences on transcription (Rogers *et al.,* 2006), leaves were sampled between 15.00 to 18.00, as described by Taylor *et al.,* (2005). In central Italy at this time irradiance stays visibly consistent and the temperature change was a decline of 2 °C from 27 to 25 °C when measured using an on sight thermometer in the shade.

Senescing leaves were selected from between four to eight individual replicate trees of each sub-plot. During senescence leaves were selected from between the ninth and 11th leaf down from the closed apical bud, as labelled and described in chapter four. Leaves of both *P. x euramericana* and *P. nigra* were sampled. Four replicate leaves were sampled for *P. x euramericana* on 21.09.04, 05.10.04, 04.11.04 and six replicate leaves were sampled on 18.10.04 . Four replicate leaves were sampled for *P. nigra* on 21.09.04, 06.10.04, 20.10.04 and eight replicate leaves were sampled on 02.11.04. The time of sampling was adjusted to account for the seasonal change in temperature and irradiance. For example, on 18.10.04 sampling took place between 14.00 and 16.00 when a two

degree temperature change between 22 and 20 °C was noted, and uniform irradiance was apparent.

For the subsequent microarray analysis described in this chapter *P. x euramericana* leaf material sampled from the ambient nitrogen sub-plot of all treatment plots from blocks one and two were selected. Leaves sampled on 31.08.04 were classed as pre-senescent and 18.10.04 as senescent material.

5.3.2 Target preparation for microarray hybridisation

5.3.2.1 RNA extraction and quantification

Under liquid N_2 at all times, each selected whole leaf was ground to a fine powder using a pestle and mortar. Ground material was added to a 50 ml falcon tube (Cellstar® greiner bio-one). A 2 % hexadecyltrimethylammonium bromide (CTAB) extraction buffer was prepared as described in Cheng *et al.* (1993), and 15 ml of pre-warmed (65 °C) CTAB was added to the ground material. The ground material remained at - 80 °C or less until suspended in the CTAB extraction buffer. Once suspended 400 µl of (2.67 % v/v) β-mercapto-ethanol (Sigma-aldrich, UK), was added to the extraction which was vortexed thoroughly. Following an incubation (65 °C for five minutes) 15 ml of CHISAM (chloroform : isoamyl alcohol, 24 : 1 v/v) was added and thoroughly mixed at room temperature. The aqueous and organic phases were separated following centrifugation at 4 500 rpm (Sorvall® legend RT) for 20 mins at room temperature (RT). The upper-phase was transferred to a new 50 ml falcon tube containing 15 mls CHISAM and the cenrifugation was repeated. The upper-phase was again taken and added to a JA-20 tube (Oakridge, USA) containing 3 mls of 10M LiCl (1:4 vol LiCl) placed on ice and stored at 4 °C over-night. Following the over-night precipitation the solution was centrifuged (Beckman J2-21 and a JA-20 rotor) at 10 000 rpm for 30 mins at 4 °C following over-night chilling of the rotor. The supernatant was removed and the pellet re-suspended in 700 µl of pre-warmed (60 °C) SSTE as described by Cheng *et al.* (1993). Following an incubation (60 °C, max two mins) 700 µl of CHISAM was added and the solution (1.4 ml) was added to a 2 ml tube (eppendorf). The solution was then centrifuged (10 000 rpm, RT for 10 mins) (Eppendorf, 5417R, Cambridge, UK). The upperphase was transferred to a new tube containing 700 µl of CHISAM and the phase separation step repeated. The upper-phase was then

transferred to 2 x vol (~1.2 ml) 99.8 % ethanol and the RNA was precipitated (-80 °C, one hour). The solution was then centrifuged (13 000 rpm, 30 mins, 4 °C), the supernatant removed and the RNA pellet was washed twice with 1 ml of 70 % ethanol by centrifugation (10 000 rpm, two mins at 4 °C). Tubes were then inverted and the pellet was air-dried for between 10 to 20 mins. When dry the pellets were re-suspended in 20 µl of DEPC-treated H_2O and stored at - 80 °C.

Stock RNA was taken (1 µl) and diluted 1:60 with DEPC-treated H_2O and nucleic acid content was quantified by measuring absorbance at 260 nm using a spectrophotometer (NanoDrop® ND-1000 Spectrophotometer, Wilmington, DE, USA.). Nucleic acid purity was estimated using the ratio absorbance at 260 nm (A_{260}) and 280 nm (A_{280}). A value of greater than 1.8 for A_{260}:A_{280} was considered of sufficient purity. The RNA quality was tested by microfluid capillary electrophoresis using the Agilent 2100 bioanaylser (Agilent Technologies, USA). Both the gel image and electropherograms were used to determine RNA quality as observed from the integrity of the two ribosomal bands (28S and 18S) and low amount of small molecular weight components (Imbeaud *et al.*, 2005).

For each RNA extraction from samples harvested on 18.10.04, 100 µg of total RNA in 15 µl of DEPC-treated H_2O were taken for cDNA synthesis. Of the 12 possible biological replicates for each treatment (six leaves per plot and two plots per treatment), the RNA extracted from nine leaves of each treatment was of sufficient quality for microarray target preparation. RNA extracted from the pre-senescent samples was pooled with respect to treatment. One pool for ambient CO_2 consisting of four replicates from plot 2 and three from plot 3, and one pool from elevated CO_2 consisting of four replicates from each of plots 1 and 4; substandard RNA (identified through electrophoresis) was not used. The cDNA sysnthesis of each pool was then carried out using 100 µg of total pooled RNA in 15 µl of DEPC-treated H_2O.

5.3.2.2 cDNA synthesis

Unless stated otherwise, all materials for cDNA sysnthesis were obtained from Invitrogen (Paisley, UK). 100 µg of total RNA in a 0.5 ml eppendorf tube was denatured with 2 µl of anchored oligo$(dt)_{20}$ primer by heating at 65 ° for 10 minutes then chilling on ice (max. 1 minute). A reverse transcription master mix was prepared. This consisted of 6 µl 5x -RT-

buffer (first strand buffer), 3 µl of 10mM DTT, 1 µl of 50x dNTP mix (a mix of dA, dC and dG, and aa-dUTP and dTTP in a ratio of 4:1 aa-dUTP:dTTP) (Amersham UK; except aa-dUTP, Sigma UK), 1 µl RNase inhibitor and 2 µl of Superscript™ reverse transcriptase. The master mix was made in bulk such that 13 µl was added to each oligo $(dt)_{20}$ primed RNA sample for over night cDNA synthesis at 48 °C. After overnight synthesis the reverse transcription reaction was inhibited by addition of 10 µl 0.5 M EDTA and any remaining RNA degraded by the addition of 10 µl 1 M NaOH and heating at 65 °C for 15 minutes. The remaining cDNA was then neutralised with 50 µl of 1M HEPES (pH 7.5).

5.3.2.3 cDNA cleanup

The recently synthesised cDNA was purified using a Qiagen PCR purification kit, consisting of QIAquick® spin columns (Qiagen, Crawley, UK). The cDNA clean up was carried out according to the manufacturer's instructions for the purification of single- or double-stranded DNA, with the following exceptions. A phosphate-ethanol wash buffer (PWB) was used instead of buffer PE and two PWB steps were included. cDNA was then eluted from the QIAquick® column membrane via two elutions each with 30 µl of 0.1 M $NaHCO_3$ (pH 9.0), 1 µl of cDNA was then taken for spectrometric quantification.

5.3.2.4 Dye coupling

The purified cDNA was taken and 35 µl 100 mM sodium acetate (pH 5.2) added. Now working under minimal light, purified cDNA was added to an aliquot of CyDye™ ester (Amersham, Buckinghamshire, UK). Cy3 and Cy5 were added to control and treatment respectively, except for nearly 50 % of the samples when this orientation was reversed to account for any dye binding bias. The samples were gently agitated and then left in the dark at room temperature for between 1.5 and 2 hours for dye binding.

5.3.2.5 Dye coupled cDNA clean up.

The recently dye coupled cDNA was purified using Qiagen PCR purification kit. The Cy3 labelled cDNA was purified according to the manufacturer's protocol with the following exceptions. An additional buffer PE wash step was included and two repeated elution steps were carried out into a fresh eppendorf tube. The Cy5 tube was treated the same

and eluted into the same eppendorf tube as the Cy3, following randomised paring between control samples and treated samples. Of the total eluate containing 200 µl of Cy3-and-Cy5 coupled cDNA 1 µl was taken and quantified spectrophometrically. The target was now prepared and concentrated down to 25 µl in a spin concentrator (Eppendorf Concentrator 5301, Eppendorf, Cambridge, UK).

5.3.3 Probe preparation

5.3.3.1 Microarray slide preparation

Microarray slides were obtained from The Platform of Integrated Clone Management (PICME, www.picme.at). This is part of the Austrian Research Centers Seibersdorf, a subunit of the ARC Seibersdorf research, GmbH. Microarray slides were taken which had been spotted, by PICME, with approximately 26 000 poplar ESTs. Slides were placed in a coplin staining jar, containing pre-hybridisation buffer, in a water bath at 42 °C, for approximately 1 hour. Pre-hybridisation buffer was prepared fresh and consisted of 50 % (v/v) formamide 5X SSC, 0.1 % SDS (w/v) and 0.1 mg ml^{-1}BSA (Sigma-Aldrich, Dorset, UK, except SDS, Fisher, Leicestershire, UK). This pre-hybridisation of slides was started approximately 30 minutes into the dye coupling reaction in an attempt to synchronise the timing of probe and target preparation. The slide was then removed from the coplin jar and washed at room temperature by placing directly into a bath containing wash buffer III (0.2xSSC) for 5 minutes. A further 5 minute wash in fresh wash buffer III was then carried out followed by the following washes; 30 seconds in H_2O of 18.0 Ω (Elga, Maxima, York, UK), 60 seconds in boiling H_2O (milliQ), and a 4 °C ethanol soak (approximately 1 minute) prior to drying by centrifugation (3000 x g for 1 minute). At no stage were slides allowed to dry prior to the final centrifugation step.

5.3.4 Hybridisation

Working in semi-darkness the dye-labelled target (25 µl) was denatured by the addition of 50 µl formamide, 25 µl of hybridisation buffer (Amersham, UK) was also added and the sample heated at 95 °C for 1 minute and then chilled on ice.

The pre-hybridised microarray slides were placed in the hybridisation chambers of a HS400 hybridisation station (Tecan, Reading, UK). Each denatured labelled target sample (100 µl) was added to the respective slide (according to manufacturer's protocol) when prompted by the primed station. Microarray hybridisation was carried out at 42 °C for 16 hours with a low agitation frequency.

5.3.4.1 Post hybridisation washing

Post hybridisation slide washing was carried out automatically while the slides remained in the chambers of the HS400 hybridisation station. Sequential washing was carried out with four different solutions increasing in stringency. Immediately post hybridisation slides were washed in the following order with wash buffer I (WB I; 0.1X SSC, 0.2 % SDS), WB II (0.1X SSC, 0.2 % SDS), WB III (0.2X SSC), H_2O (milliQ) and finally 100 % ethanol. Slides were then dried in a stream of pure N_2 gas.

5.3.5 Experimental design of hybridisations

To identify changes in gene expression between trees exposed to elevated or ambient CO_2 during senescence, three approaches were used. An overview of this experimental design is illustrated in figure 5.2. In approach one direct comparisons between senescent samples (18.10.04) exposed to either elevated or ambient CO_2 were carried out. In approach two comparisons between pre-senescent (31.08.04) and senescent material were carried out using a common pre-senescent reference pool respective to CO_2 treatment. In approach three a comparison between pre-senescent reference pools was carried out.

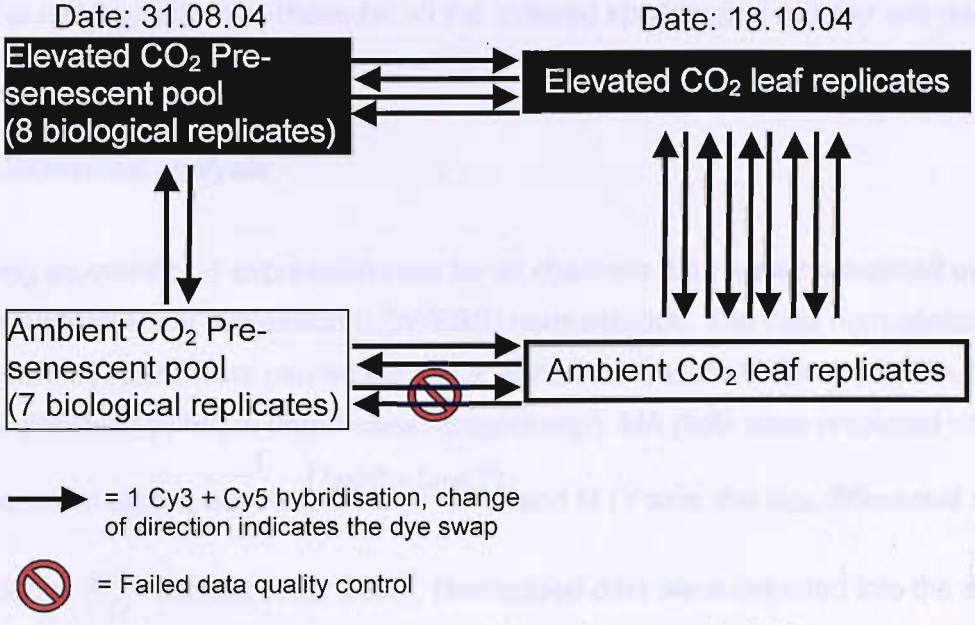

Figure 5.2: A schematic representation of the microarray hybridisation design used in this chapter

5.3.6 Data acquisition

All microarrays were scanned within the same day that hybridisation was completed. Slides were scanned using a Genetix Aquire scanner (Genetix, Hampshire, UK). The voltages of the scanner photomultiplier tubes (PMT) were adjusted to balance the digital output from the Cy3 and Cy5 dye emission channels and to ensure little if any spot saturation. This was carried out during a pre scan at 30 µm per pixel resolution, and the final scan was carried out at 5 µm resolution, PMT settings were typically between 60 to 80 %, with no more than a difference of 10% gain between channels. Scanned images were saved as TIFF files.

The raw TIFF files were analysed using GenePixPro 5.1 (Axon Instruments, Union City, California). Two TIFF files were produced for each slide respective of the maximum dye emission wavelength (now referred to as channels). The GenePIX software calculates a mean and median intensity of pixels within each spot (these values should be similar for a good quality hybridisation) and the red/green ratio against the valley background associated with that spot (Yang *et al.*, 2001). Spots with intensity below 500 or equal to 65535 (saturated) were flagged as bad. Images were also checked manually and

abnormal looking spots and those far off the indexed spotting grid (dust or salt deposits) were also flagged as bad.

5.3.7 Statistical analysis

Assuming an overall 1:1 expression ratio for all channels data were normalised using locally-weighted linear regression (LOWESS) normalisation. The data normalisation and subsequent MA plots were carried out by Dr. N.R. Street at the University of Southampton using R statistical software (http://www.r-project.org/). MA plots were produced where A (*X* axis; the mean signal) equals $\frac{(LogR + LogG)}{2}$ and M (*Y* axis; the $\log_2$ differential ratio) is equal to $\log_2 {}^{R}/_{G}$ (Dudoit *et al.*, 2000). Normalised data were imported into the analysis and visualisation software GeneSpring 7 (Silicon Genetics, Redwood City, CA). All spots flagged as bad were removed from the analysis, the dye swap was taken into account and all subsequent data analysis was carried out in GeneSpring.

5.3.7.1 Fold change

To identify genes differentially expressed by treatment, one approach standard in the literature is to regard those exhibiting greater than a two times (two-fold) change in expression ratio either up or down, as differentially expressed. With biological replication of hybridisations it is then possible to assign this two-fold change to be consistent in an arbitrarily defined *x* out of *y* hybridisations. ESTs considered as differentially expressed were those showing a consistent two-fold change in expression in at least six of the nine hybridisations during late senescence.

5.3.7.2 The t-test

For both the late senescence and pre-senescence hybridisations a *t-test* was calculated within GeneSpring to identify if a normalised expression value of an EST is statistically different from 1.0 (equal expression between treatments). For the across time analysis, senescence was assigned as either occurring in elevated or ambient CO_2. The expression changes between senescent samples and the pre-senescent reference pool with respect

to the senescence treatment were then examined by a Welch *t*-test using error model variances as recommended in the GeneSpring analysis manual (Silicon Genetics, 2004). The cross gene error model was active and based on sample replicates as recommended. No multiple testing corrections were applied.

5.3.7.3 Bayesian statistics

Differentially expressed ESTs late in senescence (18th October 2004) were identified using the 'B statistics' LIMMA packages from Bioconductor. (Smyth 2004; http://bioinf.wehi.edu.au/limma/). This uses Bayesian statistics to compute the probability of a gene being differentially expressed. A B value of zero equals a 50:50 probability of differential expression where as a B value of 3 represents approximately 95% certainty of differential expression (exp[3] / (1+exp[3])) = 0.95, or 95 %). B values are automatically adjusted for multiple testing with an FDR of 0.05. ESTs considered as significantly differentially expressed in elevated compared to ambient CO_2 late in senescence (18 October 2004) and those differentially expressed between pre-senescent and senescent tissues (were those with a B value of ≥ 3. A B value cut off of ≥ 3 was also applied to identify ESTs that were differentially expressed between 31 August 2004 and 18 October 2004, in either elevated or ambient CO_2. Genelists with B values of ≥ 3 were taken and analyzed further using GeneSpring GX. For each hybridization approach, the mean normalized expression of each EST was calculated, and those showing a B value of ≥ 3 and a 2-fold increase or 2-fold decrease in mean normalized expression in the treatment compared to the control were then selected.

5.3.8 Obtaining biological information

To provide biological information to all target EST sequences, the sequence annotation given by PICME was checked using the tBLAST X algorithm run by the DOE Joint Genome Institute (JGI, http://genome.jgi-psf.org) (Checked annotations were provided by F. Martin *et al.*, INRA, Nancy, France). These annotations were verified using the tBLAST X algorithm via *Populus* db (Starky *et al.,* 2004; www.poppel.fysbot.umu.se) and regularly checked for updates via JGI.

5.4 Results

5.4.1 Data normalisation

LOWESS regression was an effective approach to normalise the raw data obtained in each channel of each hybridisation. This can be seen when comparing the MA plots obtained for raw and normalised data, where a grouping towards the zero M value indicates a linear intensity between the red and the green channels. A typical MA plot for raw data in this chapter is shown in figure 5.3 (A) and the MA plot resulting from normalising that data is shown in figure 5.3 (B).

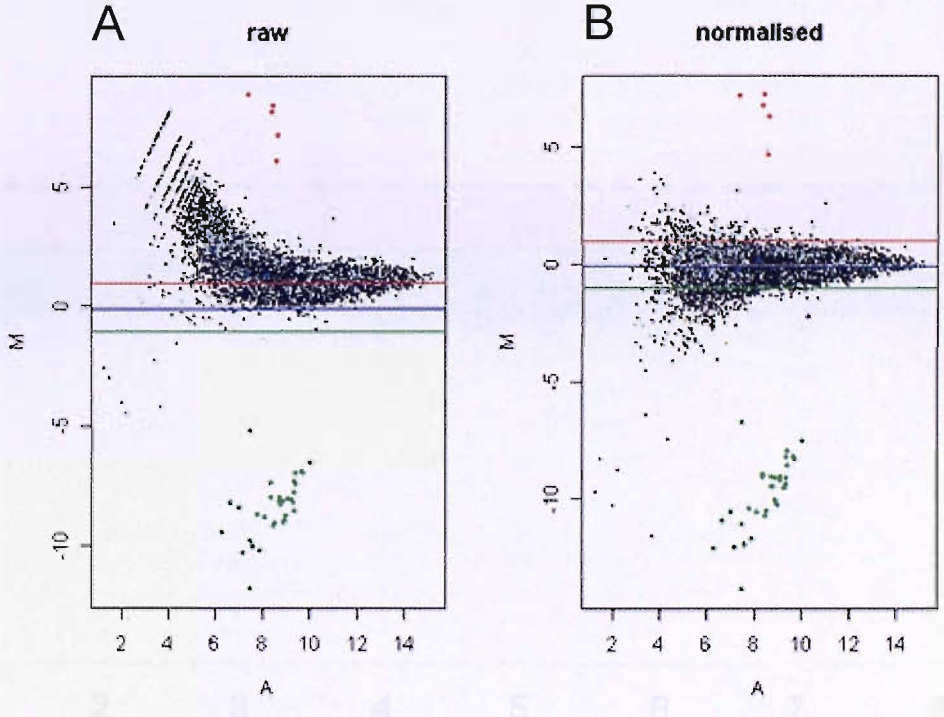

Figure 5.3: (A) An MA plot of the raw median pixel intensity of each channel and (B) the MA plot for the same data following LOWESS normalisation, the tendency towards the horizontal indicates a linear intensity between the red and green channels.

5.4.2 *Identifying differential gene expression during senescence in either elevated or ambient CO_2*

Differential gene expression was viewed in GeneSpring by a line connecting the normalised intensity of each spot between hybridisations, on a log scale; an example of this is given in figure 5.4.

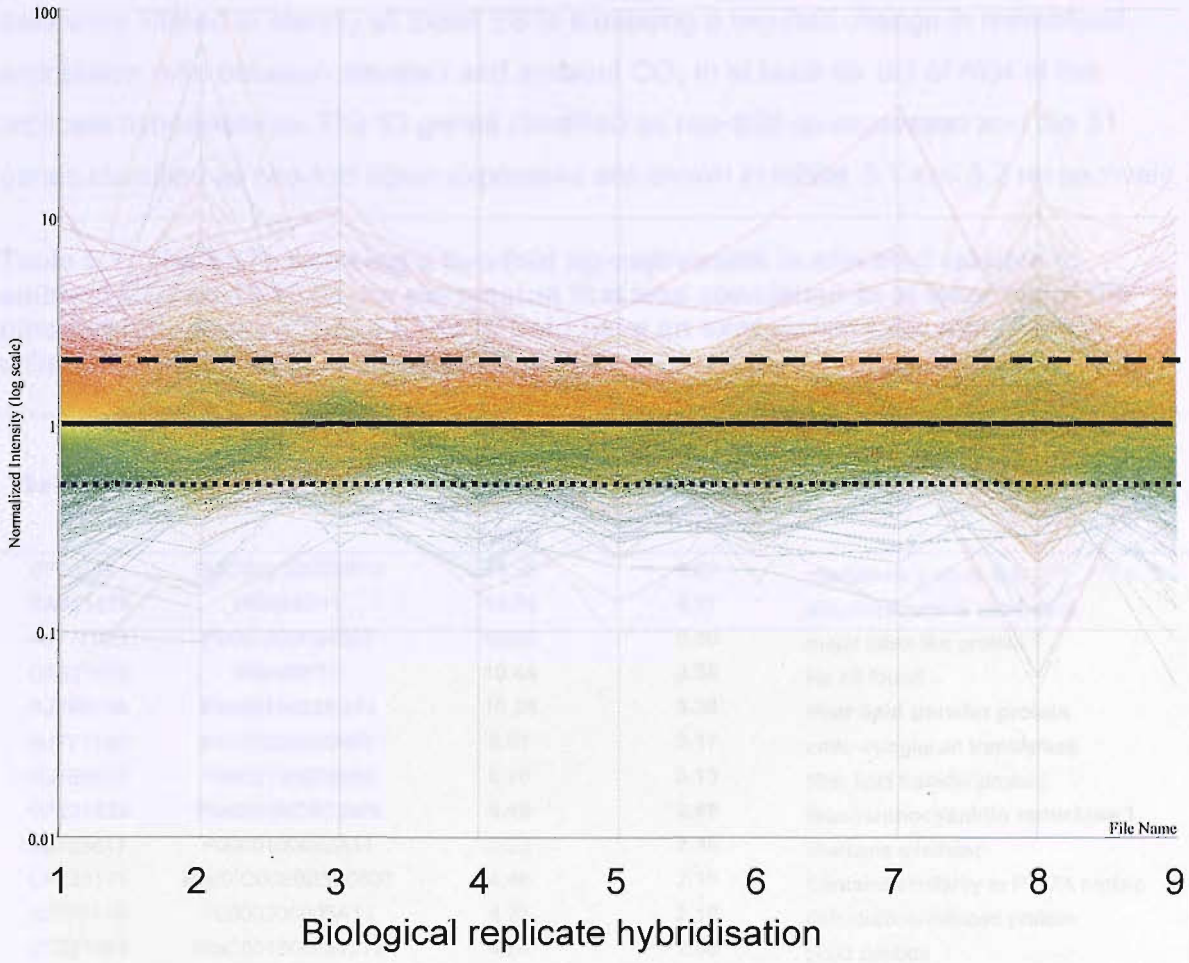

Figure 5.4: The normalised expression of the 2696 ESTs for which data exists from all nine hybridisations using targets obtained from samples taken on 18.10.04. ESTs greater than two fold up-expressed are represented by lines above (– –), no change in expression is represented by (——) and those two fold down-expressed are represented by lines below (·····).

5.4.2.1. Differential gene expression between late senescence samples

Of the 20243 possible data points, representing the normalised intensity of each poplar EST, only 13 % (2696) existed across all nine replicate hybridisations between elevated CO_2 and ambient CO_2 samples taken late in senescence (18.10.04). Of these, three ESTs were significantly differentially expressed at $p \leq 0.05$. These were annotated as fiber lipid transfer protein, dihydroflavonol reductase and leucoanthocyanidin reductase 1 ($p \leq 0.05$, in 5 out of 9 hybridisations) and are highlighted in table 5.1. Irrespective of significance, data were filtered to identify all those ESTs exhibiting a two-fold change in normalised expression ratio between elevated and ambient CO_2 in at least six out of nine of the replicate hybridisations. The 53 genes identified as two-fold up-expressed and the 31 genes identified as two-fold down-expressed are shown in tables 5.1 and 5.2 respectively.

Table 5.1: The ESTs showing a two-fold up-expression in elevated relative to ambient CO_2 on 18.10.04, an expression that was consistent in at least six of the nine hybridisations. Those ESTs in bold have an expression ratio significantly different from 1:1 in at least 5 hybridisations

GenBank	PICME id	Mean normalised expression ratio	Mean log_2 expression ratio	Annotation (tBLASTX)
CF231471	PtaC0021G8G0814	19.58	4.29	membrane protein-like
CA821476	**RSH03D11**	**19.34**	**4.27**	**dihydroflavonol reductase**
AJ772303	P0001700004E07	13.88	3.80	major latex-like protein 1
CA821652	RSH05F12	10.44	3.38	No hit found
AJ768790	**P0000100021G11**	**10.24**	**3.36**	**fiber lipid transfer protein**
AJ773160	P0000200005H07	9.01	3.17	endo-xyloglucan transferase
AJ768632	P0000100020A09	8.76	3.13	fiber lipid transfer protein
CF231825	**PtaC0026C2C0206**	**6.40**	**2.68**	**leucoanthocyanidin reductase 1**
AJ768811	P0000100022A11	5.22	2.38	chalcone synthase
CF233171	PtaJXO0020B5B0503	4.48	2.16	Contains similarity to PIR7A protein
AJ773118	P0000200005A11	4.27	2.10	dehydration-induced protein
CF231054	PtaC0016G3G0313	4.24	2.08	pop3 peptide
AJ769648	P0001000011E10	4.02	2.01	senescence-associated protein
AJ778412	P0000500004B07	4.00	2.00	pectinesterase,
AJ772957	P0000200003A06	3.97	1.99	Bad E-value
CF229570	PtaXM0027A8A0802	3.86	1.95	similar to Solanum tuberosum ci21A
CA823427	R26A04	3.85	1.95	early drought induced protein
CF231277	PtaC0019E3E0309	3.83	1.94	stable protein 1
AJ778072	P0000400039A07	3.62	1.85	arabinogalactan protein
CF232069	PtaJXO0006B3B0303	3.61	1.85	pop3 peptide
CA821690	RSH06C01	3.50	1.81	stable protein 1
CA825356	R57E09	3.40	1.77	stable protein 1

AJ769227	P0000100026G02	3.38	1.76	galactinol synthase, isoform GolS-1
AJ780302	P0000900001B06	3.26	1.71	cinnamoyl-CoA reductase
CF233601	PtaJXO0025E3E0309	3.14	1.65	unknown
CF230678	PtaC0011F4F0412	3.09	1.63	stable protein 1
AJ774165	P0000300013E02	3.07	1.62	lipid transfer protein precursor
CA823153	R21E10	3.05	1.61	unknown
CF230956	PtaC0015F10F1012	3.02	1.59	stable protein 1
AJ768358	P0000100016H11	2.95	1.56	granule-bound starch synthase
CA820871	F05B03	2.93	1.55	galactinol synthase,
CA821043	F07G07	2.89	1.53	Chain B, Solution Structure.
CA821525	RSH04A09	2.82	1.50	extensin like protein -
AJ780109	P0000800011H05	2.82	1.50	unknown [Arabidopsis thaliana]
CF233358	PtaJXO0022D10D1008	2.79	1.48	Tubulin beta-2 chain (Beta-2 tubulin)
CA824258	R39A07	2.77	1.47	unspecific monooxygenase
CA824847	R49D04	2.72	1.44	extensin like protein
CA824668	R46D01	2.67	1.41	stable protein 1
AJ777381	P0000400027D02	2.65	1.41	unknown
CA821179	F11C20	2.65	1.41	sterility protein 1
CF230621	PtaC0010H11H1115	2.53	1.34	At4g36570
AJ769000	P0000100024C01	2.50	1.32	No hit found
AJ775295	P0000300030F06	2.48	1.31	No hit found
CA825802	R67G01	2.44	1.29	early drought induced protein
CA821508	RSH03H01	2.43	1.28	Bad E-value
CA821708	RSH06D07	2.30	1.20	xyloglucan endotransglycosylase
AJ775308	P0000300030G08	2.22	1.15	unknown [Arabidopsis thaliana]
AJ778784	P0000600006B11	2.19	1.13	ribosomal protein
CA825130	R53H09	2.01	1.01	Bad E-value

Table 5.2: The ESTs showing a two-fold down-expression in elevated relative to ambient CO_2 on 18.10.04, an expression that was consistent in at least six of the nine hybridisations.

GenBank	PICME id	Mean normalised expression ratio	Mean $\log_2$ expression ratio	**Annotation (tBLASTX)**
AJ771988	P0001600013B04	0.17	-2.59	tumor-related protein [Nicotiana tabacum]
AJ777815	P0000400035D12	0.17	-2.56	CPRD2 [Vigna unguiculata]
CA825224	R55D08	0.20	-2.29	unknown [Arabidopsis thaliana]
AJ778060	P0000400038H06	0.24	-2.04	Putative flavanone 3-hydroxylase
CA826121	R73A10	0.26	-1.94	Lemir [Lycopersicon esculentum]
AJ769475	P0001000001H02	0.27	-1.88	NtEIG-E80 [Nicotiana tabacum]
CA824423	R41G12	0.28	-1.84	unknown [Arabidopsis thaliana]
AJ777537	P0000400029F05	0.31	-1.67	squalene monooxygenase [Datura innoxia]
AJ777757	P0000400034F10	0.31	-1.67	At1g30760/T5I8_22 [Arabidopsis thaliana]
AJ773363	P0000300001C03	0.32	-1.63	thaumatin-like protein [Actinidia deliciosa]
CA823952	R34A06	0.33	-1.61	glutathione S-transferase [Cucurbita maxima]
CA822481	R08H05	0.33	-1.60	unknown [Arabidopsis thaliana]
CA825479	R59G02	0.34	-1.57	unknown [Arabidopsis thaliana]
CA825784	R67E04	0.35	-1.52	kunitz trypsin inhibitor TI3 [Populus tremula]

CA821592	RSH04H06	0.36	-1.47	pathogenesis-related protein-like protein
CA821155	F11B12	0.37	-1.44	thaumatin [Vitis riparia]
AJ777197	P0000400024F07	0.37	-1.42	3-hydroxy-3-methylglutaryl-coenzyme A reductase
CA824045	R35E06	0.38	-1.38	Bad E-value
CA825136	R54A04	0.39	-1.37	Kunitz trypsin inhibitor 3
CA822900	R15F04	0.40	-1.33	Kunitz trypsin inhibitor 3
CA823789	R31D06	0.40	-1.32	P-type transporting ATPase
CF229051	PtaXM0020F12F1212	0.42	-1.27	Bad E-value
CA824360	R40F08	0.42	-1.27	kunitz trypsin inhibitor TI3
CA824929	R50E09	0.42	-1.24	Bad E-value
CA823970	R34C02	0.43	-1.23	Kunitz trypsin inhibitor 3
AJ769531	P0001000008H11	0.43	-1.21	unknown [Arabidopsis thaliana]
AJ780069	P0000800011D09	0.46	-1.12	phosphoenolpyruvate carboxykinase
CA824831	R49B06	0.48	-1.06	Bad E-value
CA820984	F06H11	0.48	-1.05	thaumatin-like protein
CA823747	R30G03	0.49	-1.03	At4g19950
AJ777113	P0000400023C05	0.53	-0.90	dicyanin [Lycopersicon esculentum]

5.4.2.2. Differential gene expression between late senescence samples using Bayesian statistics

Sixty six ESTs were classed as significantly differentially expressed using a Basysian Log odds (B-stat) cut-off value of ≥ 3 (95 % chance of differential expression). Of these 66 ESTs 15 were significantly up-regulated in elevated CO_2 13 of which also exhibited a mean expression ratio of ≥ two-fold up-regulation and of the 15 ESTs 14 represented unique gene models from the *Populus tricocarpa* sequence. The annotation of all differentially expressed probe sequences was checked against the *P. tricocarpa* sequence using the tBLASTx algorithm. The two most highly differentially expressed ESTs were identified as encoding for transcripts involved down-stream in the biosynthetic pathway of anthocyanin. The mean normalized differential expression of all significant genes was calculated from all nine hybridizations and the gene for leucoanthocyanidin dioxgenase (*LDOX*) showed a mean fold induction of 26.3 and that for dihydroflavonol reductase (*DFR*) 10.8 in elevated CO_2. All significantly up-regulated genes are given in appendix E Table A1. Fifty one of the 66 genes were significantly down-regulated in elevated CO_2 late in senescence. Forty of which had a mean normalised expression ratio ≥ two-fold down-regulated in elevated CO_2 and of the 51 ESTs 47 represented unique gene models. All 51 significantly down-regulated genes are given in appendix F Table A2.

5.4.2.3. Differential gene expression between senescence in either elevated or ambient CO_2 with respect to pre-senescent reference pools

Hybridisations between late senescence (18.10.4) and pre-senescence (31.08.04) samples with respect to CO_2 treatment were carried out to identify any changes in gene expression that occurs over the time period of autumnal senescence in elevated CO_2 (between 31.08.04 and 18.10.04), relative to the same time period in ambient CO_2. Across all six replicate hybridisations (four for progression of senescence in elevated CO_2 and two in ambient CO_2) 606 ESTs were classed as significantly ($p \leq 0.05$) differentially expressed between the progression of senescence in ambient CO_2 compared with that in elevated CO_2. The list of 606 ESTs is 11 % of those present, and is represented in figure 5.5. Those 606 ESTs that were significantly differentially expressed between treatments were further scrutinised by examining the fold change ratio. Those ESTs exhibiting two-fold up-expression during the process of senescence in elevated CO_2 only number 11 and those two-fold up-expressed during senescence in ambient CO_2 only numbered 42 and are represented in figure 5.6. Those ESTs classed as two-fold up-expressed and in common between senescence treatments are also shown in figure 5.6. Those ESTs exhibiting a two-fold down-expression during the process of senescence in either elevated or ambient CO_2 are represented in figure 5.7. With reference to figure 5.5 a general trend towards less down-expressed ESTs is evident in elevated CO_2. This can be seen clearly in figure 5.7. Of the ESTs classed as significantly differentially expressed between treatments 99 were two-fold down-expressed in ambient CO_2 while only 9 ESTs were two-fold down-expressed in elevated CO_2. Those ESTs classed as two-fold down-expressed and in common between senescence treatments number 28 and are also shown in figure 5.7.

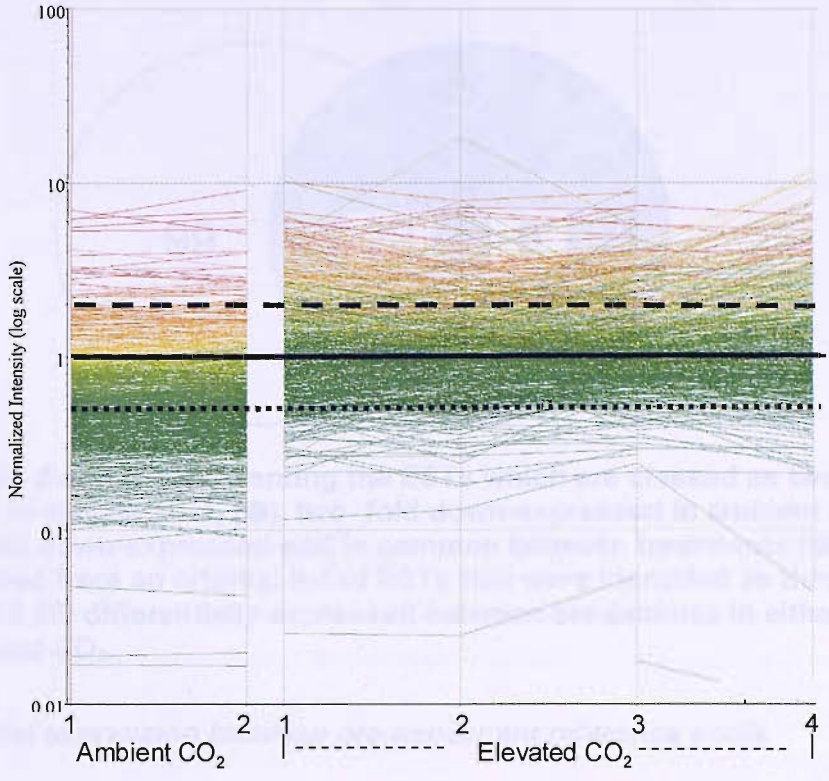

Figure 5.5: The 606 ESTs classed as significantly differentially expressed between senescence in ambient CO_2 and that in elevated CO_2. ESTs greater than two fold up-expressed are represented by lines above (— —), no change in expression is represented by (——) and those two fold down-expressed are represented by lines below (·····).

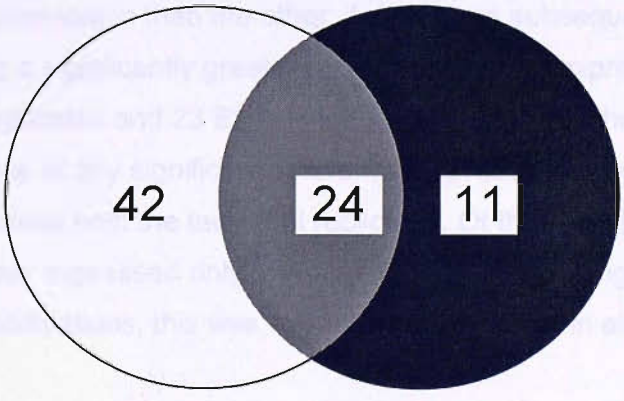

Figure 5.6: A Venn diagram representing the ESTs which are classed as two-fold up-expressed in elevated CO_2 (●), two- fold up-expressed in ambient CO_2 (○) and those two-fold up-expressed and in common between treatments (◍). These ESTs were obtained from an original list of ESTs that were identified as those significantly ($p \leq 0.05$) differentially expressed between senescence in either ambient or elevated CO_2.

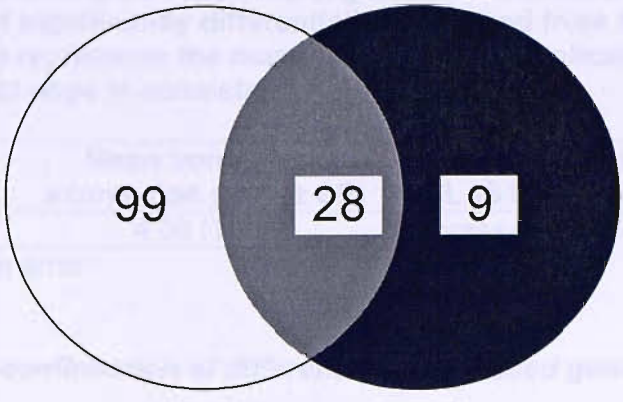

Figure 5.7: A Venn diagram representing the ESTs which are classed as two-fold down-expressed in elevated CO_2 (●), two- fold down-expressed in ambient CO_2 (○) and those two-fold down-expressed and in common between treatments (◎). These ESTs were obtained from an original list of ESTs that were identified as those significantly ($p \leq 0.05$) differentially expressed between senescence in either ambient or elevated CO_2.

5.4.2.4. Differential expression between pre-senescent reference pools

Biological variability was combined into each independent pre-senescent reference pool (31.08.04), each pool consisting of eight (elevated CO_2) or seven (ambient CO_2) biological replicates. In this analysis the biological variability is pooled to $n = 1$ and each hybridisation is a technical replicate taking into account a dye swap. A small technical variability inherent in these hybridisations is evident with one hybridisation exhibiting an increased spread of differential expression than the other. A *t*-test was subsequently carried out to identify ESTs showing a significantly greater ($p \leq 0.05$) than 1:1 expression in at least one of the two technical replicates and 23 ESTs were identified. The technical variability may account for the absence of any significant differential expression between treatment pools that was consistent across both the technical replicates. Of these 23 ESTs classed as significantly differentially expressed only one was classed as showing a two-fold change consistent in both hybridisations, this was two-fold up-expressed in elevated CO_2 and is given in table 5.3.

Table 5.3: The EST showing a two-fold up regulation in elevated relative to ambient CO_2 on 31.08.04, and significantly differentially expressed from 1:1 in at least one of the hybridisations, *n* represents the number of technical replicate hybridisations in which this two-fold change is consistent.

EST code	*n*	Mean normalised expression ratio (± SE)	Annotation *Populus*DB (tBLAST N*)
R04G03	2	4.06 (1.18)	expressed protein

* tBLAST X resulted in error

5.4.3 Independent confirmation of differentially expressed genes

Selections of differentially expressed genes identified in this microarray analysis were taken and primers designed from the EST sequence given on the PICME database (www.picme.at). Primers were designed for leucoanthocyanidin dioxgenase (*LDOX*), galactinol synthase (*Gol-S*), thaumatin and chitinase and transcript abundance was measured relative to *PDF1* a serine/threonine protein phosphatase 2A (PP2A) using reverse-transcriptase quantitive PCR (RT-qPCR). The control gene *PDF1* was used as it exhibited no differential expression between treatments. The work was carried out by Jing Zhang at the University of Southampton, and provides independent confirmation of the results presented here, for these genes, see appendix C. By using RT-qPCR *LDOX* was identified as the transcript exhibiting the most differential expression, approximately 19 (± 5.0) times up-expressed in elevated CO_2 (n = 7). The expression of this gene was examined between the pre-senescent and late senescent leaf samples, the results are shown in appendix D.

5.5. Discussion

In this chapter, and for the first time, an attempt to identify transcripts that may be responsible for an elevated CO_2 delay in autumnal senescence was carried out using cDNA microarrays. This involved combining two processes for which very little is known at the level of gene expression. These are, responses following long term field exposure to elevated CO_2, and processes occurring during natural autumnal senescence in deciduous forest trees. The most important findings are a general reduction in the amount of transcripts down-expressed during senescence in elevated relative to ambient CO_2, and later in senescence an up-expression of transcripts important in mitigating stress was evident in elevated CO_2.

5.5.1. Data analysis

For each hybridisation data were normalised by LOWESS regression. This was done to remove any systematic sources of variation that were not considered genuine biological variability. Such variation can be produced by features such as different dye labelling efficiencies, dye scanning properties, biases in the scanner and spatial effects resulting from non-uniform hybridisation. For two of the hybridisations variation between dye channel intensities was such that LOWESS regression would not normalise the data effectively. This data was subsequently eliminated from further analysis as it was considered strongly influenced by non-experimental treatment sources of variation. This shows the importance of producing and observing MA plots prior to subsequent analysis.

Obtaining confidence in assigning a number of target genes to be those significant for delayed senescence in elevated CO_2, from the many thousands on each replicate hybridisation, is no simple task. For example, of the 20243 expression ratios on each hybridisation standard statistics with a $p \leq 0.05$ would lead to the generation of 1012 false positives. Therefore multiple testing corrections such as the Bonferroni correction can be applied to the data, so ensuring significance is maintained in all tests. This has been considered as overly conservative and upon Bonferroni correction zero genes were classed as differentially expressed in Soybean growing in a FACE experiment (Ainsworth *et al.*, 2006). For data reported here and for all statistical tests carried out, no genes were classed as significantly differentially expressed when a Bonferonni correction was applied. Instead two additive processes were applied to identify target genes of interest. Those

ESTs with a consistent two-fold change in expression ratio and the standard *t-test* were used to identify genes of interest.

In the case of the late senescence samples the ideal target genes of interest would be those exhibiting a two-fold change consistant in nine out of nine hybridisations. This is because such genes could be assigned a high degree of confidence in influencing the rate of senescence under elevated CO_2. It is of importance to note, however, that of the possible 20 243 expression data points only 2696 (13 %) were present in all nine late season hybridisations following quality control measures. Therefore in identifying target genes only present in all nine hybridisations 87 % of possible data would be eliminated. Senescence at this site is characterised by natural variability between trees so a conservative cut-off point was used. Target genes were identified as those two-fold differentially expressed and consistently so in six out of nine hybridisations. In attempting to identify changes in gene expression during the progression of senescence fewer hybridisations were carried out and biological variability was reduced with the pooling of samples for the pre-senescent reference. Therefore it was considered that confidence could only be assigned to target genes that showed a consistent response between all hybridisations, (four out of four, or two out of two, for the progression of senescence in elevated CO_2 or ambient CO_2 respectively). The independent confirmation by RT-qPCR of a number of target genes supports this screening of microarray data.

5.5.2. Experimental design of hybridisations

Replicate hybridisations were carried out to allow across hybridisation confirmation of any expression ratios of interest, as discussed above, and illustrated in figure 5.2. This replication can be of two forms, technical replication would involve using the same target hybridised to additional microarrays, thus providing information on the repeatability of the hybridisation, or hybridising replicate targets, thus providing information on the biological repeatability of the treatment. In view of cost and time the latter of these two was considered more appropriate. In order to identify genes responsible for a delayed senescence in elevated CO_2 three approaches were used as illustrated in figure 5.2. Approach one, employed to identify changes in gene expression late in senescence, was to hybridise biological replicates between targets generated from samples taken 18.10.04. Nine microarray hybridisations were then carried out after randomised pairing between

control and CO_2 treatments, and a number of genes were consistently differentially expressed by CO_2 treatment. Approach two was employed to identify changes in gene expression late in senescence relative to a common pre-senescent reference pool and was similar to the approach taken by Andersson *et al.* (2004). In this case four of the replicate senescent samples from elevated CO_2 (18.10.04) were hybridised against four of the pooled pre-senescent samples from elevated CO_2 (31.08.04). This allowed identification of the changes in gene expression over the time course of senescence for trees exposed to elevated CO_2. Four of the replicate senescent samples from ambient CO_2 (18.10.04) were hybridised against four of the pooled pre-senescent samples from ambient CO_2 (31.08.04) so allowing identification of changes in gene expression during senescence in ambient CO_2, two of these could not be normalised and were subsequently omitted. This approach includes biological variability of the senescent samples but removes this variability from the pre-senescent reference pool, so attempting to minimise the documented site variability. In approach three, the two (with respect to treatment) common pre-senescent reference pools were hybridised together. The minimal replication in this form of microarray experiment is two to allow for a dye swap and so accounting for bias in dye incorporation dependent on sample treatment.

5.5.3 Differential gene expression between the pre-senescent reference pools

It is important to start the discussion about genes identified as being differentially expressed by comparing pre-senescent gene expression in elevated CO_2 with that in ambient CO_2. This is because this work can then be put in the context of the four published works in which microarray experimentation has been used on plants exposed to long-term CO_2 enrichment using FACE technology. In all cases this was on leaf material harvested during the growing season. This includes Arabidopsis (Miyazaki *et al.,* 2004), Soybean (Ainsworth *et al.,* 2006), and two poplar species, *P. tremuloides* (Gupta *et al.,* 2005) and *P. x euramericana* after three and six years growth at the POP/EUROFACE site (Taylor *et al.,* 2005). To summarise, CO_2 response appears to be controlled by a relatively small number of genes and those transcripts considered the most responsive showed generally around a two-fold change (Ainsworth *et al.,* 2006; Gupta *et al.,* 2005; Taylor *et al.,* 2005). Ainsworth *et al.,* (2006) suggest this small change in regulation is the result of the chronic nature of FACE experimentation and the use of plants acclimated to this condition, rather than using plants undergoing acute changes. Taylor *et al.* (2005) suggest that the control may occur

somewhere other than at the level of mRNA abundance. This can result from processes such as alternative splicing of mRNA and the balance between protein synthesis and degradation, which also influence protein abundance (Feder and Walser, 2005). It may also be considered that physiological response results form small changes in key transcripts or the additive effect of small changes in many transcripts that are undetected in the standard microarray analyses used in these studies and in this chapter, although this is unproven. Moreover, it is important to note that all these experiments were carried out on leaf material; therefore the transcriptional response of woody material is neglected. Nearly three times the number of transcripts responsive to elevated CO_2 was identified in stem material (277) than in leaf material (95) for *P. deltoides* exposed to a [CO_2] of up to 1200 ppm (Druart *et al.*, 2006).

Twenty three ESTs were identified as exhibiting a normalised expression ratio significantly different from 1:1 in the pre-senescent pooled microarray hybridisation. However, these 23 ESTs were not reproducibly significantly differentially expressed when the technical repeat hybridisation was taken into account. Using the fold change criteria outlined in this chapter, one EST was was two-fold up-expressed in elevated CO_2 and consistently so in both hybridisations, EST R04G03, with no functional annotation. The lack of differential expression in elevated CO_2 in the absence of development supports the findings of Taylor *et al.*, (2005) carried out using a different microarray and so using different probes to those used here. It further identifies this as a suitable starting point from which to examine the influence of elevated CO_2 on senescence as these pools can be considered to exhibit little differential response to CO_2.

5.5.4 Differential gene expression during senescence in either elevated or ambient CO_2.

Here an attempt was made to identify transcripts that may be differentially expressed between elevated and ambient CO_2 during the course of senescence (31.08.04 – 18.10.04). This approach was not a direct assessment of the transcriptional changes that occur during natural autumnal senescence in poplar as this has been carried out by others (Andersson *et al.*, 2004) using microarrays spotted with cDNA libraries specific for senescence genes. Those transcripts down expressed through the course of senescence

in elevated CO_2 relative to the same senescence time period in ambient CO_2 will first be discussed followed by those up-expressed.

Those ESTs showing a normalised expression ratio that was significantly different between the progression of senescence in elevated CO_2 and that in ambient CO_2, in all six of the hybridisations, numbered 606. The main outstanding feature was a shift towards less down expression in elevated CO_2 (figure 5.5). This became increasingly evident by the fact that 99 ESTs were specifically two-fold down-expressed in ambient CO_2 (figure 5.7). Only 9 of the ESTs considered significantly differentially expressed between treatments were specifically two-fold down-expressed in elevated CO_2 (figure 5.7). This is an important finding because although some up regulation of specific transcripts is a feature of senescence in poplar (Bhelero et al., 2003); senescence generally results in massive protein and RNA degradation (Buchanan-Wollaston et al., 2003). This was evident in poplar by a reduction in the amount of extractable RNA and ESTs annotated as ribosomal were among some of the most down-expressed (Andersson et al., 2004). Therefore this shift towards less down regulation of transcripts in elevated CO_2 may suggest that a delay in senescence is also detectable at the level of mRNA abundance. Also, 15 % of the ESTs in the list of 99 specifically down expressed in ambient CO_2 were annotated as ribosomal supporting data of Andersson et al. (2004) and suggesting reduced translation. From the list of 24 ESTs showing a greater than 2-fold up-regulation during senescence, and common to both CO_2 treatments, 22 ESTs were annotated as metallothionein. Metallothioneins represent among the most enriched genes in the autumn leaf cDNA library of poplar (Bhalerao *et al.*, 2003), and Arabidopsis (Guo *et al.*, 2004), and have a proposed role in cellular detoxification by removal of metal ions during senescence (Kohler *et al.*, 2004). The *P. euphratica* cDNA library used in the spotting of the PICME array was highly enriched in metallothioneins (Brosché *et al.*, 2005) this may explain the occurrence of these ESTs being up expressed in both treatments. Of those 11 ESTs identified as uniquely two-fold up-expressed in elevated CO_2 (figure 5.6) ESTs annotated as caffeoyl-CoA 3-O-methyltransferase and cinnamyl alcohol dehydrogenase . Both caffeoyl-CoA 3-O-methyltransferase and cinnamyl alcohol dehydrogenase are involved phenylpropanoid metabolism leading to lignin biosynthesis which provides mechanical strength to cell walls (Whetten and Sederoff, 1995). Caffeoyl-CoA 3-O-methyltransferase and many others in the lignin biosynthesis pathway was up-expressed in a *P. trichocarpa* x *P. deltoides* cross in response to leaf wounding (Smith *et al.*, 2004) and were proposed to

provide protection against pathogen infection. From the 42 ESTs identified as uniquely two-fold up-expressed in ambient CO_2 (figure 5.7) 10 ESTs present that were fragments of the same proposed gene. These 10 ESTs were annotated as dormancy associated protein. Genes encoding dormancy associated protein have been identified as part of the programmed cell death of xylem fibers (Moreau *et al.*, 2005). Genes that may be differentially expressed during the course of senescence between elevated and ambient CO_2 have been identified. Specific to ambient CO_2 99 ESTs were down expressed while in elevated CO_2 this number was nine. Genes consistently up-expressed in elevated CO_2 were involved in lignin biosynthesis, and in ambient CO_2 up expression of the fruit ripening genes thaumatin and those involved in programmed cell death were apparent.

5.5.5 Differential gene expression occurring during late (18.10.04) senescence in either elevated or ambient CO_2

Hybridisations were carried out to directly measure the differences in relative gene expression during late senescence (18.10.04) between elevated and ambient CO_2. Of the nine biological replicate hybridisations, 2696 ESTs out of a possible 20243 were consistently expressed in all hybridisations (figure 5.4). Using the data analysis described in this chapter no features exhibited a consistent ≥ two-fold change across all nine hybridisations. This was not unexpected considering the biological variability during senescence. However, in at least five of the hybridisations three ESTs were identified as exhibiting a normalised intensity ratio that was significantly different from one, using ANOVA in GeneSpring. These were annotated as *dihydroflavonol reductase* (*DFR*) having a mean normalised expression ratio of 19.34, *fiber lipid transfer protein* having a mean normalised expression ratio of 10.24 and *leucoanthocyanidin reductase 1* (*LAR*) having a mean normalised expression ratio of 6.4 (table 5.1) in the six of nine hybridisations consistently exhibiting a ≥ two-fold induction. Taking into account this cross hybridisation variability the B statistical anaylsis identified 66 ESTs as being significantly (with a ≥ 95 % probability) differentially expressed in elevated CO_2 on 18th October 2004. Both *leucoanthocyanidin dioxgenase* (*LDOX*) and *DFR* were the two most highly differentially expressed genes in elevated CO2 exhibiting a mean normalised expression ratio of 26.3 and 10.8 respectively for all nine hybridisations (table A1). *LDOX* is an enzyme involved in phenylpropanoid metabolism, specifically the flavonoid pathway and identified in *Arabidopsis* as converting leucocyanidin to anthocyanin (Pelletier *et al.*, 1997). However, this same step is reported to be catalysed in *Populus* by the enzyme anthocyanidin

synthase (Tsai *et al.,* 2006). This is a case of differing nomenclature for the same enzyme: anthocyanidin synthase is an ortholog of *LDOX* (www.genome.jp/Kegg/pathways). Orthologs are genes that have diverged between species but maintain the same function, and in poplar specific enzymes of the flavonoid pathway are encoded by multiple genes, while the same enzymes in *Arabidopsis* are encoded by single-copy genes (Tsai *et al.,* 2006). The increased activity of the flavonoid pathway potentially leading to increased anthocyanin synthesis is further supported by the up regulation of *dihydroflavonol reductase* (*DFR*) which is a key enzyme in anthocyanin biosynthesis up stream of *LDOX* (Gollop *et al.,* 2002), and terminology is consistent in poplar (Tsai *et al.,* 2006). Anthocyanins have a multi-faceted protective role in leaves (Gould, 2004). They are considered to protect from UV damage, pathogens, photoinhibiton, photooxidative stress and scavenge free radicals, so reducing ROS-associated damage (Gould, 2004). High levels of anthocyanin also accumulate in poplar under conditions considered to increase photo-oxidative stress during senescence (Keskitalo *et al.,* 2005). In elevated CO_2 of 1200 ppm up-regulation of genes involved in flavonoid metabolism were identified in *Populus* leaf material while the reverse was observed in stem material and change in the source / sink balance was suggested as a mechanism leading to increased carbon flow into flavonol metabolism (Druart *et al.,* 2006). With reference to appendix D a clear up-expression of *LDOX* is evident during the course of senescence in elevated CO_2 and over the same time course *LDOX* was down-expressed in ambient CO_2. This provides evidence that these results are not simply the consequence of a chronological shift in the timing of senescence but more likely an active switch in metabolism is occurring in elevated CO_2 leading to a delayed senescence. Further upregulation of phenylpropanoid metabolism during senescence in elevated CO_2 is provided by the up regulation of cinnamoyl-Co-A-reductase. Cinnamoyl-Co-A-reductase is also involved in lignin biosysnthesis (Whetten and Sederoff, 1995) and supports the identification of this pathway being up-expressed during senescence in elevated CO_2 (as discussed in part 5.5.4).

At this late stage in senescence galactinol synthase (*GolS*) was also up-expressed in elevated relative to ambient CO_2, so identifying an affect of elevated CO_2 on primary metabolism as well as the previously discussed influences on secondary metabolism. The first committed step in the synthesis of raffinose (a trisaccharide composed of galactose, fructose, and glucose) is catalysed by *GolS* (Taji *et al.,* 2002). In *Arabidopsis* raffinose and galactinol have been shown to provide tolerance to drought, high salinity and cold

stresses. *Galactinol synthase* has been identified as having a key role in these tolerance mechanisms and raffinose sugars also have a suggested role in thylokoid membrane stabilisation (Taji *et al.,* 2002). Additional support to the up regulation of the raffinose biosynthetic pathway is provided by up-regulation of an EST annotated as a specific isoform of *GolS* called *GolS-1* (table 5.1). *GolS-1* was induced by both drought and high salinity and was considered to provide tolerance to both these stresses in *Arabidopsis* (Taji *et al.,* 2002).

Up expression of the ESTs in elevated CO_2 reported in this chapter may be consistent with the idea of the induction of different stress responsive pathways to extend the viability of senescing cells (Buchanan-Wollaston *et al.,* 2005). This is therefore consistent with the evidence for delayed senescence in elevated CO_2 for *P. x euramericana* growing at the POP/EUROFACE site. While those ESTs down-expressed in elevated relative to ambient CO_2 late in senescence are all associated with senescence and defence processes. These are given in table 5.2 and to summarise are annotated as thaumatin which is involved in fruit maturation (Ruperti *et al.,* 2002), chitinase, and pathogenesis related proteins, involved in defence (Buchanan-Wollaston *et al.,* 2003) and possibly induced by oxidative stress (Navabpour *et al.,* 2003) and kunitz trypsin inhibitors, a class of protease inhibitors involved in wound responses in poplar (Hollick and Gordon, 1995).

5.5.6 Summary

Microarray technology has provided evidence of a delay in autumnal senescence for trees growing in elevated CO_2. This is evident by a general down regulation of gene transcription when trees growing in ambient CO_2 are compared relative to those in elevated CO_2. A down regulation of senescence-associated genes was also evident late in senescence in elevated CO_2, and up regulation of phenylpropanoid metabolism in elevated CO_2 may be a mechanism to explain this through the provision of stress tolerance.

Chapter 6:

General discussion

6.1 Overview

Recent global changes in autumnal phenology could not be totally accounted for by changes in global temperature (Menzel *et al.*, 2006). The principal finding of this thesis is that increasing atmospheric [CO_2] to 550 ppm above the current ambient [CO_2] will delay autumnal senescence for two *Populus* genotypes growing in a managed src plantation. This delay was estimated to be approximately ten days which was sufficient to positively influence the modelled NPP of the site.

Seasonal growth cessation and bud-set in poplar is genetically controlled and changing photoperiod induces this process, an induction that varies with latitudinal gradient (Böhlenius *et al.*, 2006). With this in mind, this thesis was introduced by a discussion about processes principally involving whole plant C:N and source:sink regulation that may influence the progression of leaf senescence from published data derived principally using FACE experimentation of forest trees. Earlier work at the POP/EUROFACE site has identified that the genotype *P. nigra* sets bud approximately 20 - 30 days later than *P. x euramericana* and that elevated CO_2 had no significant effect on the timing of bud-set for both species (Calfapietra *et al.*, 2003). Intriguingly, as well as the progression of autumnal senescence being delayed in elevated CO_2 so was the timing of bud-set for *P. tremuloides* growing in the AspenFACE site (Karnosky *et al.*, 2003) for locally selected clones (Isebrands *et al.*, 2001). The influence CO_2 may have on bud-set for these species was not be directly tested here. Physiological data collection was timed to identify the progression of senescence resulting approximately one month after bud-set in *P.* x *euramericana*, and from around the time of bud-set in *P. nigra*. In Chapter one a number of mechanisms by which CO_2 could influence leaf senescence were proposed and subsequently up-regulation of components involved in phenylopropanoid, and raffinose sugar metabolism have been identified, a previously unknown consequence of autumnal senescence in elevated [CO_2].

Environmental conditions present in the autumn influence the rate limiting component of photosynthesis such that the J_{max}:$V_{c,max}$ ratio is increased, meaning that autumnal photosynthesis becomes more dependent on [CO_2] (Onoda *et al.*, 2005). The dependence of autumnal photosysnthesis on [CO_2] was evident and the following species all showed increased autumnal photosynthesis: *Polygonum cuspidatum* (Onoda *et al.*, 2005),

Liquidambar styraciflua (Herrick and Thomas, 2003) and *Quercus rubra* (Cavender-Bares, *et al.*, 2000). This increased autumnal assimilation of C had either no influence on the timing of autumnal senescence (Herrick and Thomas, 2003) or a stimulatory effect (Cavender-Bares, *et al.* 2000; Onoda *et al.*, 2005). Therefore the hypothesis of Herrick and Thomas (2003) that "atmospheric CO_2 enrichment would delay senescence because leaves would retain a positive carbon balance late in the season" was disproved by their own observations.

At the on-set of this work a general consensus was that elevated CO_2 would stimulate senescence through increasing plant ontogeny, however these results were derived from determinant species (Miller *et al.*, 1999; Fangmeier *et al.,* 2000). In terms of forest trees, a variety of growth and CO_2 exposure techniques ranging from artificially simulating autumnal senescence in a glasshouse (Cavender-Bares, *et al.* 2000) to natural autumnal senescence in OTC (Li *et al.*, 2000) provided variable results. These variable results provided the drive to measure autumnal senescence across many spatial scales in whole forest canopies using a forest FACE exposure system and indeterminate species exhibiting no sink limited growth in elevated CO_2. Therefore the POP/EUROFACE site was considered because, after five years of exposure to elevated CO_2, trees still exhibited increased biomass production (Liberloo *et al.*, 2006), stimulated photosynthesis (Calfepietra *et al.*, 2005) and, importantly, no long-term down regulation of light-saturated photosynthesis was evident (Tricker *et al.*, 2005). Subsequent to the on-set of this work a delayed autumnal senescence was reported in elevated CO_2 at FACE sites for *P. tremuloides* (Karnosky *et al.*, 2003), *P. x euramericana* and *P. nigra* (Tricker *et al.*, 2004; Cotrufo *et al.*, 2005) and soybean (Dermody *et al.*, 2006). These studies provided an impetus for confirmation of these findings using a technology that could be related with current observations of phenological responses to climate change, and to further develop a mechanistic understanding of processes driving this response.

In 2003 canopy spectra were obtained using both an airborne sensor and the field portable GER 3700 and extractions of leaf chlorophyll and measurements of SLA were also taken. These measurements indicated a delayed senescence in elevated CO_2 although this finding could not be attributed to elevated CO_2 alone and appeared to be a response to site heterogeneity. In 2004 more types of data were collected over an increased temperol resolution and from all experimental blocks. This increased intensity of measurements was

carried out in an attempt to determine whether site heterogeneity or elevated CO_2 was significantly influencing autumnal senescence. The multi-scale approach of experimentation taken in this thesis is unique among forest FACE experiments and appeared very valuable. Remote sensing technology was used to effectively monitor autumnal senescence with respect to the temporal and spatial heterogeneity that is present during forest canopy senescence and a link between remotely-sensed results and gene expression was provided in this thesis. A number of knowledge gaps in our understanding of forest responses to elevated CO_2 were proposed by Karnosky (2003) and among these were phenology and stress tolerance. Data presented in this thesis identifies a link between both of these knowledge gaps.

6.2 Chapter two

The main finding in this chapter was that standard remote sensing approaches used to estimate chlorophyll content could be influenced by leaf responses to changing irradiance, irrespective of changes in chlorophyll content. This was also evident for spectral interpolation techniques commonly used in global remote sensing and, although not reported here these data are being prepared for resubmission (Tallis *et al.*, 2006 see appendix A). All remotely sensed data in this thesis were collected across narrow continuous band-widths, and remote indices and interpolation techniques using narrow continuous band-width data were identified as amoungst the most effective techniques to estimate leaf pigmentation. In the presence of all this data, the more complex data interpolation techniques for discontinuous wide band-width data were considered less effective.

One feature in the literature is the number of different techniques used to measure the highly heterogeneous process of leaf senescence in forest trees. For example, both Herrick and Thomas (2003) and Cavender-Bares *et al.* (2000) used the SPAD to estimate leaf chlorophyll content. Data presented in chapter two of this thesis show the appeal of this approach with SPAD values giving a strong correlation with leaf chlorophyll content. However, the small spatial range over which these values are obtained may limit the viability of this approach in the field, particularly in heterogeneous forest canopies. This influence of spatial variability was evident for the remotely-sensced index MNDVI. At the canopy level in elevated CO_2 MNDVI was always stimulated in *P. x euramericana* at all

times of measurement (see chapter three). While no trend could be seen for the same remotely-sensed index and species when measured at the leaf level (see chapter four). Furthermore, the percentage change in canopy MNDVI was highly represented by the percentage change in whole homogenised leaf chlorophyll content extract and not by leaf level MNDVI.

Leaf irradiance profiles are influenced by changes in mesophyll size, shape and packing (Vogelmann, 1993), and in *P.* x *euramericana* these properties have been shown to be influenced by elevated CO_2 (Taylor *et al.*, 2003). Therefore, although reflectance based non-destructive estimates capture the spatial variability of canopy senescence, direct confirmation of these results is needed, as was described in chapter four. The CCM and SPAD were both equally strongly correlated with leaf chlorophyll content and the correlation was as good as that obtained from reflectance based estimates. However, during this thesis CCM estimates of leaf chlorophyll content were carried out on ten leaves per sub-plot at the POP/EUROFACE site on a weekly basis and collected throughout the whole diurnal course of a single day during the senescence period of 2004 (data not shown). The results showed a variable week to week response not consistent with the autumnal decline in leaf chlorophyll content as evident from remote measurements (chapter three) and chlorophyll extraction (chapter four). This lead to the investigation of the influence that changing irradiance may have on non-destructive estimates of leaf chlorophyll content and subsequently both visible and NIR reflectance were identified as being responsive to leaf irradiance environment irrespective of leaf chlorophyll content. A number of effective techniques with which to monitor autumnal senescence were identified in chapter two. However, the sequential collection and interpretation of data from canopy (chapter three) to leaf (chapter four) provided the most robust approach giving confidence that those findings from gene expression studies (chapter five) could be scaled up to provide an explanation for the canopy level response.

6.3 Chapters three and four

The main findings in these chapters was a significant retention of whole canopy leaf area and chlorophyll content in *P.* x *euramericana* and *P. nigra* growing in a SRC plantation and exposed to elevated [CO_2] of 550 ppm for six years using FACE technology. These findings were all from non-destructive estimates reporting relative changes in canopy

properties. This result was substantiated in chapter four by chemical extraction of leaf chlorophyll concentration. This further identified that the reduced decline in canopy chlorophyll content estimated non-destructively, was not simply the result of increased LAI, but also the decline in chlorophyll concentration of individual leaves was reduced in elevated CO_2. It has been suggested that the dynamic relationship between climatic variables resulting in inter-annual changes in growing season length (GSL) should be incorporated in models of climate prediction (White *et al.*, 1999). Data reported here indicate that, at least for *Populus* species, increasing atmospheric [CO_2] should be considered as one variable influencing GSL in such models irrespective of the influence via radiative forcing. However, the next season die-back resulting from inadequate frost hardening (Isebrands *et al.*, 2001) in elevated CO_2 delayed senescence may have a detrimental influence on productivity complicating any modelled predictions from a CO_2 induced change in GSL. Caution should be applied when considering the estimated increase in NPP calculated in this chapter and resulting from a delayed senescence in elevated CO_2. This is because daily seasonal GPP was calculated from interpolation between meteorological variables, LAI, and photosynthetic parameters taken in 2001 (Wittig *et al.*, 2005). Nevertheless, this estimate provides evidence that a CO_2 induced shift in autumnal phenology could partly account for increased autumnal productivity (Zhou *et al.*, 2001).

The destructive sampling in chapter four allowed assessment of leaf traits associated with leaf longevity. Leaf traits such as SLA and N_{mass} were measured to link response to CO_2 enrichment with those known to correlate with leaf longevity traits existing across a number of biomes (Reich *et al.*, 1999). A link between elevated CO_2, SLA, and leaf nitrogen content and leaf longevity can be proposed, supporting earlier findings of Craine and Reich (2001) and Tricker *et al.* (2004). Observing whole spectral responses of individual leaves under controlled conditions provided information which spectral reflectance indices such as MNDVI may neglect. This was evident by observing spectral reflectance and transmittance of individual leaves between 550 nm - 900 nm over the time course of autumnal leaf senescence. The main influences on spectra were for *P. x euramericana* and by fertilization in ambient CO_2 which resulted in increased absorption of NIR energy, and elevated CO_2 in which absorption of NIR was significantly reduced in both species. The significant retention of canopy LAI in elevated CO_2 (chapter three), during this autumnal period may imply that this decreased NIR absorbance is likely to be the

response of increased leaf cellular integrity (Slaton *et al.*, 2001) in elevated CO_2 providing mechanical strength, a feature reduced upon fertilization.

Interpreting the senescence response to fertilisation is difficult. On one hand no significant interaction was seen between elevated CO_2 and fertilisation, therefore no statistical effect can be assumed, and fertilisation also had no influence on % leaf N_{mass}, so supporting this observation. However, in September of 2003 Calfapietra *et al.* (2005) calculated a significant influence of fertilisation on the N_{mass} of *P. x euramericana* leaves. When converted to a percentage N_{mass} to equal the units in this thesis, the difference classed as significant was a difference between 3.37 for fertilised leaves and 3.10 for unfertilised. This magnitude of difference had no affect on photosynthesis (Calfapietra *et al.*, 2005) so supporting the view that fertilisation does not influence growth at this site (Liberloo *et al.*, 2006). In data reported here elevated CO_2 reduced leaf % N_{mass} of *P. x euramericana* on 18.10.04, and when measured five days later fertilisation significantly reduced leaf chlorophyll concentration, a feature also significant at the canopy level when estimated using MNDVI. This implies that for *P. x euramericana* N fertilisation reduces leaf longevity, this is consistent with previous observations for grasses (Craine and Reich, 2001). The most obvious feature for *P. nigra* was a large increase in $\%N_{mass}$ for fertilised ambient CO_2-grown leaves when compared with all other treatments, a trend which also followed for SLA. Increased N fertilisation is associated with increased SLA both resulting in a negative association with leaf longevity (Reich *et al.*, 1997). The association between reduced leaf N_{mass}, reduced SLA and increased leaf longevity is consistent across global biomes and this association also fits for the leaves exposed to elevated CO_2 in this study. What does not fit is the feature that all traits increasing leaf longevity also result in decreased net photosynthesis (Reich *et al.*, 1997). In elevated CO_2 trees exhibit leaf traits for increased longevity with no change (Calfapietra *et al.*, 2005) or increased photosynthesis (Liberloo *et al.*, 2006).] Increased leaf photosynthesis along with decreased leaf N_{mass} and decreased SLA could possibly result in elevated [CO_2] by N re-allocated from Rubisco to leaf structural components and sink organs.

6.4 Chapter five

Providing evidence at the level of changing gene expression that supports the canopy and leaf measurements of preceding chapters were the most important findings of chapter five.

Data presented in this chapter also highlight the contribution of phenylpropanoid metabolism in the differential response of poplar exposed to either elevated or ambient CO_2 during senescence. This is similar to the observed up-regulation of transcripts involved in secondary metabolism and lignin biosynthesis in elevated CO_2 during the growing season of soybean (Ainsworth *et al.*, 2006).

The association between elevated CO_2 and increased photosyntheisis increasing hexose production by up to 50 % over ambient is clear for the trees studied in this thesis (Bernacchi *et al.*, 2003; Davey *et al.*, 2006). In elevated CO_2 increased carbon export from these leaves was also evident (Davey *et al.*, 2006) and NPP was stimulated (Gielen *et al.*, 2005), showing the link between elevated CO_2 and increased carbohydrate production for these poplar genotypes. Recent studies with an *Arabidopsis* mutant, *pho3*, containing a defective copy of the *SUC2* gene which was proved to be defective in sucrose export from leaves showed a clear link between increased leaf carbohydrate and increased expression of genes involved in the biosynthesis of anthocyanin (Lloyd and Zakhleniuk, 2004). Specifically and in relation to data presented in this thesis a transcriptome analysis of 22 000 genes of the *pho3* mutant revealed *LDOX* and *DFR* to be up-regulated by 190 and 31 times respectively when compared with the wild-type, and a number of transcripts involved in secondary metabolism were all among the most up-regulated (Lloyd and Zakhleniuk, 2004). The study by Lloyd and Zakhleniuk (2004) identified a link between increased leaf carbohydrate content and the induction of both *LDOX* and *DFR*, a process which may speculatively be induced by elevated CO_2. Phenylalanine ammonia lyase (PAL) is a key early enzyme catalysing the first committed step in the biosynthesis of phenylpropanoids (Dangl *et al.*, 2000). The association between elevated CO_2 and the partitioning of carbon to the synthesis of secondary metabolites was carried out using tobacco plants exposed to a [CO_2] of 1000 ppm (Matros *et al.*, 2006). The results from this study identified a direct link between elevated CO_2, increased C:N ratio of leaves and an increased activity of PAL with a concomitant increase of secondary metabolites as identified by HPLC (Matros *et al.*, 2006). PAL was increased in elevated CO_2 by between five and 11 times that measured in ambient CO_2, so providing a tentative link between the leaf carbohydrate content and the biosynthesis of secondary metabolism components. In Dangl *et al.* (2000) senescencing tissues are described as the consequence of carbon starvation resulting from reduced photosynthesis, continued export of photosynthate, and a high respiratory rate. Therefore, new carbon skeletons are sought to supply this respiratory demand such as amino acids

derived from proteolysis. In elevated CO_2 late season photosynthesis has been reported to be stimulated therefore carbon starvation may be offset and proteolysis reduced. Furthermore from the discussion summarised here it may be concluded that, in elevated CO_2 during senescence, carbon is also available for partioning to secondary metabolism and the raffinose family of oligosaccharides with a concomitant increase in leaf stress tolerence.

6.5 Summary

With the exception of chapter two the research presented in this thesis was all carried out using the POP/EUROFACE experimental site designed to estimate carbon uptake sequestration and loss of a bio-energy crop. The subject matter covered in this thesis is therefore topical considering the latest report from the DTI remarking that the UK faces difficult challenges in meeting its energy needs (DTI 2006). In 2004, 3.6% of the UK's electricity supply came from renewable energy and the UK Government has set a target to provide 10% of electricity supply from renewable energy by 2010 (DTI, 2006a). Currently nearly two-thirds of all renewable energy in the EU comes from biomass (European Commission, 2005). Poplar is grown for paper pulp and biomass, and two keys areas for future improvement of poplar are highlighted as yield and disease resistance (Taylor *et al.*, 2002). A delay in leaf senescence has been proposed as one mechanism through which yield of bio-energy crops may be enhanced (Ragauskas *et al.*, 2006). Data presented in this thesis identify an increased yield in future higher CO_2 atmospheres resulting from delayed autumnal senescence, and this delay may be attributed to increased leaf stress tolerance.

Chapter 7:

Bibliography

Adams MD, Kelley JM, Gocayne JD, Dubnick M, Polymeropoulos MH, Xiao H, Merril CR, Wu A, Olde B, Moreno RF, Kerlavage AR, McCombie WR and Venter JC. (1991) Complementary DNA sequencing: expressed sequence tags and human genome project. *Science*, **252**, 1651-1656.

Ainsworth EA, Davey PA, Hymus GJ, Osborne CP, Rodgers A, Blum H, Nösberger J and Long SP. (2003) Is stimulation of leaf photosynthesis by elevated carbon dioxide concentration maintained in the long term? A test with *Lolium perenne* grown for 10 years at two nitrogen fertilisation levels under Free Air CO_2 Enrichment. *Plant Cell and Environment*, **26**, 705 – 714.

Ainsworth EA, Rogers A, Nelson R and Long SP. (2004) Testing the "source-sink" hypothesis of down-regulation of photosynthesis in elevated [CO_2] in the field with single gene substitutions in *Glycine max*. *Agricultural and Forest Meteorology* **122,** 85-94

Ainsworth EA and Long SP. (2005) What have we learned from 15 years of free-air CO_2 enrichment (FACE)? A meta-analytic review of the responses of photosynthesis canopy. *New Phytologist*, **165**: 351-371.

Ainsworth EA, Rogers A, Vodkin LO, Walter A and Schurr U. (2006) The effects of elevated CO_2 concentration on Soybean gene expression. An analysis of growing and mature leaves. *Plant Physiology*, **142**, 135-147.

Andersson A, Keskitalo J, Sjodin A, Bhalerao R, Sterky F, Wissel K, Tandre K, Aspeborg H, Moyle R, Ohmiya Y, Brunner A, Gustafsson P, Karlsson J, Lundeberg J, Nilsson O, Sandberg G, Strauss S, Sundberg B, Uhlen M, Jansson S and Nilsson P. (2004) A transcriptional timetable of autumn senescence. *Genome Biology*, **5**, art. no.-R24.

Angert A, Biraud S, Bonfils C Henning CC, Buermann W, Pinzon J, Tucker CJ, and Fung I. (2005) Drier summers cancel out the CO_2 uptake enhancement induced by warmer springs. *Proceedings of the National Academe Science*, **102**, 10823 - 10827

The Arabidopsis Genome Initiative (2000) Analysis of the genome sequence of the flowering plant *Arabidopsis thaliana*. *Nature*, **408**, 796- 815.

Balibrea Lara M.E., Gonzalez Garcia M.-C., Fatima T., Ehness R., Lee T.K., Proels R., Tanner W and Roitsch T. (2004) Extracellular invertase is an essential component of cytokinin-mediated delay of senescence. *Plant Cell*, **16**, 1276-1287.

Beerling DJ, Heath J, Woodward FI and Mansfield TA. (1996) Drought-CO_2 interactions in trees: observations and mechanisms. *New Phytologist*, **134**, 235-242.

Bernacchi CJ, Calfapietra C, Davey PA, Wittig VE, Scarascia-Mugnozza GE, Raines CA and Long SP. (2003) Photosynthesis and stomatal conductance responses of poplars to free-air CO_2 enrichment (PopFACE) during the first growth cycle and immediately following coppice. *New Phytologist*, **159**, 609-621.

Bettarini I, Vaccari FP and Miglietta F. (1998) Elevated CO_2 concentrations and stomatal density: observations from 17 plant species growing in a CO_2 spring in central Italy. *Global Change Biology*, **4**, 17 - 22.

Betts RA. (2000) Offset of the potential carbon sink from boreal forestation by decreases in surface albedo. *Nature*, **408**, 187-190.

Bhalerao R, Keskitalo J, Sterky F, Erlandsson R, Bjorkbacka H, Birve SJ, Karlsson J, Gardestrom P, Gustafsson P, Lundeberg J and Jansson S. (2003) Gene expression in autumn leaves. *Plant Physiology*, **131**, 430-442.

Billings WD and Morris RJ. (1951) Reflection of visible and infrared radiation from leaves of different ecological groups. *American Journal of Botany*, **38**, 327-331.

Blackburn GA. (1998) Spectral indices for estimating photosynthetic pigment concentrations: a test using senescent tree leaves. *International Journal of Remote Sensing*, **19**, 657-675.

Blasting TJ and Jones S. (2004) Atmospheric carbon dioxide concentrations at 10 locations spanning latitudes 82 °N to 90 °S. Contributed by Keeling CD and Whorf TP and prepared by *CDIAC* Oak Ridge National Laboratory, Oak Ridge, Tennessee, USA.
Available at: *http://cdiac.esd.ornl.gov/ftp/ndp001a/ndp001a.pdf*

Böhlenius H, Huang T, Charbonnel-Campaa L, Brunner AM, Jansson S, Strauss SH and Nilsson O (2006) CO/FT regulatory module controls timing of flowering and seasonal growth cessation in trees. *Science*, **321**, 1040-1043.

Boisvenue C and Running SW. (2006) Impacts of climate change on natural forest productivity – evidence since the middle of the 20th century. *Global Change Biology*, **12**, 862–882.

Brosché M, Vinocur B, Alatalo ER, Lamminmaki A, Teichmann T, Ottow EA, Djilianov D, Afif D, Bogeat-Triboulot MB, Altman A, Polle A, Dreyer E, Rudd S, Lars P, Auvinen P and Kangasjarvi J. (2005) Gene expression and metabolite profiling of *Populus euphratica* growing in the Negev desert. Genome Biology, **6,** art. no.-**R101.**

Buchanan-Wollaston V. (1997) The molecular biology of leaf senescence. *Journal of Experimental Botany*, **48**, 181-199.

Buchanan-Wollaston V, Earl S, Harrison E, Mathas E, Navabpour S, Page T and Pink D. (2003) The molecular analysis of leaf senescence - a genomics approach. *Plant Biotechnology Journal*, **1**, 3-22.

Buchanan-Wollaston V, Page T, Harrison E, Breeze E, Lim PO, Nam HG, Lin J-F, Wu S-H, Swidzinski J, Ishizaki K and Leaver CJ. (2005) Comparartive transcriptome analysis reveals significant differences in gene expression and signaling pathways between developmental and dark/starvation-induced senescence in *Arabidopsis*. *The Plant Journal*, **42**, 567-585.

Bunn AG, and Goetz SJ. (2006). Trends in satellite-observed circumpolar photosynthetic activity from 1982 to 2003: The influence of seasonality, cover type, and vegetation density, *Earth Interactions*, **10**, 1-19

Calfapietra C, Gielen B, Maurizio S, De Angelis P, Miglietta F, Scarascia-Mugnozza G and Ceulemans R (2003) Do above-ground growth dynamics of poplar change with time under CO_2 enrichment? *New Phytologist*, **160**, 305-318.

Calfapietra C, Gielen B, Galema ANJ, Lukac M, De Angelis P, Moscatelli MC, Ceulemans R and Scarascia-Mugnozza G. (2003a) Free-air CO_2 enrichment (FACE) enhances biomass production in a short-rotation poplar plantation. *Tree Physiology*, 23, 805-814.

Calfapietra C, Tulva I, Eensalu E, Perez M, De Angelis P, Scarascia-Mugnozza G and Kull O. (2005) Canopy profiles of photosynthetic parameters under elevated CO_2 and N fertilization in a poplar plantation. *Environmental Pollution* **137**, 525-535.

Cao M and Woodward FI. (1998) Dynamic responses of terrestrial ecosystem carbon cycling to global climate change. *Nature*, **393**, 249 - 252.

Carter GA. Bahadur R and Norby RJ (2000). Effects of elevated atmospheric CO_2 and temperature on leaf optical properties in *Acer saccharum*. *Environmental and Experimental Botany*, **43**, 267-273

Carter GA and Knapp AK. 2001. Leaf optical properties in higher plants: linking spectral characteristics to stress and chlorophyll concentration. *American Journal of Botany* **88**: 677-684.

Cavender-Bares J, Potts M, Zacharias E and Bazzaz FA. (2000) Consequences of CO_2 and light interactions for leaf phenology, growth, and senescence in *Quercus rubra*. *Global Change Biology*, **6**, 877-887.

Chang S, Puryear J and Cairney J. (1993) A simple and efficient method for isolating RNA from pine trees. *Plant Molecular Biology Reporter*, **11**, 113-116.

Chen WJ, Black TA, Yang PC, Barr AG, Neumann HH, Nesic Z, Blanken PD, Novak MD, Eley J, Ketler RJ and Cuenca R. (1999) Effects of climatic variability on the annual carbon sequestration by a boreal aspen forest. *Global Change Biology*, **5**, 41-53.

Cheng SH, Moore BD and Seemann JR. (1998) Effects of short- and long-term elevated CO_2 on the expression of ribulose-1,5-bisphosphate carboxylase/oxygenase genes and carbohydrate accumulation in leaves of *Arabidopsis thaliana* (L) Heynh. *Plant Physiology*, **116**, 715-723.

Ciais PH, Reichstein M, Viovy N, Granier A, Oge J, Allard V, Aubinet M, Buchmann N, Bernhofer CHR, Carrara A, Chevallier F, De Noblet N, Friend AD, Friedlingstein P, Grnwald T, Heinesch B, Keronen P, Knohl A, Krinner G, Loustau D, Manca G, Matteucci G, Miglietta F, Ourcival M, Papale D, Pilegaard K, Rambal S, Seufert G, Soussana JF, Sanz MJ, Schulze ED, Vesala T and Valentini R. (2005) Europe-wide reduction in primary productivity caused by the heat and drought in 2003. *Nature*, **437**, 529-533

Chiou TJ and Bush DR. (1998) Sucrose is a signal molecule in assimilate partitioning. *Proceedings of the National Academy of Sciences of the United States of America*, **95**, 4784-4788.

Cotrufo MF, De Angelis P and Polle A (2005) Leaf litter production and decomposition in a poplar short-rotation coppice exposed to free air CO_2 enrichment (POPFACE). *Global Change Biology*, **11,** 971-982

Coupe SA, Palmer BG, Lake JA, Overy SA, Oxborough K, Woodward FI, Gray JE and Quick WP. (2006) Systemic signaling of environmental cues in *Arabidopsis* leaves. *Journal of Experimental Botany*, **57**, 329 - 341.

Cox PM, Betts RA, Jones CD, Spall SA and Totterdell IJ. (2000) Acceleration of global warming due to carbon-cycle feedbacks in a coupled climate model. *Nature*, **408**, 184-187.

Curran PJ and Hay AM. (1986) The importance of measurement error for certain procedures in remote sensing at optical wavelengths. *Photogrammetric Engineering and Remote Sensing* **52**: 229-241.

Curran PJ and Kupiec JA. (1995) Imaging spectrometry: A new tool for ecology. In Danson FM and Plummer SE, (Editors), *Advances in environmental remote sensing.* John Wiley & Sons, Chichester.

Craine JM and Reich PB. (2001) Elevated CO_2 and nitrogen supply alter leaf longevity of grassland species. *New Phytologist*, **150**, 397-403.

Cramer W, Bondeau A, Woodward FI, Prentice IC, Betts RA, Brovkin V, Cox PM, Fisher V, Foley JA, Friend AD, Kucharik C, Lomas MR, Ramankutty N, Sitch S, Smith B, White A and Young-Molling C. (2001) Global response of terrestrial ecosystem structure and function to CO_2 and climate change: results from six dynamic global vegetation models. *Global Change Biology*, **7**, 357-373

Curtis PS and Wang XZ. (1998) A meta-analysis of elevated CO_2 effects on woody plant mass, form, and physiology. *Oecologia*, **113**, 299-313.

Davey PA, Hunt S, Hymus GJ, DeLucia EH, Drake BG, Karnosky DF and Long SP. (2004) Respiratory oxygen uptake is not decreased by an instantaneous elevation of CO_2, but is increased with long-term growth in the field at elevated CO_2. *Plant Physiology*, **134**, 520-527.

Dangl JL, Dietrich RA and Thomas H. (2000) Senescence and programmed cell death. In Buchanan B, Gruissen W and Jones R (Editors) *Biochemistry and Molecular Biology of Plants* American society of plant physiologists, Maryland USA..

Davey PA, Olcer H, Zakhleniuk O, Bernacchi CJ, Calfapietra C, Long SP and Raines CA. (2006) Can fast-growing plantation trees escape biochemical down-regulation of photosynthesis when grown throughout their complete production cycle in the open air under elevated carbon dioxide? *Plant, Cell and Environment*, **29**, 1235 - 1244.

Dash J and Curran PJ. (2004) The MERIS terrestrial chlorophyll index. *International Journal of Remote Sensing*, **25,** 5403-5413

Dawson TP and Curran PJ. (1998) A new technique for interpolating the reflectance red edge position. *International Journal of Remote Sensing*, **19,** 2133-2139

Dawson TP, **North PRJ, Plummer SE and Curran PJ.** (2003) Forest ecosystem chlorophyll content: implications for remotely sensed estimates of net primary productivity. *International Journal of Remote Sensing*, **24**, 611-617.

Déjardin A, Leplé J-C, Lesage-Descauses M-C, Costa G and Pilate G. (2004) Expressed Sequence Tags from poplar wood tissues - A comparative analysis from multiple libraries. *Plant Biology*, **6**, 55 - 64.

DeLucia EH, **Hamilton JG, Naidu SL, Thomas RB, Andrews JA, Finzi A, Lavine M, Matamala R, Mohan JE, Hendrey GR, Schlesinger WH.** (1999) Net primary production of a forest ecosystem with experimental CO_2 enrichment. *Science*, **284,** 1177-1179

DemmigAdams B and Adams WW. (1996) The role of xanthophyll cycle carotenoids in the protection of photosynthesis. *Trends in Plant Science*, **1**, 21-26.

Department of Trade and Industry (2006) The energy challenge: energy review report 2006. Crown copyright 2006
Avalible at: http://www.dti.gov.uk/files/file31890.pdf (last accesed 28.11.06).

Department of Trade and Industry, (2006a).
avalible at : www.dti.gov.uk/energy/sources/renewables/index.html (last accessed 28.11.06)

Dermody O, Long S, and DeLucia EH (2006) How does elevated CO_2 or ozone affect the leaf-area index of soybean when applied independently? *New Phytologist* **169**, 145 - 155.

Diaz C, **Purdy S, Christ A, Morot-Gaudry JF, Wingler A, Masclaux-Daubresse CL** (2005) Characterization of markers to determine the extent and variability of leaf senescence in Arabidopsis. A metabolic profiling approach. *Plant Physiology*, **138,** 898-908

Dickson RE, Lewin KF, Isebrands JG, Coleman MD, Heilman WE, Riemenschneider DE, Sober J, Host GE, Zak DR, Hendrey GR, Pregitzer KS and Karnosky DF. (2000) Statistical considerations and data analysis. In *Forest atmosphere carbon transfer and storage (FACTS-II) the Aspen Free-air CO_2 and O_3 enrichment (FACE) project: an overview.* General technical report N.C. 214, United States department of agriculture (USDA), North Central research station.

Drake BG, **GonzalezMeler MA and Long SP.** (1997) More efficient plants: A consequence of rising atmospheric CO_2? *Annual Review of Plant Physiology and Plant Molecular Biology*, **48**, 609-639.

Doncaster CP and Davey AJH. (2007) *Analysis of variance: How to choose and construct models for the life sciencesl. In press.* Cambridge University academic press.

Druart N, Rodríguez-Buey M, Barron-Gafford G, Sjödin A, Bhalerao R and Hurry V. (2006) Molecular targets of elevated [CO_2] in leaves and stems of *Populus deltiodes*: implications for future tree growth and carbon sequestration. *Functional Plant Biology*, **33**, 121-131.

Dudoit S, Yang YH, Callow MJ and Speed TP. (2000) Statistical methods for identifying differentially expressed genes in replicated cDNA microarray experiments. Technical report # 578, *Statistica Sinica*, **12**, 111-139.

Duggan DJ, Bittner M, Chen Y, Meltzer P and Trent JM. (1999) Expression profiling using cDNA microarrays. *Nature Genetics Supplement*, **21**, 10-14

Durbin B and Rocke DM. (2003) Estimation of transformation parameters for microarry data. *Bioinfomatics*, **19**, 1360-1367.

Dytham C. (1999) *Choosing and using statistics, a biologist's guide.* Blackwell Science Ltd., Oxford

Ellsworth DS, Reich PB, Naumburg ES, Koch GW, Kubiske ME and Smith SD. (2004) Photosynthesis, carboxylation and leaf nitrogen responses of 16 species to elevated pCO_2 across four free-air CO_2 enrichment experiments in forest, grassland and desert. *Global Change Biology*, **10**, 2121-2138

Enquist BJ, West GB, Charnov EL and Brown JH. (1999) Allometric scaling of production and life-history variation in vascular plants. *Nature*, **401,** 907-911

Escudero A and Mediavilla S (2003) Decline in photosynthetic nitrogen use efficiency with leaf age and nitrogen resorption as determinants of leaf life span. *Journal of Ecology*, **91**, 880-889

European Commission, (2005) Biomass green energy for Europe. European Communities, 2005. Also available at: http://ec.europa.eu/research/energy/nn/nn_pu/article_1078_en.htm#biomass (last accessed 28.11.06)

Fangmeier A, Chrost B, Hogy P and Krupinska K. (2000) CO_2 enrichment enhances flag leaf senescence in barley due to greater grain nitrogen sink capacity. *Environmental and Experimental Botany*, **44**, 151-164.

FAO (2006) Global forest resources assessment 2005. Progress towards sustainable forest management. *FAO forestry paper 147.* FAO, Rome Italy.

Farquhar GD, Von Caemmerer S and Berry JA. (1980) A biochemical model of photosynthetic CO_2 assimilation in leaves and C3 species. *Planta*, **149**, 78-90.

Feder ME and Walser JC. (2005) The biological limitations of transcriptomics in elucidating stress and stress responses. *Journal of Evolutionary Biology*, **18**, 901-910

Field CB, Behrenfeld MJ, Randerson JT and Falkowski P. (1998) Primary production of the biosphere: Integrating terrestrial and oceanic components. *Science*, **281,** 237-240

Field TS and Arens NC. (2005) Form, function and environments of the early angiosperms: merging extant phylogeny and ecophysiology with fossils. *New Phytologist*, **166,** 383-408

Field TS, Lee DW and Holbrook NM. (2001) Why leaves turn red in autumn. The role of anthocyanins in senescing leaves of Red-Osier Dogwood. *Plant Physiology*, **127**, 566–574

Fogwell F. (2005) Field guide for the GER 3700, version 3.0. NERC EPFS Edinburgh. Original created by: Karen Anderson, EPFS Southampton 2002.

Francey RJ, Allison CE, Etheridge DM, Trudinger CM, Enting IG, Leuenberger M, Langenfelds RL, Michel E and Steele LP. (1999) A 1000-year high precision record of delta C-13 in atmospheric CO_2. *Tellus Series B-Chemical and Physical Meteorology*, **51,** 170-193

Gamon JA, and Qiu H. (1999) Ecological applications of remote sensing at multiple scales. In: Pugnaire FI and Valladares F (Editors) *Handbook of functional plant ecology*. Marcel Dekker Inc, New York.

Gamon JA, Serrano L and Surfus JS. (1997) The photochemical reflectance index: an optical indicator of photosynthetic radiation use efficiency across species, functional types, and nutrient levels. *Oecologia*, **112**, 492-501.

Gamon JA and Surfus JS. (1999) Assessing leaf pigment content and activity with a reflectometer. *New Phytologist*, **143**, 105-117.

Geider RJ, Delucia EH, Falkowski PG, Finzi AC, Grime JP, Grace J, Kana TM, La Roche J, Long SP, Osborne BA, Platt T, Prentice IC, Raven JA, Schlesinger WH, Smetacek V, Stuart V, Sathyendranath S, Thomas RB, Vogelmann TC, Williams P and Woodward FI. (2001) Primary productivity of planet earth: biological determinants and physical constraints in terrestrial and aquatic habitats. *Global Change Biology*, **7,** 849-882

Gibon Y, Blasing OE, Palacios-Rojas N, Pankovic D, Hendriks JHM, Fisahn J, Hohne M, Gunther M and Stitt M. (2004) Adjustment of diurnal starch turnover to short days: depletion of sugar during the night leads to a temporary inhibition of carbohydrate utilization, accumulation of sugars and post-translational activation of ADP-glucose pyrophosphorylase in the following light period. The *Plant Journal*, **39**, 847-862

Geiger M, Haake V, Ludewig F, Sonnewald U and Stitt M. (1999) The nitrate and ammonium nitrate supply have a major influence on the response of photosynthesis, carbon metabolism, nitrogen metabolism and growth to elevated carbon dioxide in tobacco. *Plant Cell and Environment*, **22**, 1177-1199.

Gepstein S, Sabehi G, Carp M-J, Hajouj T, Nesher MFO, Yariv I, Dor C and Bassani M. (2003) Large-scale identification of leaf senescence-associated genes. *The Plant Journal*, **36**, 629-642.

Gielen B, Calfapietra C, Sabatti M and Ceulemans R. (2001) Leaf area dynamics in a closed poplar plantation under free-air carbon dioxide enrichment. *Tree Physiology*, **21**, 1245-1255.

Gielen B and Ceulemans R. (2001) The likely impact of rising atmospheric CO_2 on natural and managed *Populus*: a literature review. *Environmental Pollution*, **115**, 335-358.

Gielen B, Liberloo M, Bogaert J, Calfapietra C, De Angelis P, Miglietta F, Scarascia-Mugnozza G and Ceulemans R. (2003) Three years of free-air CO_2 enrichment (POPFACE) only slightly affect profiles of light and leaf characteristics in closed canopies of *Populus*. *Global Change Biology*, **9**, 1022-1037.

Gielen B, Calapietra C, Lukac M, Wittig VE, De Angelis P, Janssens IA, Moscatelli MC, Grego S, Cotrufo MF, Godbold DL, Hoosbeek MR, Iong SP, Miglietta F, Polle A, Bernacchi CJ, Davey PA, Ceulemans R and Scarascia-Mugnozza GE. (2005) Net carbon storage in a poplar plantation (POPFACE) after three years of free-air CO_2 enrichment. *Tree Physiology*, **25**, 1399-1408.

Gitelson AA, Gritz Y and Merzlyak MN. (2003) Relationships between leaf chlorophyll content and spectral reflectance and algorithms for non-destructive chlorophyll assessment in higher plant leaves. *Journal of Plant Physiology*, **160**, 271-282.

Gitelson AA and Merzlyak MN (1994) Spectral reflectance changes associated with autumn senescence of *Aesculus-Hippocastanum* L and *Acer-Platanoides* L leaves - spectral features and relation to chlorophyll estimation. *Journal of Plant Physiology*, **143**, 286-292.

Gitelson AA, Merzlyak MN and Chivkunova OB. (2001) Optical properties and nondestructive estimation of anthocyanin content in plant leaves. *Photochemistry and Photobiology*, **74**, 38-45.

Gollop R, Even S, Colova-Tsolova V and Perl A. (2002) Expression of the grape dihydroflavonol reductase gene and analysis of its promoter region. *Journal of Experimental Botany*, **53**, 1397-1409.

Goodacre R. (2005) Making sense of the metabolome using evolutionary computation: seeing the wood with the trees. *Journal of Experimental Botany*, **56**, 245 - 254

Gould KS. (2004) Natures Swiss army knife: the diverse protective roles of anthocyanins in leaves. *Journal of Biomedicine and Biotechnology*, **2004:5**, 314-320.

Goulden ML, Munger JW, Fan S-M, Daube BC and Wofsy SC. (1996) Exchange of carbon dioxide by a deciduous forest: Response to interannual climate variability. *Science*, **271**, 1576-1578.

Grace J. (2004) Understanding and managing the global carbon cycle. *Journal of Ecology*, **92,** 189-202

Granados J and Körner C. (2002) In deep shade, elevated CO_2 increases the vigor of tropical climbing plants. *Global Change Biology*, **18**, 1109 - 1117.

Gray JE, Holroyd GH, Van Der Lee FM, Bahrami AR, Sijmons PC, Woodward FI, Schuch W and Hetherington AM. (2000) The *HIC* signalling pathway links CO_2 perception to stomatal development. *Nature*, **408**, 713 - 716.

Gunderson CA, Norby RJ and Wullschleger SD. (1993) Foliar gas exchange responses of two deciduous hardwoods during 3 years of growth in elevated CO_2 : no loss of photosynthetic enhancement. *Plant Cell and Environment*, **16**, 797-807

Guo Y, Cai Z and Gan S. (2004) Transcriptome of Arabidopsis leaf senescence. *Plant, Cell and Environment*, **27**, 521-549.

Guo JM and Trotter CM. (2004) Estimating photosynthetic light-use efficiency using the photochemical reflectance index: variations among species. *Functional Plant Biology*, **31,** 255-265

Gupta P, Duplessis S, White H, Karnosky DF, Martin F and Podila GK. (2005) Gene expression patterns of trembling aspen trees following long-term exposure to interacting elevated CO_2 and troposphere O_3. *New Phytologist*,**167**, 633-633

Haupt W and Scheuerlein R. (1990) Chloroplast Movement. *Plant Cell and Environment*, **13,** 595-614

Heineke D, Kauder F, Frommer W, Kuhn C, Gillissen B, Ludewig F and Sonnewald U. (1999) Application of transgenic plants in understanding responses to atmospheric change. *Plant Cell and Environment*, **22**, 623-628.

Hendrey GR, Ellsworth DS, Lewin KF and Nagy J. (1999) A free-air enrichment system for exposing tall forest vegetation to elevated atmospheric CO_2. *Global Change Biology*, **5,** 293-309

Hendrey GR and Miglietta F. (2006) FACE technology: past, present and future. In Nösberger J, Long SP, Norby RJ, Stitt M, Hendrey GR and Blum H (Eds.) *Ecological Studies, Vol. 187. Managed ecosystems and CO_2 Case studies, processes and perspectives*. Springer-Verlag, Berlin Heidelberg.

Herrick JD and Thomas RB. (2003) Leaf senescence and late-season net photosynthesis of sun and shade leaves of overstory sweetgum (*Liquidambar styraciflua*) grown in elevated and ambient carbon dioxide concentrations. *Tree Physiology*, **23**, 109-118.

Hikosaka K. (2003) A model of dynamics of leaves and nitrogen in a plant canopy: An integration of canopy photosynthesis, leaf life span, and nitrogen use efficiency. *American Naturalist*, **162**, 149-164.

Hikosaka K. (2005) Leaf canopy as a dynamic system: Ecophysiology and optimality in leaf turnover. *Annals of Botany* **95**, 521-533.

Hikosaka K, Onoda Y, Kinugasa T, Nagashima H, Anten NPR and Hirose T. (2005) Plant responses to elevated CO_2 concentration at different scales: leaf, whole plant, canopy and population. *Ecological Research*, **20**, 243-253.

Hoel BO and Solhaug KA. (1998) Effect of irradiance on chlorophyll estimation with the Minolta SPAD-502 leaf chlorophyll meter. *Annals of Botany*, **82,** 389-392

Hollick JB and Gordon MP. (1995) Transgenic analysis of a hybrid poplar wound-inducible promoter reveals developmental patterns of expression similar to that of storage protein genes. *Plant Physiology*, **109**, 73-85.

Hoosbeek MR, Lukac M, van Dam D, Godbold DL, Velthorst EJ, Biondi FA, Peressotti A, Cotrufo MF, De Angelis P and Scarascia-Mugnozza G. (2004) More new carbon in the mineral soil of a poplar plantation under Free Air Carbon Enrichment (POPFACE): Cause of increased priming effect? *Global Biogeochemical Cycles* **18**: art. no.-GB1040.

Hortensteiner S and Feller U. (2002) Nitrogen metabolism and remobilization during senescence. *Journal of Experimental Botany*, **53**, 927-937

Horton P, **Ruban AV and Walters RG.** (1994) Regulation of light-harvesting in green plants - indication by non-photochemical quenching of chlorophyll fluorescence. *Plant Physiology*, **106**, 415-420

Houghton JT. (2004) *Global Warming: The Complete Briefing. Third edition.* Cambridge University Press, Cambridge UK.

Hymus GJ, **Baker NR and Long SP.** (2001) Growth in elevated CO_2 can both increase and decrease photochemistry and photoinhibition of photosynthesis in a predictable manner. *Dactylis glomerata* grown in two levels of nitrogen nutrition. *Plant Physiology*, 127, 1204-1211.

Imbeaud S, Grandens E, Boulanger V, Barlet X, Zaborski P, Eveno E, Mueller O, Schroeder A and Auffray C. (2005) Towards standardization of RNA quality assessment using user-independent classifiers of microcapillary electrophoresis traces. *NucleicAcids Research*, **33**, e56.

IPCC, (2001) Chapter 3: Afforestation, Reforestation, and Deforestation (ARD) Activities. In *Land Use, Land-Use Change and Forestry*. Cambridge University Press, Cambridge UK.
availible at: http://www.grida.no/climate/ipcc/land_use/112.htm (last accessed 28.11.06)

Isebrands JG, McDonald EP, Kruger E, Hendrey G, Percy K, Pretgitzer K, Sober J and Karnosky DF. (2001) Growth responses of *Populus tremuloides* clones to interacting elevated carbon dioxide and tropospheric ozone. *Environmental Pollution*, **115**, 359-371.

Jach ME and Ceulemans R. (1999) Effects of elevated atmospheric CO_2 on phenology, growth and crown structure of Scots pine (*Pinus sylvestris*) seedlings after two years of exposure in the field. *Tree Physiology*, 19, 289-300.

Jach ME, Ceulemans R and Murray MB. (2001) Impact of greenhouse gases on the phenology of forest trees. In: Karnosky DF, Ceulemans R, Scarascia-Mugnozza GE, and Innes JL(Editors), *The impact of carbon dioxide and other greenhouse gases on forest ecosystems report No. 3 of the IUFRO Task Force on Environmental Change*. CABI Publishing USA.

Jackson RD. (1986) Remote sensing of biotic and abiotic plant stress. *Annual Review of Phytopathology*, **24**, 265-287.

Jahren AH, **Arens NC, Sarmiento G, Guerrero J and Amundson R.** (2001) Terrestrial record of methane hydrate dissociation in the Early Cretaceous. *Geology*, **29,** 159-162

Janssens IA, **Freibauer A, Ciais P, Smith P, Nabuurs G.-J, Folberth G, Schlamadinger B, Hutjes RWA, Ceulemans R, Schulze E.-D, Valentini R and Dolman AJ.** (2003) Europe's terrestrial biosphere absorbs 7 to 12% of European anthropogenic CO_2 emissions. *Science*, **300**, 1538-1542.

Jensen JR. (2000) *Remote Sensing of the Environment: an earth resource perspective.* Prentice Hall, New Jersey.

Jones MB. (1993) Plant microclimate. In: Hall DO, Scurlock JMO, Bolhar-NordenKampf HR, Leegood RC and Long SP (Editors) *Photosynthesis and Production in a Changing Environment: a field and laboratory manual* Chapman & Hall, London.

Karnosky DF, Zak DR, Pregitzer KS, Awmack CS, Bockheim JG, Dickson RE, Hendrey GR, Host GE, King JS, Kopper BJ, Kruger EL, Kubiske ME, Lindroth RL,. Mattson WJ, McDonald EP, Noormets A, Oksanen E, Parsons WFJ, Percy KE,. Podila GK, Riemenschneider DE, Sharma P, Thakur RC, Sober A, Sober J, Jones WS, Anttonen S, Vapaavuori E, Mankovska B, Heilman WE, and Isebrands JG (2003) Tropospheric O_3 moderates responses of temperate hardwood forests to elevated CO_2: A synthesis of molecular to ecosystem results from the AspenFACE project. *Functional Ecololgy*, **17**, 289-304.

Kasahara M, **Kagawa T, Oikawa K, Suetsugu N, Miyao M and Wada M.** (2002) Chloroplast avoidance movement reduces photodamage in plants. *Nature*, **420,** 829-832

Kaufmann RH and Stock JH. (2003) Testing hypothesis about mechanisms for the unknown carbon sink: A time series analysis. *Global Biogeochemical Cycles*, **17**, 1072, doi:10.1029/2002GB001962.

Keeling CD (1998) Rewards and penalties of monitoring the Earth. *Annual Review of Energy and Environment*, **23,** 25-82

Keeling CD, **Chin JFS and Whorf TP**. (1996) Increased activity of northern vegetation inferred from atmospheric CO_2 measurements. *Nature*, **382,** 146-149

Keeling CD and Whorf TP. (2004). Atmospheric CO_2 records from sites in the SIO air sampling network. In Trends: A compendium of data on global change. carbon dioxide information analysis center, Oak Ridge National Laboratory, U.S. Department of Energy, Oak Ridge, Tenn., U.S.A. Available at: *http://cdiac.ornl.gov/ftp/trends/co2/maunaloa.co2* (last accessed 28.11.06)

Keskitalo J, Bergquist G, Gardeström and Jansson S. (2005) A cellular timetable of autumnal senescence. *Plant Physiology*, **139**, 1635-1648.

Klironomos JN, Allen MF, Rillig MC, Piotrowski J, Makvandi-Nejad S, Wolfe B and Powell JR. (2005) Abrupt rise in atmospheric CO_2 overestimates community response in a model plant-soil system. *Nature*, **433**, 621-624.

Koch KE. (1996) Carbohydrate-modulated gene expression in plants. *Annual Review of Plant Physiology and Plant Molecular Biology*, **47**, 509-540.

Kohler A, Delaruelle C, Martin D, Encelot N and Martin F. (2003) The poplar root transcriptome: analysis of 7000 expressed sequence tags. *FEBS letters*, **542**, 37-41.

Kohler A, Blaudez D, Chalot M and Martin F. (2004) Cloning and expression of multiple metallothioneins from hybrid poplar. *New Phytologist*, **164**, 83 - 93.

Knapp AK and Carter GA. (1998) Variability in leaf optical properties amoung 26 species from a broad range of habitats. *American Journal of Botany,* **85**, 940-946.

Knorr W, Prentice IC, House JI and Holland EA (2005) Long-term sensitivity of soil carbon turnover to warming. *Nature*, **433,** 298-301

Körner C (2003) Ecological impacts of atmospheric CO_2 enrichment on terrestrial ecosystems. *Philosophical Transactions of the Royal Society of London Series a-Mathematical Physical and Engineering Sciences*, **361,** 2023-2041

Körner C, Asshoff R, Bignucolo O, Hattenschwiler S, Keel SG, Pelaez-Riedl S, Pepin S, Siegwolf RTW and Zotz G. (2005) Carbon flux and growth in mature deciduous forest trees exposed to elevated CO_2. *Science*, **309,** 1360-1362

Lack AJ and Evans DE. (2001) Instant Notes: Plant Biology. BIOS Scientific Publishers Ltd, Oxford.

Lake JA, Woodward FI and Quick WP. (2002) Long-distance CO_2 signaling in plants. *Journal of Experimental Botany*, **53**, 183 - 193.

Lawlor DW (2001) *Photosynthesis*, Third edition. BIOS Scientific Publishers Ltd., Oxford

Levizou E, Drilias P, Psaras GK and Maneta Y. (2005) Non-destructive assessment of leaf chemistry and physiology through spectral reflectance measurements may be misleading when changes in trichome density co-occur. *New Phytologist*, **165**, 436-472.

Liberloo M, Gielen B, Calfapietra C, Veys C, Pilgiacelli R, Scarascia-Mugnozza G and Ceulemans R (2004). Growth of a poplar short rotation coppice under elevated atmospheric CO_2 concentrations (EUROFACE) depends on fertilization and species. *Annals of Forest Science*, **61**, 299-307.

Liberloo M, Dillen SY, Calfapietra C, Marinari S, Luo ZB, De Angelis P and Ceulemans R (2005).Elevated CO_2 concentration, fertilization and their interaction: growth stimulation in a short-rotation poplar coppice (EUROFACE). *Tree Physiology*, 25, 179-189.

Liberloo M, Calfapietra C, Lukac, M, Godbold D, Luo ZB, Polle A, Hoosbeek M, Kull O, Marek M, Raines C, Rubino M, Taylor G, Scarascia-Mugnozza G and Ceulemans R. (2006) Woody biomass production during the second rotation of a bio-energy *Populus* plantation increases in a future high CO_2 world. *Global Change Biology*, **12**, 1094-1106.

Liberloo M, Tulva I, Raïm O and Ceulemans R..(2007) Photosynthetic stimulation under long-term CO_2 enrichment and fertilization is sustained across a closed *Populus* canopy profile (EUROFACE). New Phytologist, 173, 537-549.

Li, J-H, Dijkstra P, Hymus GJ, Wheeler RM, Piastuch WC, Hinkle CR, and Drake BG. (2000) Leaf senescence of *Quercus myrtifolia* as affected by long-term CO_2 enrichment in its native environment. *Global Change Biology*, **6**, 727-733.

Li-cor (1990) LAI-2000 Plant Canopy Analyser Instruction Manual.

Lieth H (1974) Introduction to phenology and the modeling of seasonality. In: Lieth H (Editor) *Phenology and seasonality modeling*. Chapman & Hall Publishing, London.

Lim PO, Woo HR and Nam HG. (2003) Molecular genetics of leaf senescence in *Arabidopsis. Trends in Plant Sciences*, **8**, 272-278.

Lloyd JC and Zakhleniuk OV. (2004) Responses of primary and secondary metabolism to sugar accumulation revealed by microarray expression analysis of the *Arabidopsis* mutant, *pho3. Journal of Experimental Botany*, **55**, 1221 - 1230.

Long SP, **Humphries S and Falkowski PG** (1994) Photoinhibition of photosynthesis in nature. *Annual Review of Plant Physiology and Plant Molecular Biology*, **45,** 633-662

Long SP, **Ainsworth EA, Rogers, A and Ort DR.** (2004) Rising atmospheric carbon dioxide: Plants FACE the future. *Annual Review of Plant Biology*, **55**, 591-628.

Long SP, Ainsworth EA, Bernacchi CJ, Davey PA, Hymus GJ, Leakey ADB, Morgan PB and Osborne CP. (2006) Long-term responses of photosynthesis and stomata to elevated [CO_2] in managed systems. In Nösberger J, Long SP, Norby RJ, Stitt M, Hendrey GR and Blum H (Editors), *Ecological Studies, Vol. 187. Managed ecosystems and CO_2 Case studies, processes and perspectives*. Springer-Verlag, Berlin Heidelberg.

Long SP, Ainsworth EA, Leakey ADB, Nösberger J and Ort DR. (2006a) Food for thought: lower-than-expected crop yield stimulation with rising CO_2 concentrations. *Science*, **312**, 1918-1921.

Lucht W, Prentice CI, Myneni RB, Sitch S, Friedlingstein P, Cramer W, Bousquet P, Buermann W and Smith B.(2002) Climatic control of the high-latitude vegetation greening trend and Pinatubo effect. Science, **296**, 1687-1688.

Ludewig F, **Sonnewald U, Kauder F, Heineke D, Geiger M, Stitt M, Muller-Rober BT, Gillissen B, Kuhn C and Frommer WB**. (1998) The role of transient

starch in acclimation to elevated atmospheric CO_2. *FEBS Letters*, **429**, 147-151.

Lukac M, **Calfapietra C and Godbold DL**. (2003) Production, turnover and mycorrhizal colonization of root systems of three *Populus* species grown under elevated CO_2 (POPFACE). *Global Change Biology*, **9**, 838-848.

Maclellan C. (2006) Guidelines for post processing GER 1500 spectral data files using FSF excel template. NERC Field Spectroscopy Facility, Edinburgh. Obtained via http://fsf.nerc.ac.uk

Malhi Y. (2002) Carbon in the atmosphere and terrestrial biosphere in the 21st century. *Philosophical Transactions of the Royal Society of London Series a-Mathematical Physical and Engineering Sciences*, **360,** 2925-2945

Makino A, **Harada M, Sato T, Nakano H and Mae T**. (1997) Growth and N allocation in rice plants under CO_2 enrichment. *Plant Physiology*, **115**, 199-203.

Makino A and Mae T. (1999) Photosynthesis and plant growth at elevated levels of CO_2. *Plant and Cell Physiology*, **40**, 999-1006.

Makino A, **Nakano H, Mae T, Shimada T and Yamamoto N.** (2000) Photosynthesis, plant growth and N allocation in transgenic rice plants with decreased Rubisco under CO_2 enrichment. *Journal of Experimental Botany*, **51**, 383-389.

Martínez DE and Guiamet JJ. 2004. Distortion of the SPAD 502 chlorophyll meter readings by changes in irradiance and leaf water status. *Agronomie*, **24**, 41-46.

Matros A, Amme S, Kettig B, Buck-Sorlin GH, Sonnewald U and Mock H-P. (2006) Growth at elevated CO_2 concentrations leads to modified profiles of secondary metabolites in tobacco cv. SamsunNN and to increased resistance against infection with *potato virus Y. Plant, Cell and Environment*, **29**, 126-137.

McDonald MS. (2003) *Photobiology of higher plants*. John Wiley & Sons Ltd, Chichester

McKersie BD, Senaratna T, Walker MA, Kendall EJ and Hetherington PR. (1988) Deterioration of membranes during aging in plants: evidence for free radical mediation. In Noodén LD and Leopold AC (Editors) *Senecence and aging in plants*. Academic Press Inc. London.

Menzel A, **and Fabian P**. (1999) Growing season extended in Europe. *Nature*, **397**, 659-659.

Menzel, A, Sparks TH, Estrella N Koch E, Aasa A, Ahas R, Alm-kübler K, Bissolli P, Braslavská O, Briede A, Chmielewski FM, Crepinsek Z, Curnel Y, Dahl Å, Defila C, Donnelly A, Filella Y, Jatczak K, Måge F, Mestre A, Nordli Ø, Peñuelas J, Pirinen P, Remišová V, Scheifinger H, Striz M, Susnik A, Van Vliet AJH, Wielgolaski F-E, Zach S, Zust A (2006). European phenological response to climate change matches the warming pattern. *Global Change Biology*, **12**, 1-8.

Merzlyak MN, Gitelson AA, Chivkunova OB and Rakitin VY. (1999) Non-destructive optical detection of pigment changes during leaf senescence and fruit ripening. *Physiologia Plantarum*, **106**, 135-141.

Merzlyak MN, Gitelson AA, Chivkunova OB, Solovchenko AE and Pogosyan SI. (2003) Application of reflectance spectroscopy for analysis of higher plant pigments. *Russian Journal of Plant Physiology*, **50**, 704-710.

Merzlyak MN, Melo TB and Naqvi KR. (2004) Estimation of leaf transmittance in the near infrared region through reflectance measurements. *Journal of Photochemistry and Photobiology B-Biology*, **74,** 145-150.

Miglietta F, Raschi A, Resti R, and Badiani M. (1993) Growth and ontomorphogenesis of soybean (*Glycine-max* Merril) in an open, naturally CO_2-enriched environment. *Plant Cell and Environment.* **16**, 909-918.

Miglietta F, Magliulo V, Bindi M, Cerio L, Vaccari FP, Loduca V and Peressotti A. (1998) Free air CO_2 enrichment of potato (*Solanum tuberosum* L.): development, growth and yield. *Global Change Biology*, **4**, 163-172.

Miglietta F, Peressotti A, Vaccari FP, Zaldei A, DeAngelis P and Scarascia-Mugnozza G. (2001) Free-air CO_2 enrichment (FACE) of a poplar plantation: the POPFACE fumigation system. *New Phytologist*, **150**, 465-476.

Miller A, Tsai CH, Hemphill D, Endres M, Rodermel S and Spalding M. (1997) Elevated CO_2 effects during leaf ontogeny - A new perspective on acclimation. *Plant Physiology*, **115**, 1195-1200.

Miyazaki S, Fredricksen M, Hollis KC, Poroyko V, Shepley D, Galbraith DW, Long SP and Bohnert HJ. (2004) Transcript expression profiles of Arabidopsis thaliana grown under controlled conditions and open-air elevated concentrations of CO_2 and of O_3. *Field Crops Research*, **90,** 47-59

Monteith JL and Moss CJ. (1977) Climate and the efficiency of crop production in Britian (and discussion). *Philosophical Transactions of the Royal Society of London Series B-Biological Sciences*, **281**, 277-294

Moran R and Porath D (1980) Chlorophyll determination in intact tissues using N,N-Dimethylformamide. *Plant Physiology*, **65,** 478-479

Moore B, Zhou L, Rolland F, Hall Q, Cheng WH, Liu YX, Hwang I, Jones T and Sheen J. (2003) Role of the Arabidopsis glucose sensor HXK1 in nutrient, light, and hormonal signaling. *Science*, **300**, 332-336.

Moore BD, Cheng SH, Rice J and Seemann JR. (1998) Sucrose cycling, Rubisco expression, and prediction of photosynthetic acclimation to elevated atmospheric CO_2. *Plant Cell and Environment*, **21**, 905-915.

Moore BD, Cheng SH, Sims D and Seemann JR. (1999) The biochemical and molecular basis for photosynthetic acclimation to elevated atmospheric CO_2. *Plant Cell and Environment*, **22**, 567-582.

Moreau C, Aksenov N, Lorenzo MG, Segerman B, Funk C, Nilsson P, Jansson S and Tuominen H. (2005) A genomic approach to investigate developmental cell death in woody tissues of *Populus* trees. *Genome Biology*, **6**, R344.

Morecroft MD, Stokes VJ and Morison JIL. (2003) Seasonal changes in the photosynthetic capacity of canopy oak (*Quercus robur*) leaves: the impact of slow development on annual carbon uptake. *International Journal of Biometeorology*, **47**, 221 - 226.

Myneni RB, Dong J, Tucker CJ, Kaufmann RK, Kauppi PE, Liski J, Zhou L, Alexeyev V and Hughes MK. (2001) A large carbon sink in the woody biomass of Northern forests. *Proceedings of the National Academy of Sciences of the United States of America*, **98**, 14784-14789.

Myneni RB, Keeling CD, Tucker CJ, Asrar G and Nemani RR. (1997) Increased plant growth in the northern high latitudes from 1981 to 1991. *Nature*, **386**, 698-702.

Navabpour S, Morris K, Allen R, Harrison E, Mackerness S A-H and Buchanan-Wollaston V. (2003) Expression of senescence-enhanced genes in response to oxidative stress. *Journal of Experimental Botany*, **54**, 2285-2292

Nelson ND and Isebrands JD. (1983) Late-season photosynthesis and photosynthate distribution in an intensively-cultured *Populus-nigra* x *laurifolia* clone. *Photosynthetica*, **17**, 537-549

Nemani RR, Keeling CD, Hashimoto H, Jolly WM, Piper SC, Tucker CJ, Myneni RB and Running SW. (2003) Climate-driven increases in global terrestrial net primary production from 1982 to 1999. *Science*, **300,** 1560-1563.

Nielsen TH, Krapp A, Roper-Schwarz U and Stitt M. (1998) The sugar-mediated regulation of genes encoding the small subunit of Rubisco and the regulatory subunit of ADP glucose pyrophosphorylase is modified by phosphate and nitrogen. *Plant Cell and Environment*, **21**, 443-454.

Noodén LD. (1988) The phenomena of senescence and aging. In Noodén LD and Leopold AC, (Editors), *Senecence and aging in plants.* Academic Press Inc. London.

Norby RJ, Hanson PJ, O'Neill EG, Tschaplinski TJ, Weltzin JF, Hansen RA, Cheng WX, Wullschleger SD, Gunderson CA, Edwards NT and Johnson DW. (2002) Net primary productivity of a CO_2-enriched deciduous forest and the implications for carbon storage. *Ecological Applications*, **12**, 1261-1266.

Norby RJ, Sholtis JD, Gunderson CA and Jawdy SS. (2003) Leaf dynamics of a deciduous forest canopy: no response to elevated CO_2. *Oecologia*, **136**, 574-584

Norby RJ, Todd DE, Fults J and Johnson DW. (2001) Allometric determination of tree growth in a CO_2-enriched sweetgum stand. *New Phytologist*, **150**, 477-487.

Norby RJ, Wullschleger SD, Gunderson CA, Johnson DW and Ceulemans R. (1999) Tree responses to rising CO_2 in field experiments: implications for the future forest. *Plant Cell and Environment*, **22**, 683-714.

Norby RJ, Hartz-Rubin JS, Verbrugge MJ. (2003) Phenological responses in maple to experimantal atmospheric warming and CO_2 enrichment. *Global Change Biology*, **9**, 1792-1801.

Norby RJ, Ledford J, Reilly CD, Miller NE and O`Neill EG (2004). Fine-root production dominates response of a deciduous forest to atmospheric CO_2 enrichment. *Proceedings of the National Academy of Science USA*, **101**, 9689-9693

Norby RJ, DeLucia EH, Gielen B, Calfapietra C, Giardina CP, King JS, Ledford J, McCarthy HR, Moore DJP, Ceulemans R, De Angelis P, Finzi AC, Karnosky DF, Kubiske ME, Lukac M, Pregitzer KS, Scarascia-Mugnozza G, Schlesinger WH and Oren R. (2005) Forest response to elevated CO_2 is conserved across a broad range of productivity. *Proceedings of theNational Academy of Science USA*, **102**, 18052-18056.

Nösberger J and Long SP. (2006) Introduction. In Nösberger J, Long SP, Norby RJ, Stitt M, Hendrey GR and Blum H (Editors), *Ecological Studies, Vol. 187. Managed ecosystems and CO_2 Case studies, processes and perspectives.* Springer-Verlag, Berlin Heidelberg.

Olsen JE, Junttila O, Nilsen J, Eriksson ME, Martinussen I, Olsson O, Sandberg G and Moritz T. (1997) Ecotpic expression of oat phytochrome A in hybrid aspen changes critical daylength for growth and prevents cold acclimatization. *The Plant Journal*, **12**, 1339 - 1350.

Onoda Y, Hikosaka K and Hirose T. (2005) Seasonal change in the balance between capacities of RuBP carboxylation and RuBP regeneration affects CO_2 response of photosynthesis in *Polygonum cuspidatum. Journal of Experimental Botany* 56: 755-763

Oren R, Ellsworth DS, Johnsen KH, Phillips N, Ewers BE, Maier C, Schafer KVR, McCarthy H, Hendrey G, McNulty SG and Katul GG. (2001) Soil fertility limits carbon sequestration by forest ecosystems in a CO_2-enriched atmosphere. *Nature*, **411,** 469-472

Osmond B, Ananyev G, Berry J, Langdon C, Kolber Z, Lin GH, Monson R, Nichol C, Rascher U, Schurr U, Smith S and Yakir D. (2004) Changing the way we think about global change research: scaling up in experimental ecosystem science. *Global Change Biology*, **10,** 393-407

Parmesan C and Yohe G. (2003) A globally coherent fingerprint of climate change impacts across natural systems. *Nature*, **421**, 37-42

Paul MJ and Driscoll SP. (1997) Sugar repression of photosynthesis: The role of carbohydrates in signalling nitrogen deficiency through source:sink imbalance. *Plant Cell and Environment*, **20**,110-116

Paul MJ and Foyer CH. (2001) Sink regulation of photosynthesis. *Journal of Experimental Botany*, **52**, 1383-1400.

Pearson PN and Palmer MR. (2000) Atmospheric carbon dioxide concentrations over the past 60 million years. *Nature*, **406**, 695-699

Pelletier MK, Murrell JR and Shirley BW. (1997) Characterization of Flavonol Synthase and Leucoanthocyanidin Dioxygenase genes in *Arabidopsis*. *Plant Physiology*, **113**, 1437-1445.

Peñuelas J and Filella I (1998) Visible and near-infrared reflectance techniques for diagnosing plant physiological status. *Trends in Plant Science*, **3**, 151-156

Peñuelas J and Filella I. (2001) Phenology - Responses to a warming world. *Science*, **294**, 793-795.

Peñuelas J and Inoue Y. (2000) Reflectance assessment of canopy CO_2 uptake. *International Journal of Remote Sensing*, **21**, 3353-3356.

Petit JR, Jouzel J, Raynaud D, Barkov NI, Barnola J-M, Basile I, Bender M, Chappellaz J, Davis M, Delaygue G, Delmotte m, Kotlyakov VM, Legrand M, Lipenkov VJ, Iorius C, Pépin L, Ritz C, Saltzman E and Stievenard M. (1999) Climate and atmospheric history of the past 420, 000 years from the Vostok ice core, Antarctica. *Nature*, **399**, 429 - 435.

Pieters AJ, Paul MJ and Lawlor DW. (2001) Low sink demand limits photosynthesis under P-i deficiency. *Journal of Experimental Botany*, **52**, 1083-1091.

Pinter PJ, Kimball BA, Wall GW, LaMorte RL, Hunsaker DJ, Adamsen FJ, Frumau KFA, Vugts HF, Hendrey GR, Lewin KF, Nagy J, Johnson HB, Wechsunge F, Leavitt SW, Thompson TL, Matthias AD and Brooks TJ. (2000) Free-air CO_2 enrichment (FACE): blower effects on wheat canopy microclimate and plant development. *Agricultural and Forest Meteorology*, **103,** 319-333

Plummer SE, Danson, FM and Wilson, AK. (1995) Advances in remote sensing technology. In Danson FM and Plummer SE (Editors) *Advances in environmental remote sensing.*. John Wiley & Sons Chichester.

Pourtau N, Marès M, Purdy S, Quentin N, Ruël A and Wingler A (2004) Interactions of abscisic acid and sugar signalling in the regulation of leaf senescence. *Planta* **219**, 765-772.

Pourtau N, Jennings R, Pelzer E, Pallas J and Wingler A. (2006) Effect of sugar-induced senescence on gene expression and implications for the regulation of senescence in *Arabidopsis*. *Planta*, **224**, 556–568.

Prentice IC, Farquhar G, Fasham M, Goulden M, Heimann M, Jaramillo V, Kheshgi H, Le Quere C and Scholes RJ. (2001) The carbon cycle and atmospheric carbon dioxide. In Houghton JT, Ding Y, Griggs DJ, Noger M, van der Linden PJ, Dai X, Maskell K and Johnson CA (Editors), *Climate change 2001: The scientific basis*. Contribution of working Group I to the Third Assessment Report of the Intergovernmental panel on Climate Change. Cambridge University Press, Cambridge.

Priestley J and Hey W. (1772) Observations on different kinds of air. *Philosophical Transactions*, **62**, 147-264

Pritchard SG, Rogers HH, Prior SA and Peterson CM. (1999) Elevated CO_2 and plant structure: a review. *Global Change Biology*, **5**, 807-837.

Quirino BF, Noh YO, Himelblau E and Amasino RM. (2000) Molecular aspects of leaf senescence. *Trends in Plant Sciences*, **5**, 278-282.

Rae A, Ferris R, Tallis MJ and Taylor G. (2006) Elucidating genomic regions determining enhanced leaf growth and delayed senescence in elevated CO_2. *Plant, Cell and Environment*, **29**, 1730-1741.

Ragauskas A, Williams CK, Davidson BH, Britovsek G, Cairney J, Eckert CA, Frederick Jr WJ, Hallett JP, Leak DJ, Liotta CL, Mielenz JR, Murphy R, Templer R and Tschaplinski T. (2006) The path forward for biofuels and biomaterials. *Science*, **311**, 484 - 489.

Reich PB, Walters MB and Ellsworth DS. (1992) Leaf life-span in relation to leaf, plant and stand characteristics among diverse ecosystems. *Ecological Monographs*, **62**, 365-392

Reich PB, Walters MB and Ellsworth DS. (1997). From tropics to tundra: Global convergence in plant functioning. *Proceedings of the National Academy of Sciences of the United States of America*, **94**, 13730-13734.

Reich PB, Ellsworth DS, Walters MB, Vose JM, Gresham C, Volin JC and Bowman WD. (1999) Generality of leaf trait relationships: A test across six biomes. *Ecology*, **80**, 1955-1969.

Richardson AD, Duigan SP and Berlyn GP. (2002) An evaluation of non-invasive methods to estimate foliar chlorophyll content. *New Phytologist*, **153**, 185-194.

Richardson AD, Bailey AS, Denny EG, Martin W, and Keefe JO. (2006) Phenology of a northern hardwood forest canopy. *Global Change Biology* **12**, 1-15.

Rogers A, Ainsworth EA and Kammann C. (2006) FACE value: Perspectives on the future of free-air CO_2 enrichment studies. In Nösberger J, Long SP, Norby RJ, Stitt M, Hendrey GR and Blum H (Editorss.) *Ecological Studies, Vol. 187. Managed ecosystems and CO_2 Case studies, processes and perspectives.* Springer-Verlag berlin Heidelberg.

Roitsch T. (1999) Source-sink regulation by sugar and stress. *Current Opinion in Plant Biology*, **2**, 198-206.

Roitsch T and González M-C. (2004) Function and regulation of plant invertases: sweet sensations. *Trends in Plant Science*, **9**, 606 - 613.

Root TL, Price JT, Hall KR, Schneider SH, Rosenzweig, C and Pounds JA. (2003) Fingerprints of global warming on wild animals and wild plants *Nature* **421**, 57-60.

Ruperti B, Cattivelli L, Pagni S and Ramina A. (2002) Ethylene-responsive genes are differentially regulated during abscission, organ senescence and wounding in peach (*Prunus persica*). *Journal of Experimental Botany*, **53**, 439-437.

Sage RF. (1994) Acclimation of photosynthesis to increasing atmospheric CO_2 - the gas-exchange perspective. *Photosynthesis Research*, **39**, 351-368.

Scarascia-Mugnozza G, De Angelis P, Sabatti M, Calfapietra C, Migletta F, Raines C, Godbold D, Hoosbeek M, Taylor, G, Polle A and Ceulemans R. (2005) Centenary congress article. Global change and agro-forestry ecosystems: Adaptation and mitigation in a FACE experiment on a poplar plantation. *Plant Biosystems*, **139**, 255-264.

Scarascia-Mugnozza G, Calfapietra C, Ceulemans R, Gielen B, Cotrufo MF, De Angelis P, Godbold D, Hoosbeek MR, Kull O, Lukac M, Marek M, Migletta F, Polle A, Raines C, Sabatti M, Anselmi N and Taylor G. (2006) Responses to elevated [CO_2] of a short rotation, multispecies poplar plantation: the POPFACE / EUROFACE experiment. In Nösberger J, Long SP, Norby RJ, Stitt M, Hendrey GR and Blum H (Editors.) *Ecological Studies, Vol. 187. Managed ecosystems and CO_2 Case studies, processes and perspectives.* Springer-Verlag, Berlin Heidelberg.

Schlesinger WH, Bernhardt ES, DeLucia EH, Ellsworth DS, Finzi AC, Hendrey GR, Hofmockel KS, Lichter J, Matamala R, Moore D, Oren R, Pippen JS and Thomas RB. (2006) The Duke forest FACE experiment: CO_2 enrichment of a loblolly pine forest. In Nösberger J, Long SP, Norby RJ, Stitt M, Hendrey GR and Blum H (Editors.) *Ecological Studies, Vol. 187. Managed ecosystems and CO_2 Case studies, processes and perspectives.* Springer-Verlag, Berlin Heidelberg.

Schloss AL, Kicklighter DW, Kaduk J and Wittenberg U. (1999) Comparing global models of terrestrial net primary productivity (NPP): comparison of NPP to climate and the Normalized Difference Vegetation Index (NDVI). *Global Change Biology*, **5**, 25-34.

Schwanz P and Polle A. (1998) Antioxidative systems, pigment and protein contents in leaves of adult Mediterranean oak species (*Quercus pubescens* and *Q-ilex*) with lifetime exposure to elevated CO_2. *New Phytologist*, **140**, 411-423.

Sellers PJ, Bounoua L, Collatz GJ, Randall DA, Dazlich DA, Los SO, Berry JA, Fung I, Tucker CJ, Field CB, and Jensen TG. (1996) Comparison of radiative and physiological effects of doubled atmospheric CO_2 on climate. *Science* **271**, 1402-1406.

Sigurdsson BD. (2001) Elevated CO_2 and nutrient status modified leaf phenology and growth rhythm of young *Populus trichocarpa* trees in a 3-year field study. *Trees-Structure and Function*, **15**, 403-413.

Sims DA and Gamon JA. (2002) Relationships between leaf pigment content and spectral reflectance across a wide range of species, leaf structures and developmental stages. *Remote Sensing of Environment*, **81**, 337-354.

Sims DA, Luo Y and Seeman JR. (1998) Importance of leaf verse whole plant CO_2 environment for photosynthetic acclimation. *Plant, Cell and Environment*, **21**, 1189-1196.

Slaton MR, Hunt Jr ER and Smith WK. (2001) Estimating near-infrared leaf reflectance from leaf structural characteristics. *Americana Journal of Botany*, **88**, 278-284

Slayback DA, Pinzon JE, Los SO and Tucker CJ. (2003) Northern hemisphere photosynthetic trends 1982 - 99. *Global Change Biology*, **9**, 1 - 15.

Smith CM, Rodriguez-Buey M, Karlsson J and Campbell M. (2004) The response of the poplar transcriptome to wounding and subsequent infection by a viral pathogen. *New Phytologist*, **164**, 123-136

Smith KL, Steven MD and Colls JJ. (2004) Use of hyperspectral derivative ratios in the red-edge region to identify plant stress responses to gas leaks. *Remote Sensing of Environment*, **92**, 207-217

Smyth GK. (2004) Linear models and empirical Bayes methods for assessing differential expression in microarray experiments. *Statistical Applications in Genetics and Molecular Biology* 3: No. 1, Article 3

Sokal RR and Rohlf FJ. (1998) *Biometry*. (Third edition.). WH. Freeman and Company, New York

Southern E, Mir K and Shchepinov. (1999) Molecular interactions on microarrays. *Nature Genetics Supplement*, **21**, 5-9.

Sterky F, Regan S, Karlsson J, Hertzberg M, Rohde A, Holmberg A, Amini B, Bhalerao R, Larsson M, Villarroel R, Montagu MV, Sandberg G, Olsson O, Teeri TT, Boerjan W, Gustafsson P, Uhlén M, Sundberg B and Lundeberg J. (1998) Gene discovery in the wood-forming tissues of poplar: Analysis of 5,692 expressed sequence tags. *Proceedings of the National Academy of Sciences*, **95**, 13330-13335.

Sterky F, Bhalerao RR, Unneberg P, Segerman B, Nilsson P, Brunner AM, Charbonnel-Campaa L, Lindvall JJ, Tandre K, Strauss SH, Sunderb B, Gustafsson P, Uhlén M, Bhalerao RP, Nilsson O, Sandberg S, Karlsson J, Lundeberg J and Jansson S. (2004) A *Populus* EST resource for plant functional genomics. *Proceedings of the National Academy of Science*, **101**, 13951-13956.

Stitt M. (1991) Rising CO_2 levels and their potential significance for carbon flow in photosynthetic cells. *Plant Cell and Environment*, **14**, 741-762.

Stitt M and Krapp A. (1999) The interaction between elevated carbon dioxide and nitrogen nutrition: the physiological and molecular background. *Plant Cell and Environment*, **22**, 583-621.

Stöckli R and Vidale PL. (2004) European plant phenology and climate as seen in a 20-year AVHRR land-surface parameter dataset. *International Journal Remote Sensing*, **25**, 3303- 3330

Street NR, Skogström O, Sjödin A, Tucker J, Rodríguez-Ascosta M, Nilsson P, Jansson S and Taylor G. (2006) The genetics and genomics of the drought response in *Populus*. *The Plant Journal*, **48**, 321 - 341.

Taiz L and Zeiger E. (2002) *Plant Physiology*, Third edition. Sinauer Associates, Inc., Publishers, Massachusetts.

Taji T, Ohsumi C, Iuchi S, Seki M, Kasuga M, Kobayashi M, Yamaguchi-Shinozaki K and Shinozaki K. (2002) Important roles of drought- and cold-

inducible genes for galactinol synthase in stress tolerance in *Arabidopsis thaliana*. *The Plant Journal*, **29**, 417-426.

Taylor G. (2002). *Populus*. *Arabidopsis* for forestry. Do we need a model tree? *Annals of Botany* **90**: 681-689.

Taylor G, Tricker PJ, Zhang FZ, Alston VJ, Miglietta F and Kuzminsky E. (2003) Spatial and temporal effects of free-air CO_2 enrichment (POPFACE) on leaf growth, cell expansion, and cell production in a closed canopy of poplar. *Plant Physiology*, **131**, 177-185.

Taylor G, Street NR, Tricker PJ, Sjodin A, Graham L, Skogstrom O, Calfapietra C, Scarascia-Mugnozza G and Jansson S. (2005) The transcriptome of *Populus* in elevated CO_2. *New Phytologist*, **167**, 143-154

Terashima I, Araya T, Miyazawa S, Sone K and Yano S. (2005) Construction and maintenance of the optimal photosynthetic systems of the leaf, herbaceous plant and tree: an eco-developmental treatise. *Annals of Botany*, **95**, 507-519

The Royal Society. (2001) The role of land carbon sinks in mitigating global climate change. Availible at: http://www.royalsoc.ac.uk/displaypagedoc.asp?id=11505 (last accessed 28.11.06)

Thomas SC. (2005). Increased leaf reflectance in tropical trees under elevated CO_2. *Global Change Biology*, **11**, 197-202.

Thompson SL, Govindasamy B, Mirin A, Caldeira K, Delire C, Milovich J, Wickett M and Erickson D. (2004) Quantifying the effects of CO_2-fertilized vegetation on future global climate and carbon dynamics. *Geophysical Research Letters* **31,** L23211.

Tricker PJ, Calfapietra C, Kuzminsky E, Puleggi R, Ferris R, Nathoo M, Pleasants LJ, Alston V, De Angelis P and Taylor G. (2004) Long-term acclimation of leaf production, development, longevity and quality following 3 yr exposure to free-air CO_2 enrichment during canopy closure in *Populus*. *New Phytologist*, **162**, 413-426.

Tricker PJ, Trewin H, Kull O, Clarkson GJJ, Eensalu E, Tallis MJ, Colella A, Doncaster CP, Sabatti M and Taylor G (2005) Stomatal conductance and not stomatal density determines the long-term reduction in leaf transpiration of poplar in elevated CO_2. *Oecologia*, **143**, 652-660

Tsai C-J, Harding SA, Tschaplinski TJ, Lindroth RL and Yuan Y. (2006) Genome-wide analysis of the structural genes regulating defense phenylpropanoid metabolism in *Populus*. *New Phytologist*, **172**, 47-62.

Tucker CJ, Slayback DA, Pinzon JE, Los SO, Myneni RB and Taylor MG. (2001) Higher northern latitude normalized difference vegetation index and growing season trends from 1982 to 1999. *International Journal of Biometeorology*, **45**, 184-190.

Tuskan GA and DiFazio S *et al.*, (2006) The genome of black cottonwood, *Populus trichocarpa* (Torr. & Gray). *Science*, **313**, 1596-1604.

UN, (1998) Kyoto protocol to the United Nations framework convention on climate change.
Avalible at: http://unfccc.int/resource/docs/convkp/kpeng.pdf (last accessed 28.11.06)

Underwood AJ (1997) *Experiments in Ecology: Their Logical Design and Interpretation Using Analysis of Variance*. Cambridge Univ Press, Cambridge UK

Vogelmann TC. (1993) Plant tissue optics. *Annual Review of Plant Physiology and Plant Molecular Biology*, **44**, 231-251.

Wada M, Kagawa T and Sato Y. (2003) Chloroplast movement. *Annual Review of Plant Biology,* **54**, 455-468

Wait DA, Jones CG, Wynn J and Woodward FI. (1999) The fraction of expanding to expanded leaves determines the biomass response of *Populus* to elevated CO_2. *Oecologia*, **121**, 193-200

Walter A, **Christ MM, Barron-gafford GA, Grieve KA, Murthy R and Rascher U.** (2005) The effect of elevated CO_2 on diel leaf growth cycle, leaf carbohydrate content and canopy growth performance of *Populus deltoides*. *Global Change Biology*, **11**, 1207-1219

Ward JK and Kelly JK. (2004) Scaling up evolutionary responses to elevated CO_2: lessons from *Arabidopsis*. *Ecology Letters,* **7**, 427-440.

Watson JD, Gilman M, Witkowski J and Zoller M. (1992) Recombinant DNA (*second edition*). Scientfic American books, New York.

Weaver LM and **Amasino RM**. (2001) Senescence is induced in individually darkened Arabidopsis leaves but inhibited in whole darkened plants. *Plant Physiology*, **127**, 876-886.

Weaver LM, **Gan SS, Quirino B and Amasino RM**. (1998) A comparison of the expression patterns of several senescence- associated genes in response to stress and hormone treatment. *Plant Molecular Biology*, **37**, 455-469.

Wellburn AR (1994). The spectral determination of chlorophyll-a and chlorophhyll-b, as well as total carotenoids, using various solvents with spectrophotometers of different resolution. *Journal of Plant Physiology*, **144**, 307-313.

Whetten R and Sederoff R. (1995) Lignin biosynthesis. *The Plant Cell*, **7**, 1001 - 1013.

White MA, Running SW and Thornton PE. (1999) The impact of growing-season length on carbon assimilation and evapotranspiration over 88 years in the eastern US deciduous forest. *International Journal of Biometeorology*, **42**, 139 - 145.

Widholm JM and Ogren WL. (1969) Photorespiratory-induced senescence of plants under conditions of low carbon dioxide. *Proceedings of the National Academy of Sciences, USA*, **63**, 668 - 675.

William A, Hoch WA, Singsaas EL and McCown BH. (2003) Resorption protection. Anthocyanins facilitate nutrient recovery in autumn by shielding leaves from potentially damaging light levels. *Plant Physiology*, **133**, 1296–1305,

Williams WE, Gorton HL, and Witiak SM. (2003) Chloroplast movements in the field. *Plant, Cell and Environment* 26: 2005 - 2014.

Willmer C and Fricker M. (1996). Stomata, *second edition*. In: Black, M and Charlwood B (*Series editors*), *Topics in plant functional biology: 2.. Chapman & Hall,London*

Wingler A, von Schaewen A, Leegood RC, Lea PJ and Quick PW. (1998) Regulation of Leaf Senescence by Cytokinin, Sugars, and Light . Effects on NADH-Dependent Hydroxypyruvate Reductase. *Plant Physiology*, **116**, 329-335.

Wingler A, Mares M and Pourtau N. (2004) Spatial patterns and metabolic regulation of photosynthetic parameters during leaf senescence. *New Phytologist*, **161**, 781-789.

Wingler A, Purdy S, MacLean JA and Pourtau N. (2006) The role of sugars in integrating environmental signals during the regulation of leaf senescence. *Journal of Experimental Botany*, **57**, 391–399.

Wittig VE, Bernacchi CJ, Zhu X-G, Calfapietra C, Ceulemans R, De Angelis p, Gielen B, Miglietta F, Morgan PB and Long SP. (2005). Gross primary production is stimulated for three *Populus* species grown under free-air CO_2 enrichment from planting through canopy closure. *Global Change Biology*, **11**, 644-656.

Wright IJ, Reich PB, Westoby M, Ackerly DD, Baruch Z, Bongers F, Cavender-bares J, Chaplin T, Cornelissen JHC, Diemer M, Flexas J, Garnier E, Groom PK, Gullas J, Hikosaka K, Lamont BB, Lee T, Lee W, Lusk C, Midgley JJ, Navas M-L, Niinemets Ü, Oleksyn J, Osada N, Poorter, H, Poot P, Prior L, Pyankov VI, Roumet C, Thomas SC, Tjoelker MG, Veneklaas EJ and Villar R. (2004) The world-wide leaf economics spectrum. *Nature*, **2403**, 1-7.

Woo HY, Kim JH, Nam HG, Lim PO (2004) The delayed leaf senescence mutants of *Arabidopsis*, *ore1*, *ore3*, and *ore9* are tolerant to oxidative stress. *Plant Cell Physiology*, **45**, 923-932.

Woolley JT. (1971) Reflectance and transmittance of light by leaves. *Plant Physiology*, **47**, 656-662.

Xiao WY, Sheen J and Jang JC. (2000) The role of hexokinase in plant sugar signal transduction and growth and development. *Plant Molecular Biology*, **44**, 451-461.

Yang YH, Buckley MJ and Speed TP. (2001) Analysis of cDNA microarray images. *Briefings in Bioinformatics*, **2**, 341-349.

Yong JWH, Wong SC, Letham DS, Hocart CH and Farquhar GD. (2000) Effects of elevated CO_2 and nitrogen nutrition on cytokinins in the xylem sap and leaves of cotton. *Plant Physiology*, **124**, 767-779.

Yoshida S. (2003) Molecular regulation of leaf senescence. *Current Opinion in Plant Biology*, **6**, 79-84.

Zarco-Tejada PJ, Pushnik JC, Dobrowski S and Ustin SL. (2003) Steady-state chlorophyll a fluorescence detection from canopy derivative reflectance and double-peak red-edge effects. *Remote Sensing of Environment*, **84**, 283-294

Zhou L, **Tucker C J, Kaufmann RK, Slayback D, Shabanov NV and Myneni RB.** (2001) Variations in northern vegetation activity infrerred from satellite data of vegetation index during 1981 to 1999. *Journal of Geophysical Research*, **106**, 20069-20083.

Zimmermann P and Zentgraf U. (2005) The correlation between oxidative stress and leaf senescence during plant development. *Cellular and Molecular Biology Letters*, **10**, 515-534.

Appendix

Appendix A: Publications

Publications arising from this work

Tallis MJ, Dash J, Curran PJ and Taylor G. Changing levels of low irradiance influences spectral estimates of leaf chlorophyll content. **New Phytologist** (*preparation for resubmission*)

Bixia X, Taylor G, Rae AM, **Tallis MJ** and Karnosky DF. Applications of Genomics to Poplar Improvement: A Primer for Forest Managers. (*in preparation*).

Taylor G, **Tallis MJ**, Giardina CP, Percy KE, Miglietta F *et al.* Future atmospheric CO_2 leads to delayed autumnal senescence and increased carbon gain in *Populus.* **Global Change Biology** (*accepted*)

Tallis MJ, Street N, Zhang J, Gielen B, Calfapietra C, DeAngelis P, Miglietta F and Taylor G. Delayed autumnal senescence in a high CO_2 world: altered gene expression in *Populus* following six years of exposure to free air CO_2 enrichment in the POPFACE experiment. (*In preparation*).

International conference presentations

Tallis MJ, Migletta F. Street NR, and Taylor G. *Elevated atmospheric CO_2 delays autumnal senescence for Poplar.* ***Key-note presentation***: **4th International poplar symposium, Nanjing, China 2006**

Taylor G, **Tallis MJ**, Rae AM and Miglietta F. *Does exposure to elevated CO_2 delay the onset of autumnal senescence? Evidence from leaf, canopy and remote measurements.* **International Botanical Congress, *Vienna 2005***

Dash J, **Tallis MJ**, Curran PJ and Taylor G. *The relationship between irradiance and the red edge position of a leaf.* **Remote Sensing and Photogrammetry Society Conference, *Portsmouth 2005***

International poster presentations

Tallis MJ, Migletta F. Street NR, Gielen B, and Taylor G. *Why is autumn getting later?* **Society of Experimental Biology Conference, Canterbury 2006.**

Tallis MJ, Miglietta F, and Taylor G. *Delayed autumnal senescence in elevated atmospheric CO_2.* **International FACE workshop Ascona Switizerland 2004**

Tallis MJ, Miglietta F, and Taylor G. *Does elevated atmospheric CO_2 delay autumnal senescence?* **Society of Experimental Biology Conference, Edinburgh 2004. (Irene Menton Prize Winner).**

Publications associated with this work

Rae AM, Ferris R, **Tallis MJ** and Taylor G (2006). Elucidating genomics regions for increased leaf growth and delayed leaf senescence in elevated CO_2 **Plant Cell and Environment** , **29**, 1730-1741.

Tricker PJ, Trewin H, Kull O, Clarkson GJJ, Eensalu E, **Tallis MJ**, Colella A, Doncaster CP, Sabatti M, Taylor G (2005) Stomatal conductance and not stomatal density determines the long-term reduction in leaf transpiration of poplar in elevated CO_2. **Oecologia** 143: 652-660

Taylor G, Tricker PJ, Graham LE, **Tallis MJ**, Rae AM, Trewin H, Street NR (2006). The potential of genomics and genetics to understand plant responses to elevated atmospheric [CO_2]. **Ecological Studies, Vol. 187.** J. Nösberger, SP Long, RJ Norby, M Stitt, GR Hendry, H Blum (Eds.) *In Managed Ecosystems and CO_2; Case studies, processes, and perspectives.* Springer-Verlag Berlin Heidelberg.

Presentations associated with this work

Dash J, **Tallis MJ.** *MTCI validation mid-term review.* **European Space Agency (ESA ESRIN) Frascati, Italy 2006**

Appendix B:

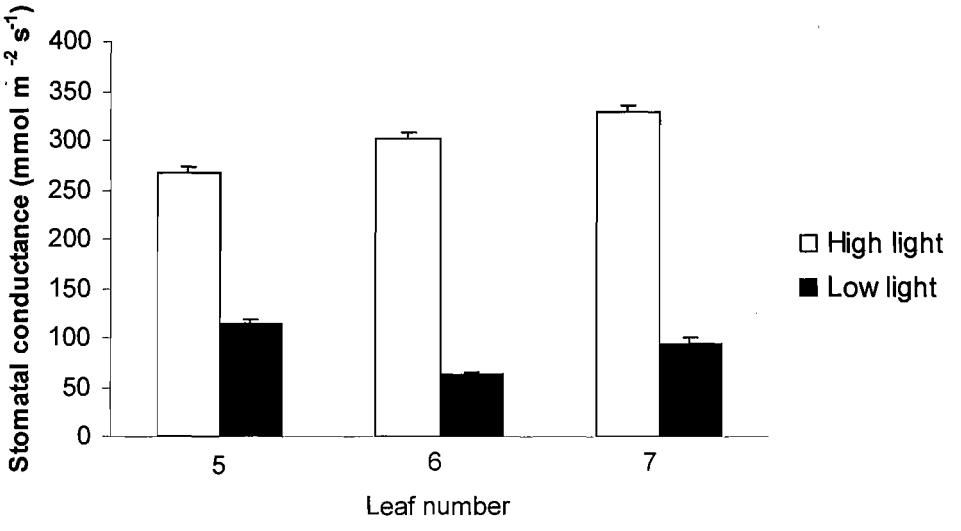

Appendix B: The stomatal conductance of *Populus deltoides* leaves *insitu* taken under two irradiance environments. Bars represent the mean (± 1 SE) of 10 replicate measurements per leaf for trees exposed to 2 hrs of high irradiance (700 μmol s^{-1} m^{-2}) or low irradiance (20 μmol s^{-1} m^{-2}).

Appendix C:

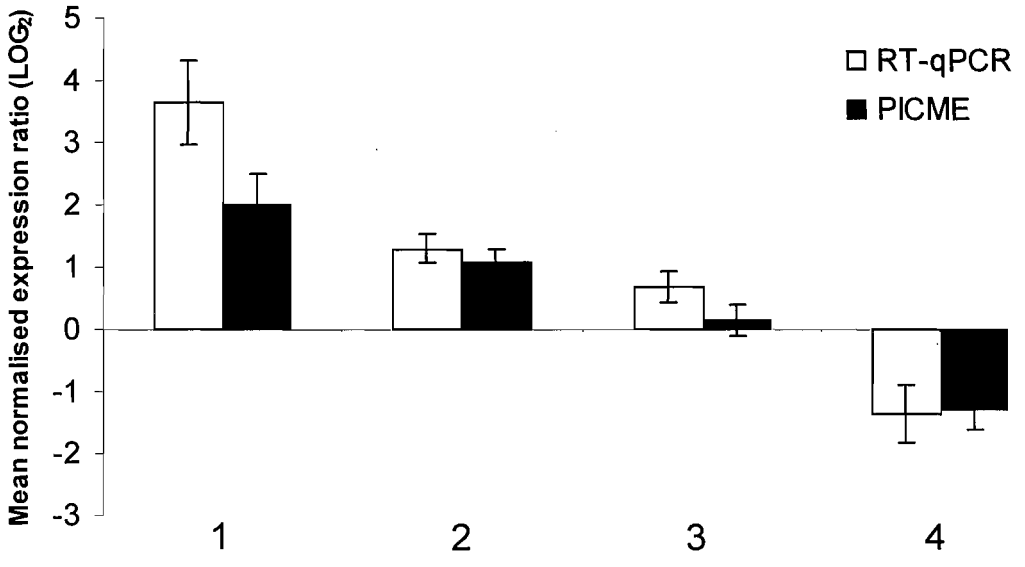

Appendix C: The comparison between the Log_2 expression ratios from microarray hybridisation (n =7) and RT-qPCR (n = 7) for the relative expression in elevated CO_2. Expression ratios are for EST sequences annoated as: (1) *LDOX*, (2) *GOLS*, (3) *GOLS-1*, and (4) *thaumatin*. The mean expression ratio calculated using RT-qPCR included the mean of between 2 and 3 technical repeats for each biological replicate and was calculated relative to the expression of the control gene *PDF1* (a serine/threonine protein phosphatase 2A (PP2A)).

Appendix D:

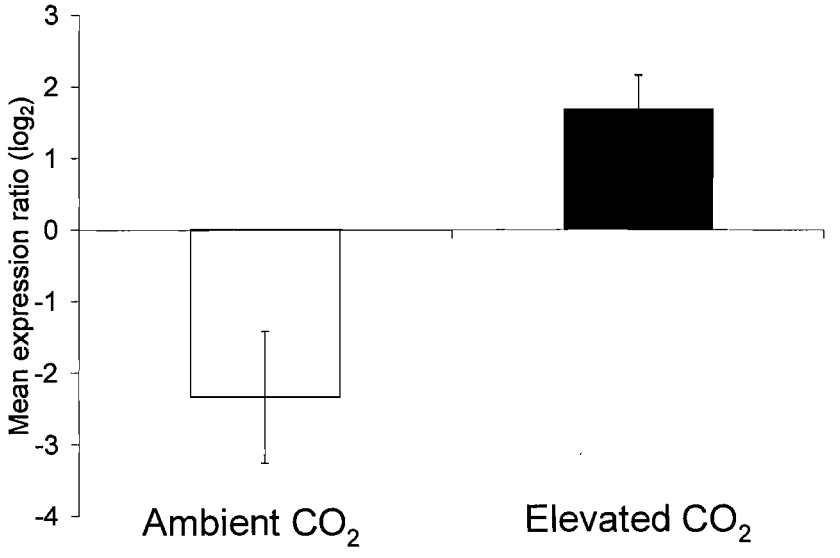

Appendix D: The mean expression ratio of *LDOX* calculated from expression in senescent leaves (18.10.04) / expression in pre-senescent leaves (31.08.04) (n = 4 at each time point). The relative change in expression are given for ambient CO_2 and elevated CO_2.

Appendix E

Table A1

The mean normalised expression ratios, statistics and annotations for the 15 significantly up-regulated (E/A) ESTs (18 October). The Benjamini-Hochberg corrected *P* value and the B statistics are given for each EST. Common annotations (in bold) are for ESTs representing the same gene model in the *P. trichocarpa* genome.

GenBank	PICME id	Mean normalised expression ratio	Mean $\log_2$ expression ratio	adjusted *P* value	*B* statistic	Annotation (tBLASTX)
CA826016	R71B12	26.31	3.27	≤0.01	3.91	leucoanthocyanidin dioxgenase
CA821476	RSH03D11	10.76	2.38	≤0.01	3.91	dihydroflavonol reductase
AJ768555	P0000100019B10	7.11	1.96	≤0.01	3.97	BURP domain-containing protein
AJ774308	P0000300015F01	6.90	1.93	≤0.01	4.29	endo-xyloglucan transferase
AJ768790	P0000100021G11	6.66	1.90	≤0.01	3.61	fiber lipid transfer protein
CA823427	R26A04	3.39	1.22	≤0.01	3.18	early drought induced protein
AJ774165	P0000300013E02	2.80	1.03	≤0.01	4.23	lipid transfer protein precursor
CF232035	PtaJXO0005G12G1214	2.78	1.02	≤0.01	3.05	Bad E-value
CF230956	***PtaC0015F10F1012***	***2.76***	***1.02***	≤0.01	***3.99***	***stable protein 1***
CA821043	***F07G07***	***2.74***	***1.01***	≤0.01	***5.10***	***Chain B, Solution Structure Of Hypothetical Arabidopsis Thaliana Protein At3g17210.***
CA824847	R49D04	2.63	0.97	≤0.01	3.65	extensin like protein
CF228982	PtaXM0019G12G1214	2.34	0.85	≤0.01	3.56	alpha-tubulin
CF230120	PtaC0004A9A0901	2.08	0.73	≤0.01	3.60	aquaporin
CA824021	R35A08	1.90	0.64	≤0.01	3.83	aquaporin
CA820768	F03A03	1.77	0.57	≤0.01	3.48	ATP synthase CF0 A chain

Appendix F

Table A2

The mean normalised expression ratios, statistics and annotations for the 51 significantly down-regulated (E/A) ESTs (18 October). The Benjamini-Hochberg corrected *P* value and the B statistics are given for each EST. Common annotations (in bold) are for ESTs representing the same gene model in the *P. trichocarpa* genome.

GenBank	PICME id	Mean normalised expression ratio	Mean $\log_2$ expression ratio	adjusted *P* value	*B* statistic	Annotation (tBLASTX)
AJ770105	P0001100007C01	0.06	-2.85	0.006	4.30	AT5g59750/mth12_150
AJ777815	P0000400035D12	0.14	-1.99	0.006	3.54	CPRD2
CF228720	PtaXM0016E8E0810	0.14	-1.96	0.006	3.22	Bad E-value
AJ771988	P0001600013B04	0.14	-1.93	0.005	7.40	tumor-related protein
CA825224	R55D08	0.18	-1.70	0.006	6.48	unknown
AJ778060	P0000400038H06	0.21	-1.58	0.006	5.86	Putative flavanone 3-hydroxylase
CA826121	R73A10	0.22	-1.53	0.006	4.47	Lemir
AJ769541	P0001000009B03	0.22	-1.50	0.006	4.23	CjMDR1
AJ769475	P0001000001H02	0.23	-1.46	0.006	4.63	NtEIG-E80
AJ770437	P0001100012B01	0.24	-1.42	0.006	3.92	ABA-responsive protein-like [
CF229310	PtaXM0023H5H0515	0.25	-1.37	0.006	3.70	unknown
AJ776430	P0000400013A05	0.26	-1.36	0.006	3.03	Bad E-value
AJ777537	P0000400029F05	0.26	-1.34	0.006	3.13	squalene monooxygenase
AJ777757	P0000400034F10	0.27	-1.32	0.006	3.54	At1g30760/T5I8_22
AJ773363	***P0000300001C03***	***0.28***	***-1.28***	***0.006***	***4.62***	***thaumatin-like protein***
AJ773455	P0000300002F10	0.28	-1.26	0.006	4.56	Bad E-value
CA825479	R59G02	0.30	-1.20	0.006	3.03	unknown
CA822481	R08H05	0.30	-1.19	0.006	4.60	unknown
AJ777648	P0000400033B05	0.31	-1.16	0.006	3.07	disease resistance gene homolog

CA821592	RSH04H06	0.31	-1.16	0.006	3.97	pathogenesis-related protein-like protein
CA823910	R33D01	0.32	-1.14	0.006	3.57	calmodulin-related protein
CA825784	R67E04	0.32	-1.14	0.006	3.39	kunitz trypsin inhibitor TI3
CF228949	PtaXM0019C7C0705	0.33	-1.10	0.006	3.19	Bad E-value
CA821155	***F11B12***	***0.34***	***-1.09***	***0.006***	***5.21***	***thaumatin***
AJ777197	P0000400024F07	0.34	-1.07	0.006	4.38	3-hydroxy-3-methylglutaryl-coenzyme A reductase (HMG-CoA reductase)
CA823789	R31D06	0.35	-1.04	0.006	3.25	P-type transporting ATPase
CA825136	***R54A04***	***0.35***	***-1.04***	***0.006***	***4.21***	***Kunitz trypsin inhibitor 3***
CB239784	***RSH16F06***	***0.36***	***-1.02***	***0.006***	***3.86***	***Kunitz trypsin inhibitor 3***
CA822900	***R15F04***	***0.37***	***-1.00***	***0.006***	***3.47***	***Kunitz trypsin inhibitor 3***
CA823575	R28D05	0.37	-0.99	0.006	4.31	Bad E-value
AJ777541	P0000400029F09	0.39	-0.94	0.006	3.40	oxidoreductase
CA823970	***R34C02***	***0.40***	***-0.91***	***0.006***	***4.16***	***Kunitz trypsin inhibitor 3***
AJ769531	P0001000008H11	0.40	-0.91	0.006	3.13	unknown
AJ780069	P0000800011D09	0.44	-0.82	0.006	3.55	phosphoenolpyruvate carboxykinase
AJ778123	P0000400039G05	0.44	-0.82	0.006	3.03	lysophospholipase-like protein
AJ769546	P0001000009C03	0.45	-0.81	0.006	4.56	No hit found
CA825274	R56C09	0.45	-0.80	0.006	3.21	Bad E-value
AJ769528	P0001000008H08	0.47	-0.75	0.006	4.27	cinnamyl alcohol dehydrogenase
AJ769525	P0001000008H03	0.49	-0.72	0.006	3.62	ABC transporter family protein
AJ774960	P0000300026C05	0.49	-0.71	0.006	5.61	1-aminocyclopropane-1-carboxylate oxidase
CF227381	PtaD4A12B0503	0.50	-0.70	0.006	3.71	ferulate-5-hydroxylase
CF234757	PtaJXT0014G6G0614	0.50	-0.69	0.006	3.47	squalene synthase
CA823758	R30H09	0.50	-0.69	0.01	3.29	protein S
CF233557	PtaJXO0025A10A1002	0.52	-0.66	0.01	3.05	PVR3-like protein
AJ771476	P0001600001G01	0.53	-0.63	0.01	3.12	No hit found